Universidad del País Vasco | Euskal Herriko Unibertsitatea

Facultad de Medicina y Enfermería / Medikuntza eta Erizaintza Fakultatea

Departamento de Genética, Antropología Física y Fisiología Animal / Genetika, Antropologia Fisikoa eta Animalien Fisiologia Saila

Tesis doctoral / Doktorego tesia

MiR-Pharmacogenetics in

Childhood Acute Lymphoblastic Leukemia Treatment

Maitane Umerez Igartua

Leioa, 2018

MiR-Pharmacogenetics

in Childhood Acute Lymphoblastic Leukemia Treatment

Maitane Umerez Igartua

PhD Thesis

Department of Genetics, Physic Anthropology and Animal Physiology

2018

"De gente bien nacida es agradecer los beneficios que recibe"
El Quijote (1605)

Quiero aprovechar estas líneas para dar las gracias a todas aquellas personas que han estado a mi lado y han hecho posible este proyecto.

En primer lugar a África, gracias por creer en mí y darme la oportunidad de llevar a cabo esta tesis. Hecho la vista atrás a 2011, asignatura de Genética, cuando conseguiste sembrar en mí la curiosidad por la farmacogenética y pude dibujar las primeras pinceladas con mi proyecto de fin de máster. Opté por la vía FIR sin yo saber que años más tarde me brindarías la ocasión de seguir trazando el camino hacia una tesis doctoral que hoy es una realidad, gracias.

El camino ha sido duro, pero sin ninguna duda ha sido amortiguado por grandes investigadoras y mejores personas que con sus acuarelas han hecho de esta tesis su mejor versión.

¡Muchísimas gracias Ángela! Por tu ayuda incondicional, por guiarme cuando lo necesitaba; probablemente sin tu apoyo no lo hubiera conseguido, eres maravillosa y llegarás hasta dónde te lo propongas, no tengo ninguna duda, te lo mereces.

No puedo olvidarme de: Leire y Carmen, entre tabla y tabla, análisis y coteje, jeje siempre dispuestas a ayudar, sois muy trabajadoras y así me lo habéis demostrado, eskerrik asko. Nerea y Jone, mila-mila esker zuen laguntzagatik, denborak gehien estutzen zuenean hor egon zinetelako. Y agradecer por supuesto a Idoia, Borja y Eli, por formar parte del equipo y colaborar en dar forma a este trabajo.

Empecé a brocha gorda, pero sin duda todo lo que me habéis enseñado me ha permitido llegar a perfilar mis conocimientos y hoy puedo decir que aquel boceto se ha convertido en obra, expuesta al mundo, orgullosa, contenta y con ganas de seguir abriendo las puertas a más páginas que seguir coloreando.

¿Y qué sería de mi vida sin mí paleta de colores? Nere bizitza ez litzateke berdina izango ingurukoengatik ez balitza! Abestiak esaten duen bezala, taupada bakoitzaz koloreztatu zuribeltza, taupada bakoitzaz irribarre bat…eta bi, hiru…mila!

Kuadritxangitarrok, Amaia, Maialen, Eneida, Marijo, Leire, Irati eta Sandra, eskerrik asko zuen babesagatik, zuen aldamenian lan orduak alde batera jareta denbora geldittuko nekelako. Zapatu Sakratu gehixau dakulako aurretik, topa!

Garazi eta Jaione, betirako deiketan dian horreittako bi lagun! Ikasketak elkartu ginttuen baina adiskidetasunak irmo mantendu gaittu urtiek aurrera egin ahala. Garazi, urtebete pasatxo da zure tesian niri dedikatutako hitzak irakurri nittunetik, zuk ez dozu gutxiago merezi (inork baino hobeto ulerketan dozulako momentu honen garrantzia). Jaione zer esanik ez, orain urrinago bizi arren elkarketan garen bakoitzian ondiok Gasteizko pisuko garai zoro hareittan bagina modura dalako. Neskak, ea noizko hurrengo patxaran homeopatikua! Jajajaja.

Eskerrik asko farmaziako lagun danori (Aitziber, Mikel, Pili, Arantza, Pablo, Josu, David, June, Garbiñe, Josune, Asun, Belén, Miren, Larraitz, Araceli, Nekane, Maritxu, Laura, Berta, Koro, Gonzalo, Carmen y Maripi), aún recuerdo cuando en 2014 os pedía consejo llena de dudas antes de tomar la decisión sobre este camino. Gracias por interesaros en todo momento sobre mis avances. Mila esker Josean por entender mi situación y darme la oportunidad de adaptar mis horarios y compaginar Donostia con Leioa. Y gracias a Marta, Shandra, Lurdes, Mertxe y a todos aquellos que han estado de alguna forma presentes durante estos años.

Eta bukatu aurretik, ikasteko nork erakutsi izan bihar dalako eta horretan onenak izan dittutelako txikittatik aldamenian, nere eskerrik kuttunena nere familixiari. Tia Lurdes, zuk erakutsi dostazu pereza ez dala existitten (nere kasuan "umereza" pittin bat bai seguru!). Tio Jabi, porque sé que soy tu "*farmaféutica*" favorita, gracias por sacarme una sonrisa cada vez que me llamas así. Tia Marian, hainbeste aldiz zure bizkotxo paregabiakin goxatu dostazulako mila mila esker. Amaiur, ahizpa eta laguna, txikittatik jolasian, ni oinaztu eta zu trumoi, ekaitz perfektua! Gaur egun be elkarren eskutik ibilbidian, holaxe jarraitu dagila urte askuan! Eta nola ez, Ama, Aitta, iparrorratz, bidelagun, eskerrik asko beti nere albuan izatiagatik eta naizena izatera heltzen lagunketiagatik.

Publications

The work of this thesis is reflected in the following publications:

Iparraguirre L, Gutierrez-Camino A, **Umerez M,** Martin-Guerrero I, Astigarraga I, Navajas A, Sastre A, Garcia de Andoin N, García-Orad A. MiR-pharmacogenetics of methotrexate in childhood B-cell acute lymphoblastic leukemia. *Pharmacogenet Genomics. 2016 Nov;26(11):517-525. (Genetics & Heredity Q3, JCR: 2,250; Genetics Q2, SJR: 0.993).*

Umerez M, Gutierrez-Camino A, Martin-Guerrero I, Garcia de Andoin N, Santos B, Sastre A, Echebarria-Barona A, Astigarraga I, Navajas A, Garcia-Orad A. Mir-pharmacogenetics of Vincristine and peripheral neurotoxicity in childhood B-cell acute lymphoblastic leukemia. *Pharmacogenomics J. 2017 Dec 27. doi: 10.1038/s41397-017-0003-3. [Epub ahead of print]. (Genetics & Heredity Q2, JCR: 3,812; Pharmacology Q1, SJR: 1.352)*

Umerez M, Gutierrez-Camino A, Santos B, Martin-Guerrero I, Garcia de Andoin N, Sastre A, Navajas A, Astigarraga I, Garcia-Orad A. Pharmacoepigenetics in childhood acute lymphoblastic leukemia: Involvement of miRNA polymorphisms in hepatotoxicity. *Epigenomics. 2018 Apr 1; 10(4):409-417. doi: 10.2217/epi-2017-0138. (Genetics & Heredity Q1, JCR: 4.979; Genetics Q1, SJR: 1.679)*

Umerez M, Gutierrez-Camino A, Lopez-Lopez E, Santos B, Martin-Guerrero I, García de Andoin N, Sastre A, Navajas A, Astigarraga I, García-Orad A. Pharmacoepigenetics in childhood acute lymphoblastic leukemia: Involvement of miRNA polymorphisms in mucositis. *(Under review in Pharmacogenomics). (Pharmacology & Pharmacy Q3, JCR: 2,302; Pharmacology Q2, SJR: 0.877)*

Furthermore, during the development of this thesis, I have also published the following articles:

Umerez M, Gutierrez-Camino A, Muñoz-Maldonado C, Martin-Guerrero I, Garcia-Orad A. MTHFR polymorphisms in childhood acute lymphoblastic leukemia: Influence on methotrexate therapy. *Pharmgenomics Pers Med. 2017 Mar 27;10:69-78. (Pharmacology Q1, SJR: 1.165)*

Umerez M, García-Obregón S, Martín-Guerrero I, Astigarraga I, Gutierrez-Camino A, García-Orad A. Role of miRNAs in treatment response and toxicity of childhood acute lymphoblastic leukemia. *Pharmacogenomics. 2018 Mar; 19(4):361-373.). (Pharmacology & Pharmacy Q3, JCR: 2,302; Pharmacology Q2, SJR: 0.877)*

Abbreviation	Explanation
3´UTR	3'UTR regulation
6-MP	6-mercaptopurine
ABCB1	ATP binding cassette subfamily B member 1
ABCC1	ATP binding cassette subfamily C member 1
ABCC10	ATP binding cassette subfamily C member 10
ABCC2	ATP binding cassette subfamily C member 2
ABCC3	ATP binding cassette subfamily C member 3
ABCC4	ATP binding cassette subfamily C member 4
ABCG2	ATP binding cassette subfamily G member 2
ADME	Absorption, distribution, metabolism, elimination
AKR1A1	Aldo-keto reductase family 1 member A1
AKR1C3	Aldo-keto reductase family 1 member C3
ALDH1	Aldehyde dehydrogenase, cytosolic 1-like
ALDH1A1	Aldehyde dehydrogenase 1 family member A1
ALDH3A1	Aldehyde dehydrogenase 3 family member A1
ALDH5A1	Aldehyde dehydrogenase 5 family member A1
ALT	Alanine aminotrasferase
ALL	Acute lymphoblastic leukemia
AraC	Cytarabine
ASO	Allele specific oligos
ASP	L-asparaginase
AST	Aspartate aminotransferase
B-ALL	B-cell lineage acute lymphoblastic leukemia
BAX	Bcl-2-like protein 4
BCLW	Bcl-2 like protein
BM	Bone marrow
bp	Base pair
CAT	Catalase
CBR1	Carbonyl reductase 1
CBR3	Carbonyl reductase 3
CeGen	Spanish national genotyping center
CI	Confidence interval
CIPN	chemotherapy-induced peripheral neuropathy
CNS	Central nervous sistem
CPA	Cyclophosphamide
CPdB	Consensuspath database
CPK	Creatin phosphokinase
CYP2A6	Cytochrome P450 family 2 subfamily A member 6
CYP2B6	Cytochrome P450 family 2 subfamily B member 6
CYP2C19	Cytochrome P450 family 2 subfamily C member 19
CYP2C8	Cytochrome P450 family 2 subfamily C member 8
CYP2C9	Cytochrome P450 family 2 subfamily C member 9
CYP3A4	Cytochrome P450 family 3 subfamily A member 4
CYP3A5	Cytochrome P450 family 3 subfamily A member 5
Chr	Chromosome

Abbreviations

DAMPs	Damage-associated pattern molecules
DEXA	Dexamethasone
DHFR	Dihydrofolate reductase
DICER	Ribonuclease type III
DLK	Dual leucine zipper kinase
DNA	Deoxyribonucleic acid
DNR	Daunorubicin
DROSHA	Double-stranded RNA-specific endoribonuclease
dsRNA	Double-stranded RNA
DTR	Deep tendon reflex
EFS	Event free survival
EIF2C1	Eukaryotic translation initiation factor 2C, 1
EIF2C2	Eukaryotic translation initiation factor 2C, 2
epiADR	Epiadriamycin
ER	Endoplasmic reticulum
ERCC1	ERCC excision repair 1, endonuclease non-catalytic subunit
ERCC2	ERCC excision repair 2, TFIIH core complex helicase subunit
ERCC4	ERCC excision repair 4, endonuclease catalytic subunit
ETV6	Ets variant 6
FDR	False discovery rate
GPX1	Glutathione peroxidase 1
GWAS	Genome wide association study
HR	High risk
IP3R	Inositol 1,4,5-triphosphate receptor
ISCIII	Instituto de Salud Carlos III
LSO	Locus specific oligos
MAF	Minor allele frequency
MAPK	Mitogen-activated protein kinase
MFE	Minimum free energy
MGMT	O-6-methylguanine-DNA methyltransferase
miRNA	MicroRNA
MLH1	MutL homolog 1
MRD	Minimal residual disease
mRNA	Messenger RNA
MSH2	MutS homolog 2
MTHFD1	Methylenetetrahydrofolate dehydrogenase, cyclohydrolase and formyltetrahydrofolate synthetase 1
MTHFR	5,10-methylenetetrahydrofolate reductase
MTR	Methionine synthase
MTRR	Methionine synthase reductase
MTX	Methotrexate
NA	Not available
NFKB1	Nuclear factor kappa B subunit 1
NFKBIE	NFKB inhibitor epsilon
NMN	Nicotinamide mononucleotide
NMNAT	Nicotinamide mononucleotide adenylyltransferase

NOS1	Nitric oxide synthase 1
NOS2	Nitric oxide synthase 2
NOS3	Nitric oxide synthase 3
NQO1	NAD(P)H quinone dehydrogenase 1
OR	Odds ratio
OS	Overall survival
PCR	Polymerase chain reaction
PD	Pharmacodynamic
PDN	Prednisone
PK	Pharmacokinetic
PLD	Phospholipase D
POR	Cytochrome p450 oxidoreductase
pre-miRNA	Precursor miRNA
pri-miRNA	Primary miRNA
Puma	p53 upregulated modulator of apoptosis
RALBP1	RalA binding protein 1
RFC1	Reduced folate carrier
RISC	RNA-inducing silencing complex
RNA	Ribonucleic Acid
ROS	Reactive oxygen species
SARM1	Sterile α-motif-containing and armadillo-motif-containing protein
SD	Standard deviation
SHMT1	Serine hydromethyl transferase
SLC19A1	Solute carrier family 19 member 1
SLC22A16	Solute carrier family 22 member 16
SLC22A6	Solute carrier family 22 member 6
SLC22A8	Solute carrier family 22 member 8
SLC46A1	Solute carrier family 46 member 1
SLCO1A2	Solute carrier organic anion transporter family member 1A2
SLCO1B1	Solute carrier organic anion transporter family member 1B1
SLCO1B3	Solute carrier organic anion transporter family member 1B3
SNP	Single nucleotide polymorphism
SNS	Symphatetic nervous system
SOD1	Superoxide dismutase 1
SR	Standard risk
ssRNA	Single stranded RNA
STS	Soft tissue sarcoma
TdT	Terminal deoxytransferase
TIT	Triple intrathecal
TLR	Toll like receptor
TOP2A	DNA topoisomerase II alpha
TP53	Tumor protein p53
TS	Thymidylate synthetase
TUBB*	Tubulin
ULN	Upper limit of normal
VCR	Vincristine

Abbreviations

VHR	Very high risk
WHO	World health organization
Wlds	Wallerian degeneration slow
XDH	Xanthine dehydrogenase

Index

INTRODUCTION

1. ACUTE LYMPHOBLASTIC LEUKEMIA

1.1. Introduction

Acute Lymphoblastic Leukemia (ALL) is the most common childhood cancer, being the leading cause of death by disease in developed countries for this population. The last three decades, ALL survival rates have raised remarkably reaching up to 90% (Tasian and Hunger, 2017). This improvement on outcome has been achieved, at least in part, due to the intensive treatment protocols that are based on the risk stratification of patients and the administration of a combination of several drugs along the different treatment phases. However, as counterpart to this survival improvement, some patients experience severe toxicities that often require a dose reduction or even treatment discontinuation, with the consequent negative impact on survival (Ceppi et al., 2014; Salazar et al., 2012). Hence, nowadays one of the challenging fields in childhood ALL is the investigation of reliable toxicity markers, being pharmacogenetics a promising tool to achieve this goal.

1.2. Definition

ALL is a neoplasm of the lymphoid cell lineage precursor, the lymphoblast, which may affect to the B-cell or the T-cell lineages. Acquisition by the lymphoblast of a series of genetic abnormalities disturbs its normal maturation process (Figure 1) leading to differentiation arrest and proliferation of the transformed cell, which is typically distinguished by its small to medium-size, scant cytoplasm, moderately condensed to dispersed chromatin and inconspicuous nucleoli.

As a consequence of this immature clone proliferation, invasion of bone marrow (BM) and peripheral blood occurs, causing marrow function failure and blastic infiltration of organs and tissues, mainly lymph nodes, liver, spleen, central nervous system (CNS) and testes.

ALL represents the third part of pediatric cancer diagnoses and accounts for about 75-80% of all acute leukemia cases in children.
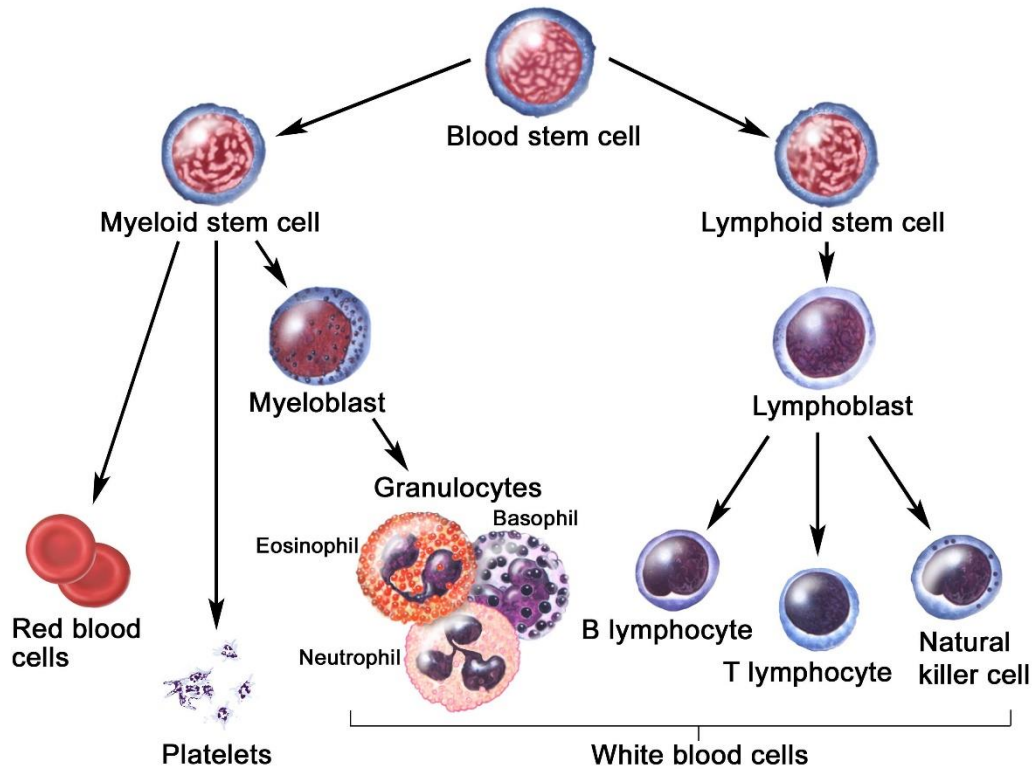
© 2007 Terese Winslow
U.S. Govt. has certain rights

Figure 1. Normal blood cell development.
Source: (https://www.cancer.gov/types/leukemia/hp/child-all-treatment-pdq)

1.3. Childhood ALL epidemiology

Approximately 75% of the cases occur in children under six years of age and there is a frequency peak between the ages of 2 and 5 years (Swerdlow et al., 2008). The worldwide incidence is estimated at 1-4.75/100,000 cases per year. ALL is slightly more common in males than females. Additionally, racial and ethnic differences have been described. Hispanics are more likely to develop acute leukemia than Caucasians and these show higher incidence than African-Americans (Lim et al., 2014).

In Spain, according to the National Child Tumor Registry (RETI-SEHOP, 1980-2016), the incidence of ALL is 37.1% (CI95%: 35.2-39.0) of all pediatric malignancies in children <14 years old (Figure 2).

Standardized rate by world population (ASRw)
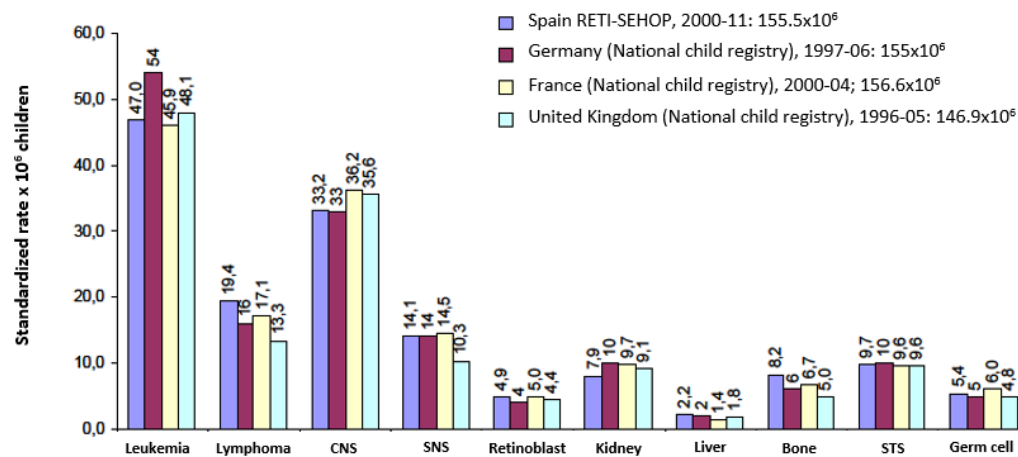
Abbreviations: CNS, central nervous system; SNS, sympathetic nervous system; STS, soft tissue sarcoma; Epit, epithelial.
Figure 2. Childhood cancer incidence in Spain (RETI-SEHOP) and other European countries.
Source: Adapted from RNTI-SEHOP (https://www.uv.es/rnti/cifrasCancer.html)

The 80–85% of all ALL cases have their origin in the B-cell lineage (Silverman et al., 2000). From now on, we are going to focus on this majority ALL subtype, the B-cell precursor acute lymphoblastic leukemia (B-ALL).

1.4. Clinical and pathological features

Most patients with B-ALL present with signs and symptoms consequence of bone marrow failure: thrombocytopenia (presence of petechiae, ecchymosis or hemorrhage), anemia (shown as paleness and asthenia) and/or neutropenia (infection risk increase, reason for which it is not rare ALL debuting with fever without an apparent infectious focus). The leukocyte count may be decreased, normal or markedly elevated. Bone pain and arthralgia may be pronounced due to infiltration of bone marrow or even the bone tissue or the articulation structures. At exploration, lymphadenopathy, hepatomegaly and splenomegaly are frequently present. Sometimes central nervous system and testes in male patients might be affected because of blasts predilection for these tissues (Swerdlow et al., 2008). Symptoms duration may be between days to months and the disease presentation could go from an asymptomatic analytical alteration to a medical emergency.

Morphologically the B-ALL tumor lymphoblasts in blood smears and bone marrow aspirates vary from small cells with scant cytoplasm, condensed nuclear chromatin and indistinct nucleoli to larger cells with moderate amounts of light blue to blue-grey cytoplasm occasionally vacuolated, dispersed nuclear chromatin and multiple variably prominent nucleoli (Swerdlow et al., 2008). In bone marrow biopsies, the tumor lymphoblasts are small to medium-sized, with scant

cytoplasm, with round to oval, indented or convoluted nuclei, finely dispersed chromatin and indistinct or small nucleoli (Swerdlow et al., 2008).

Inmunophenotypically, the lymphoblasts in B-ALL are almost always positive for the B-cell markers CD19, cytoplasmic CD79a and cytoplasmic CD22; while none of these by itself is specific, positivity in combination or at high intensity strongly supports the B lineage. The degree of differentiation of B-lineage lymphoblasts has clinical and genetic correlates. In the earliest stage, so called early precursor B-ALL or proB-ALL, the blasts express CD19, cytoplasmic CD79a, cytoplasmic CD22 and nuclear TdT. In the intermediate stage, so called common ALL, the blasts express CD10. In the most mature precursor B differentiation stage, so called pre-B-ALL, the blasts express cytoplasmic μ chains. The immunophenotype of precursor B-ALL differs in almost all cases from that seen in normal B-cell precursors. These differences can be very useful in the evaluation of minimal residual disease (MRD) of follow-up bone marrow specimens (Hashimoto et al., 2002; Swerdlow et al., 2008).

On a chromosomal structural basis, certain genetic alterations tightly related to ALL have been described (Table 1).

Table 1. Chromosomal translocations and chromosome number changes and their frequency in B-cell ALL (Malouf and Ottersbach, 2017).

Cytogenetic abnormality	Frequency Children (2-18 years old)
TEL/AML1 or ETV6-RUNX1 t(12;21)(p13;q22)	12-15 %
ETV6-RUNX1-like	6 %
E2A/PBX1 t(1;19)(q23;p13.3)	2-6 %
DUX4-rearranged	8 %
Hyperdiploidy	20-30 %
Trisomy 4 and 10	20-25 %
MLL/AF4 t(4;11)(q21;q23)[A]	2-20 %
BCR/ABL t(9;22)(q34;q11)	1-3 %
BCR/ABL1-like	15-20 %
Hypodiploidy	1-2 %
Intrachromosomal amplification of chromosome 21 (iAMP21)	2-3 %

Notes: A, over 50 fusion partner genes have been identified for *MLL*. The most common partner genes are *AF4* transcription factor on chromosome 4q21, but also *ENL* on chromosome 19p13 and *AF9* on chromosome 9p22.

Some of this genetic alterations have been associated with prognosis, for example, normal karyotype or TEL/AML positivity are associated with favourable prognosis whereas BCR/ABL or MLL presence is related to unfavourable prognosis.

1.5. Prognostic factors and risk stratification

Nowadays, the most important prognostic factors to be considered are: age, leukocyte count at diagnosis, immunophenotype, extramedullary affectation, ploidy, cytogenetic or genomic alterations, early treatment response and MRD, factors that confer a favorable or unfavorable prognosis (Table 2).

Table 2. Prognostic factors in childhood ALL that confer favorable or unfavorable prognosis.

Favorable	Unfavorable
Age between 1-9 years	Age < 1 year or > 10 years
Diagnostic leukocyte count <20 x 10^9/L	Diagnostic leukocyte count > 20 x 10^9/L
Common immunophenotype	T-ALL > pre-pre B-ALL > pre-B-ALL > B-ALL
No CNS involvement	CNS involvement
Normal karyotype, hyperdiploidy (51-81 chromosomes), *TEL/AML +*.	Almost tetraploidy (82-94 chromosomes), hipodiploidy (30-45 chromosomes), almost haploidy (24-29 chromosomes), BCR/ABL +, MLL +
Blasts in BM < 5% at day + 14 of treatment	Blasts in BM >5% at day + 14 of treatment

Abbreviations: T-ALL, T-cell acute lymphoblastic leukemia; B-ALL, B-cell acute lymphoblastic leukemia; CNS, central nervous system; BM, bone marrow.

Introduction

The evaluation of these factors at the moment of diagnosis allows the stratification of patients according to their disease risk (Table 3).

Table 3. Criteria for risk group stratification in childhood ALL therapy.

STANDARD RISK (SR)

A patient must meet all the following criteria to be included in this group
Age 1-9 years
Common ALL immunophenotype (CD19+, CD10+, cytoplasmic μ chains -)
White blood cell count at diagnosis <20x10^9/l
No extramedullary involvement (CNS, testes)
Absence of unfavourable cytogenetics
<5% blasts in bone marrow at day +14
<0.1% MRD at the end of the induction phase of treatment

HIGH RISK (HR)

The existence of at least one of these criteria determines the inclusion of the patient at high risk:
Age ≥10 years
Any immunophenotype except for the one indicated in SR
White blood cell count between 20 and 200x10^9/l
Extramedullary involvement (CNS, testes)
Unfavourable cytogenetics
≥5% blasts in bone marrow at day +14
≥0.1% MRD at the end of induction

VERY HIGH RISK (VHR)

The existence of at least one of these criteria determines the inclusion of the patient at very high risk:
White blood cell count >200x10^9/l
Very unfavourable cytogenetics
HR with ≥5% blasts in bone marrow at day +14/+21
HR with ≥0.1% MRD at the end of consolidation

Nowadays this strategy of stratifying patients has been used to adjust the treatment.

2. CHILDHOOD ALL TREATMENT: LAL/SHOP PROTOCOL

ALL therapy is based on complex, well established, risk adapted treatment protocols, where a combination of multiple drugs is administered sequentially along different phases. The protocol used up to recent years in Spain for ALL treatment was the one approved by the Society of Pediatric Hematology and Oncology (SEHOP), called LAL/SHOP. It has several versions (94, 99, 2005), with slight differences among them. LAL/SHOP 2005 protocol is described in Figure 3. In 2013 the LAL/SHOP 2005 protocol was updated to a similar LAL/SEHOP-PETHEMA 2013 protocol.
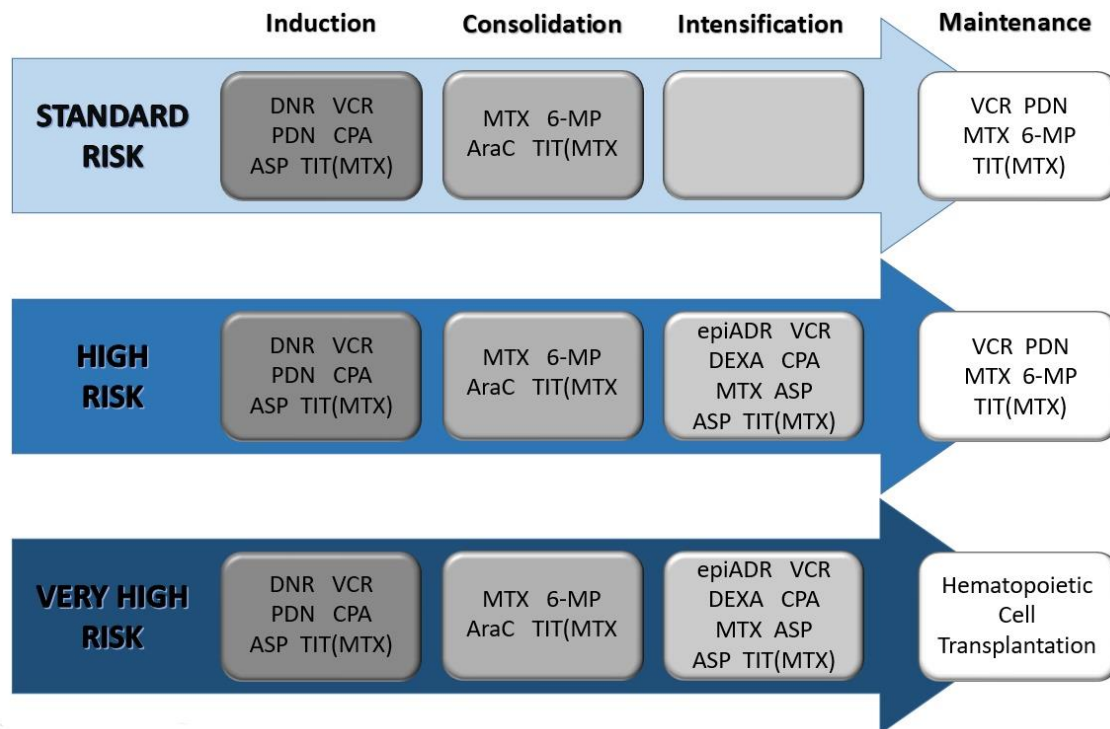
Abbreviations: DNR, daunorubicin; VCR, vincristine; PDN, prednisone; CPA, cyclophosphamide; ASP, L-asparaginase; TIT, triple intrathecal; MTX, methotrexate; 6-MP, 6-mercaptopurine; AraC, cytarabine; epiADR, epiadriamycin; DEXA:dexamethasone.
Figure 3. LAL/SHOP 2005 treatment protocol diagram.

Firstly, in all the risk groups an induction phase is conducted during about 5 weeks. The goal of this phase is to eradicate more than the 99% of the initial leukemic cell burden in bone marrow in order to restore normal hematopoiesis. LAL/SHOP 2005 protocol includes: **prednisone** (PDN) (glucocorticoid, immunosuppressive effect; intravenous or oral 60 mg/m^2/day for 28 days, 30 mg/m^2/day the following 4 days, and 15 mg/m^2/day 4 more days), **daunorubicine** (DNR) (anthracycline with capacity to block topoisomerase and bind to DNA; one 48h continuous infusion of 120 mg/m^2), **vincristine** (VCR) (vinca alkaloid that interferes with microtubules blocking the mitosis on metaphase; weekly bolus of 1.5 mg/m^2, maximum 2 mg, for 4 weeks), **L-asparaginase** (ASP) (enzyme that hydrolyzes asparagine and interferes with the synthesis of proteins; 10 doses of intramuscular 5,000 U/m^2 on alternate days), and **cyclophosphamide** (CPA) (DNA alkylating agent that blocks transcription and replication processes; one infusion of 1000 mg/m^2). Furthermore, **triple intrathecal therapy** (TIT) (combination of methotrexate (MTX), cytarabine (AraC) and hydrocortisone; two doses adjusted by age group) is started to avoid the invasion of the CNS.

Secondly, once normal hematopoiesis is restored the consolidation phase begins, which is maintained for around 8 weeks. In this second phase, the treatment is enhanced to prevent the onset of therapy-resistant clones. All the risk groups receive the same consolidation therapy. At

this stage, **methotrexate** (folate analogue that exerts its antitumor effect by inhibiting the synthesis of purines, pyrimidines and proteins; 5 g/m^2 or 3 g/m^2, total three doses given in 24 h infusion with subsequent folinic acid rescue) and **6-mercaptopurine** (6-MP) (purine analogue that exerts its effect by incorporation into DNA; oral 30 mg/m^2/day for 6 weeks) are used. Monitoring of MTX concentration in plasma is carried out every day until the concentration is below 0.2 μM. Furthermore, consolidation phase is completed with **cytarabine** (AraC) (cytosine analogue that inhibits DNA polymerase; four doses of 1 g/m^2) and TIT (four doses).

Finally, a maintenance phase is applied, which can be extended for about two years and is intended to preserve remission with reinductions. Reinductions are applied monthly for the first 6 months and consist of PDN (40 mg/m^2/day for 7 days), VCR (1.5 mg/m^2, maximum 2 mg) and TIT (only for the first 4 months of maintenance phase). Moreover oral or intramuscular MTX (20 mg/m^2/weekly) and oral 6-MP (60 mg/m^2/day) are still used.

For HR and VHR groups the treatment is strenghthened in several ways. Firstly, an additional intensification phase between the consolidation and maintenance phases is applied. During this intensification phase, several drugs including epirubicin, VCR, dexamethasone, CPA, MTX, ASP, AraC and TIT are administered. Appart from this extra phase, for HR group patients, during induction, ASP goes to 10,000 U/m^2 and two CPA infusions and three TIT are administered. Moreover, during maintenance phase the reinductions are applied for the first 8 months and ASP and CPA are also used. In the VHR group, treatment is further intensified with several consolidation phases and treatment is concluded with hematopoietic cell transplantation.

This strategy of adjusting treatment according to risk groups, has improved survival rates, reaching nowadays the 5 year event free survival rates up to 80-90 % (Bhojwani et al., 2015; Liang et al., 2010; Mitchell et al., 2010; Möricke et al., 2010). In Spain, according to RETI data, it is estimated that 5 year survival from diagnosis has increased notably from 56% in the 80´s to 83% during last years (Figure 4, RETI-SEHOP 1980-2016).
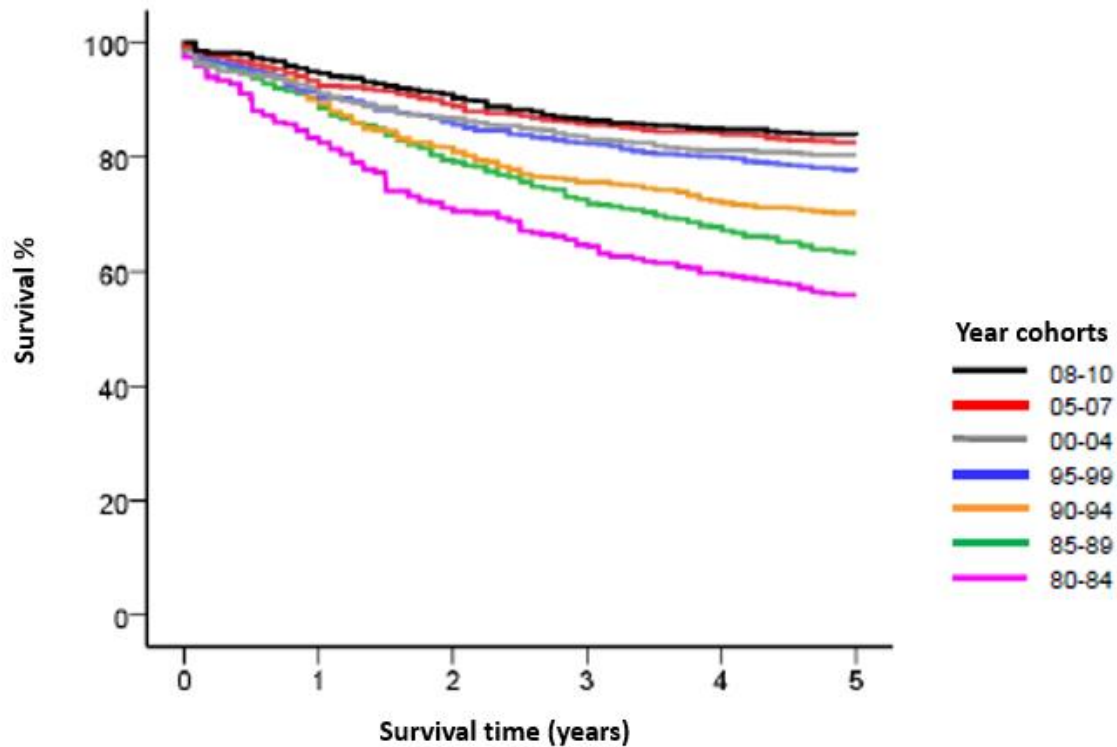
Figure 4. Childhood ALL 5 year from diagnosis survival rates per incidence year cohorts. 0-14 years, 1980-2010, N=3989 cases.
Source: Adapted from RETI-SEHOP (https://www.uv.es/rnti/informes.html).

One of the most important problems associated with these treatment protocols is that, in spite of clinical success, some patients experience severe toxicity, requiring a dose reduction or even treatment cessation, with the consequent negative impact on survival (Ceppi et al., 2014; Salazar et al., 2012). Risk stratification adapted therapy has allowed to avoid excessive chemotherapy in some patients (Geng and Wang, 2015; Hunger et al., 2005; Pui and Evans, 2013). However, toxicity persists in patients of the three risk groups.

3. TOXICITIES OF CHILDHOOD ACUTE LYMPHOBLASTIC LEUKEMIA THERAPY

Drugs are administered to a defined posology (dose and frequency) to reach certain concentrations in the target tissue with the unique purpose of achieving the sought effect. However, the effect of these drugs in other tissues, cells or intracellular routes can lead to the development of undesirable effects, toxicity.

When a drug is administered, it goes through the sequential steps of absorption, distribution, metabolism and excretion, processes that are known under the ADME denomination. The drugs administered through a route different to the intravenous, e.g. oral or intramuscular, will suffer an absorption process till the bloodstream. Once in the blood, they will be distributed to the

different tissues where they are intended to act. Next, the molecules will be metabolized, predominantly in the liver to be finally eliminated from the organism (mainly by renal excretion and biliary excretion to a less extent, depending of the drug). This four ADME steps are defined as pharmacokinetics (PK), i.e. how a drug moves through an individual´s body and affects the drug effect by altering the concentrations reached in its site of action (Preskorn and Hatt, 2013). On the other hand, everything referred to the therapeutic response, generally determined by the drug affinity and activity at its site of action is defined as pharmacodynamics (PD) (Preskorn and Hatt, 2013).

The PK/PD processes for each drug are comprised inside a pathway in which nowadays most involved genes are known. Any modification in these PK/PD genes could act as predisposing factors that disturb the optimal drug response and conduct to adverse event development (Turner et al., 2015), as they could lead to alterations of drug concentrations or production of intermediaries that contribute to toxicity or interrupt drug effects. The elucidation of modifications in PK/PD genes of specific drugs bring the opportunity to diminish even more the toxicities they induce.

The LAL/SHOP treatment protocol contemplates the evaluation of toxicities on each treatment phase, in order to act accordingly taking the appropriate supporting cares, reducing doses or even discontinuing drugs. Some adverse events secondary to LAL/SHOP treatment protocols can be associated to the administration of specific antileukemic agents, e.g. anthracyclines produced cardiomyopathy, ASP-induced hypersensitivity or VCR induced peripheral neuropathy (Moriyama et al., 2015). In contrast, other toxicities can be linked to the use of several drugs. For instance, hepatic toxicity has been associated to ASP exposure during induction and to MTX during consolidation phase (Liu et al., 2017). Other example could be mucositis, which has been linked to several antileukemic agents such as MTX, DNR or CPA. Table 4 shows the most common toxicities of the drugs used in childhood ALL treatment.

Table 4. ALL treatment toxicities and the drugs that induce them.

Toxicity	Drug
Neurotoxicity	
Peripheral neuropathy	Vincristine[++], Cyclophosphamide*.
Paralytic ileus	Vincristine[+].
Hepatic toxicity	
Hypertransaminasemia	L-Asparraginase[++], Methotrexate[++], Daunorubicin[++], 6-Mercaptopurine[+], Citarabine[+].
Hyperbilirubinemia	Daunorubicin[++], L-Asparraginase[++], Methotrexate[++], 6-Mercaptopurine[+].
Digestive toxicity	
Mucositis	Methotrexate[++], Daunorubicin[++], Cyclophosphamide[+], 6-Mercaptopurine[+], Citarabine[++].
Nausea/vomits	Daunorubicin[++], Cyclophosphamide[++], Methotrexate[++], Vincristine[++], L-Asparraginase[++], 6-Mercaptopurine[+], Citarabine[++].
Diarrhea	Daunorubicin[++], Methotrexate[+],Vincristine[+], L-Asparraginase[++], Citarabine[++].
Nephrotoxicity	
Cystitis	Cyclophosphamide[++].
Renal dysfunction	Citarabine*.
Hematologic toxicity	
Anemia	Daunorubicin[++], Vincristine[++], L-Asparraginase[+], Cyclophosphamide*, Methotrexate[+], 6-Mercaptopurine[+], Citarabine[+].
Neutropenia	Daunorubicin[++], L-Asparraginase[+], Cyclophosphamide[++].
Thrombocytopenia	Daunorubicin[++], Vincristine[++], L-Asparraginase[+], Cyclophosphamide*, Methotrexate[+], 6-Mercaptopurine[++], Citarabine[+].
Other	
Hyperglycemia	Prednisone[+], L-Asparraginase[++].
Hypersensitivity	L-Asparraginase[++], Methotrexate*, 6-Mercaptopurine*, Citarabine*.
Exanthema	Methotrexate[+].
Cardiotoxicity	Daunorubicin[++], Cyclophosphamide*.
Gastrointestinal hemorrhage	Daunorubicin[++], Methotrexate*.
Infection	Daunorubicin[++], Cyclophosphamide[+], Citarabine[++].

Notes: Drug official product information declare each toxicity as very common (≥1/10) (denoted as ++), common (<1/10 to ≥1/100) (denoted as +) or uncommon <1/100 to ≥ 1/1000) (denoted as *) (Accord Healthcare S.L.U., 2017a, 2017b; Baxter Oncology GmbH, 2017; Pfizer, 2017a, 2017b; Silver pharma S.L., 2017; Spezialpräparate, 2017).

We have focused our study in: neurotoxicity induced by VCR, the clearest drug/toxicity pairing; hepatic toxicity and gastrointestinal toxicity, both produced by several ALL therapy drugs and high MTX plasma levels.

Introduction

3.1. VCR-induced neurotoxicity

VCR is an important component of childhood ALL, however, despite its clinical efficacy, VCR can cause sensory and motor neurotoxicity (Carozzi et al., 2015), the main VCR adverse event and a limiting factor for its use.

The most common neurotoxicity form is the peripheral neuropathy which is presented primarily as a distal sensory-motor polyneuropathy (Legha, 1986). This toxicity seems to be related to plasmatic VCR peak concentrations (Dougherty et al., 2007; Groninger et al., 2005). These plasmatic concentrations will be determinated by the frequency and number of administered VCR doses as well as by VCR PK (Figure 5).
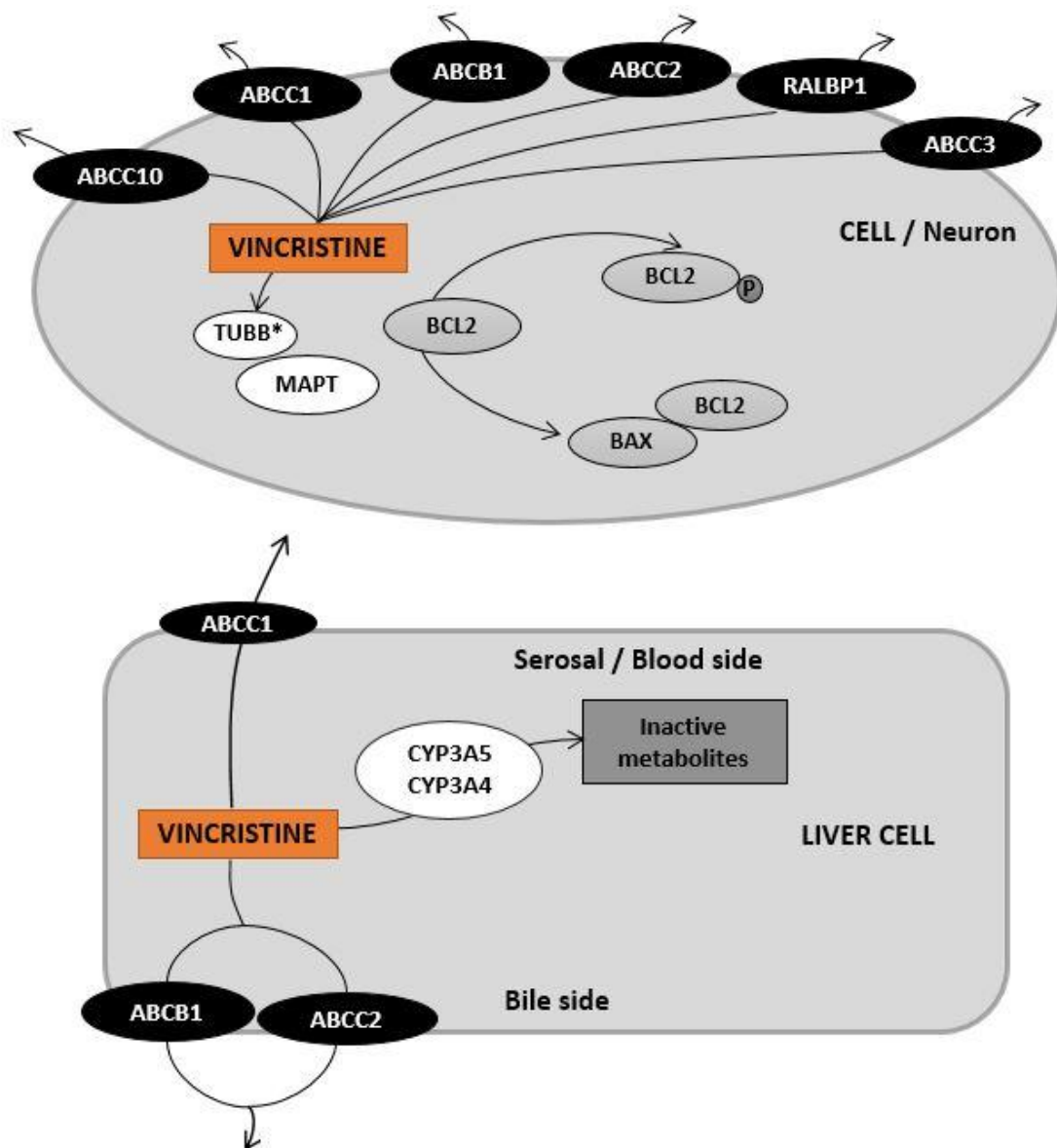
Figure 5. VCR PK/PD pathways.

VCR is predominantly metabolized through CYP3A enzymes subfamily, playing an important role in vincristine clearance (Dennison et al., 2006). Membrane transporters including ABCB1, ABCC1, ABCC2, ABCC3, ABCC10 and RALBP1 also have a relevant role in vincristine transport and elimination. The biliary excretion of vincristine is mediated by ABCB1 and ABCC2, whereas vincristine is transported into the blood by ABCC1 (Figure 5) (Leveque and Jehl, 2007).

Based on an PD view, VCR inhibits cell proliferation by binding to tubulin and blocking microtubules polymerization (Islam and Iskander, 2004), which leads to a mitotic block and cell apoptosis (Jordan and Wilson, 2004), which could explain neurodegeneration. Consequently, genes coding beta-tubulin proteins and/or in microtubule-associated proteins such as TUBB, MAPT or CEP72, could alter the stabilization of microtubules, modifying the cells sensitivity to vincristine and provoking differences in the effect of this drug among patients.

On the other hand, studies in patients and animal models implicate axonal degeneration as the principal anatomopathologic lesion behind the neurotoxicity process, suggesting that VCR could either directly or indirectly trigger a "dying back" axon degeneration that proceeds in a distal-to-proximal manner. Potential mechanisms for initiating axon degeneration include defects in axon transport (Argyriou et al., 2012; van den Bent, 2005; Rosenthal and Kaufman, 1974), altered mitochondrial function, or altered Ca+2 homeostasis.

The neuronal crucial points in which VCR could interfere are (Figure 6): (1) in the nucleus during axon development, target-derived neurotrophins control the transcription equilibrium of pro-survival/pro-death genes, Bcl-2-like protein 2 (*BCLW*) and p53 upregulated modulator of apoptosis (*Puma*) respectively; (2) during axonal transport, *BCLW* transcripts and cell soma-derived factor nicotinamide mononucleotide adenylyltranferase (*NMNAT2*) are transported toward distal axons; (3) in mitochondria and endoplasmic reticulum (ER), translated *BCLW* modulates mitochondrial function which inhibits caspase cascade and maintains Ca2+ homeostasis preventing activation of Ca2+-dependent calpains and finally (4) SARM1 pathway, where VCR and axotomy activates *SARM1* and DLK/MAPK signaling, leading to activation of calpains, the ultimate convergence point for executing axon degeneration (Fukuda et al., 2017). Therefore, alterations in any of these points where VCR could act might consequently modify the way in which VCR produces the axonal degeneration and neurotoxicity.
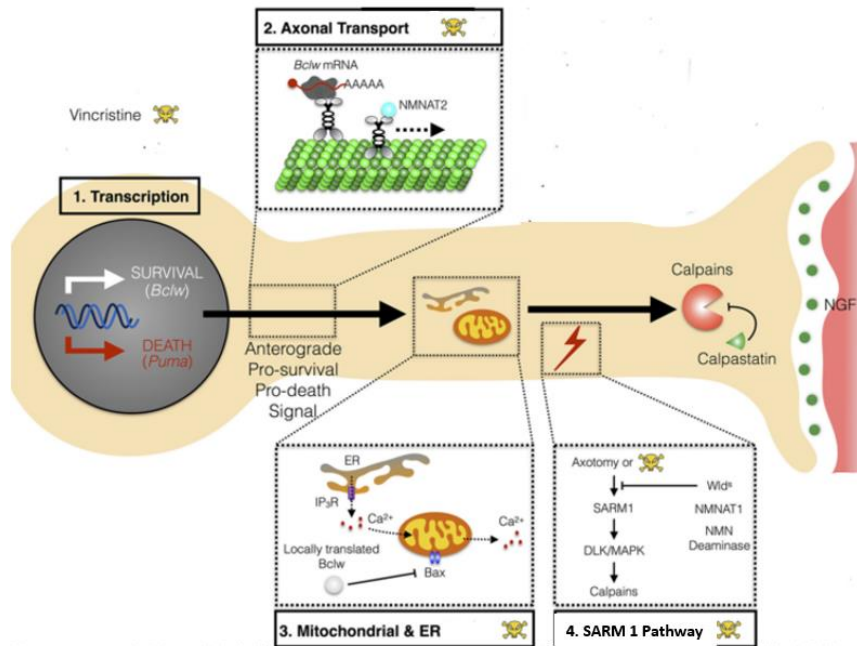
Abbreviations: ER, endoplasmic reticulum; **IP3R**, inositol 1,4,5-triphosphate receptor; **BAX**, Bcl-2-like protein 4; **SARM1**, sterile α-motif-containing and armadillo-motif-containing protein; **DLK**, dual leucine zipper kinase; **MAPK**, mitogen-activated protein kinase; **Wlds**, Wallerian degeneration slow; **NMN**, nicotinamide mononucleotide; **CIPN**, chemotherapy-induced peripheral neuropathy.

Figure 6. Mechanisms of axon degeneration proposed for VCR. Axon degeneration is determined by factors that can either enhance death and/or inhibit survival pathways.

Source: adapted from Fukuda et al. 2017 (Fukuda et al., 2017).

Currently it does not exist any treatment to prevent the neurotoxicity and if the toxicity is established the only action to be taken is the VCR discontinuation until recovery, dose reduction or interval prolongation (Argyriou et al., 2012; Ceppi et al., 2014), which could in turn, reduce survival (Carozzi et al., 2015; Ceppi et al., 2014; Postma et al., 1993). Therefore, one of the challenges in medicine is to predict which patients are going to develop VCR-related neurotoxicity in order to adjust the treatment in advance.

3.2. Hepatic toxicity

One of the most common drug-related toxicities in childhood ALL patients is hepatotoxicity (Y Liu et al. 2017), which is partly defined as an elevation of serum aminotransferases (alanine aminotransferase (ALT) or aspartate aminotransferase (AST)) and bilirubin (BI) levels. This elevation is caused by alterations in hepatic cells membrane or cell death (Navarro and Senior, 2006) that are induced by different mechanisms (Figure 7): (1) disruption of intracellular calcium homeostasis, which produces the disassembly of actin fibrils at cell surface, and then, cell lysis; (2) generation of enzyme-drug adducts, whose products lead to enzymes dysfunction, loss of ionic gradients, decrease in ATP levels and, therefore, cell death; (3) formation of antibodies and

cytokines recruitment, which causes inflammation due to the migration of adducts to cell surface, (4) cell apoptosis due to immune response or cell damage; and (5) mitochondria alterations, such as disruptions of fatty acid β-oxidation (Lee, 2003).
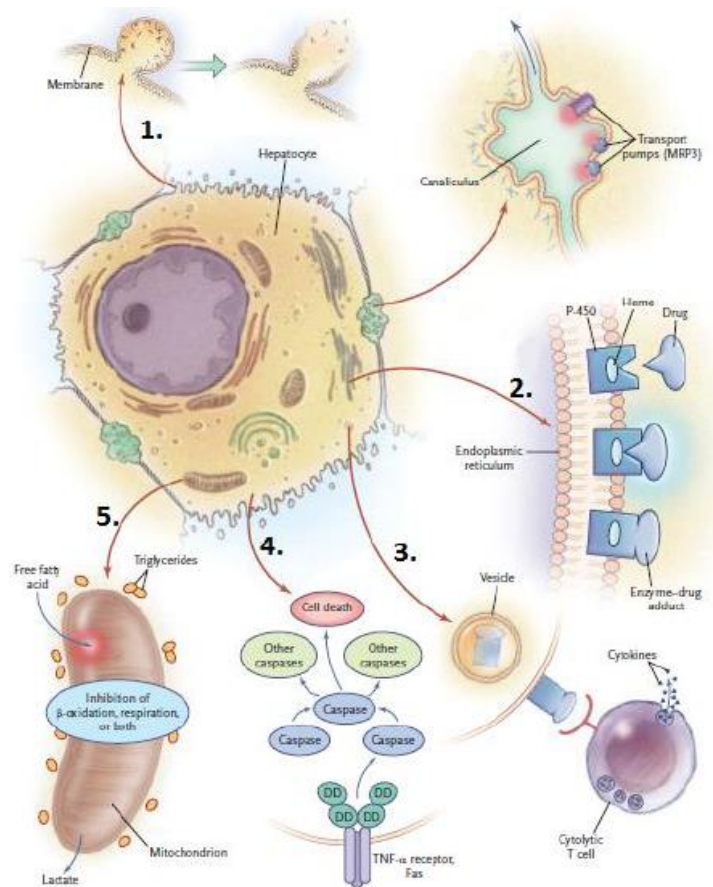
Figure 7. Proposed hepatic toxicity mechanisms.
Source: Adapted from Lee 2013 (Lee, 2003).

Approximately 66.5% of childhood ALL patients show liver toxicity at some point during ALL treatment (Ladas et al. 2010). The point in which hepatotoxicity is developed could depend on the drug administered (Iorga, Dara, and Kaplowitz 2017). In fact, in the induction phase, Liu and colleagues linked hepatotoxicity to ASP exposure whereas on the other hand, during consolidation phase, high-dose MTX is well-known to cause liver toxicity (Y Liu et al. 2017).

ASP is an enzyme that metabolizes extracellular asparagines into aspartic acid. Its antileukemic effect is based on the relative inability of leukemic cells to synthesize asparagine, as opposed to normal cells. The depletion of asparagines diminishes protein synthesis, leading to leukemic cell death (Ho et al., 1970; Onuma et al., 1971). In this case, the hepatotoxicity mechanism is unknown, nevertheless, it has been suggested that it might be similar to the mechanism that causes hepatic steatosis (Liu et al., 2017), caused by the accumulation of fatty acids in liver microvesicles secondary to the interruption of fatty acid oxidation in the mitochondria.

Introduction

Moreover, this interruption results in an increase reactive oxygen species (ROS). Therefore, mitochondria alteration, increased ROS concentration and the accumulation of fatty acid microvesicles in the liver lead to cell apoptosis (Liu et al., 2016), which result in an increase hepatic enzyme levels and therefore, hepatotoxicity.

Regarding MTX, a key component for most ALL treatment protocols, is a folate analogue that once inside the cell, is metabolized into MTX polyglutamates (MTXPGs). Both MTX and MTXPGs inhibit DHFR, responsible for the convertion of dihydrofolates to active tetrahydrofolates, causing depletion of intracellular tetrahydrofolate. On the other hand, MTXPGs target other folate-dependent enzymes such as TYMS, leading to nucleic acid and protein synthesis inhibition and consequent cell death, particularly in rapidly dividing cells (Krajinovic and Moghrabi, 2004). Finally, the role of membrane transporter proteins is essential for MTX elimination from the cell and from the organism through bile and urine efflux (Mikkelsen et al., 2011). These proteins include ATP-binding cassette transporters, such as ABCB1 (Swerts et al., 2006), and organic anion transporters, such as SLCO1B1 (Abe et al., 2001; Trevino et al., 2009) (Figure 8). In this case, the urderlying toxicity route seems to be directly related to its mechanism of action, i.e. inhibition of nucleic acid and protein synthesis and the generation of DNA strand breaks that can trigger cell apoptosis (Celtikci et al., 2009) (Figure 8). In addition, other mechanisms for MTX-induced hepatic toxicity have been proposed, such as a reduction of hepatic folate repositories, the accumulation of toxic polyglutamates (Dávila-Fajardo et al., 2013) or an increase in homocysteine concentration in which MTHR and MTR enzymes activity will play an important role (Celtikci et al., 2009) (Figure 8).

Hepatic level toxicity could lead to treatment interruptions or dose reductions which influence negatively in survival. For this reason the prediction of the patients in risk of suffering hepatic toxicity in each treatment phase and insight into de underlying responsible drugs is challenging in order to adjust the treatment before drug administration.
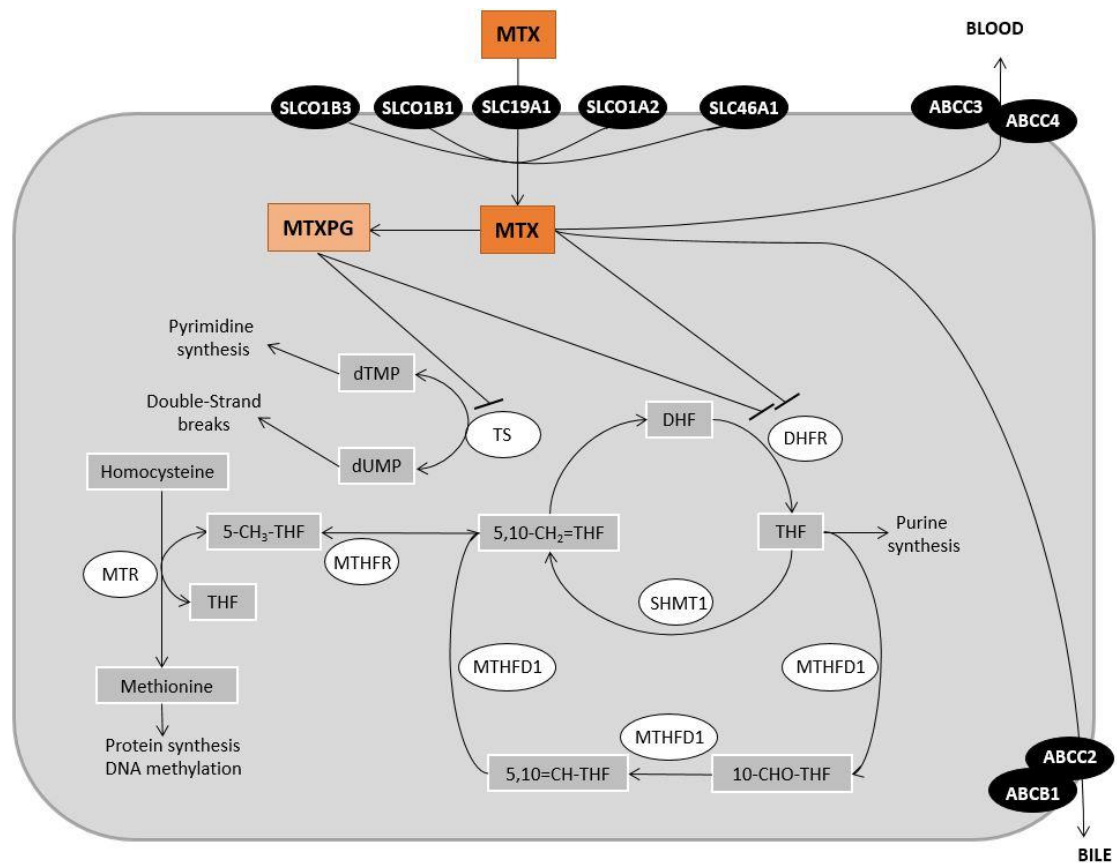
Figure 8. MTX PK/PD pathways.

3.3. Gastrointestinal toxicity

Similarly of importance are the adverse drug events related to the gastrointestinal tract, such as mucositis, diarrhea or vomits. Mucositis is one of the most debilitating and frequent acute side effect of antileukemic chemotherapy in childhood ALL (Sangild et al. 2017; Schmiegelow et al. 2017). This toxicity is characterized by the breakdown of the mucosal barrier, which in mild forms, is presented as mucosal erythema and in most advanced clinical form as deep and painful ulcerative lesions of the oral cavity and gastrointestinal tract (Sonis 2004c, 2004b, 2004a; Van Sebille et al. 2015). As a consequence, children suffer from abdominal pain, vomits and diarrhea, which result in weight loss, need for nutritional support and an increased risk of infections (Kuiken et al. 2017).

The mucosal lesion results from the cumulative impact of a number of biological pathways that originate in the submucosa and ultimately target the oral epithelium. Figure 9 depicts the proposed pathophysiologic five-stage process from initiation to healing (Sonis, 2007).

Introduction
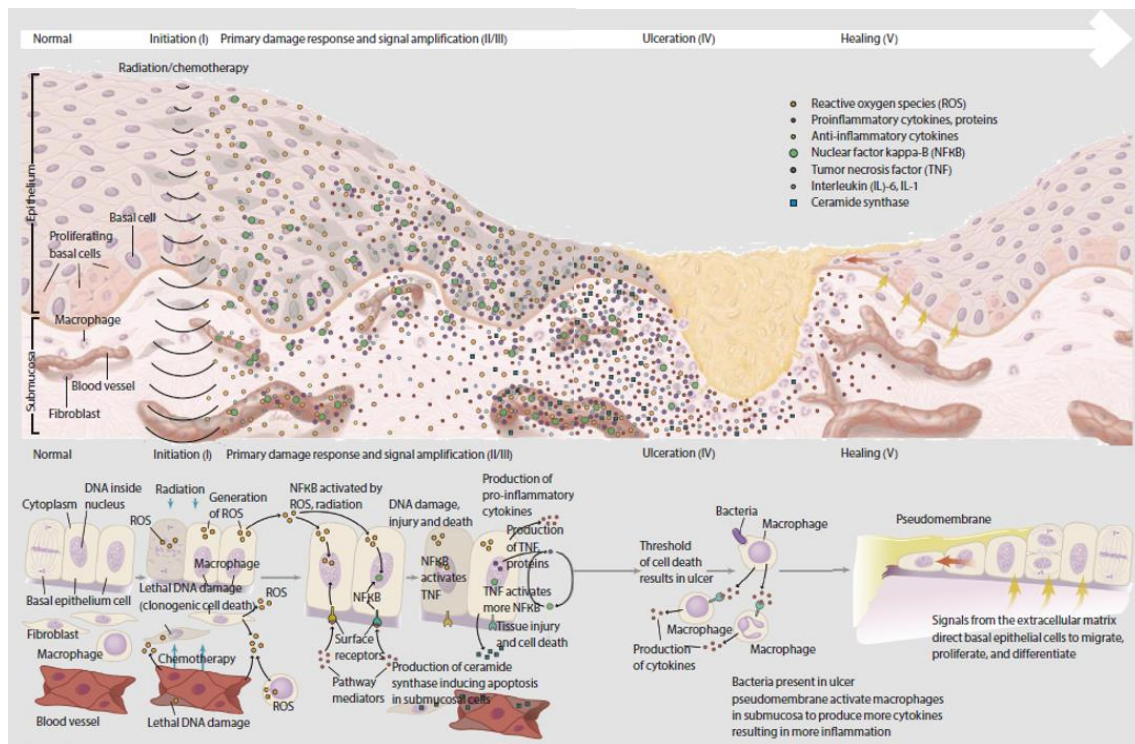
Figure 9. Mucositis pathogenesis in five phase process: initiation, primary damage response (messaging and signaling), amplification, ulceration and healing (Sonis, 2007).

During initiation phase chemotherapy induces basal epithelial cells death and the damaged tissue generates reactive oxygen species (ROS) and releases endogenous damage-associated pattern molecules (DAMPs), which then bind to specific receptors. Chemotherapy by itself or ROS and DAMPs initiate a series of cascading biological events, including the activation of a number of transcription factors, such as nuclear factor Kappa-B (NF-κB) giving way to primary damage response. As a result of NF-κB activation, genes associated with the production of proinflammatory cytokines and cytokine modulators, stress responders (eg, COX-2, inducible NO-synthase, superoxide dismutase), and cell adhesion molecules, may be expressed, which have demonstrated activity in the pathogenesis of mucositis. Other pathways have also been identified as playing significant roles in regimen-related mucosal injuries. Among the most significant are those associated with nitrogen metabolism, Toll-like receptor signaling, B-cell-receptor signaling, P13K/AKT signaling and mitogen-activated protein kinase (MAPK) signaling, to name a few. During amplification phase, the mediators provoke a series of positive feedback loops that serve to amplify and prolong tissue injury through their effects on transcription factors. Consequently, gene up-regulation occurs with resultant increases in injurious cytokine production.

Mucositis can be linked to several antileukemic agents such as MTX, previously mentioned, CPA or DNR (Cinausero et al. 2017; Schmiegelow et al. 2017). CPA is an antineoplasic in the class of

alkylating agents which has the ability to add alkyl groups to many electronegative groups under conditions present in cells (Baxter Oncology GmbH, 2017). They stop tumor growth by cross-linking guanine bases in DNA double-helix strands. This makes the strands unable to uncoil and separate. As this is necessary in DNA replication, the cells can no longer divide. Metabolism and activation occurs at the liver. 75% of the drug is activated by CYPs isoforms, and then is eliminated primarily in the form of metabolites (Figure 10).

DNR is an antineoplasic in the anthracycline class. General properties of drugs in this class include: interaction with DNA in a variety of different ways including intercalation, DNA strand breakage and inhibition with the enzyme topoisomerase II. DNR may also inhibit polymerase activity, affect regulation of gene expression, and produce free radical damage to DNA. Several transporters have been shown to be involved in its transport (Figure 11).

The gastrointestinal manifestations may cause treatment delays, unplanned interruptions or even premature discontinuation of therapy (Cinausero et al. 2017), which in turn may result in impaired survival. Therefore, it would be of great interest to predict which patients are going to suffer from mucositis in order to prevent its development.
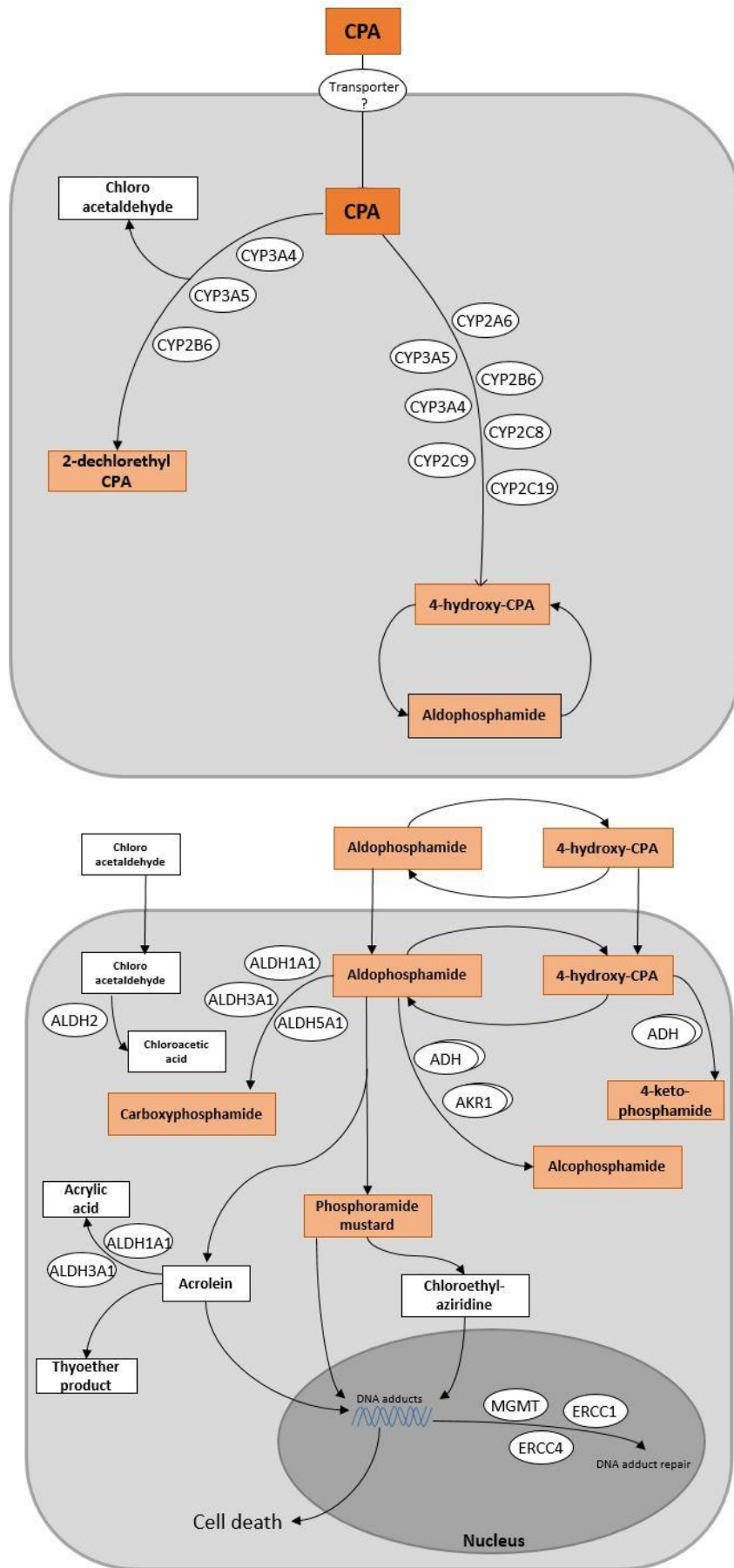
Introduction

Figure 10. CPA PK/PD pathways.
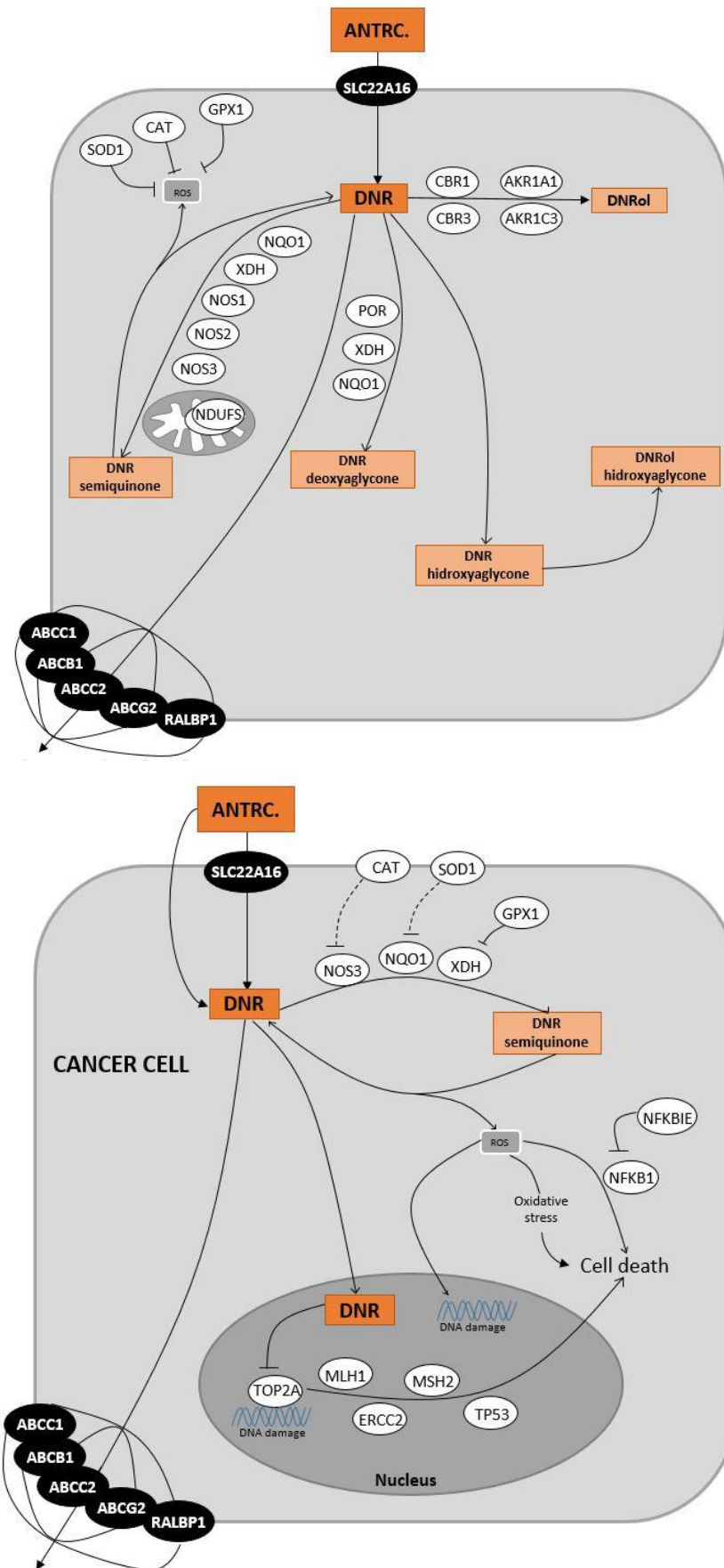
Figure 11. Anthracyclines PK/PD pathways.

3.4. MTX plasmatic levels

MTX is the backbone in ALL therapy but it has a very narrow therapeutic range, i.e. it has little difference between toxic and therapeutic concentrations and thereby, at high doses it easily causes toxicity and it has been shown that the frequency of global toxicity in patients with plasmatic concentrations above 0.2 μM was significantly higher than in patients with lower concentrations, the same for the frequency of renal toxicity or vomiting (Lopez-Lopez et al., 2011). MTX toxicities depend on the reached drug concentrations, but also the time it is acting, so MTX correct elimination has to be assured. For this reason, during high dose MTX therapy plasmatic levels are monitored tightly from 2 h after infusion end and until the levels are under 0.2 μmol/l. ADME process proteins, and particularly MTX transporters (Figure 12) play an important role in drug elimination and thus in the MTX plasmatic concentrations.
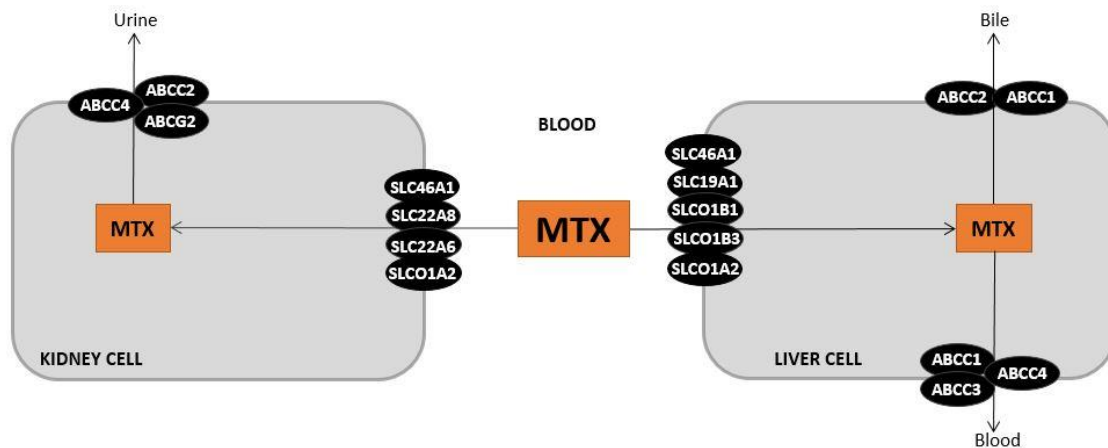
Figure 12. MTX tranporters in kidney and liver cell.

In the same way, as for the rest of the toxicities, is of great interest to predict which patients will present high plasmatic levels due to a less efficient MTX elimination, to adjust the treatment from the beginning and avoid the toxicities it carries.

To summarize, children that undergo ALL therapy will suffer toxicities that vary from mild to more severe adverse events that will be recoverable in most of the cases but that occasionally could also leave long term damages. In this regard, pharmacogenetic studies offer a great tool to better adjust childhood ALL therapy and therefore reduce adverse evets (Ansari and Krajinovic, 2007).

4. PHARMACOGENETICS IN ALL

Pharmacogenetics is a tool that aims to predict which drugs will be the most effective and safe for a patient based on individual genetic features (Shomron 2010; Rukov and Shomron 2011). Germline genetic variations such as insertions and deletions (gain/loss of a short sequence fragment), structural variations (gain/loss of a large sequence fragment, e.g. copy number variation) or single nucleotide polymorphisms (SNP) are important determinants of the interpatient variability in ALL therapy toxicities.

Most of the studies on pharmacogenomics research focused on the role of SNPs, the simplest form of DNA variation. SNPs are single base substitutions of one nucleotide by another, observed in the general population at a frequency greater than 1% (Figure 13). SNPs occur throughout the genome at a frequency of about one in 200-300 base pairs (bp). Recent large-scale studies have identified approximately 15 million SNPs in the human genome (1000 Genomes Project Consortium et al., 2010) which can be found across genes as well as in non-genic regions and being possible to affect gene function, including drug PK/PD genes. The presence of these SNPs could explain why the toxicity profile or the severity grade exhibit by patients is different in spite of undergoing the same treatment protocol.
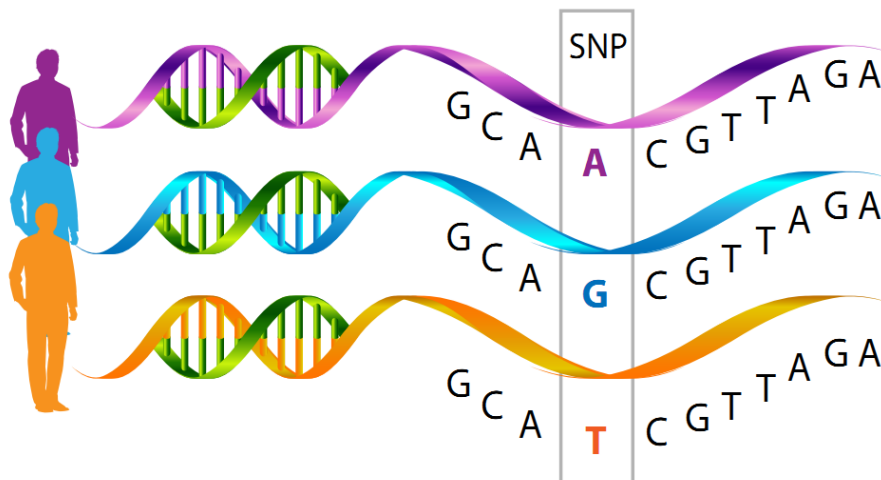
Figure 13. SNP schematic image, showing the A/G/T allele for a locus in three individuals.
Source: https://www.whatisdna.net/wiki/single-nucleotide-polymorphisms/

In this context, great research effort has been invested, both by candidate gene strategy and genome wide association studies (GWAS).

The candidate gene strategy examines those genes suspected in the pathophysiologic pathways of toxicity, based on what is already known about the drug transport, metabolism, or mechanism of action/toxicity. In the last years, high-throughput genotyping technology has allowed the

Introduction

screening of genetic variation across the entire genome, so called GWAS. The GWAS approach involves scanning the entire genome in order to identify germline variants that differ in prevalence between the affected and non-affected population, giving arise to interesting novel causative pathways as no hypothesis are generated prior to the study (Maxwell and Cole, 2017; Moriyama et al., 2015).

4.1. ALL pharmacogenetics

In childhood ALL therapy numerous studies have been carried out in the field of pharmacogenetics, discovering variants mainly in genes involved in drug PK and PD pathways that can explain some of the risk to develop the drug-specific adverse effects in ALL.

Regarding the neurotoxicity induced by VCR, one of the most interesting results was found by Diouf et al., in a GWAS performed in a large group of pediatric patients with ALL (Diouf et al., 2015). This study showed association between peripheral neuropathy in later phases of treatment and the SNP rs924607 in the promoter region of *CEP72*, a gene involved in the PD pathway. Other SNPs in *ABCC2*, *ABCB1* or *CYP3A5*, all of them of the PK pathway, have been found associated with neurotoxicity (Ceppi et al., 2014; Egbelakin et al., 2011; Lopez-Lopez et al., 2016; Plasschaert et al., 2004). Some of these SNPs could change the expression regulation or are located in intronic regions and therefore any other change that affect drug PK/PD genes could be implicated in neurotoxicity.

Concerning hepatotoxicity, several polymorphisms have been identified in association with plasmatic transaminases elevation. A noteworthy example is the SNP rs738409 in *PNPLA3,* found in a GWAS strongly associated with hepatotoxicity in children with ALL during the induction (Liu et al., 2017), result that has been replicated recently by our group (Gutierrez-Camino et al., 2017a). During consolidation phase, other significant polymorphisms have been found in MTX PK/PD genes, e.g. *RFC1* (80G>A) (Gregers et al., 2010), *ABCB1* (3435C>T) (Gregers et al., 2015a) and *MTHFR* (677C>T and 1298A>C) (Umerez et al., 2017), with no clear markers for hepatic toxicity. Regarding hepatotoxicity measured as an elevation of bilirubin, to the best of our knowledge no studies have been performed. Until now few reliable variants have been found in association with hepatic toxicity, therefore more studies are required.

When we consider gastrointestinal toxicity, we have come across with studies that identify associations between mucositis and polymorphism in MTX pathway genes during consolidation phase. Most of these polymorphisms are located in genes involved in MTX PK pathway, such as *ABCB1*, *ABCC1*, *ABCC2* or *ABCC4* (Bektaş-Kayhan et al., 2012; Liu et al., 2014a; Lopez-Lopez et

al., 2013). However, this toxicity is poorly analyzed during other treatment phases in which additional mucotoxic drugs such as DNR and CPA are administered.

Regarding MTX plasma levels, in the past few years, a large number of studies have analyzed the relationship between genetic polymorphism and MTX clearance. Some of the most interesting results have been found in MTX transporters. The most convincing results up to present have been found for *SLCO1B1* transporter. Two SNPs in this transporter, rs4149081 and rs11045879, were identified in association with MTX clearance for the first time by Treviño et al. in a GWAS performed in children with ALL (Trevino et al. 2009). After that first report, these variants and others in *SLCO1B1* have been confirmed in subsequent studies (Lopez-Lopez et al. 2011; Ramsey et al. 2013; Radtke et al. 2013; Lopez-Lopez et al. 2013; Ramsey et al. 2012). As a result of these studies, other works have focused their interest on the analysis of variants in MTX transporters, finding several SNPs in genes such as *SLC19A1*, *ABCC2*, or *ABCC4* also associated with MTX levels (Lopez-Lopez et al. 2013; Laverdiere et al. 2002). Interestingly, rs9516519 in *ABCC4*, a SNP that is located in a putative microRNA (miRNA) binding site has been associated with MTX plasmatic levels (Lopez-Lopez et al., 2013) suggesting that variants in miRNA could also explain MTX plasmatic level disturbances.

All these results, suggest that interference mechanisms mediated by noncoding RNA molecules such as miRNAs might contribute to toxicity development as they could regulate drug PK/PD genes expression (Lopomo and Coppedè, 2017).

4.2. MicroRNAs

MiRNAs comprise a large family of 18-22 nucleotide-long single strand RNAs that have emerged as key regulators of gene expression at a post-transcriptional level, inducing gene silencing. MiRNAs are transcribed from different locations in the genome by RNA polymerase II into long primary transcripts called pri-miRNAs (dsDNA, 300-5000 bp). The pri-miRNAs are characterized by a central region of double-stranded RNA (dsRNA) of about 30-40 nucleotides, a terminal loop and two single stranded RNA (ssRNA) opposite among each other. These pri-miRNAs are processed in the nucleus by the complex formed by DROSHA RNase and DGCR8 containing dsRNA binding domains. DsRNA sequence determines its secondary structure and its capacity to bind with processing proteins.

After processing of pri-miRNAs, these smaller molecules (about 70 nucleotides) are known as pre-miRNAs. The pre-miRNAs are exported from the nucleus to the cytoplasm through Exportine5 (XPO5) and RAN GTPase (Bohnsack et al., 2004; Kim, 2004) protein. In the cytoplasm,

the pre-miRNAs are processed by Dicer (Hutvágner et al., 2001; Merritt et al., 2010) and TARBP2 enzyme, which eliminate the loop, generating a dsRNA molecule known as miRNA duplex (Song et al., 2003). The miRNA duplex is separated to form the mature miRNA as a single strand. The selected strand of the miRNA duplex is incorporated into multiprotein complex known as RISC (RNA-inducing silencing complex), composed of the EIF2C1 (AGO1), EIF2C2 (AGO2), SND1, GEMIN3, GEMIN4 and CCR-NOT complex genes (Inada and Makino, 2014). The mature miRNA is transported by the RISC complex to messenger RNAs (mRNAs), target of the regulation (Li et al., 2014). The miRNA binds to the complementary bases in the 3´ UTR region of the mRNA (Figure 14).
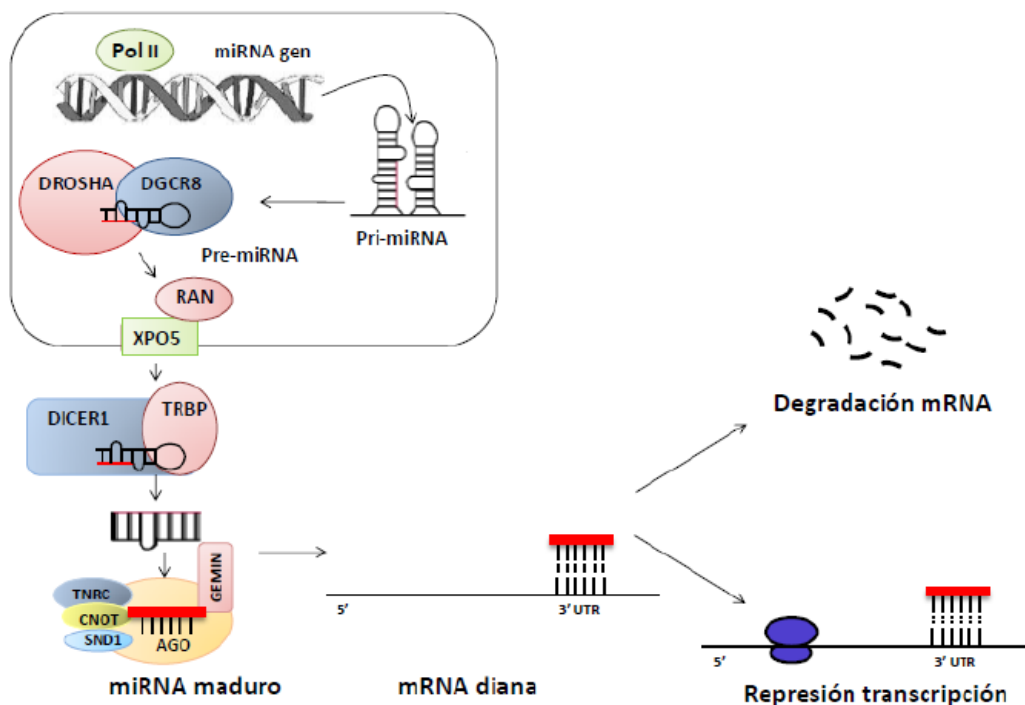
Figure 14. MiRNA biogenesis and mechanism of action.
Source: Adapted from Ryan et al 2010 (Ryan, Robles, and Harris 2010).

MiRNAs have a characteristic sequence for target recognition of approximately 7 bp, known as seed region. The miRNA acts by specific binding of the seed sequence to a complementary target sequence. The regulation mechanism depends on the degree of miRNA-mRNA complementarity: direct cleavage and degradation of the mRNA, when the complementarity is perfect; protein translation blocking/inhibition in the case of imperfect base pairing (Gregory et al., 2006).

Since the sequence complementary to a miRNA seed is short, a miRNA may degrade or repress translation of many target mRNAs containing complementary sequences to the seed region. But

there is also the possibility that a gene can be regulated by multiple miRNAs. MiRNAs sharing all or part of the nucleotide sequence of the seed region can be grouped into families. Members of the same family of miRNAs are potential regulators of the same set of mRNAs (Friedman et al., 2008; Lewis et al., 2005). For each miRNA, there are many putative targets predicted by different databases, however, nowadays miRNA targets are not completely defined and few interactions are validated experimentally.

MiRNA mediated gene regulation can be affected by both, changes in the levels of miRNAs (upregulation or downregulation) or changes in the seed sequence (binding capacity modification). Therefore, SNPs in pre-miRNAs (miR-SNP) which determine the miRNAs secondary structure, may affect their stability or processing efficiency, affecting their own levels and SNPs in the seed region, the sequence that determines the miRNA binding, could affect the accurate recognition of its targets (Figure 15) (Ryan et al., 2010).
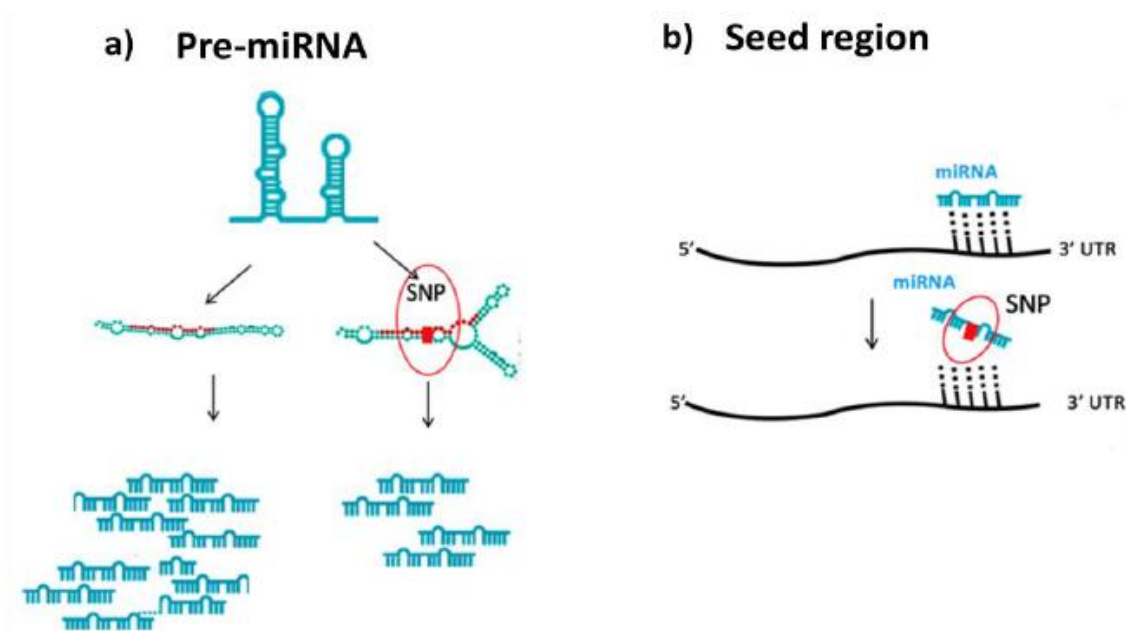
Figure 15. SNPs in miRNA effect in: a) Pre-miRNA: miRNA levels upregulation or downregulation due to secondary structure modification or miRNA processing alteration; b) Seed region: miRNA-mRNA complementarity affectation or lose.

Through this mechanism of regulation, miRNAs could regulate more than 50 % of human genes, including genes involved in pharmacokinetic and pharmacodynamics (PK/PD) pathways of drugs (Li et al., 2016; Nakajima and Yokoi, 2011). Consequently SNPs in miRNAs could alter drugs PK/PD genes and could explain the susceptibility of some patients to develop drug toxicity.

Introduction

4.3. MiR Pharmacogenetics

The principle of the involvement of miRNAs in drug response entails that increased miRNA expression down-regulates genes encoding proteins that promote drug efficacy. Conversely, lowered miRNA levels may result in up-regulated genes with products that inhibit drug function (Rukov et al., 2014)].

In fact, interactions between miRNAs, target gene expression and drug response have been already shown. For instance, overexpression of miR-21 inhibited *PDCD4* expression and prevented apoptosis in cells under arsenic trioxide treatment (Li et al., 2010). Another examples are miR-15 and miR-16, whose downregulation caused the overexpression of BCL2, and in turn, the development of multidrug resistant phenotype in cancer cells (Xia et al., 2008). Both processes (increased and lowered miRNA expression) may affect drug function and therefore make miRNAs potent regulators of drug efficacy (Rukov et al., 2014). Given this important role of miRNAs, studies analyzing changes in miRNA function are acquiring relevance in pharmacogenomics.

Concerning SNPs in miRNAs, several examples of SNPs linked to chemotherapeutic agents induced toxicities can be found in the literature. Such an example could be the association of hsa-miR-196a2 rs11614913 polymorphism with severe overall toxicity in advanced non-small cell lung cancer patients treated with platinum-based chemotherapy (Zhan et al., 2012). As other example, rs895819 in miR-27a has been pointed out as a clinically useful marker to identify patients in risk of severe fluoropyrimidines toxicity when combined with the determination of dihydropyrimidine dehydrogenase gene variants (Meulendijks et al., 2016). Rs895819 G variant allele was associated with increased miR-27a levels and reduced fluoropyrimidines metabolizing dihydropyrimidine dehydrogenase expression, which as a result would prolonged the half-life of administered fluoropyrimidines and in turn increase the susceptibility to severe toxicity (Amstutz et al., 2015).

With regard to childhood B-ALL, there is a previous study performed by our group in which 46 SNPs in 42 pre-miRNAs were analyzed in an attempt to establish treatment toxicity markers. This study identified several SNPs in association to different ALL treatment toxicities. For instance, rs56103835 in miR-453 (also known as miR-323b) was found to be significantly associated with MTX plasma clearance (Lopez-Lopez et al., 2014a). Interestingly, this miRNA has as putative target gene *ABCC4*, which is involved in MTX transport. Additionally, we also found that

rs2114358 in miR-1206 was associated with MTX-induced mucositis during consolidation phase (Gutierrez-Camino et al., 2017b).

Given the fact that since the aforementioned study (only 46 miR-SNPs studied) the number of annotated miRNAs has increased substantially up to 2500 (Kozomara and Griffiths-Jones, 2014) and that nowadays miRNA targets are not completely defined and any miRNA could be involved in the regulation of genes involved in drug response, it is of great interest to determine whether any of the currently described variants in miRNAs are associated with the susceptibility to develop toxicities during childhood ALL therapy.

HYPOTHESIS AND OBJECTIVES

5. HYPOTHESIS

Childhood ALL survival rates have increased due in part to intensive therapy, however the toxicities provoked by this treatment have often a negative impact on survival rates.

Pharmacogenomic studies have already identified variants that could affect drug PK/PD genes as markers to predict toxicity development in childhood ALL. Nowadays it is known that miRNAs can affect the expression of drug PK/PD pathway genes and preliminary studies have already suggested that miRNA genetic variants affecting their levels or function can alter PK/PD pathway genes.

Therefore, in this work we propose that variants in miRNAs that could target genes of PK/PD genes, as well as other toxicity-related genes might be involved in the risk to develop the toxicities that appear during childhood B-ALL therapy and can be used as toxicity markers.

6. OBJECTIVES

The main goal of the present study was to determine if miRNA genetic variants could be associated with the most common toxicities developed during childhood B-ALL therapy.

In order to achieve this goal, we analyzed the association between 213 miRNA SNPs and the most common toxicities induced by B-ALL therapy in a cohort of 179 homogeneously treated childhood ALL patients. We set the following specific objetives:

1. To determine the miRNA genetic variants associated with peripheric neurotoxicity produced by VCR during the induction phase.
2. To determine the miRNA genetic variants associated with hepatic toxicity due to ASP and MTX during induction and consolidation phase.
3. To determine the miRNA genetic variants associated with gastrointestinal toxicity in relation to DNR, CPA and MTX during induction phase.
4. To determine the miRNA genetic variants associated with elevated MTX plasmatic levels during consolidation phase.

MATERIALS AND METHODS

7. STUDY POPULATION

7.1. Patients

This study included a total of 179 pediatric patients diagnosed with a B-ALL. The samples of B-ALL patients were collected from 2000 to 2013 at the Pediatric Oncology Units of 3 Spanish reference hospitals (Cruces University Hospital, Donostia University Hospital, and La Paz University Hospital). All patients were homogeneously treated with the LAL/SHOP 94, 99 or 2015 protocols. Populatin characteristics are shown in Table 5.

Table 5. Demographic characteristics of the B-ALL patients included in the study.

No. of patients, n	179
Sex	
Females, n (%)	74 (41.34)
Males, n (%)	105 (58.66)
Mean age at diagnosis ± SD, years	5.12 ± 3.23
No. of patients per treatment protocol, n (%)	
LAL/SHOP 94, n (%)	9 (5.02)
LAL/SHOP 99, n (%)	60 (33.52)
LAL/SHOP 2005, n (%)	108 (60.34)
No data, n (%)	2 (1.12)

Abbreviations: SD, standard deviation.

The study was approved by medical ethical committee (CEISH/102R/2011) and signed informed consent was obtained from parents or guardians and patients (in case they were <12 years) according to the Declaration of Helsinki.

Demographic and clinical data were collected from patients´ medical files by two independent researchers, objectively and blinded to genotypes. For each patient the collected data included: sex and age at diagnosis; neurotoxicity signs and symptoms for all treatment phases; hepatic function data defined by highest plasma levels of transaminases (aspartate aminotransferase (AST) and alanine aminotransferase (ALT)) and bilirubin for all treatment phases; presence of digestive tube involving toxicities (nausea/vomits, mucositis and diarrhea) for all treatment phases; renal function data defined by highest serum creatinine levels for all treatment phases and administered MTX dose (3 g/m^2 or 5 g/m^2) and plasma levels at 48h, 72h and 96h during consolidation phase (Table 6).

Table 6. Evaluated toxicities and their detected frequencies per treatment phase in the studied ALL population.

	Induction Phase	Consolidation Phase	Intensification Phase	Maintenance Phase
Neurotoxicity, n (%)				
Grade 1-4	47 (26.26)	11 (6.15)	9 (5.03)	1 (0.56)
Grade 1-2	28 (15.64)	–	–	–
Grade 3-4	19 (10.61)	–	–	–
Hypertransaminasemia, n (%)				
Grade 2-4	55 (30.73)	49 (27.37)	15 (8.38)	19 (10.61)
Grade 2	25 (13.97)	28 (15.64)	–	–
Grade 3-4	29 (16.20)	19 (10.61)	–	–
No data	1 (0.56)	2 (1.12)	9 (5.03)	9 (5.03)
Hyperbilirubinemia, n (%)				
Grade 1-4	29 (16.20)	14 (7.82)	7 (3.91)	7 (3.91)
No data	9 (5.03)	11 (6.15)	9 (5.03)	9 (5.03)
Mucositis, n (%)				
Grade 2-4	36 (20.11)	16 (8.94)	15 (8.38)	0 (0.00)
No data	9 (5.03)	11 (6.15)	9 (5.03)	9 (5.03)
Diarrhea, n (%)				
Grade 2-4	22 (12.29)	10 (5.59)	12 (6.70)	0 (0.00)
No data	9 (5.03)	11 (6.15)	9 (5.03)	9 (5.03)
Nausea/Vomits, n (%)				
Grade 2-4	45 (25.14)	40 (22.35)	21 (11.73)	5 (2.79)
No data	9 (5.03)	11 (6.15)	9 (5.03)	9 (5.03)
Nephrotoxicity, n (%)				
Grade 1-4	6 (3.35)	7 (3.91)	5 (2.79)	0 (0.00)
No data	8 (4.47)	11 (6.15)	9 (5.03)	9 (5.03)
MTX dose in consolidation, n (%)*				
3 g/m^2	–	77 (43.02)	–	–
5 g/m^2	–	101 (56.42)	–	–
MTX plasma levels in consolidation, n (%)				
Total (at any moment)	–	62 (34.64)	–	–
48 h (plasma level >1 µM)	–	43 (24.02)	–	–
72 h (plasma level >0,2 µM)	–	56 (31.28)	–	–
48 h (plasma level >1 µM) and 72 h (>0.2 µM)	–	41 (22.91)	–	–
96 h (plasma level >0.2 µM)	–	33 (18.44)	–	–
Hematologic toxicity ^				
Anemia (grade ≥2)	71/75	56/71	–	–
Neutropenia (grade ≥2)	71/75	58/75	–	–
Trhombocitopenia (grade ≥2)	65/75	58/75	–	–

Notes: *, no MTX data was collected for one patient; – , not applicable or not measured;.^, hematologic data collected for 75 patients from 2 hospitals.

7.2. Toxicity evaluation

Neurotoxicity was graded according to the WHO Peripheral Nervous System toxicity criteria (Table 7); three phenotypes were considered: any grade neurotoxicity (grades 1–4), low-grade neurotoxicity (grades 1–2) and high-grade neurotoxicity (grades 3–4).

Table 7. WHO toxicity grading scale for determining the severity of adverse events for peripheral neurotoxicity.

PERIPHERAL NERVOUS SYSTEM				
PARAMETER	GRADE 1	GRADE 2	GRADE 3	GRADE 4
Neuropathy/Lower Motor Neuropathy		Mild transient paresthesia only	Persistent or progressive paresthesias, burning sensation in feet, or mild dysesthesia; no weakness; mild to moderate deep tendon reflex changes; no sensory loss	Onset of significant weakness, decrease or loss of DTRs, sensory loss in "stocking glove" distribution, radicular sensory loss, multiple cranial nerve involvement; bladder or bowel dysfunction, fasciculations, respiratory embarrassment from chest wall weakness.
Myopathy or Neuromuscular Junction Impairment	Normal or mild (<2 x ULN) CPK elevation	Mild proximal weakness and/or atrophy not affecting gross motor function. Mild myalgias, +/- mild CPK elevation (<2 x ULN)	Proximal muscle weakness and/or atrophy affecting motor function +/- CPK elevation; or severe myalgias with CPK >2 x ULN;	Onset of myasthenia- like symptoms (fatigable weakness with external, variable ophthalmoplegia and/or ptosis), or neuromuscular junction blockade (acute paralysis) symptoms

Hepatic toxicity was measured as an elevation on plasma levels of AST or ALT aminotrasferases and bilirubine. Hypertrasaminasemia was graded according to the Spanish Society of Pediatric Hematology and Oncology standards, adapted from the WHO criteria (Table 8). Hepatotoxicity was considered beginning from a hypertransaminasemia of grade 2 to 4 (>2.6*ULN) and high hepatotoxicity with a grade 3 to 4 (>5.1*ULN). Regarding hyperbilirubinemia, patients were also classified by severity grade (Table 8) which was considered from grade 1.

Table 8. LAL-SHOP protocol toxicity grading scale for determining the severity of hepatotoxicity, adapted from WHO criteria.

	Toxicity grade 1	Toxicity grade 2	Toxicity grade 3	Toxicity grade 4
AST (SGOT)	1.25 - 2.5 x ULN	2.6 - 5 x ULN	5.1 - 10 x ULN	> 10 x ULN
ALT (SGPT)	1.25 - 2.5 x ULN	2.6 - 5 x ULN	5.1 - 10 x ULN	> 10 x ULN
Hyperbilirubinemia	1.1-1.5 x ULN	1.6-2.5 x ULN	2.6-5 x ULN	>5 x ULN

Materials and Methods

Digestive toxicity was evaluated as the presence of mucositis, diarrhea or nausea/vomits during all the treatment phases, and were grade from 1 to 4 according to the WHO criteria (Table 9). We considered toxicity from grade 2 to 4.

Table 9. LAL-SHOP protocol toxicity grading scale for determining the severity of gastrointestinal toxicity, adapted from WHO criteria.

	Toxicity grade 1	**Toxicity grade 2**	**Toxicity grade 3**	**Toxicity grade 4**
Mucositis	Mild discomfort/pain, erythema	Erythema, ulcer (possibility to eat solids)	Ulcers (Only liquid diet possible)	Impossibility to eat
Diarrhea	Transient (<2 days)	Tolerable but >2 days	Intolerable, requires treatment	Hemorrhage, dehydration
Nausea/Vomits	Nausea	Transient vomits	Vomits that require treatment	Untreatable vomits

MTX levels were considered high if the plasmatic concentration was over 1 µmol/l at 48 h or over 0.2 µmol/l at 72 h or 96 h after at least one of the three doses administered during the consolidation phase. In addition, global high MTX plasma levels were considered if the MTX levels were higher than the established threshold in any of the cycles.

Nephrotoxicity was considered from grades 1 to 4 beginning from a serum creatinine level >1.26 x ULN (Table 10).

Table 10. LAL-SHOP protocol toxicity grading scale for determining the severity of nephrotoxicity, adapted from WHO criteria.

	Toxicity grade 1	**Toxicity grade 2**	**Toxicity grade 3**	**Toxicity grade 4**
Creatinine	1.26-2.5 x ULN	2.6-5 x ULN	5.1-10 x ULN	>10 x ULN

In the present study, all the toxicities mentioned in table 6 were analyzed except for nephrotoxicity, due to the low patient number that suffered from this toxicity in our study population. Moreover, we neither analyzed hematologic toxicity because during data collection period we observed that almost every patient included in the study suffered from some grade of anemia, neutropenia or thrombocitopenia (during induction phase 71 patients from the 75 total patients for which hematologic data was collected), thus we did not have two comparable groups for the realization of an association study.

8. SAMPLE PROCESSING

8.1. DNA extraction

Germline genomic DNA was extracted using the phenol-chloroform method (Sambrook, J, 2001) from remission peripheral blood isolated granulocytes or bone marrow slides (with <5 % blast cells).

8.2. DNA quantification and quality checking

DNA concentration and quality were estimated with NanoDrop® ND-1000 Spectrophotometer. The ratio of absorbance at 260 and 280 nm was used to assess the purity of DNA. A ratio of ~1.8 was generally accepted as "pure" for DNA.

9. MICRORNA GENE POLYMORPHISMS SELECTION

Since only a few SNPs in pre-miRNAs (miR-SNP) have been studied in relation to ALL therapy toxicity and taking into account that:

1. SNPs located in the *seed* region of pre-miRNAs could destabilize the miRNA-mRNA interaction or even change miRNA targets.
2. miR-SNPs could influence the processing and/or target selection (miRNA-mRNA interaction) (Slaby et al., 2012).
3. miRNAs could regulate a wide range of genes that up to present are not completely defined and therefore any miRNA may be involved in the regulation of genes that affect to the development of toxicities during ALL therapy.
4. The number of miR-SNPs with a minor allele frequency (MAF) higher than 1% described for the Caucasian population was methodologically manageable at the moment of selection.

We decided to include in the study all the SNPs in pre-miRNAs described at the moment of selection (May 2014).

For miR-SNPs search, all the miRNAs described in mirbase (www.mirbase.org) at the moment of the selection were introduced in SNIPER database (http://www.integratomics-time.com/miRNA-SNiPer/). Afterwards, MAF for each SNP was found through dbSNP (https://www.ncbi.nlm.nih.gov/snp/). All the known miR-SNPs at the moment of the selection with a MAF higher than 1 % (MAF≥0.01) in European/Caucasoid populations were selected, a total of 213 SNPs in 206 miRNAs (Table 11).

Materials and Methods

Table 11. Selection of polymorphisms in pre-miRNAs.

	Gene	SNP	Allele	Chromosome	Location
1	hsa-mir-449b	rs10061133	A>G	5	54466544
2	mir-1302-4	rs10173558	T>C	2	208133995
3	hsa-mir-5196	rs10406069	G>A	19	35836530
4	hsa-mir-4745	rs10422347	C>T	19	804959
5	hsa-mir-548ae-2	rs10461441	T>T	5	57825920
6	hsa-mir-2053	rs10505168	A>G	8	113655752
7	hsa-mir-4700	rs1055070	T>G	12	121161048
8	hsa-mir-943	rs1077020	T>T	4	1988193
9	hsa-mir-6074	rs10878362	T>T	12	66417493
10	hsa-mir-544b	rs10934682	T>G	3	124451312
11	hsa-mir-603	rs11014002	T>T	10	24564653
12	hsa-mir-1343	rs11032942	T>T	11	34963459
13	mir-624	rs11156654	T>A	14	31483955
14	hsa-mir-5579	rs11237828	T>T	11	79133220
15	hsa-mir-1265	rs11259096	T>C	10	14478618
16	hsa-mir-196a-2	rs11614913	C>T	12	54385599
17	hsa-mir-548at	rs11651671	T>T	17	40646803
18	hsa-mir-5092	rs11713052	C>G	3	124870376
19	hsa-mir-4792	rs11714172	T>G	3	24562877
20	hsa-mir-3192	rs11907020	T>C	20	18451325
21	hsa-mir-4653	rs11983381	A>G	7	100802786
22	hsa-mir-548a-1	rs12197631	T>T	6	18572056
23	hsa-mir-202	rs12355840	T>C	10	135061112
24	hsa-mir-3117	rs12402181	G>A	1	67094171
25	hsa-mir-1269b	rs12451747	T>T	17	12820632
26	hsa-mir-4744	rs12456845	T>C	18	46576058
27	hsa-mir-4433	rs12473206	T>T	2	64567916
28	hsa-mir-4274	rs12512664	A>G	4	7461769
29	hsa-mir-4277	rs12523324	T>T	5	1708983
30	hsa-mir-4293	rs12780876	T>A	10	14425204
31	hsa-mir-612	rs12803915	G>A	11	65211979
32	hsa-mir-4309	rs12879262	G>C	14	103006047
33	hsa-mir-300	rs12894467	C>T	14	101507727
34	hsa-mir-1294	rs13186787	T>T	5	153726769
35	hsa-mir-3152	rs13299349	G>A	9	18573360
36	hsa-mir-548ac	rs1414273	T>T	1	117102649
37	hsa-mir-3175	rs1439619	A>C	15	93447631
38	hsa-mir-5007	rs1572687	C>T	13	55748673
39	hsa-mir-3612	rs1683709	C>T	12	128778703
40	hsa-mir-5700	rs17022749	T>T	12	94955603
41	hsa-mir-2110	rs17091403	C>T	10	115933905
42	hsa-mir-4422	rs17111728	T>C	1	55691384
43	mir-1908	rs174561	T>C	11	61582708
44	hsa-mir-3143	rs17737028	A>G	6	27115467
45	hsa-mir-633	rs17759989	A>G	17	61021611
46	hsa-mir-3652	rs17797090	G>A	12	104324266
47	hsa-mir-4733	rs17885221	C>T	17	29421443
48	hsa-mir-5197	rs2042253	A>G	5	143059433
49	hsa-mir-605	rs2043556	A>G	10	53059406
50	hsa-mir-4511	rs2060455	T>T	15	66011630
51	hsa-mir-3620	rs2070960	C>T	1	228284991
52	hsa-mir-1206	rs2114358	T>C	8	129021179
53	hsa-mir-4494	rs215383	G>A	12	47758032
54	hsa-mir-3130-1	rs2241347	T>T	2	207647981
55	hsa-mir-4707	rs2273626	C>A	14	23426182
56	hsa-mir-492	rs2289030	C>G	12	95228286
57	hsa-mir-1229	rs2291418	C>T	5	179225324
58	hsa-mir-564	rs2292181	G>C	3	44903434
59	hsa-mir-149	rs2292832	T>T	2	241395503
60	hsa-mir-604	rs2368392	C>T	10	29834003

Table 11. Selection of polymorphisms in pre-miRNAs (Continuation).

	Gene	SNP	Allele	Chromosome	Location
61	hsa-mir-4432	rs243080	C>T	2	60614572
62	hsa-mir-4636	rs257095	A>G	5	9053945
63	hsa-mir-1208	rs2648841	C>A	8	129162433
64	hsa-mir-3183	rs2663345	T>T	17	925764
65	hsa-mir-4804	rs266435	C>G	5	72174432
66	hsa-mir-6128	rs2682818	C>A	12	81329536
67	hsa-mir-4308	rs28477407	C>T	14	55344901
68	hsa-mir-378d-1	rs28645567	G>A	4	5925054
69	hsa-mir-4472-1	rs28655823	G>C	8	143257760
70	hsa-mir-1255a	rs28664200	T>C	4	102251501
71	hsa-mir-146a	rs2910164	G>C	5	159912418
72	hsa-mir-5695	rs2967897	G>G	19	13031210
73	hsa-mir-4803	rs3112399	T>A	5	71465361
74	hsa-mir-577	rs34115976	C>G	4	115577997
75	hsa-mir-4669	rs35196866	T>T	9	137271318
76	hsa-mir-2278	rs356125	G>A	9	97572244
77	hsa-mir-5189	rs35613341	C>G	16	88535407
78	hsa-mir-6076	rs35650931	G>C	14	50433227
79	hsa-mir-449c	rs35770269	A>T	5	54468124
80	hsa-mir-3166	rs35854553	A>T	11	87909673
81	hsa-mir-3936	rs367805	G>A	5	131701279
82	hsa-mir-6499	rs3734050	C>T	5	150901699
83	hsa-mir-499a	rs3746444	T>C	20	33578251
84	hsa-mir-5090	rs3823658	G>A	7	102106201
85	hsa-mir-4751	rs4112253	C>G	19	54786022
86	hsa-mir-96	rs41274239	A>G	7	129414574
87	hsa-mir-187	rs41274312	G>A	18	33484792
88	hsa-mir-154	rs41286570	G>G	14	10152612
89	hsa-mir-216a	rs41291179	A>T	2	56216090
90	hsa-mir-122	rs41292412	C>T	18	56118358
91	hsa-mir-3135b	rs4285314	T>T	6	32717702
92	hsa-mir-548ap	rs4414449	T>C	15	86368898
93	hsa-mir-6084	rs45530340	C>C	1	20960230
94	hsa-mir-548ap	rs4577031	A>T	15	86368959
95	hsa-mir-4268	rs4674470	T>C	2	220771223
96	hsa-mir-941-1	rs4809383	C>T	20	62550780
97	hsa-mir-548j	rs4822739	C>G	22	26951185
98	hsa-mir-5680	rs487571	T>T	8	103137693
99	hsa-mir-595	rs4909237	C>T	7	158325503
100	hsa-mir-608	rs4919510	C>G	10	102734778
101	hsa-mir-548al	rs515924	A>G	11	74110353
102	hsa-mir-3671	rs521188	A>G	1	65523519
103	hsa-mir-4424	rs56088671	T>T	1	178646884
104	hsa-mir-323b	rs56103835	T>C	14	101522556
105	hsa-mir-548aw	rs56195815	T>T	9	135821099
106	hsa-mir-5189	rs56292801	G>A	16	88535341
107	hsa-mir-1283-1	rs57111412	T>T	19	54191743
108	hsa-mir-559	rs58450758	T>T	2	47604866
109	hsa-mir-656	rs58834075	C>T	14	101533093
110	hsa-mir-888	rs5965660	T>G	X	145076302
111	hsa-mir-3928	rs5997893	G>A	22	31556103
112	hsa-mir-4762	rs60308683	T>T	22	46156446
113	hsa-mir-4326	rs6062431	G>C	20	61918164
114	hsa-mir-4467	rs60871950	G>A	7	102111936
115	hsa-mir-596	rs61388742	T>C	8	1765425
116	hsa-mir-3922	rs61938575	G>A	12	104985443
117	hsa-mir-412	rs61992671	G>A	14	101531854
118	hsa-mir-4772	rs62154973	C>T	2	103048780
119	hsa-mir-585	rs62376935	C>T	5	168690635
120	hsa-mir-4482	rs641071	T>T	10	106028157

Table 11. Selection of polymorphisms in pre-miRNAs (Continuation).

	Gene	SNP	Allele	Chromosome	Location
121	hsa-mir-3679	rs6430498	G>A	2	134884700
122	hsa-mir-423	rs6505162	T>T	17	28444183
123	hsa-mir-646	rs6513496	T>C	20	58883534
124	hsa-mir-4731	rs66507245	T>T	17	15154966
125	hsa-mir-3622a	rs66683138	T>T	8	27559214
126	hsa-mir-6128	rs67042258	G>A	11	56511354
127	hsa-mir-3167	rs670637	T>T	11	126858392
128	hsa-mir-4642	rs67182313	A>G	6	44403438
129	hsa-mir-4431	rs6726779	T>C	2	52929680
130	MIR3910-1, MIR3910-2	rs67339585	T>T	9	94398581
131	hsa-mir-3135a	rs6787734	T>T	3	20179097
132	hsa-mir-4305	rs67976778	T>T	13	40238175
133	hsa-mir-3144	rs68035463	C>A	6	120336327
134	hsa-mir-1255b-1	rs6841938	T>T	4	36428048
135	hsa-mir-3683	rs6977967	A>G	7	7106636
136	hsa-mir-3686	rs6997249	T>T	8	130496365
137	hsa-mir-4427	rs701213	T>T	1	233759918
138	hsa-mir-378h	rs702742	A>G	5	154209024
139	hsa-mir-548aj-2	rs7070684	T>T	10	12172775
140	hsa-mir-1283-2	rs71363366	C>G	19	54261549
141	hsa-mir-140	rs7205289	C>C	16	69967005
142	hsa-mir-2117	rs7207008	T>A	17	41522213
143	hsa-mir-4741	rs7227168	C>T	18	20513374
144	hsa-mir-3188	rs7247237	C>T	19	18392894
145	hsa-mir-3689f	rs72502717	T>T	9	137742597
146	hsa-mir-105-2	rs72631816	T>A	X	151562938
147	hsa-mir-222	rs72631825	G>A	X	45606471
148	hsa-mir-16-1	rs72631826	T>T	13	50623143
149	hsa-mir-106b	rs72631827	G>G	7	99691652
150	hsa-mir-323b	rs72631831	G>G	7	1062656
151	hsa-mir-183	rs72631833	G>G	7	129414804
152	hsa-mir-3972	rs72646786	C>T	1	17604437
153	hsa-mir-3976	rs72855836	G>A	18	5840810
154	hsa-mir-4999	rs72996752	A>G	19	8454236
155	hsa-mir-4459	rs73112689	T>T	5	53371399
156	hsa-mir-1178	rs7311975	T>C	12	120151493
157	hsa-mir-647	rs73147065	T>T	20	62574006
158	hsa-mir-4532	rs73177830	T>T	20	56470471
159	hsa-mir-548h-4	rs73235381	T>T	8	26906402
160	hsa-mir-1269a	rs73239138	G>A	4	67142620
161	hsa-mir-4739	rs73410309	T>T	17	77681036
162	hsa-mir-4474	rs74428911	G>T	9	20502274
163	hsa-mir-6504	rs74469188	T>C	16	81644970
164	hsa-mir-3615	rs745666	C>G	17	72744798
165	hsa-mir-518d	rs74704964	C>T	19	54238208
166	hsa-mir-2682	rs74904371	C>T	1	98510847
167	hsa-mir-5702	rs74949342	C>G	2	227523436
168	hsa-mir-4719	rs7500280	T>T	16	76902847
169	hsa-mir-4477a	rs75019967	A>A	9	68415338
170	hsa-mir-4742	rs7522956	A>C	1	224585958
171	hsa-mir-520f	rs75598818	G>A	19	54185492
172	hsa-mir-944	rs75715827	T>C	3	189547735
173	hsa-mir-4298	rs75966923	C>A	11	1880730
174	hsa-mir-182	rs76481776	C>T	7	129410227
175	hsa-mir-4521	rs76800617	A>G	17	8090294
176	hsa-mir-1303	rs77055126	T>T	5	154065348
177	hsa-mir-4634	rs7709117	A>G	5	174178774
178	hsa-mir-576	rs77639117	A>T	4	110409933
179	hsa-mir-4743	rs78396863	G>C	18	46196971
180	hsa-mir-6075	rs78541299	G>A	5	1510904

Table 11. Selection of polymorphisms in pre-miRNAs (Continuation).

	Gene	SNP	Allele	Chromosome	Location
181	hsa-mir-6083	rs78790512	G>A	3	124093220
182	hsa-mir-4789	rs78831152	C>T	3	175087408
183	hsa-mir-4786	rs78832554	G>A	2	240882476
184	hsa-mir-4481	rs7896283	A>G	10	12695177
185	hsa-mir-1307	rs7911488	A>G	10	105154089
186	hsa-mir-597	rs79397096	G>A	8	9599276
187	hsa-mir-3976	rs79512808	T>G	5	82136024
188	hsa-mir-5707	rs80128580	G>A	7	158384368
189	hsa-mir-3176	rs8054514	T>G	16	593277
190	hsa-mir-4520a	rs8078913	C>T	17	6558768
191	hsa-mir-4698	rs832733	T>T	12	47581629
192	hsa-mir-550a-3	rs850108	T>T	7	29720404
193	hsa-mir-4751	rs8667	G>A	19	50436371
194	hsa-mir-4671	rs877722	A>T	1	234442257
195	mir-27a	rs895819	T>C	19	13947292
196	hsa-mir-4519	rs897984	T>T	16	30886643
197	hsa-mir-5689	rs9295535	T>T	6	10439968
198	hsa-mir-3141	rs936581	G>A	5	153975576
199	hsa-mir-5186	rs9842591	C>A	3	151283691
200	hsa-mir-5680	rs9877402	A>G	3	120768492
201	hsa-mir-548h-3	rs9913045	T>T	17	13446924
202	MIR4302	rs11048315	G>A	12	26026988
203	MIR3908	rs111803974	T>T	12	124021017
204	MIR299, MIR380	rs111906529	T>C	14	101489703
205	MIR520G	rs112328520	C>T	19	54225501
206	mir-1282	rs11269	G>G	15	44085909
207	MIR4532	rs113808830	C>T	20	56470456
208	hsa-mir-4479	rs116932476	G>A	9	139781193
209	MIR296	rs117258475	G>A	20	57392686
210	hsa-mir-6717	rs117650137	G>A	14	21491532
211	MIR3649	rs117723462	T>G	12	1769533
212	MIR4436B2	rs163642	T>T	2	111042483
213	MIR3689	rs62571442	A>G	9	137742124

10. SNPS GENOTYPING

MiR-SNPs genotyping was performed in the National Genotyping Center (CeGen-ISCIII) using the GoldenGate Genotyping Assay with Veracode technology according to the published Illumina protocol was used. GoldenGate® platform allows a multiplex PCR assay, which enables the processing of a large number of SNPs simultaneously, minimizing time and required reactants and materials.

The GoldenGate® assay consists of several steps. Firstly, the DNA sample (250 ng at 50 ng/μl) is marked with biotin or Streptavidin. This mark is useful for the subsequent union of the primers that are specifically designed for each SNP. Three primers are designed: two of them are specific for each SNP allele, are called Allele-Specific Oligos (ASO) and the third hybridizes several bases downstream from the SNP site, is the Locus-Specific Oligo (LSO). The LSO contains a unique code that identifies each SNP. Following hybridization the second step is the extension of the ASOs and ligation of the extended product with the LSO. Then this regions are amplified through PCR with universal primers. This primers are marked with different colorants for each ASO (Cy-3 and Cy-5) allowing the identification of each allele of the SNP. This products are hybridized to a matrix where SNPs could be read through fluorescence signal (Figure 16).
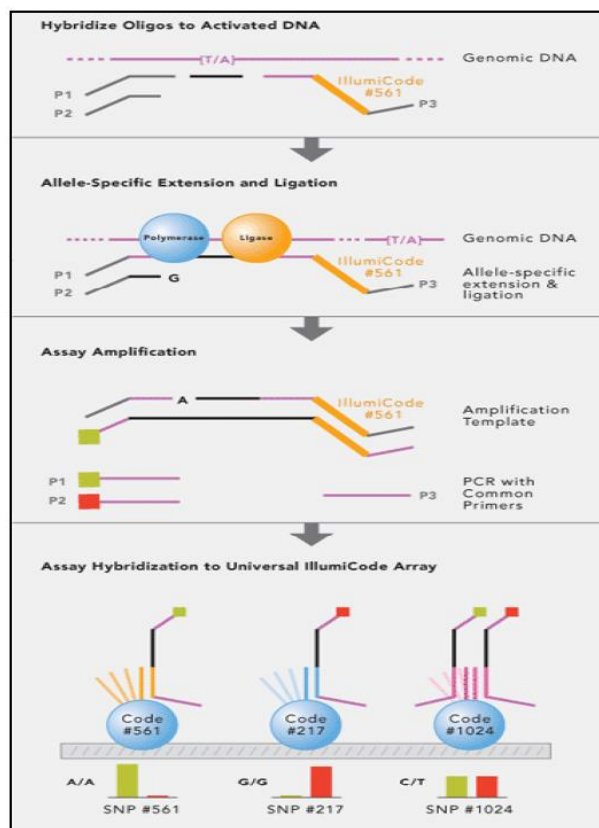
Figure 16. Genotyping GoldenGate® assay overview.

Each reaction required a total of 400 ng of DNA. The DNA was re-quantified at the Spanish Genotyping Center using PicoGreen technique (Invitrogen Corp., Carlsbad, CA) and diluted to a final concentration of 50 ng/µl. With this technique, the concentration of DNA is determined by means of a fluorescent dye that binds to double stranded DNA (PicoGreen®, Molecular Probes), which is then quantified with a fluorometer.

Data were analyzed with GenomeStudio software for genotype clustering and calling. Duplicate samples and CEPH trios (Coriell Cell Repository, Camden, NJ) were genotyped across the plates. SNPs showing Mendelian allele-transmission errors or showing discordant genotypes were excluded from the analysis.

In total, 53 out of the 213 selected SNPs (24.88%) were excluded from the study due to the fail in genotyping of more than 20% of the samples (Table 12).

Table 12. SNPs excluded from the study

	SNP	Gene
1	rs10461441	hsa-mir-548ae-2
2	rs1077020	hsa-mir-943
3	rs10878362	hsa-mir-6074
4	rs11014002	hsa-mir-603
5	rs11032942	hsa-mir-1343
6	rs11237828	hsa-mir-5579
7	rs11651671	hsa-mir-548at
8	rs12197631	hsa-mir-548a-1
9	rs12451747	hsa-mir-1269b
10	rs12473206	hsa-mir-4433
11	rs12523324	hsa-mir-4277
12	rs13186787	hsa-mir-1294
13	rs1414273	hsa-mir-548ac
14	rs17022749	hsa-mir-5700
15	rs2060455	hsa-mir-4511
16	rs2241347	hsa-mir-3130-1
17	rs2292832	hsa-mir-149
18	rs2663345	hsa-mir-3183
19	rs35196866	hsa-mir-4669
20	rs4285314	hsa-mir-3135b
21	rs487571	hsa-mir-5680
22	rs56088671	hsa-mir-4424
23	rs56195815	hsa-mir-548aw
24	rs57111412	hsa-mir-1283
25	rs58450758	hsa-mir-559
26	rs60308683	hsa-mir-4762
27	rs641071	hsa-mir-4482
28	rs6505162	hsa-mir-423
29	rs66507245	hsa-mir-4731
30	rs66683138	hsa-mir-3622a
31	rs67339585	hsa-mir-3910-1 hsa-mir-3910-2
32	rs6787734	hsa-mir-3135a
33	rs67976778	hsa-mir-4305
34	rs6841938	hsa-mir-1255b-1
35	rs6997249	hsa-mir-3686
36	rs701213	hsa-mir-4427
37	rs7070684	hsa-mir-548aj-2
38	rs72502717	hsa-mir-3689f
39	rs73112689	hsa-mir-4459
40	rs73147065	hsa-mir-647
41	rs73177830	hsa-mir-4532
42	rs73235381	hsa-mir-548h-4
43	rs73410309	hsa-mir-4739
44	rs7500280	hsa-mir-4719
45	rs77055126	hsa-mir-1303
46	rs7911488	hsa-mir1307
47	rs832733	hsa-mir-4698
48	rs850108	hsa-mir-550a-3
49	rs897984	hsa-mir-4519
50	rs9295535	hsa-mir-5689
51	rs9913045	hsa-mir-548h-3
52	rs111803974	hsa-mir-3908
53	rs163642	hsa-mir-4436B2

11. STATISTICAL ANALYSES

The genotyping success rate was calculated with Haploview (4.2.) software.

The relationship between toxicities and covariables such as age, sex or number of specific drug doses was measured using multivariate logistic regression models and correlation coefficients. The relationship between toxicity in different phases or between the gastrointestinal toxicities (mucositis, diarrhea and vomiting) during induction was measured using univariate logistic regression models and correlation coefficients. The association between miRNA polymorphisms and the different ALL treatment toxicities was evaluated using the χ2 or Fisher's exact test. The effect sizes of the associations were estimated by the odds ratio (OR) from univariate logistic regression. The most significant test among dominant and recessive genetic models was selected. The dominant model proposes that a unique copy of the risk allele is sufficient to modify the risk whereas the recessive model postulates that both copies are needed. In all cases the significance level was set at 5%. Analyses were performed by using R v3.0.1 software.

Due to the large number of SNPs under study, and consequent considerable number of comparisons, false positives are not rare. Therefore, the results were adjusted for multiple comparisons using the false discovery rate (FDR) correction (calculated considering the number of significant SNPs) (Benjamini et al., 2001) and Bonferroni correction (a more conservative method because is calculated contemplating all the studied comparisons) (Rice et al., 2008). The OpenEpi software was used to measure the statistical power of the associations (Sullivan et al., 2009).

12. BIOINFORMATICS ANALYSES

12.1. MiRNAs secondary structures prediction

For miRNAs showing significant results, the impact of the SNPs in the minimum free energy (MFE) was calculated for each allele using the RNAfold web tool (http://rna.tbi.univie.ac.at/cgi-bin/RNAWebSuite/RNAfold.cgi) and miRNAs most stable secondary structures were predicted (Gruber et al., 2008). From miRNA variant MFE, the energy change (ΔΔG) of the hairpin structure was calculated.

12.2. Target genes selection

MiRNA target genes were selected based on miRWalk database (http://zmf.umm.uni-heidelberg.de/apps/zmf/mirwalk2/) (Dweep and Gretz, 2015). Only those targets confirmed by

at least 6 of the twelve different prediction algorithms provided by miRWalk (miRWalk, miRDB, PITA, MicroT4, miRMap, RNA22, miRanda, miRNAMap, RNAhybrid, miRBridge, PICTAR2 and Targetscan) were selected.

12.3. Pathways analysis

For the identification on the genes involved in drug toxicity development, a first strategy based on known drug related ADME genes was applied. Alternatively a second approach to identify other putative target genes was conducted by pathway enrichment analysis.

In the first strategy, for each miRNA the list of the predicted genes was crossed with the list of genes involved in drugs pharmacokinetic and pharmacodinamic pathways identified by Pharmacogenomic Knowledge Base (PharmGKB) (https://www.pharmgkb.org/) and literature review.

In the second strategy, enriched pathway analyses of putative target genes were determined with ConsensusPath database (CPdB) (http://consensuspathdb.org/) using the over-representation analysis module (Kamburov et al., 2013). The miRWalk target gene list was analyzed against the default collection of KEGG (http://www.genome.jp/kegg/) (Kanehisa et al., 2017), Reactome (http://www.reactome.org/) (Fabregat et al., 2016) and BioCarta (http://cgap.nci.nih.gov/Pathways/BioCarta_Pathways) pathways databases. A conservative p-value cutoff (0.0001) was used.

RESULTS

MiR-pharmacogenetics of Vincristine and peripheral neurotoxicity in childhood B-cell acute lymphoblastic leukemia

Umerez, Maitane[1]*, PhD student; Gutierrez-Camino, Ángela[1]*, PhD; Martín-Guerrero Idoia[1], PhD; García de Andoin, Nagore[2,3], MD; Santos, Borja[1], PhD; Sastre, Ana[4],MD; Echebarria-Barona, Aizpea[5], PhD; Astigarraga, Itziar[3,5,6], PhD; Navajas, Aurora[5,6]PhD; Garcia-Orad, Africa[1,6], PhD.

*These authors share first authorship

[1]Department of Genetics, Physic Anthropology and Animal Physiology, University of the Basque Country, UPV/EHU, Leioa, Spain; [2]Department of Pediatrics, University Hospital Donostia, San Sebastian, Spain; [3]Department of Pediatrics, University of the Basque Country, UPV/EHU, Leioa, Spain, [4]Department of Oncohematology, University Hospital La Paz, Madrid, Spain; [5]Department of Pediatrics, University Hospital Cruces, Barakaldo, Spain; [6]BioCruces Health Research Institute, Barakaldo, Spain.

Abstract

Vincristine (VCR), an important component of childhood acute lymphoblastic leukemia (ALL) therapy, can cause sensory and motor neurotoxicity. This neurotoxicity could lead to dose reduction or treatment discontinuation, which could in turn reduce survival. In this line, several studies associated peripheral neurotoxicity and polymorphisms in genes involved in pharmacokinetics (PK) and pharmacodynamics (PD) of VCR. Nowadays, it is well known that these genes are regulated by microRNAs (miRNAs) and SNPs in miRNAs could modify their levels or function. Therefore, the aim of this study was to determine whether SNPs in miRNAs could be associated with VCR-induced neurotoxicity. To achieve this aim, we analyzed all the SNPs in miRNAs (minor allele frequency (MAF) ≥0.01) which could regulate VCR-related genes in a large cohort of Spanish children with B-cell precursor ALL (B-ALL) homogeneously treated with LAL/SHOP protocols. We identified the A allele of rs12402181 in the seed region of miR-3117-3p, that could affect the binding with *ABCC1* and *RALBP1* gene, and C allele of rs7896283 in pre-mature sequence of miR-4481, which could be involved in peripheral nerve regeneration, significantly associated with VCR-induced neurotoxicity. These findings point out the possible involvement of two SNPs in miRNA associated with VCR-related neurotoxicity.

Keywords: B-cell acute lymphoblastic leukemia, vincristine, microRNAs, single nucleotide polymorphisms.

INTRODUCTION

Vincristine (VCR) is an important component of childhood acute lymphoblastic leukemia (ALL) therapy, the most common childhood cancer (Johnston et al., 2010). Despite its clinical efficacy, VCR can cause sensory and motor neurotoxicity (Carozzi et al., 2015), a disabling adverse event that can appear in any of the treatment phases. The frequency, number and concentration of the doses of VCR administered in the different protocols may affect the incidence of neurotoxicity and the treatment phase in which it appears more frequently (induction or maintenance) (Gutierrez-Camino et al., 2016). However, independently of when it appears, neurotoxicity could lead to VCR dose reduction or treatment discontinuation (Ceppi et al., 2014) which could in turn, reduce survival (Carozzi et al., 2015; Ceppi et al., 2014; Postma et al., 1993). Therefore, one of the challenges in medicine is to predict which patients are going to develop VCR-related neurotoxicity in order to adjust the treatment in advance.

In the past few years several studies analyzed the relationship between genetic variants and VCR-related neurotoxicity, mainly focused on genes involved in pharmacokinetics (PK) and pharmacodynamics (PD) of VCR (Ceppi et al., 2014; Diouf et al., 2015; Egbelakin et al., 2011; Hartman et al., 2010; Lopez-Lopez et al., 2016; Moore et al., 2011; Plasschaert et al., 2004). In this line, one of the most interesting results was found by Diouf et al. in a Genome Wide Association Study (GWAS) performed in a large group of pediatric patients with ALL (Diouf et al., 2015). This study showed association between peripheral neuropathy in later phases of treatment and the SNP rs924607 in the promoter region of *CEP72*. Interestingly, this SNP is additionally located in a non-coding RNA called LOC100996325. Moreover, three out of the other four significant SNPs identified in this GWAS (rs17032980, rs12786200 and rs4463516) were also located in non-coding regions (Diouf et al., 2015).

Nowadays, it is well known that non-coding RNAs, such as microRNAs (miRNAs), regulate more than 50% of our genes, including genes involved in PK and PD of different drugs (Li et al., 2016; Nakajima and Yokoi, 2011). Genetic variants in miRNAs can modify their levels or function and consequently, might affect the expression of their target genes. In this line, in a recent study of our group, we found association between rs2114358 in miR-1206 and methotrexate (MTX)-induced oral mucositis (Gutierrez-Camino et al., 2017b) and other three SNPs in miR-5198, miR-595 and miR-453 and MTX plasma levels (Iparraguirre et al., 2016; Lopez-Lopez et al., 2014b). These miRNAs might regulate *SLC46A1*, *SLC19A1* and *SLCO1A2* MTX transport genes, and then, expression changes in these transporters could alter MTX clearance. In consequence, we can

hypothesize that variants in miRNAs targeting VCR PK and PD genes could also be associated with VCR-induced neurotoxicity in children with B-ALL.

Therefore in this study, we analyzed all the SNPs in miRNAs (minor allele frequency (MAF) ≥0.01) which could regulate VCR-related genes in a large cohort of Spanish children with B-ALL homogeneously treated.

MATERIALS AND METHODS

Patients

The patients included in this retrospective study were 179 Spanish children diagnosed with B-ALL at the Pediatric Oncology Units of three Spanish hospitals (University Hospital La Paz, University Hospital Donostia and University Hospital Cruces) from 2000 to 2013. Written informed consent was obtained from all patients or their parents before sample collection. University of the Basque Country (UPV/EHU) ethics committee board approval (CEISH/102R/2011) was obtained.

Treatment and toxicity evaluation

All the patients included in the study were homogeneously treated according to the Spanish LAL-SHOP 94/99/2005 protocols. These protocols were described previously (Lopez-Lopez et al., 2016). Briefly, four doses of VCR (1.5 mg/m^2) given on a weekly basis were administrated at induction. In later phases of treatment, except consolidation, between 6 and 16 doses (1.5 mg/m^2) were administrated on a monthly or weekly basis depending on phase and risk group. In addition to VCR, these treatment protocols also included daunorubicin, prednisone, cyclophosphamide, and asparaginase and intrathecal methotrexate-cytarabine-hydrocortisone therapy. High-risk patients in the LAL/SHOP 99 also received an only dose of 3 g/m^2 of methotrexate on day +15. The later phases of treatment were more heterogeneous based on risk group segregation. None of these other drugs induce peripheral neurotoxicity as a common adverse event.

Toxicity data for all the treatment phases were collected blinded to genotypes from the patients' medical files by the same two expert researchers in all cases. Patients were evaluated at three hospitals by physicians that were familiar with assessing VCR neuropathy, using the same standards and same frequency of evaluation among the different centers. Neurotoxicity was graded according to the WHO Peripheral Nervous System toxicity criteria (See Table 7); three phenotypes were considered: any grade neurotoxicity (grades 1–4), low-grade neurotoxicity

(grades 1–2) and high-grade neurotoxicity (grades 3–4). Other relevant data including age, sex, number of VCR doses and risk group were systematically collected from the clinical records.

In the present study, we focused the neurotoxicity analysis at induction because all the patients received the same number of VCR doses, most neurotoxicity cases of our cohort were developed during the induction and finally, no other drugs that usually cause neurotoxicity were administered in this phase. Moreover, we also analyzed the three phenotypes in any of the treatment phases (induction, consolidation, intensification or maintenance), and we defined it as global neurotoxicity.

Genes and polymorphisms selection

Taking into account that, nowadays, miRNAs targets are not completely defined and the fact that any miRNA could be implicated direct or indirectly in the regulation of VCR-related genes, we selected all the miRNA genes that had SNPs described at the time of the study (May 2014). For the SNP selection, we used mirbase (http://www.mirbase.org/), miRNA SNIPER (http://bioinfo.life.hust.edu.cn/miRNASNP2/index.php), and dbSNP (http://www.ncbi.nlm.nih.gov/SNP/) databases, as well as literature review.

From a total of 1910 SNPs in 969 miRNAs, we selected those SNPs with a MAF more than 0.01 in European/Caucasoid populations. With these criteria, a final number of 213 SNPs in 206 miRNAs were finally selected for the study (See Table 11).

Genotyping

Genomic DNA was extracted from patients' peripheral blood or bone marrow when complete remission was achieved using the phenol–chloroform method, as previously described (Sambrook, J, 2001). DNA was quantified using PicoGreen (Invitrogen Corp., Carlsbad, California, USA). For each sample, 400 ng of DNA were genotyped using the GoldenGate Genotyping Assay (Illumina Inc., San Diego, California, USA) with Veracode technology according to the published Illumina protocol. Data were analyzed with GenomeStudio (Illumina Inc.) software for genotype clustering and calling. Duplicate samples and CEPH trios (Coriell Cell Repository, Camden, New Jersey, USA) were genotyped across the plates. SNPs showing Mendelian allele-transmission errors or showing discordant genotypes were excluded from the analysis.

Statistical analysis

The association between neurotoxicity and genetic polymorphisms was evaluated by the χ2 or Fisher's exact test. The effect sizes of the associations were estimated by the odds ratios (OR). To account for the possible confounding effect of VCR dose, multivariate logistic regressions were used when global toxicity was analyzed. The most significant test among dominant and recessive genetic models was selected. In all cases the significance level was set at 5%. The results were adjusted for multiple comparisons using the false discovery rate (FDR) correction, assuming 5 % level of significance for all tests (Benjamini et al., 2001). The OpenEpi software was used to measure the statistical power of the associations (Sullivan et al., 2009). Analyses were performed using the R v3.3.0. software.

Bioinformatics analysis

- *miRNAs secondary structures prediction*

The RNAfold web tool (http://rna.tbi.univie.ac.at/cgi-bin/RNAWebSuite/RNAfold.cgi) (Gruber et al., 2008) was used to calculate the impact of the SNPs in the minimum free energy secondary structures and the energy change (ΔΔG) of the hairpin structure of the miRNAs showing significant results.

- *Gene targets selection and pathways analysis*

Target genes for each of the significant miRNAs were extracted based on miRWalk database (http://zmf.umm.uni-heidelberg.de/apps/zmf/mirwalk2/index.html) (Dweep et al., 2011). Only those genes confirmed by at least six of the 12 prediction programs hosted in miRWalk were included.

Regarding pathway analysis with significant miRNAs, following a first approach, we considered genes involved in VCR PK and PD (*ABCB1, ABCC1, ABCC10, ABCC2, ABCC3, CYP3A4, CYP3A5* and *BAX, BCL2, RALBP1, CEP72, MAPT, TUBB1, TUBB2A,TUBB2B, TUBB3, TUBB4*) (Figure 17) selected based on the Pharmacogenomic Knowledge Base (PharmGKB) (https://www.pharmgkb.org/) and by literature review. Then, in a second approach to identify other target genes that could be involved in VCR-induced neurotoxicity, we performed a pathway enrichment analysis using the ConsensusPathDB web tool (CPdB) (http://consensuspathdb.org/) (Kamburov et al., 2013) using the over-representation analysis module. The miRWalk target gene lists were analyzed against the default collection of KEGG (Kanehisa et al., 2017), Reactome (Fabregat et al., 2016)

and BioCarta (https://cgap.nci.nih.gov/Pathways/BioCarta_Pathways) pathway databases. A conservative *p*-value cutoff (0.0001) was used.
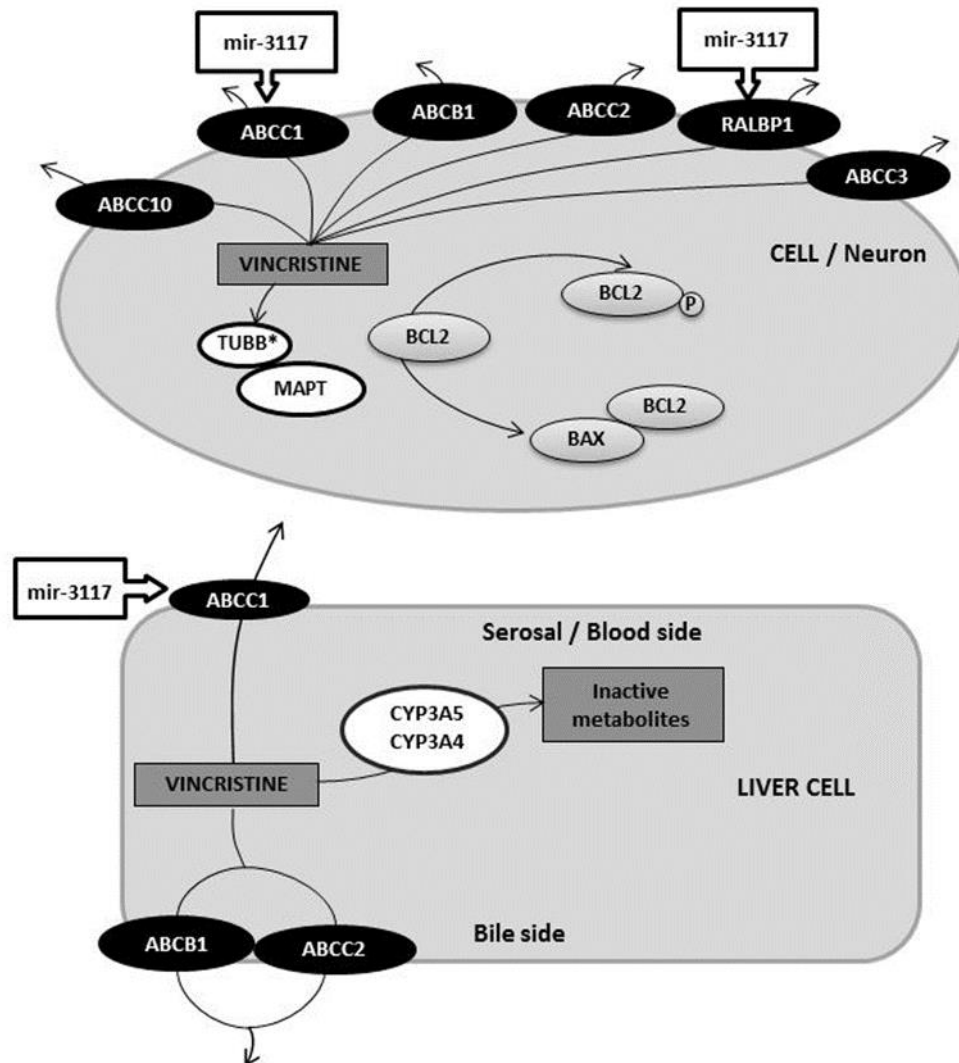
Figure 17. Genes of the VCR PK/PD pathways and the most significant miRNA in this study, miR-3117, targeting the corresponding genes.

RESULTS

Patient's baseline characteristics

In this study, we included a total of 179 patients with childhood B-ALL from whom VCR neurotoxicity data were available in 175 patients (Table 13). The majority of neurotoxicity cases appeared during induction phase (47/55 patients, 85.45%). Only 8 patients developed peripheral neurotoxicity in later treatment phases (3 patients in consolidation, 4 patients in intensification and 1 patient in maintenance) (Table 14).

Table 13. Characteristics of the childhood B-ALL patients

Number of patients	175
Sex, n (%)	
Female	72 (41.14)
Male	103 (58.86)
Age at diagnosis (mean ±SD) (years)	5.12 ± 3.23
Female	5.10 ± 3.22
Male	5.70 ± 3.20
Treatment protocol, n (%)[1]	
LAL-SHOP 94/99	68 (38.86)
LAL-SHOP 2005	105 (60.00
Neurotoxicity, n (%)	
Induction	
Grades 1-4	47 (26.86)
Grades 1-2	28 (16.00)
Grades 3-4	19 (10.86)
Global	
Grades 1-4	55 (31.43)
Grades 1-2	32 (18.29)
Grades 3-4	24 (13.71)

Abbreviations: B-ALL, B-cell acute lymphoblastic leukemia; SD, standard deviation.
Notes: [1]there was not information about treatment protocol for two patients.

Table 14. VCR Peripheral Neurotoxicity data

	Induction			Global		
	Grades 1-4 n (%)	Grades 1-2 n (%)	Grades 3-4 n (%)	Grades 1-4 n (%)	Grades 1-2 n (%)	Grades 3-4 n (%)
No neurotoxicity	128 (73.14)	128 (73.14)	128 (73.14)	120 (68.57)	120 (68.57)	120 (68.57)
Neurotoxicity	47 (26.86)	28 (16.00)	19 (10.86)	55 (31.43)	32 (18.29)[2]	24 (13.71)[2]
NA	0 (0.00)	19 (10.86)[1]	28 (16.00)[1]	0 (0.00)	23 (13.14)[1]	31 (17.71)[1]

Abbreviations: NA, not available.
Notes: [1] when only grades 1-2 or grades 3-4 toxicity was present, the patient was codified as NA for the other grade toxicity;.[2] one patient present both, grades 1-2 and grades 3-4 toxicity.

Genotyping results

Successful genotyping was carried out for 155 out of 179 DNA samples (86.59 %). During the genotyping process, 53 out of 213 SNPs (24.88 %) (See Table 12) failed in more than 20% of the samples and were eliminated from the study. These failures were due to no PCR amplification, insufficient intensity for cluster separation, or poor or no cluster definition. Successful genotyping was obtained for 160 SNPs (75.12%).

Association study

To investigate whether genetic variation in miRNAs may influence VCR-induced neurotoxicity, we tested the association between the 160 successfully genotyped SNPs in 154 miRNAs and peripheral neurotoxicity data. The study population consisted of 155 Spanish childhood B-ALL patients who were homogeneously treated and whose genotype and toxicity data were available. The main analyses were performed at induction phase, when 85.45% of the neurotoxicity cases were detected. We evaluated the severity of peripheral neuropathy considering patients developing neurotoxicity of any grade (1-4) (47 patients), low grade (1-2) (28 patients) and high grade (3-4) (19 patients).

The most significant result in this study was found for rs12402181 in miR-3117 (Table 15). The AG+AA genotypes were associated with a 0.16-fold decreased grades 1-4 neurotoxicity risk (P = 0.00042) and the AA genotype was never found in patients with peripheral neurotoxicity. A statistical power of 70 % was calculated from 39 toxicity patients (MAF = 3.8 %) and 116 patients without toxicity (MAF = 18%). The significant association was consistently found in induction phase for low and high toxicity grade analyses with 0.0069 and 0.0099 p values respectively.

The second most significant result was found for rs7896283 in miR-4481. The CC genotype was associated with a 2.6-fold increased risk of VCR-induced neurotoxicity (P = 0.017). A statistical power of 54 % was calculated from 39 toxicity patients (MAF = 51 %) and 97 patients without toxicity (MAF = 32 %). In this case the C allele was associated with high grade neurotoxicity (P=0.0148) (Table 15). The third most significant polymorphism was rs35650931 in miR-6076. The CC genotype was protective and was not found in any of the toxicity cases (P = 0.017). This association was also found for grades 1-2 neurotoxicity (P = 0.014) (Table 15). Other 9 SNPs showed significant association (p<0.05) with VCR-induced neurotoxicity during induction phase (Table 16).

When global VCR-induced neurotoxicity occurring in any of the phases was analyzed, again the most significant results were found for rs12402181 in miR-3117 and rs7896283 in miR-4481 (Table 17).

None of the SNPs reached significant P-values when FDR correction was applied. However rs12402181 in mir-3117 almost reached a significant p-value (p=0.06) after FDR correction.

Table 15. SNPs in miRNAs showing the most significant associations with VCR neurotoxicity during induction phase in pediatric B-ALL. Genotypic and allelic frequencies.

miRNA SNP	Position Localization	Genotype/ Allele	Grades 1-4 Tox (n=175)		Model OR (95% CI) P-value	Grades 1-2 Tox (n=156)		Model OR (95% CI) P-value	Grades 3-4 Tox (n=147)		Model OR (95% CI) P-value
			No tox N=128	Tox N=47		No tox N=128	Tox N=28		No tox N=128	Tox N=19	
hsa-mir-3117 rs12402181	Chr.: 1 in_seed	GG AG AA	76 (65.5) 37 (31.9) 3 (2.6)	36 (92.3) 3 (7.7) 0 (0.0)	Dominant 0.16 (0.05-0.55) **0.00042**	76 (65.5) 37 (31.9) 3 (2.6)	21 (91.3) 2 (8.7) 0 (0.0)	Dominant 0.18 (0.04-0.81) **0.0069**	76 (65.5) 37 (31.9) 3 (2.6)	15 (93.8) 1 (6.2) 0 (0.0)	Dominant 0.13 (0.02-0.99) **0.0099**
		G A	189 (81.5) 43 (18.5)	75 (96.1) 3 (3.8)	0.176 (0.053-0.584) **0.0016**	189 (81.5) 43 (18.5)	44 (95.7) 2(4.3)	0.2 (0.047-0.856) **0.0170**	189 (81.5) 43(18.5)	31(96.9) 1(3.1)	0.142 (0.019-1.067) 0.0283
hsa-mir-4481 rs7896283	Chr.: 10 pre-miRNA	TT CT CC	46 (47.4) 40 (41.2) 11 (11.3)	10 (25.6) 18 (46.2) 11 (28.2)	Dominant 2.62 (1.15-5.95) **0.0173**	46 (47.4) 40 (41.2) 11 (11.3)	6 (26.1) 12 (52.2) 5 (21.7)	Dominant 2.56 (0.93-7.03) 0.0578	46 (47.4) 40 (41.2) 11 (11.3)	4 (25.0) 6 (37.5) 6 (37.5)	Recesive 4.69 (1.43-15.43) **0.0148**
		T C	132 (68) 62 (32)	38 (48.7) 40 (51.3)	2.241 (1.310-3.834) **0.0029**	132 (68) 62 (32)	24 (52.2) 22 (47.8)	1.952 (1.016-3.748) **0.0425**	132 (68) 62 (32)	14 (43.8) 18 (56.3)	2.737 (1.279-5.858) **0.0078**
hsa-mir-6076 rs35650931	Chr.: 14 pre-miRNA	GG CG CC	93 (80.2) 21 (18.1) 2 (1.7)	37 (94.9) 2 (5.1) 0 (0.0)	Dominant 0.22 (0.05-0.97) **0.0175**	93 (80.2) 21 (18.1) 2 (1.7)	23 (100.0) 0 (0.0) 0 (0.0)	Dominant 0 (0.0) **0.0140**	93 (80.2) 21 (18.1) 2 (1.7)	14 (87.5) 2 (12.5) 0 (0.0)	Dominant 0.58 (0.12-2.72) 0.4636
		G C	207 (89.2) 25 (10.8)	76 (97.4) 2 (2.6)	0.218 (0.050-0.942) **0.0261**	207 (89.2) 25 (10.8)	46 (100) 0 (0)	0 (-) **0.0196**	207 (89.2) 25 (10.8)	30 (93.8) 2 (6.3)	0.552 (0.124-2.450) 0.4283

Abbreviations: B-ALL, B cell acute lymphoblastic leukemia; VCR, vincristine; miRNA, microRNA; SNP, single nucleotide polymorphism; Tox, toxicity; OR, odds ratio; CI, confidence interval; Chr, chromosome; NA, not available.

Notes: Bold denote significant P-values.

Table 16. List of the twelve miRNA SNPs associated to VCR-induced neurotoxicity during induction phase in childhood ALL.

miRNA SNP	Position Localization	Genotype /Allele	Grades 1-4 Tox (n=175)		Model OR. (95% CI) P-value	Grades 1-2 Tox (n=156)		Model OR. (95% CI) P-value	Grades 3-4 Tox (n=147)		Model OR. (95% CI) P-value
			No tox N=128	Tox N=47		No tox N=128	Tox N=28		No tox N=128	Tox N=19	
hsa-mir-3117 rs12402181	Chr.: 1 in_seed	GG AG AA	76 (65.5) 37 (31.9) 3 (2.6)	36 (92.3) 3 (7.7) 0 (0.0)	Dominant 0.16 (0.05-0.55) **0.00042**	76 (65.5) 37 (31.9) 3 (2.6)	21 (91.3) 2 (8.7) 0 (0.0)	Dominant 0.18 (0.04-0.81) **0.0069**	76 (65.5) 37 (31.9) 3 (2.6)	15 (93.8) 1 (6.2) 0 (0.0)	Dominant 0.13 (0.02-0.99) **0.0099**
		G A	189 (81.5) 43 (18.5)	75 (96.1) 3 (3.8)	0.176 (0.053-0.584) **0.0016**	189 (81.5) 43 (18.5)	44 (95.7) 2(4.3)	0.2 (0.047-0.856) **0.0170**	189 (81.5) 43(18.5)	31(96.9) 1(3.1)	0.142 (0.019-1.067) 0.0283
hsa-mir-4481 rs7896283	Chr.: 10 pre-miRNA	TT CT CC	46 (47.4) 40 (41.2) 11 (11.3)	10 (25.6) 18 (46.2) 11 (28.2)	Dominant 2.62 (1.15-5.95) **0.0173**	46 (47.4) 40 (41.2) 11 (11.3)	6 (26.1) 12 (52.2) 5 (21.7)	Dominant 2.56 (0.93-7.03) 0.0578	46 (47.4) 40 (41.2) 11 (11.3)	4 (25.0) 6 (37.5) 6 (37.5)	Recesive 4.69 (1.43-15.43) **0.0148**
		T C	132 (68) 62 (32)	38 (48.7) 40 (51.3)	2.241 (1.310-3.834) **0.0029**	132 (68) 62 (32)	24 (52.2) 22 (47.8)	1.952 (1.016-3.748) **0.0425**	132 (68) 62 (32)	14 (43.8) 18 (56.3)	2.737 (1.279-5.858) **0.0078**
hsa-mir-6076 rs35650931	Chr.: 14 pre-miRNA	GG CG CC	93 (80.2) 21 (18.1) 2 (1.7)	37 (94.9) 2 (5.1) 0 (0.0)	Dominant 0.22 (0.05-0.97) **0.0175**	93 (80.2) 21 (18.1) 2 (1.7)	23 (100.0) 0 (0.0) 0 (0.0)	Dominant 0 (0.0) **0.0140**	93 (80.2) 21 (18.1) 2 (1.7)	14 (87.5) 2 (12.5) 0 (0.0)	Dominant 0.58 (0.12-2.72) 0.4636
		G C	207 (89.2) 25 (10.8)	76 (97.4) 2 (2.6)	0.218 (0.050-0.942) **0.0261**	207 (89.2) 25 (10.8)	46 (100) 0 (0)	0 (-) **0.0196**	207 (89.2) 25 (10.8)	30 (93.8) 2 (6.3)	0.552 (0.124-2.450) 0.4283
hsa-mir-577 rs34115976	Chr.: 4 pre-miRNA	CC CG GG	78 (68.4) 34 (29.8) 2 (1.8)	21 (53.8) 14 (35.9) 4 (10.3)	Recesive 6.40 (1.12-36.44) **0.0302**	78 (68.4) 34 (29.8) 2 (1.8)	12 (52.2) 7 (30.4) 4 (17.4)	Recesive 11.79 (2.02-68.91) **0.0049**	78 (68.4) 34 (29.8) 2 (1.8)	9 (56.2) 7 (43.8) 0 (0.0)	Dominant 1.69 (0.58-4.88) 0.3416
		C G	190 (83.3) 38 (16.7)	56 (71.8) 22 (28.2)	1.964 (1.074-3.593) **0.0267**	190 (83.3) 38 (16.7)	31 (67.4) 15 (32.6)	2.42 (1.192-4.911) 0.0125	190 (83.3) 38 (16.7)	25 (78.1) 7 (21.9)	1.4 (0.565-3.470) 0.4658
hsa-mir-5197 rs2042253	Chr.: 5 pre-miRNA	AA AG GG	63 (54.3) 50 (43.1) 3 (2.6)	28 (73.7) 9 (23.7) 1 (2.6)	Dominant 0.42 (0.19-0.95) **0.03157**	63 (54.3) 50 (43.1) 3 (2.6)	18 (81.8) 3 (13.6) 1 (4.5)	Dominant 0.26 (0.08-0.83) **0.012045**	63 (54.3) 50 (43.1) 3 (2.6)	10 (62.5) 6 (37.5) 0 (0.0)	Dominant 0.71 (0.24-2.09) 0.5343
		A G	176 (75.9) 56 (24.1)	65 (85.5) 11 (14.5)	0.532 (0.262-1.078) 0.0763	176 (75.9) 56 (24.1)	39 (88.6) 5 (11.4)	0.403 (0.151-1.072) 0.0612	176 (75.9) 56 (24.1)	26 (81.3) 6 (18.8)	0.725 (0.284-1.852) 0.5003
hsa-mir-449c rs35770269	Chr.: 5 in_seed	AA AT TT	57 (49.6) 42 (36.5) 16 (13.9)	12 (30.8) 24 (61.5) 3 (7.7)	Dominant 2.21 (1.02-4.79) **0.0389**	57 (49.6) 42 (36.5) 16 (13.9)	10 (43.5) 12 (52.2) 1 (4.3)	Recesive 0.28 (0.04-2.23) 0.1566	57 (49.6) 42 (36.5) 16 (13.9)	2 (12.5) 12 (75.0) 2 (12.5)	Dominant 6.88 (1.50-31.64) **0.0029**
		A T	156 (67.8) 74 (32.2)	48 (61.5) 30 (38.5)	1.32 (0.773-2.246) 0.3102	156 (67.8) 74 (32.2)	32 (69.6) 14(30.4)	0.92 (0.464-1.832) 0.8173	156 (67.8) 74 (32.2)	16 (50) 16 (50)	2.10 (1.000-4.446) 0.0466

Abbreviations: B-ALL, B cell acute lymphoblastic leukemia; VCR, vincristine; miRNA, microRNA; SNP, single nucleotide polymorphism; Tox, toxicity; OR, odds ratio; CI, confidence interval; Chr, chromosome.

Notes: Bold denote significant P-values.

Table 16. List of the twelve miRNA SNPs associated to VCR-induced neurotoxicity during induction phase in childhood ALL. (Continuation)

miRNA SNP	Position Localization	Genotype /Allele	Grades 1-4 Tox (n=175)		Model OR. (95% CI) P-value	Grades 1-2 Tox (n=156)		Model OR. (95% CI) P-value	Grades 3-4 Tox (n=147)		Model OR. (95% CI) P-value
			No tox N=128	Tox N=47		No tox N=128	Tox N=28		No tox N=128	Tox N=19	
hsa-mir-1208 rs2648841	Chr.: 8 pre-miRNA	CC	88 (77.9)	23 (60.5)	Dominant 2.30 (1.04-5.05) **0.0410**	88 (77.9)	12 (54.5)	Dominant 2.93 (1.13-7.58) **0.0291**	88 (77.9)	11 (68.8)	Dominant 1.60 (0.51-5.04) 0.4323
		AC	22 (19.5)	14 (36.8)		22 (19.5)	10 (45.5)		22 (19.5)	4 (25.0)	
		AA	3 (2.7)	1 (2.6)		3 (2.7)	0 (0.0)		3 (2.7)	1 (6.2)	
		C	198 (87.6)	60 (78.9)	1.886 (0.957-3.718) 0.0640	198 (87.6)	34 (77.3)	2.080 (0.927-4.668) 0.0712	198 (87.6)	26 (81.3)	1.632 (0.617-4.313) 0.3195
		A	28 (12.4)	16 (21.1)		28 (12.4)	10 (22.7)		28 (12.4)	6 (18.8)	
hsa-mir-5090 rs3823658	Chr.: 7 in_seed	GG	95 (81.9)	25 (65.8)	Dominant 2.35 (1.04-5.34) **0.0444**	95 (81.9)	14 (63.6)	Dominant 2.59 (0.96-6.95) 0.0677	95 (81.9)	11 (68.8)	Dominant 2.06 (0.65-6.55) 0.2387
		AG	19 (16.4)	12 (31.6)		19 (16.4)	8 (36.4)		19 (16.4)	4 (25.0)	
		AA	2 (1.7)	1 (2.6)		2 (1.7)	0 (0.0)		2 (1.7)	1 (6.2)	
		G	209 (90.1)	62 (81.6)	2.052 (0.996-4.225) 0.0477	209 (90.1)	36 (81.8)	2.02 (0.839-4.863) 0.1113	209 (90.1)	26 (81.3)	2.097 (0.782-5.624) 0.1340
		A	23 (9.9)	14 (18.4)		23 (9.9)	8 (18.2)		23 (9.9)	6 (18.8)	
hsa-mir-202 rs12355840	Chr.: 10 pre-miRNA	TT	62 (63.3)	18 (47.4)	Dominant 1.91 (0.90-4.08) 0.0926	62 (63.3)	8 (36.4)	Dominant 3.01 (1.15-7.88) **0.0215**	62 (63.3)	10 (62.5)	Recesive 1.24 (0.14-11.36) 0.8522
		CT	31 (31.6)	19 (50.0)		31 (31.6)	14 (63.6)		31 (31.6)	5 (31.2)	
		CC	5 (5.1)	1 (2.6)		5 (5.1)	0 (0.0)		5 (5.1)	1 (6.2)	
		T	155 (79.1)	55 (72.4)	1.443 (0.785-2.655) 0.2363	155 (79.1)	30 (68.2)	2.140 (1.043-4.391) 0.12	155 (79.1)	25 (78.1)	1.059 (0.428-2.619) 0.9021
		C	41 (20.9)	21 (27.6)		41 (20.9)	14 (31.8)		41 (20.9)	7 (21.9)	
hsa-mir-4326 rs6062431	Chr.: 20 pre-miRNA	GG	59 (51.8)	26 (68.4)	Dominant 0.50 (0.23-1.08) 0.0699	59 (51.8)	17 (77.3)	Dominant 0.32 (0.11-0.91) **0.0229**	59 (51.8)	9 (56.2)	Recesive 0.48 (0.06-3.89) 0.4478
		CG	41 (36.0)	10 (26.3)		41 (36.0)	4 (18.2)		41 (36.0)	6 (37.5)	
		CC	14 (12.3)	2 (5.3)		14 (12.3)	1 (4.5)		14 (12.3)	1 (6.2)	
		G	159 (69.7)	62 (81.6)	0.52 (0.273-0.992) **0.0448**	159 (69.7)	38 (86.4)	0.364 (0.147-0.900) **0.0238**	159 (69.7)	24 (75)	0.77 (0.329-1.795) 0.5414
		C	69 (30.3)	14 (18.4)		69 (30.3)	6 (13.6)		69 (30.3)	8 (25)	
mir-1908 rs174561	Chr.: 11 pre-miRNA	TT	67 (61.5)	17 (44.7)	Dominant 1.97 (0.93-4.16) 0.0738	67 (61.5)	14 (63.6)	Recesive 0 (0.0) 0.5887	67 (61.5)	3 (18.8)	Dominant 6.91 (1.86-25.70) **0.0011**
		CT	36 (33.0)	20 (52.6)		36 (33.0)	8 (36.4)		36 (33.0)	12 (75.0)	
		CC	6 (5.5)	1 (2.6)		6 (5.5)	0 (0.0)		6 (5.5)	1 (6.2)	
		T	170 (78)	54 (71)	1.44 (0.800-2.604) 0.2220	170 (78)	36 (81.8)	0.79 (0.343-1.806) 0.5712	170 (78)	18 (56.3)	2.755 (1.277-5.940) **0.0079**
		C	48 (22)	22 (29)		48 (22)	8 (18.2)		48 (22)	14 (43.7)	
hsa-mir-4745 rs10422347	Chr.: 19 5p in_mature; 3p pre-miRNA	CC	88 (78.6)	35 (89.7)	Dominant 0.42 (0.14-1.30) 0.1043	88 (78.6)	19 (82.6)	Dominant 0.77 (0.24-2.48) 0.6581	88 (78.6)	16 (100.0)	Dominant 0 (0.0) **0.0409**
		CT	22 (19.6)	4 (10.3)		22 (19.6)	4 (17.4)		22 (19.6)	0 (0.0)	
		TT	2 (1.8)	0 (0.0)		2 (1.8)	0 (0.0)		2 (1.8)	0 (0.0)	
		C	198 (88.4)	74 (94.9)	0.412 (0.139-1.219) 0.0994	198 (88.4)	42 (91.3)	0.73 (0.240-2.188) 0.5671	198 (88.4)	32 (100)	0 (-) **0.0420**
		T	26 (11.6)	4 (5.1)		26 (11.6)	4 (8.7)		26 (11.6)	0 (0)	

Abbreviations: B-ALL, B cell acute lymphoblastic leukemia; VCR, vincristine; miRNA, microRNA; SNP, single nucleotide polymorphism; Tox, toxicity; OR, odds ratio; CI, confidence interval; Chr, chromosome.

Notes: Bold denote significant P-values.

Table 17. List of the twelve miRNA SNPs associated to VCR-induced global neurotoxicity in childhood ALL.

miRNA SNP	Position Localization	Genotype /Allele	Grades 1-4 Tox (n=175)		Model OR. (95% CI) P-value/D corrected P	Grades 1-2 Tox (n=152)		Model OR. (95% CI) P-value/D corrected P	Grades 3-4 Tox (n=144)		Model OR. (95% CI) P-value/D corrected P
			No tox N=120	Tox N=55		No tox N=120	Tox N=32		No tox N=120	Tox N=24	
hsa-mir-3117 rs12402181	Chr.: 1 in_seed	GG	72 (65.5)	40 (88.9)	Dominant	72 (65.5)	23 (85.2)	Dominant	72 (65.5)	18 (90.0)	Dominant
		AG	35 (31.8)	5 (11.1)	0.24 (0.09-0.65)	35 (31.8)	4 (14.8)	0.33 (0.11-1.02)	35 (31.8)	2 (10.0)	0.21 (0.05-0.96)
		AA	3 (2.7)	0 (0.0)	**0.0017/0.0026**	3 (2.7)	0 (0.0)	**0.0357/0.0464**	3 (2.7)	0 (0.0)	**0.0173/0.0272**
		G	179 (81.4)	85 (94.4)	0.271 (0.104-0.710)	179 (81.4)	50 (92.6)	0.349 (0.119-1.022)	179 (81.4)	38 (95)	0.23 (0.053-0.991)
		A	41 (18.6)	5 (5.6)	**0.0033**	41 (18.6)	4 (7.4)	0.0460	41 (18.6)	2 (5)	**0.0327**
hsa-mir-4481 rs7896283	Chr.: 10 pre-miRNA	AA	45 (49.5)	11 (24.4)	Dominant	45 (49.5)	6 (22.2)	Dominant	45 (49.5)	5 (25)	Dominant
		AG	36 (39.6)	22 (48.9)	3.02 (1.37-6.69)	36 (39.6)	13 (48.1)	3.42 (1.26-9.27)	36 (39.6)	9 (45)	2.93 (0.98-8.75)
		GG	10 (11.0)	12 (26.7)	**0.0045/0.0103**	10 (11.0)	8 (29.6)	**0.0099/0.0186**	10 (11.0)	6 (30)	0.0416/0.0838
		A	126 (69.2)	44 (48.9)	2.352 (1.399-3.955)	126 (69.2)	25 (46.3)	2.61 (1.403-4.855)	126 (69.2)	19 (47.5)	2.487 (1.240-4.987)
		G	56 (30.8)	46 (51.1)	**0.0011**	56 (30.8)	29 (53.7)	**0.0020**	56 (30.8)	21 (52.5)	**0.0089**
hsa-mir-646 rs6513496	Chr.: 20 pre-miRNA	TT	64 (58.7)	35 (77.8)	Dominant	64 (58.7)	22 (81.5)	Dominant	64 (58.7)	13 (65.0)	Dominant
		CT	39 (35.8)	8 (17.8)	0.41 (0.18-0.90)	39 (35.8)	4 (14.8)	0.32 (0.11-0.92)	39 (35.8)	6 (30.0)	0.77 (0.28-2.07)
		CC	6 (5.5)	2 (4.4)	**0.0214/0.0102**	6 (5.5)	1 (3.7)	**0.0221/0.0135**	6 (5.5)	1 (5.0)	0.5959
		T	167 (76.6)	78 (86.7)	0.504 (0.254-0.998)	167 (76.6)	48 (88.9)	0.409 (0.166-1.012)	167 (76.6)	32 (80)	0.819 (0.355-1.888)
		C	51 (23.4)	12 (13.3)	**0.0465**	51 (23.4)	6 (11.1)	0.0471	51 (23.4)	8 (20)	0.6384
hsa-mir-4432 rs243080	Chr.: 2 pre-miRNA	CC	33 (31.1)	10 (22.7)	Recesive	33 (31.1)	6 (23.1)	Recesive	33 (31.1)	4 (20.0)	Recesive
		CT	51 (48.1)	17 (38.6)	2.40 (1.12-5.18)	51 (48.1)	11 (42.3)	2.02 (0.79-5.15)	51 (48.1)	8 (40.0)	2.55 (0.93-6.99)
		TT	22 (20.8)	17 (38.6)	**0.0261/0.0230**	22 (20.8)	9 (34.6)	0.1482	22 (20.8)	8 (40.0)	0.0769
		C	117 (55.2)	37 (42)	1.698 (1.027-2.806)	117 (55.2)	23 (44.2)	1.553 (0.843-2.859)	117 (55.2)	16 (40)	1.847 (0.928-3.676)
		T	95 (44.8)	51 (58)	**0.0381**	95 (44.8)	29 (55.8)	0.1560	95 (44.8)	24 (60)	0.0776
hsa-mir-449c rs35770269	Chr.: 5 in_seed	AA	55 (50.5)	14 (31.1)	Dominant	55 (50.5)	12 (44.4)	Recesive	55 (50.5)	3 (15.0)	Dominant
		AT	39 (35.8)	27 (60.0)	2.26 (1.08-4.70)	39 (35.8)	14 (51.9)	0.24 (0.03-1.91)	39 (35.8)	14 (70.0)	5.77 (1.60-20.83)
		TT	15 (13.8)	4 (8.9)	**0.0264/0.0351**	15 (13.8)	1 (3.7)	0.1046	15 (13.8)	3 (15.0)	**0.0020/0.0029**
		A	149 (68.3)	55 (61.1)	1.374 (0.824-2.291)	149 (68.3)	38 (70.4)	0.909 (0.475-1.742)	149 (68.3)	20 (50)	2.159 (1.091-4.272)
		T	69 (31.7)	35 (38.9)	0.2219	69 (31.7)	16 (29.6)	0.7742	69 (31.7)	20 (50)	**0.0248**
hsa-mir-5197 rs2042253	Chr.: 5 pre-miRNA	AA	59 (53.6)	32 (72.7)	Dominant	59 (53.6)	20 (76.9)	Dominant	59 (53.6)	13 (65.0)	Dominant
		AG	48 (43.6)	11 (25.0)	0.43 (0.20-0.93)	48 (43.6)	5 (19.2)	0.35 (0.13-0.93)	48 (43.6)	7 (35.0)	0.62 (0.23-1.68)
		GG	3 (2.7)	1 (2.3)	**0.0269/0.0175**	3 (2.7)	1 (3.8)	**0.0259/0.0187**	3 (2.7)	0 (0.0)	0.3429
		A	166 (75.5)	75 (85.2)	0.533 (0.274-1.035)	166 (75.5)	45 (86.5)	0.478 (0.204-1.123)	166 (75.5)	33 (82.5)	0.652 (0.273-1.559)
		G	54 (24.5)	13 (14.8)	0.0604	54 (24.5)	7 (13.5)	0.0848	54 (24.5)	7 (17.5)	0.3334

Abbreviations: B-ALL, B cell acute lymphoblastic leukemia; VCR, vincristine; miRNA, microRNA; SNP, single nucleotide polymorphism; Tox, toxicity; OR, odds ratio; CI, confidence interval; D corredted P, dose corrected P-value; Chr, chromosome.

Notes: Bold denote significant P-values.

Table 17. List of the twelve miRNA SNPs associated to VCR-induced global neurotoxicity in childhood ALL. (Continuation).

miRNA SNP	Position Localization	Genotype /Allele	Grades 1-4 Tox (n=175)		Model OR. (95% CI) P-value/D corrected P	Grades 1-2 Tox (n=152)		Model OR. (95% CI) P-value/D corrected P	Grades 3-4 Tox (n=144)		Model OR. (95% CI) P-value/D corrected P
			No tox N=120	Tox N=55		No tox N=120	Tox N=32		No tox N=120	Tox N=24	
hsa-mir-1208 rs2648841	Chr.: 8 pre-miRNA	CC	84 (78.5)	27 (61.4)	Dominant	84 (78.5)	15 (57.7)	Dominant	84 (78.5)	12 (60.0)	Dominant
		AC	20 (18.7)	16 (36.4)	2.30 (1.07-4.93)	20 (18.7)	11 (42.3)	2.68 (1.08-6.62)	20 (18.7)	7 (35.0)	2.43 (0.89-6.66)
		AA	3 (2.8)	1 (2.3)	**0.0336/0.0237**	3 (2.8)	0 (0.0)	**0.0358/0.0243**	3 (2.8)	1 (5.0)	0.0905
		C	188 (87.9)	70 (79.5)	1.859 (0.96-3.6)	188 (87.9)	41 (78.8)	1.94 (0.888-4.239)	188 (87.9)	31 (77.5)	2.099 (0.899-4.901)
		A	26 (12.1)	18 (20.5)	0.0630	26 (12.1)	11 (21.2)	0.0924	26 (12.1)	9 (22.5)	0.0813
hsa-mir-6128 rs67042258	Chr.: 11 pre-miRNA	GG	56 (50.9)	20 (44.4)	Recesive	56 (50.9)	10 (37.0)	Recesive	56 (50.9)	9 (45.0)	Recesive
		AG	43 (39.1)	25 (55.6)	0 (0.0)	43 (39.1)	17 (63.0)	0 (0.0)	43 (39.1)	11 (55.0)	0 (0,0)
		AA	11 (10.0)	0 (0.0)	**0.0347/0.0047**	11 (10.0)	0 (0.0)	0.1211/0.0234	11 (10.0)	0 (0.0)	0.2130/0.0487
		G	155 (70.5)	65 (72.2)	0.917 (0.532-1.581)	155 (70.5)	37 (68.5)	1.096 (0.576-2.084)	155 (70.5)	29 (72.5)	0.905 (0.426-1.919)
		A	65 (29.5)	25 (27.8)	0.7556	65 (29.5)	17 (31.5)	0.7807	65 (29.5)	11 (27.5)	0.7936
hsa-mir-6504 rs74469188	Chr.: 16 in_mature	TT	75 (81.5)	29 (65.9)	Dominant	75 (81.5)	18 (69.2)	Dominant	75 (81.5)	13 (65.0)	Dominant
		CT	17 (18.5)	13 (29.5)	2.28 (1.01-5.16)	17 (18.5)	7 (26.9)	1.96 (0.73-5.25)	17 (18.5)	6 (30.0)	2.38 (0.82-6.85)
		CC	0 (0.0)	2 (4.5)	**0.0488/0.0321**	0 (0.0)	1 (3.8)	0.1896	0 (0.0)	1 (5.0)	0.1189
		T	167 (90.8)	71 (80.7)	2.352 (1.137-4.868)	167 (90.8)	43 (82.7)	2.056 (0.857-4.931)	167 (90.8)	32 (80)	2.456 (0.977-6.172)
		C	17 (9.2)	17 (19.3)	**0.0187**	17 (9.2)	9 (17.3)	0.1008	17 (9.2)	8 (20)	0.0501
hsa-mir-577 rs34115976	Chr.: 4 pre-miRNA	CC	73 (67.6)	26 (57.8)	Recesive	73 (67.6)	15 (55.6)	Recesive	73 (67.6)	12 (60.0)	Dominant
		CG	33 (30.6)	15 (33.3)	5.17 (0.91-29.32)	33 (30.6)	8 (29.6)	9.22 (1.59-53.37)	33 (30.6)	8 (40.0)	1.39 (0.52-3.71)
		GG	2 (1.9)	4 (8.9)	0.0541/0.0272	2 (1.9)	4 (14.8)	**0.0107/0.0034**	2 (1.9)	0 (0.0)	0.5137
		C	179 (82.9)	67 (74.4)	1.661 (0.919-3)	179 (82.9)	38 (70.4)	2.037 (1.029-4.033)	179 (82.9)	32 (80)	1.209 (0.516-2.835)
		G	37 (17.1)	23 (25.6)	0.0907	37 (17.1)	16 (29.6)	**0.0386**	37 (17.1)	8 (20)	0.6613
hsa-mir-4642 rs67182313	Chr.: 6 pre-miRNA	AA	71 (65.1)	32 (71.1)	Dominant	71 (65.1)	15 (55.6)	Recesive	71 (65.1)	18 (90.0)	Dominant
		AG	35 (32.1)	11 (24.4)	0.76 (0.36-1.62)	35 (32.1)	10 (37.0)	2.83 (0.45-17.82)	35 (32.1)	2 (10.0)	0.21 (0.05-0.94)
		GG	3 (2.8)	2 (4.4)	0.4707	3 (2.8)	2 (7.4)	0.2912	3 (2.8)	0 (0.0)	**0.0162/0.0168**
		A	177 (81.2)	75 (83.3)	0.863 (0.451-1.654)	177 (81.2)	40 (74.1)	1.511 (0.753-3.034)	177 (81.2)	38 (95)	0.227 (0.053-0.980)
		G	41 (18.8)	15 (16.7)	0.6578	41 (18.8)	14 (25.9)	0.2436	41 (18.8)	2 (5)	**0.0312**
mir-1908 rs174561	Chr.: 11 pre-miRNA	TT	64 (62.1)	20 (45.5)	Dominant	64 (62.1)	14 (53.8)	Recesive	64 (62.1)	7 (35.0)	Dominant
		CT	33 (32.0)	23 (52.3)	1.97 (0.96-4.02)	33 (32.0)	12 (46.2)	0 (0,0)	33 (32.0)	12 (60.0)	3.05 (1.12-8.30)
		CC	6 (5.8)	1 (2.3)	0.0620/0.0413	6 (5.8)	0 (0.0)	0.3472	6 (5.8)	1 (5.0)	**0.0252/0.0095**
		T	161 (78.2)	63 (71.6)	1.42 (0.804-2.508)	161 (78.2)	40 (76.9)	1.073 (0.52-2.216)	161 (78.2)	26 (65)	1.926 (0.929-3.993)
		C	45 (21.8)	25 (28.4)	0.2262	45 (21.8)	12 (23.1)	0.8482	45 (21.8)	14 (35)	0.0746

Abbreviations: B-ALL, B cell acute lymphoblastic leukemia; VCR, vincristine; miRNA, microRNA; SNP, single nucleotide polymorphism; Tox, toxicity; OR, odds ratio; CI, confidence interval; D corredted P, dose corrected P-value; Chr, chromosome.

Notes: Bold denote significant P-values.

Bioinformatic analysis

- *Effect of genetic variants on the pre-miRNA secondary structure*

The SNP rs12402181 was located in the seed region of miR-3117-3p. The change from G to A allele did not show either an energy change or alteration in the secondary structure (Figure 18, a). For rs7896283 in miR-4481, located in pre-miRNA sequence, the substitution of the T allele for a C allele induced an energy change (ΔΔG) of -1.2 kcal/mol (from −17.3 to −18.5 kcal/mol). This allelic change also induced a modification on the secondary structure (Figure 18, b). Regarding rs35650931 in miR-6076, also located in the pre-miRNA sequence, the substitution of the G allele for a C allele induced a modest energy change of 0.3 kcal/mol (from −41.20 to −40.90 kcal/mol) and an alteration on the secondary structure (Figure 18, c).
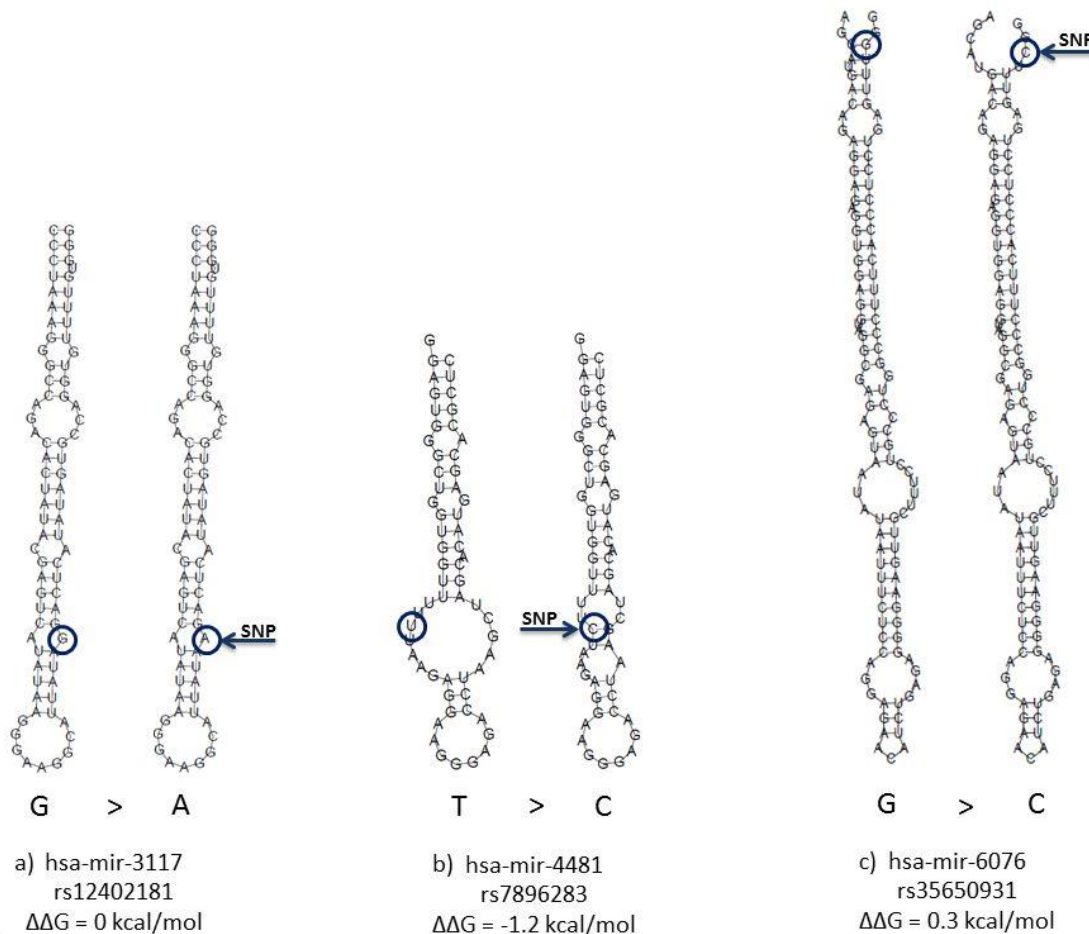
Figure 18. Energy change (ΔΔG) and minimum free-energy structures of the three most significant miRNA SNPs (a. miR-3117, b. miR-4481 and c. miR-6076) due to the presence of different alleles, extracted from RNAfold web tool. For each miRNA, the SNP alleles are marked with a circle and the arrow points out the variant allele.

- *Target prediction and pathway analysis*

Following the first approach, we searched for miRNA targets among VCR PK/PD genes. For mir-3117 we found two transporter genes, *ABCC1* and *RALBP1* (Figure 17) whereas none for miR-4481 or miR-6076.

In a second approach for miR-4481 or miR-6076, pathway enrichment analyses were performed in order to detect other neurotoxicity-related genes. For miR-4481, we found five possible pathways, and four of them were related to the nervous system (Table 18). The axon-guidance pathway was the most significant pathway and was identified by both Reactome ($p=1.36 \times 10^{-7}$) and KEGG ($p=7.83 \times 10^{-6}$) databases. MiR-4481 targeted a total of 40 genes in this pathway (Table 19). The other two pathways were glutamatergic-synapse and Neuronal system. Regarding miR-6076, we did not find any pathway apparently related with neurotoxicity.

Table 18. List of the five pathways predicted by pathway enrichment analysis in Consensus Path DB for miR-4481.

No.	Pathway	Database	p-value	q-value	Set Size	Candidates contained
1	Axon guidance	Reactome	1.36e-07	0.000146	487	33 (6.8%)
2	Developmental Biology	Reactome	4.59e-07	0.000246	748	42 (5.6%)
3	Axon guidance - Homo sapiens (human)	KEGG	7.83e-06	0.0028	177	16 (9.0%)
4	Glutamatergic synapse - Homo sapiens (human)	KEGG	4.26e-07	0.00023	114	12 (10.5%)
5	Neuronal System	Reactome	5.94e-05	0.0127	251	22 (6.3%)

Table 19. In-silico predicted Axon guidance pathway genes that overlap with miR-4481 target genes according to Reactome or KEGG databases.

Entrez-gene	Gene name	Database
8829	NRP1 : neuropilin 1	Reactome, KEGG
2046	EPHA8 : EPH receptor A8	Reactome, KEGG
5362	PLXNA2 : plexin A2	Reactome, KEGG
1943	EFNA2 : ephrin A2	Reactome, KEGG
1944	EFNA3 : ephrin A3	Reactome, KEGG
10298	PAK4 : p21 (RAC1) activated kinase 4	Reactome, KEGG
3897	L1CAM : L1 cell adhesion molecule	Reactome, KEGG
9901	SRGAP3 : SLIT-ROBO Rho GTPase activating protein 3	Reactome, KEGG
137970	UNC5D : unc-5 netrin receptor D	Reactome, KEGG
200734	SPRED2 : sprouty related EVH1 domain containing 2	Reactome
7408	VASP : vasodilator-stimulated phosphoprotein	Reactome
9260	PDLIM7 : PDZ and LIM domain 7	Reactome
1641	DCX : doublecortin	Reactome
6324	SCN1B : sodium voltage-gated channel beta subunit 1	Reactome
4629	MYH11 : myosin heavy chain 11	Reactome
9462	RASAL2 : RAS protein activator like 2	Reactome
8986	RPS6KA4 : ribosomal protein S6 kinase A4	Reactome
5156	PDGFRA : platelet derived growth factor receptor alpha	Reactome
8831	SYNGAP1 : synaptic Ras GTPase activating protein 1	Reactome
2906	GRIN2D : glutamate ionotropic receptor NMDA type subunit 2D	Reactome
8515	ITGA10 : integrin subunit alpha 10	Reactome
2263	FGFR2 : fibroblast growth factor receptor 2	Reactome
8874	ARHGEF7 : Rho guanine nucleotide exchange factor 7	Reactome
9826	ARHGEF11 : Rho guanine nucleotide exchange factor 11	Reactome
10048	RANBP9 : RAN binding protein 9	Reactome
55800	SCN3B : sodium voltage-gated channel beta subunit 3	Reactome
4627	MYH9 : myosin heavy chain 9	Reactome
64283	ARHGEF28 : Rho guanine nucleotide exchange factor 28	Reactome
784	CACNB3 : calcium voltage-gated channel auxiliary subunit beta 3	Reactome
6327	SCN2B : sodium voltage-gated channel beta subunit 2	Reactome
28964	GIT1 : GIT ArfGAP 1	Reactome
2886	GRB7 : growth factor receptor bound protein 7	Reactome
8682	PEA15 : phosphoprotein enriched in astrocytes 15	Reactome
5293	PIK3CD : phosphatidylinositol-4,5-bisphosphate 3-kinase catalytic subunit delta	KEGG
6405	SEMA3F : semaphorin 3F	KEGG
6387	CXCL12 : C-X-C motif chemokine ligand 12	KEGG
10500	SEMA6C : semaphorin 6C	KEGG
7976	FZD3 : frizzled class receptor 3	KEGG
57715	SEMA4G : semaphorin 4G	KEGG
5535	PPP3R2 : protein phosphatase 3 regulatory subunit B, beta	KEGG

DISCUSSION

In the present study, we have analyzed the correlation of 160 SNPs in 154 miRNAs and VCR-neurotoxicity during induction phase, in 155 children with ALL homogeneously treated with the Spanish LAL-SHOP 94/95/2005 protocols. The most interesting and significant result was found for rs12402181 in miR-3117, whose AA genotype could increase the efflux of VCR from the cells, through *ABCC1* and *RALBP1* gene. Additionally, although less significant, a second interesting SNP that could be involved in the regulation of the axon guidance pathway genes was identified, rs7896283 in miR-4481.

The most significant association in this study was found for the rs12402181 in mir-3117, in which AG/AA genotypes showed a 0.2-fold decreased risk of peripheral neurotoxicity under a dominant model. This significant result was consistently obtained in all the analyses. This SNP is located in the seed region of miR-3117-3p, therefore, the change of the G allele for the A allele could affect the accurate recognition of its target mRNA sequences. *In silico* analysis determined that miR-3117-3p targeted two VCR transport genes, *ABCC1* and *RALBP1*. *ABCC1* gene encodes the multidrug resistance protein 1 (MRP1), which mediates the ATP-dependent efflux of a broad range of antineoplastic agents, including vinca alkaloids such as VCR (Franca et al., 2017; Kunicka and Soucek, 2014). Actually, polymorphisms in *ABCC1* that could affect its function have been already associated with VCR-related neuropathy (Franca et al., 2017; Lopez-Lopez et al., 2016). On the other hand, the second putative target of miR-3117-3p, *RALBP1*, was identified as a highly active protein involved in the process of removing vinca alkaloids (Awasthi et al., 2005). It has been reported that the inhibition of RALBP1 was associated with drug accumulation and increased cytotoxicity (Drake et al., 2007). Therefore, the rs12402181 A variant allele could affect the binding of miR-3117-3p with ABCC1 and RALBP1 mRNAs and in turn, increase their expression. A higher expression of *ABCC1* and *RALBP1* genes could result in an elevated VCR efflux from the cell, explaining the decreased risk of VCR-induced neurotoxicity. Even though the effect of rs12402181 seems to decrease cells sensitivity to VCR, when overall survival (OS) and event free survival (EFS) were analyzed no association was found (data not shown).

The second most significant result was observed for rs7896283 CT/CC genotypes in miR-4481, which showed a 2.62-fold increase risk of neurotoxicity in induction phase (grades 1-4) under a dominant model. This SNP also showed significant association with high neurotoxicity (grades 3-4), and remained significant when global analyses were performed. The rs7896283 C allele is located in the pre-miRNA sequence and the substitution of the T allele for a C allele induces a

negative energy change. This change could turn the miRNA hairpin from an unstable to a stable status (ΔΔG=-1.2 kcal/mol). It has been proposed that the increase in the structure stability of the pre-miRNA may enhance the product of the mature miRNA (Gong et al., 2012), and thus, it could lead to a decreased expression of its targets. In this case, we did not find genes related to VCR PK or PD targeted by miR-4481. However, by pathway enrichment analysis, we identified five putative pathways that could be involved in VCR-induced neurotoxicity. Interestingly, four out of these five pathways were related to the nervous system. In addition, both KEGG and Reactome databases predicted axon guidance as the most significant pathway targeted by miR-4481. Axon guidance is involved in spontaneous regeneration of peripheral nerves when they are damaged (Chiono and Tonda-Turo, 2015). Therefore, the risk rs7896283 C allele may increase miR-4481 stability and in consequence its mature levels, leading to a decrease in the expression of its target genes. Then, less expression in genes involved in peripheral nerves regeneration could be the explanation of the increased peripheral neuropathy.

Other 10 SNPs showing significant association with VCR-induced neurotoxicity during induction phase for which we could not explain its function, such as rs35650931 in mir-6076, were found (Table 16).

This study has some limitations that might be addressed, such as the relatively high failure rate in genotyping technique. However, this high chance of failure was accepted from the beginning of the study, because despite the predicted low score for genotyping, no other design option to amplify the polymorphisms in question was possible. Another possible weakness is that the SNPs did not reach a significant P-value when FDR was applied. However, it is interesting to point out that rs12402181 in mir-3117, after FDR correction, almost reach a significant p-value (p=0.06), and this association was consistent in all the analysis. Moreover, the statistical power to detect a degree of interaction between this SNP and neurotoxicity was 70 %, which gives strength to our results. In contrast, the statistical power for the second significant result in this study was only of 54 %. Finally, we have to take into account the inaccuracy of the prediction algorithms of the databases used to determine the target gene and pathways,(Akhtar et al., 2016; Lee et al., 2015) but nowadays this limitation has to be assumed.

In this study, we identified rs12402181 in the seed region of miR-3117-3p and rs7896283 in pre-mature sequence of miR-4481 significantly associated with VCR-induced neurotoxicity. In miR-3117-3p, the SNP could cause the loss of binding with its target genes *ABCC1* and *RALBP1,* which could affect VCR efflux. In miR-4481, the SNP could alter miRNA levels and therefore, affect the expression of genes involved in peripheral nerves regeneration. These findings point out the

possible involvement of two SNPs in miRNAs associated with VCR-related neurotoxicity. It would be of great interest to replicate these findings in a larger cohort of children with B-ALL.

ACKNOWLEDGEMENTS

CONFLICT OF INTERESTS

The authors declare no conflict of interest

REFERENCIAS

Akhtar, M.M., Micolucci, L., Islam, M.S., Olivieri, F., and Procopio, A.D. (2016). Bioinformatic tools for microRNA dissection. Nucleic Acids Res. 44, 24–44.

Awasthi, S., Hallene, K.L., Fazio, V., Singhal, S.S., Cucullo, L., Awasthi, Y.C., Dini, G., and Janigro, D. (2005). RLIP76, a non-ABC transporter, and drug resistance in epilepsy. BMC Neurosci. 6, 61.

Benjamini, Y., Drai, D., Elmer, G., Kafkafi, N., and Golani, I. (2001). Controlling the false discovery rate in behavior genetics research. Behav. Brain Res. 125, 279–284.

Carozzi, V.A., Canta, A., and Chiorazzi, A. (2015). Chemotherapy-induced peripheral neuropathy: What do we know about mechanisms? Neurosci. Lett. 596, 90–107.

Ceppi, F., Langlois-Pelletier, C., Gagne, V., Rousseau, J., Ciolino, C., De Lorenzo, S., Kevin, K.M., Cijov, D., Sallan, S.E., Silverman, L.B., et al. (2014). Polymorphisms of the vincristine pathway and response to treatment in children with childhood acute lymphoblastic leukemia. Pharmacogenomics 15, 1105–1116.

Chiono, V., and Tonda-Turo, C. (2015). Trends in the design of nerve guidance channels in peripheral nerve tissue engineering. Prog. Neurobiol. 131, 87–104.

Diouf, B., Crews, K.R., Lew, G., Pei, D., Cheng, C., Bao, J., Zheng, J.J., Yang, W., Fan, Y., Wheeler, H.E., et al. (2015). Association of an inherited genetic variant with vincristine-related peripheral neuropathy in children with acute lymphoblastic leukemia. JAMA 313, 815–823.

Drake, K.J., Singhal, J., Yadav, S., Nadkar, A., Pungaliya, C., Singhal, S.S., and Awasthi, S. (2007). RALBP1/RLIP76 mediates multidrug resistance. Int. J. Oncol. 30, 139–144.

Dweep, H., Sticht, C., Pandey, P., and Gretz, N. (2011). miRWalk--database: prediction of possible miRNA binding sites by "walking" the genes of three genomes. J. Biomed. Inform. 44, 839–847.

Egbelakin, A., Ferguson, M.J., MacGill, E.A., Lehmann, A.S., Topletz, A.R., Quinney, S.K., Li, L., McCammack, K.C., Hall, S.D., and Renbarger, J.L. (2011). Increased risk of vincristine neurotoxicity associated with low CYP3A5 expression genotype in children with acute lymphoblastic leukemia. Pediatr. Blood Cancer 56, 361–367.

Fabregat, A., Sidiropoulos, K., Garapati, P., Gillespie, M., Hausmann, K., Haw, R., Jassal, B., Jupe, S., Korninger, F., McKay, S., et al. (2016). The Reactome pathway Knowledgebase. Nucleic Acids Res. 44, D481-7.

Franca, R., Rebora, P., Bertorello, N., Fagioli, F., Conter, V., Biondi, A., Colombini, A., Micalizzi, C., Zecca, M., Parasole, R., et al. (2017). Pharmacogenetics and induction/consolidation therapy toxicities in acute lymphoblastic leukemia patients treated with AIEOP-BFM ALL 2000 protocol. Pharmacogenomics J. 17, 4–10.

Gong, J., Tong, Y., Zhang, H.-M., Wang, K., Hu, T., Shan, G., Sun, J., and Guo, A.-Y. (2012). Genome-wide identification of SNPs in microRNA genes and the SNP effects on microRNA target binding and biogenesis. Hum. Mutat. 33, 254–263.

Gruber, A.R., Lorenz, R., Bernhart, S.H., Neubock, R., and Hofacker, I.L. (2008). The Vienna RNA websuite. Nucleic Acids Res. 36, W70-4.

Gutierrez-Camino, A., Martin-Guerrero, I., Lopez-Lopez, E., Echebarria-Barona, A., Zabalza, I., Ruiz, I., Guerra-Merino, I., and Garcia-Orad, A. (2016). Lack of association of the CEP72 rs924607 TT genotype with vincristine-related peripheral neuropathy during the early phase of pediatric acute lymphoblastic leukemia treatment in a Spanish population. Pharmacogenet. Genomics 26, 100–102.

Gutierrez-Camino, A., Oosterom, N., den Hoed, M.A.H., Lopez-Lopez, E., Martin-Guerrero, I., Pluijm, S.M.F., Pieters, R., de Jonge, R., Tissing, W.J.E., Heil, S.G., et al. (2017). The miR-1206 microRNA variant is associated with methotrexate-induced oral mucositis in pediatric acute lymphoblastic leukemia. Pharmacogenet. Genomics 27, 303–306.

Hartman, A., van Schaik, R.H.N., van der Heiden, I.P., Broekhuis, M.J.C., Meier, M., den Boer, M.L., and Pieters, R. (2010). Polymorphisms in genes involved in vincristine pharmacokinetics or pharmacodynamics are not related to impaired motor performance in children with leukemia. Leuk. Res. 34, 154–159.

Iparraguirre, L., Gutierrez-Camino, A., Umerez, M., Martin-Guerrero, I., Astigarraga, I., Navajas, A., Sastre, A., Garcia de Andoin, N., and Garcia-Orad, A. (2016). MiR-pharmacogenetics of methotrexate in childhood B-cell acute lymphoblastic leukemia. Pharmacogenet. Genomics 26, 517–525.

Johnston, W.T., Lightfoot, T.J., Simpson, J., and Roman, E. (2010). Childhood cancer survival: a report from the United Kingdom Childhood Cancer Study. Cancer Epidemiol. 34, 659–666.

Kamburov, A., Stelzl, U., Lehrach, H., and Herwig, R. (2013). The ConsensusPathDB interaction database: 2013 update. Nucleic Acids Res. 41, D793-800.

Kanehisa, M., Furumichi, M., Tanabe, M., Sato, Y., and Morishima, K. (2017). KEGG: new perspectives on genomes, pathways, diseases and drugs. Nucleic Acids Res. 45, D353–D361.

Kunicka, T., and Soucek, P. (2014). Importance of ABCC1 for cancer therapy and prognosis. Drug Metab. Rev. 46, 325–342.

Lee, Y.J.D., Kim, V., Muth, D.C., and Witwer, K.W. (2015). Validated MicroRNA Target Databases: An Evaluation. Drug Dev. Res. 76, 389–396.

Li, M.-P., Hu, Y.-D., Hu, X.-L., Zhang, Y.-J., Yang, Y.-L., Jiang, C., Tang, J., and Chen, X.-P. (2016). MiRNAs and miRNA Polymorphisms Modify Drug Response. Int. J. Environ. Res. Public Health 13.

Lopez-Lopez, E., Gutierrez-Camino, A., Bilbao-Aldaiturriaga, N., Pombar-Gomez, M., Martin-Guerrero, I., and Garcia-Orad, A. (2014). Pharmacogenetics of childhood acute lymphoblastic leukemia. Pharmacogenomics 15, 1383–1398.

Lopez-Lopez, E., Gutierrez-Camino, A., Astigarraga, I., Navajas, A., Echebarria-Barona, A., Garcia-Miguel, P., Garcia de Andoin, N., Lobo, C., Guerra-Merino, I., Martin-Guerrero, I., et al. (2016). Vincristine pharmacokinetics pathway and neurotoxicity during early phases of treatment in pediatric acute lymphoblastic leukemia. Pharmacogenomics 17, 731–741.

Moore, A.S., Norris, R., Price, G., Nguyen, T., Ni, M., George, R., van Breda, K., Duley, J., Charles, B., and Pinkerton, R. (2011). Vincristine pharmacodynamics and pharmacogenetics in children with cancer: a limited-sampling, population modelling approach. J. Paediatr. Child Health 47, 875–882.

Nakajima, M., and Yokoi, T. (2011). MicroRNAs from biology to future pharmacotherapy: regulation of cytochrome P450s and nuclear receptors. Pharmacol. Ther. 131, 330–337.

Plasschaert, S.L.A., Groninger, E., Boezen, M., Kema, I., de Vries, E.G.E., Uges, D., Veerman, A.J.P., Kamps, W.A., Vellenga, E., de Graaf, S.S., et al. (2004). Influence of functional polymorphisms of the MDR1 gene on vincristine pharmacokinetics in childhood acute lymphoblastic leukemia. Clin. Pharmacol. Ther. 76, 220–229.

Postma, T.J., Benard, B.A., Huijgens, P.C., Ossenkoppele, G.J., and Heimans, J.J. (1993). Long-term effects of vincristine on the peripheral nervous system. J. Neurooncol. 15, 23–27.

Sambrook, J, R.D. (2001). Molecular cloning: a laboratory manual (New York: NY: Cold Spring Harbor Laboratory Press).

Sullivan, K.M., Dean, A., and Soe, M.M. (2009). OpenEpi: a web-based epidemiologic and statistical calculator for public health. Public Health Rep. 124, 471–474.

Pharmacoepigenetics in childhood acute lymphoblastic leukemia: Involvement of miRNA polymorphisms in hepatotoxicity

Umerez, Maitane[1*], PhD student; Gutierrez-Camino, Ángela[1*], PhD; Santos, Borja[1], PhD; Martín-Guerrero, Idoia[1], PhD; García de Andoin, Nagore[2,3], MD; Sastre, Ana[4],MD; Navajas, Aurora[5,6]PhD; Astigarraga, Itziar[3,5,6], PhD; Garcia-Orad, Africa[1,6], PhD.

*These authors share first authorship

[1]Department of Genetics, Physic Anthropology and Animal Physiology, University of the Basque Country, UPV/EHU, Leioa, Spain; [2]Department of Pediatrics, University Hospital Donostia, San Sebastian, Spain; [3]Department of Pediatrics, University of the Basque Country, UPV/EHU, Leioa, Spain, [4]Department of Oncohematology, University Hospital La Paz, Madrid, Spain; [5]Department of Pediatrics, University Hospital Cruces, Barakaldo, Spain; [6]BioCruces Health Research Institute, Barakaldo, Spain.

Abstract

Aims: Hepatotoxicity is one of the most common drug-related toxicity during the treatment of childhood acute lymphoblastic leukemia (ALL). Many genes involved in liver-specific signaling pathways are tightly controlled by miRNAs, and miRNA function could be modulated by SNPs. In consequence, we hypothesized that variants in miRNAs could be associated with drug-induced hepatotoxicity. **Methods:** We analyzed 213 SNPs in 206 miRNAs in a cohort of 179 children with ALL homogeneously treated. **Results:** rs2648841 in miR-1208 was the most significant SNP during consolidation phase after FDR correction, probably through an effect of its target genes *DHFR*, *MTR* and *MTHFR*. **Conclusions:** These results point out the possible involvement of SNPs in miRNAs in toxicity to chemotherapy in children with ALL.

Keywords: Hepatotoxicity, SNPs, miRNAs, childhood acute lymphoblastic leukemia, chemotherapy, methotrexate.

INTRODUCTION

Acute lymphoblastic leukemia (ALL) is the most common childhood cancer, accounting for 30% of all pediatric malignancies in developed countries (Johnston et al., 2010). In the last decades, survival has increased, approaching and even exceeding 90% in some countries, due, in part, to the progress made in treatment protocols (Pui et al., 2015). However, despite the clinical success of therapy, patients often suffer from toxicity, requiring a dose reduction or treatment discontinuation (Salazar et al., 2012), which may affect survival. In this context, it has gained relevance to reduce toxicity of cancer treatment (den Hoed et al., 2015).

One of the most common drug-related toxicities in childhood ALL patients is hepatotoxicity (Liu et al., 2017).This toxicity is partly defined as an increase of serum aminotransferases as result of hepatocyte cell death induced by drugs. Approximately 66.5% of childhood ALL patients show liver toxicity at some point during ALL treatment (Ladas et al., 2010). The point in which hepatotoxicity is developed could depend on the drug administered (Iorga et al., 2017). In fact, in the induction phase, Liu and colleagues linked hepatotoxicity to asparaginase (ASP) exposure whereas on the other hand, during consolidation phase, high-dose methotrexate (MTX) is well-known to cause liver toxicity (Liu et al., 2017).

Independently of when it appears, one of the challenges in medicine is to predict which patients are going to develop drug-induced hepatotoxicity in order to adjust the treatment in advance. In this line, pharmacogenetic studies have reported associations between genetic variants and hepatotoxicity during the treatment of childhood patients with ALL (Erčulj et al., 2012; Gregers et al., 2010, 2015b; Liu et al., 2017). For instance, Liu and colleagues in a Genome Wide Association Study (GWAS) identified the SNP rs738409 in *PNPLA3* strongly associated with hepatotoxicity in children with ALL during the induction (Liu et al., 2017), result recently replicated (Gutierrez-Camino et al., 2017a). Regarding consolidation, considering MTX as the main cause of hepatotoxicity, most of the studies focused their analysis on few variants in genes of pharmacokinetic or pharmacodynamics pathways of MTX, such as *RFC1* (80G>A) (Gregers et al., 2010), *ABCB1* (3435C>T) (Gregers et al., 2015a) and *MTHFR* (677C>T and 1298A>C) (Umerez et al., 2017), with no clear markers for hepatic toxicity. In this context, pharmacoepigenetics arises as a tool to identify new predictive markers. This recent subdiscipline includes the study of microRNA (miRNAs), non-coding RNAs that regulate gene expression at the post-trancriptional level, and entails that increased or lowered miRNA expression may affect genes that promote drug efficacy or inhibit drug function (Rukov et al., 2014). Genetic variants in miRNAs can modify their levels or function and consequently, might affect the expression of

their target genes. In fact, several studies have already found association between drug-related toxicities and SNPs in miRNAs (Amstutz et al., 2015; Gutierrez-Camino et al., 2017b; Iparraguirre et al., 2016; Zhan et al., 2012).

At present, it is known that many genes involved in liver-specific signaling pathways, including those involved in drug metabolism and transport, are tightly controlled by miRNAs (Lauschke et al., 2017). In consequence, we can hypothesize that variants in miRNAs targeting ASP-related genes in induction and MTX-related genes in consolidation could be also associated with drug-induced hepatotoxicity in children with B-cell precursor acute lymphoblastic leukemia (B-ALL). In this study, we analyzed all the SNPs in miRNAs (minor allele frequency (MAF) ≥0.01) which could be associated with hepatotoxicity in a large cohort of Spanish children with B-ALL homogeneously treated.

MATERIAL AND METHODS

Patients

This is a retrospective study including 179 Spanish children diagnosed with B-ALL at the Pediatric Oncology Units of three Spanish hospitals (University Hospital Cruces, University Hospital Donostia and University Hospital La Paz from 2000 to 2013). Written informed consent was obtained from all patients or their parents before sample collection. This study obtained the approval (CEISH/102R/2011) of the University of the Basque Country (UPV/EHU).

Treatment and toxicity evaluation

All the patients included in the study were homogeneously treated with the Spanish standard LAL-SHOP 94/99/2005 protocols. At the induction phase, 10 doses of 5,000-15,000 μ/m^2 of asparaginase, depending on treatment arm, were administered. This phase also included vincristine, daunorubicin, prednisone, cyclophosphamide and intrathecal methotrexate-cytarabine-hydrocortisone therapy. High-risk patients in the LAL/SHOP 99 also received a single dose of 3 g/m^2 of methotrexate on day +15. In the consolidation phase, patients were treated with three high MTX doses (each dose consisted of 3 or 5 g/m^2), 6-mercaptopurine, four doses of cytarabine and four doses of triple intrathecal therapy.

Toxicity data were collected blinded to genotypes from the patients' medical files by the same two expert researchers in all cases. We focused our analysis on hepatic toxicity measured as elevation of both aspartate aminotransferase (AST) and alanine aminotransferase (ALT)

following the guidelines valid at the time of inclusion of patients and data collection (Bénichou, 1990; Robles-Diaz et al., 2014). These hepatic enzymes are measured, at least, once a week during induction and, during consolidation, it is mandatory before MTX administration. If transaminases levels are high, the treatment is delayed, especially at consolidation phase. Hepatotoxicity was graded according to the Spanish Society of Pediatric Hematology and Oncology standards, adapted from the WHO criteria (See Table 8). Hepatotoxicity was considered from grade 2 to 4 (>2.6 x Upper Limit of Normal, ULN) and high hepatotoxicity from grade 3 to 4 (>5.1 x ULN). The highest value of both AST and ALT in plasma at induction and consolidation phases was recorded. Additionally, because hepatic damage can be also detected by elevation of bilirubin (BI), these data were also collected. BI toxicity was considered from grade 1 to 4 (>1.1 x ULN) (See Table 8). The highest value at induction and consolidation phases was recorded. Other data such as sex and age were systematically recorded from the clinical records.

Genes and polymorphism selection

Taking into account that miRNAs targets are not completely defined nowadays and that any miRNA could be implicated direct or indirectly in the regulation of genes involved in hepatotoxicity development, we selected all the miRNA genes that have SNPs described at the time of the study (May 2014). Of a total of 1910 SNPs in 969 miRNAs, we selected those SNPs with a MAF>0.01 in European/Caucasoid populations. For the SNP selection, we used mirbase (http://www.mirbase.org/),   miRNA   SNIPER (http://bioinfo.life.hust.edu.cn/miRNASNP2/index.php),   and   dbSNP (http://www.ncbi.nlm.nih.gov/SNP/) databases, as well as literature review (See Table 11).

Genotyping

Genomic DNA was extracted from peripheral blood or bone marrow of patients with ALL in remission using the phenol–chloroform method, as previously described (Sambrook, J, 2001). DNA was quantified using PicoGreen (Invitrogen Corp., Carlsbad, California, USA).

For each sample, 400 ng of DNA was genotyped using the GoldenGate Genotyping Assay (Illumina Inc., San Diego, California, USA) with Veracode technology according to the published Illumina protocol. Data were analyzed with GenomeStudio (Illumina Inc.) software for genotype clustering and calling. Duplicate samples and CEPH trios (Coriell Cell Repository, Camden, New Jersey, USA) were genotyped across the plates. SNPs showing Mendelian allele-transmission errors or showing discordant genotypes were excluded from the analysis.

Statistical analysis

The relationship between hepatotoxicity, measured as transaminases elevation, during induction and consolidation was measured using univariate logistic regression models and correlation coefficients. To account for the possible confounding effect of age, sex and MTX dose and MTX plasma levels on hepatotoxicity, multivariate logistic regressions were used. The association between hepatotoxicity and genetic polymorphisms was evaluated by the $\chi 2$ or Fisher's exact test. The effects sizes of associations were estimated by the odds ratios. The most significant test among dominant and recessive models was selected. In all cases the significant level was set at 5%. The results were adjusted for multiple comparisons using the false discovery rate (FDR) correction (Benjamini et al., 2001). Analyses were performed by using the R v3.3.0. software.

Bioinformatics analysis

- *miRNAs secondary structures prediction*

The RNAfold web tool (http://rna.tbi.univie.ac.at/cgi-bin/RNAWebSuite/RNAfold.cgi) (Gruber et al., 2008) was used to calculate the impact of the SNPs in the minimum free energy secondary structures and the energy change ($\Delta\Delta G$) of the hairpin structure of the miRNAs showing significant results.

- *Gene targets selection*

MiRNA target genes were selected based on miRWalk database (Dweep and Gretz, 2015). Only those genes confirmed by at least six of the 12 prediction programs hosted in miRWalk (http://www.umm.uni-heidelberg.de/apps/zmf/mirwalk/index.html) were included. The potential miRNA target genes related to ASP and MTX were selected by literature review and using the Pharmacogenomic Knowledge Base (PharmGKB) (https://www.pharmgkb.org/).

RESULTS

Patient's baseline characteristics

In this study we included a total of 179 childhood patients and we focused our analyses on transaminases elevation. Transaminases data were available for 170 patients at induction phase and for 168 at consolidation phase (Table 20). During the induction phase, 55 out of 170 patients (32.3%) presented elevation of transaminases (grade ≥2), 29 of them (17.1%) high elevation (grade ≥3). At consolidation phase, 49 out of 168 individuals (29.2%) had increased transaminases of grade ≥2, 19 of them (11.3%) with high increase (grade ≥3). Only 20 patients

who had transaminases elevation during induction also developed it at consolidation, and no association between both events was found (p=0.16). We did not find association between transaminases and the covariates age, sex, MTX dose received and MTX plasma levels; thus, we did not include these covariates in the subsequent association analyses.

Table 20. Patients´ characteristics.

Characteristics	Induction phase	Consolidation phase
Number of patients	170	168
Sex, n (%)		
Male	100 (58.8)	100 (59.5)
Female	70 (41.2)	68 (40.5)
Age at diagnosis, mean ± SD (years)		
Male	5.27 ± 3.24	5.28 ± 3.24
Female	4.91 ± 3.28	4.98 ± 3.30
Treatment protocol, n (%)		
LAL/SHOP 94/99	63 (37.1)	62 (36.9)
LAL/SHOP 2005	107 (62.9)	106 (63.1)
Hepatotoxicity, n (%)		
Transaminases elevation	55 (32.3)	49 (29.2)
Bilirubin elevation	29 (17.1)	14 (8.3)

Abbreviations: SD, standard deviation.

Regarding BI, few patients presented toxicity levels. At induction, 29 patients presented high levels of BI (only 4 of them presented other grade different from 1) and at consolidation, 14 patients (only two of them presented an elevation higher than grade 1) (Table 20).

Genotyping results

Successful genotyping was carried out for 158 out of 179 DNA samples (88.3%) and for 160 SNPs (75.12%). Genotyping failures were due to no PCR amplification, insufficient intensity for cluster separation, or poor or no cluster definition.

Association study

To investigate whether genetic variation in miRNAs influences hepatotoxicity, measured as an elevation of transaminases, we tested the association between the 160 successfully genotyped polymorphisms in 154 miRNAs and hepatic toxicity data. This analysis was performed at induction and consolidation phases in a cohort of 158 Spanish children with B-ALL.

In the induction phase, when we analyzed hepatotoxicity of grade ≥2 we found three SNPs significantly associated, located in miR-4707, miR-3689d2 and miR-300. When we focused our analysis on high hepatotoxicity (grade ≥3), two SNPs, located in miR-5197 and miR-3936, were associated (Table 21). None of them remained significant after FDR correction.

Table 21. SNPs in miRNAs showing the most significant associations with hepatotoxicity (≥2 grade) and hepatotoxicity (≥3 grade) during induction phase in pediatric B-ALL. Genotypic and allelic frequencies.

miRNA SNP	Position Localization	Genotype/ Allele	Hepatotoxicity grade ≥2 (n=170)		Model OR (95% CI) P-value/FDR	Hepatotoxicity grade≥3(n=144)		Model OR (95% CI) P-value
			NO Tox n=115 (%)	TOX n=55 (%)		NO Tox n=115 (%)	TOX n=29 (%)	
miR-4707 rs2273626	Chr: 14 In seed	AA	25 (24.5)	21 (44.7)	Dominant	25 (24.5)	9 (33.3)	Recessive
		AC	56 (54.9)	15 (31.9)	0.40 (0.19-0.83)	56 (54.9)	10 (37.0)	1.62 (0.62-4.22)
		CC	21 (20.6)	11 (23.4)	**0.014/0.59**	21 (20.6)	8 (29.6)	0.328/0.648
		A	106 (52)	57 (60.6)	0.70 (0.42-1.15)	106 (52)	28 (51.9)	1.0 (0.55-1.83)
		C	98 (48)	37 (39.4)	0.162	98 (48)	26 (48.1)	0.988
miR-3689d2 rs62571442	Chr: 9 pre-miRNA	AA	26 (25.5)	13 (27.7)	Recessive	26 (25.5)	7 (25.9)	Recessive
		AG	61 (59.8)	20 (42.6)	2.46 (1.07-5.65)	61 (59.8)	12 (44.4)	2.44 (0.91-6.58)
		GG	15 (14.7)	14 (29.8)	**0.035/0.59**	15 (14.7)	8 (29.6)	0.085/0.648
		A	113 (55.4)	46 (48.9)	1.296 (0.74-2.11)	113 (55.4)	26 (48.1)	1.337 (0.73-2.43)
		G	91 (44.6)	48 (51.1)	0.299	91 (44.6)	28 (51.9)	0.342
miR-300 rs12894467	Chr: 14 pre-miRNA	CC	42 (40.8)	15 (31.9)	Recessive	42 (40.8)	9 (33.3)	Recessive
		CT	53 (51.5)	23 (48.9)	2.81 (1.01-7.83)	53 (51.5)	13 (48.1)	2.70 (0.80-9.05)
		TT	8 (7.8)	9 (19.1)	**0.049/0.59**	8 (7.8)	5 (18.5)	0.121/0.648
		C	137 (66.5)	53 (56.4)	1.53 (0.93-2.53)	137 (66.5)	31 (57.4)	1.47 (0.79-2.71)
		T	69 (33.5)	41 (43.6)	0.091	69 (33.5)	23 (42.6)	0.213
miR-5197 rs2042253	Chr: 5 pre-miRNA	AA	64 (62.7)	23 (48.9)	Dominant	64 (62.7)	11 (40.7)	Dominant
		AG	36 (35.3)	22 (46.8)	1.76 (0.87-3.53)	36 (35.3)	14 (51.9)	2.45 (1.03-5.83)
		GG	2 (2.0)	2 (4.3)	0.113/0.59	2 (2)	2 (7.4)	**0.040/0.648**
		A	164 (80.4)	68 (72.3)	1.568 (0.88-2.76)	164 (80.4)	36 (66.7)	2.05 (1.05-3.97)
		G	40 (19.6)	26 (27.7)	0.119	40 (19.6)	18 (33.3)	**0.031**
miR-3936 rs367805	Chr:5 pre-miRNA	GG	53 (52.5)	19 (40.4)	Dominant	53 (52.5)	7 (25.9)	Dominant
		AG	41 (40.6)	23 (48.9)	1.63 (0.81-3.28)	41 (40.6)	17 (63)	3.15 (1.23-8.12)
		AA	7 (6.9)	5 (10.6)	0.171/0.63	7 (6.9)	3 (11.1)	**0.012/0.648**
		G	147 (72.8)	61 (64.9)	1.446 (0.85-2.44)	147 (72.8)	31 (57.4)	1.98 (1.06-3.69)
		A	55 (27.2)	33 (35.1)	0.167	55 (27.2)	23 (42.6)	**0.029**

Abbreviations: B-ALL, B cell acute lymphoblastic leukemia; miRNA, microRNA; SNP, single nucleotide polymorphism; Tox, toxicity; OR, odds ratio; CI, confidence interval; FDR, False Discovery Rate; Chr, chromosome.
Notes: Bold denote significant P-values.

In the consolidation phase, analyzing hepatic toxicity of grade ≥2, three SNPs were found associated, located in miR-1208, miR-3615 and miR-3144. When the analysis were restricted to high hepatotoxicity (grade ≥3), nine SNPs located in miR-1208, miR-4745, miR-4467, miR-5189, miR-1908, miR-5197, miR-4634 and miR-4472-1, were significantly associated (Table 22 and Table 23). The only result which reached a significant p-value when FDR correction was applied was rs2648841 in miR-1208 with hepatotoxicity of grade ≥2, in which GT+TT genotype showed a 0.1-fold decreased risk (p=0.00006). The T allele conferred protection for this toxicity with a p-value of 0.0004. When the analysis were focused on high hepatotoxicity (grade ≥3), this association was also found (p=0.001) (Table 22).

Table 22. The most significant SNP in miRNA associated with hepatotoxicity (grade ≥2) and hepatotoxicity (grade ≥3) during consolidation phase in pediatric B-ALL.

miRNA/SNP	Position Localization	Genotype /Allele	Hepatotoxicity grade≥2 (n=168)		Model OR (95% CI) P-valued	Hepatotoxicity grade≥3 (n=138)		Model OR (95% CI) P-value
			NO Tox n=119 (%)	TOX n=49 (%)		NO Tox n=119 (%)	TOX n=19 (%)	
miR-1208 rs2648841	Chr: 8 pre-miRNA	GG	68 (66.7)	40 (95.2)	Dominant	68 (66.7)	18 (100)	Dominant
		GT	31 (30.4)	2 (4.8)	0.10 (0.02-0.44)	31 (30.4)	0 (0.0)	0 (0.0)
		TT	3 (2.9)	0 (0.0)	**0.00006***	3 (2.9)	0 (0.0)	**0.0016**
		G	167 (81.9)	82 (97.6)	0.11 (0.02-0.46)	167 (81.9)	36 (100)	0
		T	37 (18.1)	2 (2.4)	**0.0004**	37 (18.1)	0 (0)	**0.0055**

Abbreviations: B-ALL, B cell acute lymphoblastic leukemia; miRNA, microRNA; SNP, single nucleotide polymorphism; Tox, toxicity; OR, odds ratio; CI, confidence interval; FDR, False Discovery Rate; Chr, chromosome.

Notes: *, significant after FDR correction (0.0062); bold denote significant P-values.

Table 23. SNPs in miRNAs showing the most significant associations with hepatotoxicity (grade ≥2) and hepatotoxicity (grade ≥3) during consolidation phase in pediatric B-ALL. Genotypic and allelic frequencies.

miRNA/SNP	Position Localization	Genotype/ Allele	Hepatotoxicity grade≥2 (n=168)		Model OR (95% CI) P-value/Corrected P-value	Hepatotoxicity grade≥3 (n=138)		Model OR (95% CI) P-value/Corrected P-value
			NO Tox n=119 (%)	TOX n=49 (%)		NO Tox n=119 (%)	TOX n=19 (%)	
miR-1208 rs2648841	Chr: 8 pre-miRNA	GG	68 (66.7)	40 (95.2)	Dominant	68 (66.7)	18 (100)	Dominant
		TG	31 (30.4)	2 (4.8)	0.10 (0.02-0.44)	31 (30.4)	0 (0.0)	0 (0.0)
		TT	3 (2.9)	0 (0.0)	**0.00006/0.0062**	3 (2.9)	0 (0.0)	**0.0016/0.16**
		G	167 (81.9)	82 (97.6)	0.11 (0.026-0.468)	167 (81.9)	36 (100)	0
		T	37 (18.1)	2 (2.4)	**0.0004**	37 (18.1)	0 (0)	**0.0055**
miR-3615 rs745666	Chr: 17 pre-miRNA	CC	43 (40.6)	14 (34.1)	Recessive	43 (40.6)	4 (22.2)	Dominant
		CG	54 (50.9)	17 (41.5)	3.48 (1.30-9.33)	54 (50.9)	11 (61.1)	2.16 (0.52-8.88)
		GG	9 (8.5)	10 (24.4)	**0.014/0.43**	9 (8.5)	3 (16.7)	0.125/0.56
		C	140 (66)	45 (54.9)	1.59 (0.95-2.68)	140 (66)	19 (52.8)	1.74 (0.85-3.55)
		G	72 (34)	37 (45.1)	0.075	72 (34)	17 (47.2)	0.125
miR-3144 rs68035463	Chr: 6 pre-miRNA	CC	53 (50.0)	22 (53.7)	Recessive	53 (50.0)	10 (58.8)	Recessive
		AC	47 (44.3)	11 (26.8)	4.04 (1.31-12.50)	47 (44.3)	5 (29.4)	2.22 (0.41-12.04)
		AA	6 (5.7)	8 (19.5)	**0.015/0.43**	6 (5.7)	2 (11.8)	0.382/0.64
		C	153 (72.2)	55 (67.1)	1.273 (0.735-2.206)	153 (72.2)	25 (73.5)	0.934 (0.412-2.117)
		A	59 (27.8)	27 (32.9)	0.389	59 (27.8)	9 (26.5)	0.869
miR-4745 rs10422347	Chr:19 In mature	CC	89 (86.4)	30 (73.2)	Dominant	89 (86.4)	10 (55.6)	Dominant
		CT	13 (12.6)	10 (24.4)	2.33 (0.96-5.68)	13 (12.6)	7 (38.9)	5.09 (1.71-15.08)
		TT	1 (1.0)	1 (2.4)	0.066/0.59	1 (1)	1 (5.6)	**0.004/0.21**
		C	191 (92.7)	70 (85.4)	2.18 (0.97-4.89)	191 (92.7)	27 (75)	4.244 (1.69-10.64)
		T	15 (7.3)	12 (14.6)	0.0534	15 (7.3)	9 (25)	**0.001**
miR-4467 rs60871950	Chr:7 In mature	AA	26 (25.2)	16 (38.1)	Dominant	26 (25.2)	10 (55.6)	Dominant
		AG	45 (43.7)	17 (40.5)	0.55 (0.26-1.18)	45 (43.7)	6 (33.3)	0.27 (0.10-0.76)
		GG	32 (31.1)	9 (21.4)	0.127/0.59	32 (31.1)	2 (11.1)	**0.012/0.41**
		A	97 (47.1)	49 (58.3)	0.63 (0.381-1.062)	97 (47.1)	26 (72.2)	0.342 (0.157-0.746)
		G	109 (52.9)	35 (41.7)	0.082	109 (52.9)	10 (27.8)	**0.005**
miR-5189 rs35613341	Chr:16 pre-miRNA	CC	53 (50.5)	16 (38.1)	Dominant	53 (50.5)	4 (22.2)	Dominant
		CG	40 (38.1)	20 (47.6)	1.66 (0.80-3.44)	40 (38.1)	10 (55.6)	3.57 (1.10-11.55)
		GG	12 (11.4)	6 (14.3)	0.172/0.59	12 (11.4)	4 (22.2)	**0.022/0.44**
		C	146 (69.5)	52 (61.9)	1.40 (0.82-2.38)	146 (69.5)	18 (50)	2.28 (1.11-4.67)
		G	64 (30.5)	32 (38.1)	0.208	64 (30.5)	18 (50)	**0.021**
miR-1908 rs174561	Chr: 11 pre-miRNA	TT	55 (54.5)	27 (67.5)	Dominant	55 (54.5)	14 (82.4)	Dominant
		CT	39 (38.6)	12 (30.0)	0.58 (0.27-1.24)	39 (39.6)	3 (17.6)	0.26 (0.07-0.95)
		CC	7 (6.9)	1 (2.5)	0.153/0.59	7 (6.9)	0 (0.0)	**0.023/0.44**
		T	149 (73.8)	66 (82.5)	0.596 (0.30-1.15)	149 (73.8)	31 (91.2)	0.272 (0.08-0.92)
		C	53 (26.2)	14 (17.5)	0.120	53 (26.2)	3 (8.8)	**0.027**

Abbreviations: B-ALL, B cell acute lymphoblastic leukemia; miRNA, microRNA; SNP, single nucleotide polymorphism; Tox, toxicity; OR, odds ratio; CI, confidence interval; Chr, chromosome.
Notes: Bold denote significant P-values.

Table 23. SNPs in miRNAs showing the most significant associations with hepatotoxicity (grade ≥2) and hepatotoxicity (grade ≥3) during consolidation phase in pediatric B-ALL. Genotypic and allelic frequencies (Continuation).

miRNA/SNP	Position Localization	Genotype/ Allele	Hepatotoxicity grade≥2 (n=168)		Model OR (95% CI) P-value/Corrected P-value	Hepatotoxicity grade≥3 (n=138)		Model OR (95% CI) P-value/Corrected P-value
			NO Tox n=119 (%)	TOX n=49 (%)		NO Tox n=119 (%)	TOX n=19 (%)	
miR-5189 rs56292801	Chr:16 pre-miRNA	GG	58 (55.2)	19 (45.2)	Dominant	58 (55.2)	5 (27.8)	Dominant
		AG	39 (37.1)	19 (45.2)	1.49 (0.73-3.07)	39 (37.1)	11 (61.1)	3.21 (1.07-9.65)
		AA	8 (7.6)	4 (9.5)	0.272/0.593	8 (7.6)	2 (11.1)	**0.029/0.44**
		G	155 (73.8)	57 (67.9)	1.33 (0.76-2.31)	155 (73.8)	21 (58.3)	2.01 (0.97-4.17)
		A	55 (26.2)	27 (32.1)	0.303	55 (26.2)	15 (41.7)	0.057
miR-5197 rs2042253	Chr: 5 pre-miRNA	AA	65 (61.9)	22 (52.4)	Recessive	65 (61.9)	9 (50)	Recessive
		AG	39 (37.1)	17 (40.5)	8.00 (0.81-79.23)	39 (37.1)	7 (38.9)	13 (1.11-151.78)
		GG	1 (1.0)	3 (7.1)	0.050/0.59	1 (1)	2 (11.1)	**0.036/0.44**
		A	169 (80.5)	61 (72.6)	1.55 (0.8-2.8)	169 (80.5)	25 (69.4)	1.81 (0.82-3.98)
		G	41 (19.5)	23 (27.4)	0.140	41 (19.5)	11 (30.6)	0.134
miR-4634 rs7709117	Chr: 5 pre-miRNA	AA	23 (22.3)	8 (19.0)	Recessive	23 (22.3)	2 (11.1)	Recessive
		AG	63 (61.2)	24 (57.1)	1.58 (0.66-3.81)	63 (61.2)	9 (50)	3.22 (1.09-9.49)
		GG	17 (16.5)	10 (23.8)	0.314/0.606	17 (16.5)	7 (38.9)	**0.040/0.44**
		A	109 (52.9)	40 (47.6)	1.23 (0.74-2.05)	109 (52.9)	13 (36.1)	1.988 (0.95-4.13)
		G	97 (47.1)	44 (52.4)	0.413	97 (47.1)	23 (63.9)	0.062
miR-4472-1 rs28655823	Chr:8 In seed	GG	83 (79.0)	37 (88.1)	Dominant	83 (79)	18 (100)	Dominant
		CG	20 (19.0)	5 (11.9)	0.51 (0.18-1.45)	20 (19)	0 (0.0)	0 (0.0)
		CC	2 (1.9)	0 (0.0)	0.185/0.591	2 (1.9)	0 (0.0)	**0.040/0.44**
		G	186 (88.6)	79 (94)	0.491 (0.18-1.33)	186 (88.6)	36 (100)	0 (-)
		C	24 (11.4)	5 (6)	0.154	24 (11.4)	0 (0.0)	**0.032**

Abbreviations: B-ALL, B cell acute lymphoblastic leukemia; miRNA, microRNA; SNP, single nucleotide polymorphism; Tox, toxicity; OR, odds ratio; CI, confidence interval; Chr, chromosome.
Notes: Bold denote significant P-values.

Regarding BI, during induction, a total of 11 SNPs were associated with high BI levels from grade 1 to 4 (Table 24). During consolidation, a total of 4 SNPs were associated. None of them remained significant after FDR correction (Table 24).

Table 24. SNPs in miRNAs showing the most significant associations with hyperbilirrubinemia during induction and consolidation phases in pediatric B-ALL. Genotypic and allelic frequencies.

miRNA SNP	Position Localization	Genotype / Allele	Bilirubin Induc (n=170) NO Tox n=141 (%)	TOX n=29 (%)	Model OR (95% CI) P-value	Bilirubin Cons (n=168) NO Tox n=154 (%)	TOX n=14 (%)	Model OR (95% CI) P-value
hsa-mir-4634 rs7709117	Chr.: 5 pre-miRNA	AA	30 (24.8)	1 (3.8)	Dominant	31 (23.5)	0 (0.0)	Recessive
		AG	69 (57)	20 (76.9)	8.24 (1.07-63.44)	80 (60.6)	7 (53.8)	4.53 (1.38-14.83)
		GG	22 (18.2)	5 (19.2)	**0.00639**	21 (15.9)	6 (46.2)	**0.01624**
		A	129 (53.3)	22 (42.3)	1.557 (0.85-2.852)	142 (53.8)	7 (26.9)	3.159 (1.285-7.768)
		G	113 (46.7)	30 (57.7)	0.15	122 (46.2)	19 (73.1)	**0.0089**
hsa-mir-3188 rs7247237	Chr.: 19 pre-miRNA	CC	67 (54.5)	14 (51.9)	Recessive	74 (54.8)	6 (46.2)	Dominant
		CT	49 (39.8)	7 (25.9)	4.73 (1.45-15.49)	49 (36.3)	6 (46.2)	1.42 (0.45-4.43)
		TT	7 (5.7)	6 (22.2)	**0.01351**	12 (8.9)	1 (7.7)	0.5503
		C	183 (74.4)	35 (64.8)	1.577 (0.842-2.954)	197 (73)	18 (69.2)	1.199 (0.5-2.877)
		TT	63 (25.6)	19 (35.2)	0.1528	73 (27)	8 (30.8)	0.6835
hsa-mir-1208 rs2648841	Chr.: 8 pre-miRNA	GG	86 (71.7)	24 (92.3)	Dominant	98 (74.8)	10 (76.9)	Recessive
		TG	32 (26.7)	1 (3.8)	0.21 (0.05-0.94)	31 (23.7)	2 (15.4)	5.37 (0.45-63.69)
		TT	2 (1.7)	1 (3.8)	**0.014847**	2 (1.5)	1 (7.7)	0.2341
		G	204 (85)	49 (94.2)	0.347 (0.103-1.173)	227 (86.6)	22 (84.6)	1.179 (0.384-3.626)
		T	36 (15)	3 (5.8)	0.0761	35 (13.4)	4 (15.4)	0.7734
hsa-mir-4642 rs67182313	Chr.: 6 pre-miRNA	AA	88 (72.1)	13 (48.1)	Dominant	88 (65.7)	10 (76.9)	Dominant
		AG	31 (25.4)	12 (44.4)	2.79 (1.19-6.54)	41 (30.6)	3 (23.1)	0.57 (0.152.19)
		GG	3 (2.5)	2 (7.4)	**0.01884**	5 (3.7)	0 (0.0)	0.3978
		A	207 (84.8)	38 (70.4)	2.356 (1.192-4.654)	217 (81)	23 (88.5)	0.555 (0.16-1.92)
		G	37 (15.2)	16 (29.6)	**0.0119**	51 (19)	3 (11.5)	0.3463
hsa-mir-577 rs34115976	Chr.: 4 pre-miRNA	CC	71 (58.7)	22 (81.5)	Dominant	83 (62.4)	9 (69.2)	Dominant
		CG	44 (36.4)	4 (14.8)	0.32 (0.11-0.91)	43 (32.3)	4 (30.8)	0.74 (0.22-2.52)
		GG	6 (5)	1 (3.7)	**0.02071**	7 (5.3)	0 (0.0)	0.6224
		C	186 (76.9)	48 (88.9)	0.415 (0.169-1.021)	209 (78.6)	22 (84.6)	0.667 (0.221-2.013)
		G	56 (23.1)	6 (11.1)	0.0495	57 (21.4)	4 (15.4)	0.4693
hsa-mir-4636 rs257095	Chr.: 5 pre-miRNA	AA	95 (77.2)	18 (66.7)	Recessive	103 (76.3)	8 (61.5	Recessive
		AG	28 (22.8)	7 (25.9)	0 (0.0)	31 (23.0)	4 (30.8)	11.17 (0.66-189.99)
		GG	0 (0)	2 (7.4)	**0.03141**	1 (0.7)	1 (7.7)	0.1265
		A	218 (88.6)	43 (79.6)	1.992 (0.922-4.303)	237 (87.8)	20 (76.9)	2.155 (0.807-5.754)
		GG	28 (11.4)	11 (20.4)	0.0753	33 (12.2)	6 (23.1)	0.1181
hsa-mir-6128 rs2682818	Chr.: 8 pre-miRNA	CC	97 (79.5)	21 (77.8)	Recessive	109 (81.3)	8 (61.5)	Dominant
		AC	25 (20.5)	4 (14.8)	0 (0.0)	23 (17.2)	5 (38.5)	2.72 (0.82-9.04)
		AA	0 (0)	2 (7.4)	**0.03183**	2 (1.5)	0 (0.0)	0.11531
		C	219 (89.8)	46 (85.2)	1.523 (0.646-3.59)	241 (89.9)	21 (80.8)	2.125 (0.741-6.093)
		A	25 (10.2)	8 (14.8)	0.333	27 (10.1)	5 (19.2)	0.1524

Table 24. SNPs in miRNAs showing the most significant associations with hyperbilirrubinemia during induction and consolidation phases in pediatric B-ALL. Genotypic and allelic frequencies (Continuation).

miRNA SNP	Position Localization	Genotype	Bilirubin Induc (n=170)		Model OR (95% CI) P-value	Bilirubin Cons (n=168)		Model OR (95% CI) P-value
		Allele	NO Tox n=141 (%)	TOX n=29 (%)		NO Tox n=154 (%)	TOX n=14 (%)	
hsa-mir-604 rs2368392	Chr.: 10 pre-miRNA	CC	75 (61)	13 (48.1)	Recessive	80 (59.3)	6 (46.2)	Recessive
		CT	46 (37.4)	11 (4.7)	7.56 (1.20-47.71)	52 (38.5)	5 (38.5)	8.00 (1.21-53.06)
		TT	2 (1.6)	3 (11.1)	**0.03267**	3 (2.2)	2 (15.4)	0.05213
		C	196 (79.7)	37 (68.5)	1.801 (0.938-3.46)	212 (78.5)	17 (65.4)	1.935 (0.82-4.566)
		T	50 (20.3)	17 (31.5)	0.0747	58 (21.5)	9 (34.6)	0.1264
hsa-mir-548ap rs4577031	Chr.: 15 pre-miRNA	AA	52 (42.3)	9 (33.3)	Recessive	53 (39.3)	6 (46.2)	Recessive
		AT	62 (50.4)	12 (44.4)	3.62 (1.17-11.24)	70 (51.9)	5 (38.5)	1.86 (0.37-9.41)
		TT	9 (7.3)	6 (22.2)	**0.03337**	12 (8.9)	2 (15.4)	0.4757
		A	166 (67.5)	30 (55.6)	1.66 (0.912-3.023)	176 (65.2)	17 (65.4)	0.991 (0.425-2.31)
		T	80 (32.5)	24 (44.4)	0.0955	94 (34.8)	9 (34.6)	0.9837
hsa-mir-548ap rs4414449	Chr.: 15 in_mature	TT	46 (40.4)	8 (30.8)	Recessive	47 (37.9)	5 (38.5)	Recessive
		CT	56 (49.1)	11 (42.3)	3.13 (1.09-8.98)	61 (49.2)	6 (46.2)	1.23 (0.25-6.05)
		CC	12 (10.5)	7 (26.9)	**0.04092**	16 (12.9)	2 (15.4)	0.805
		T	148 (64.9)	27 (51.9)	1.713 (0.932-3.147)	155 (62.5)	16 (61.5)	1.042 (0.454-2.391)
		C	80 (35.1)	25 (48.1)	0.0808	93 (37.5)	10 (38.5)	0.9233
hsa-mir-5197 rs2042253	Chr.: 5 pre-miRNA	AA	76 (62.3)	11 (40.7)	Dominant	80 (59.7)	7 (53.8)	Dominant
		AG	42 (34.4)	16 (59.3)	2.4 (1.03-5.63)	50 (37.3)	6 (46.2)	1.27 (0.40-3.99)
		GG	4 (3.3)	0 (0)	**0.04115**	4 (3.0)	0 (0.0)	0.6833
		A	194 (79.5)	38 (70.4)	1.634 (0.843-3.166)	210 (78.4)	20 (76.9)	1.086 (0.417-2.83)
		G	50 (20.5)	16 (29.6)	0.1434	58 (21.6)	6 (23.1)	0.8656
hsa-mir-4481 rs7896283	Chr.: 10 pre-miRNA	AA	43 (38.7)	11 (45.8)	Recessive	46 (36.5)	7 (87.5)	Dominant
		AG	46 (41.4)	12 (50.0)	0.18 (0.02-1.37)	59 (46.8)	0 (0)	0.08 (0.01-0.69)
		GG	22 (19.8)	1 (4.2)	0.03591	21 (16.7)	1 (12.5)	**0.003636**
		A	132 (59.5)	34 (70.8)	0.604 (0.307-1.189)	151 (59.9)	14 (87.5)	0.214 (0.048-0.96)
		G	90 (40.5)	14 (29.2)	0.142	101 (40.1)	2 (12.5)	**0.0279**
hsa-mir-5007 rs1572687	Chr.: 13 pre-miRNA	CC	37 (30.1)	12 (44.4)	Dominant	39 (28.9)	8 (61.5)	Dominant
		CT	64 (52.0)	8 (29.6)	0.54 (0.23-1.26)	70 (51.9)	2 (15.4)	0.25 (0.08-0.82)
		TT	22 (17.9)	7 (25.9)	0.15727	26 (19.3)	3 (23.1)	**0.020464**
		C	138 (56.1)	32 (59.3)	0.878 (0.483-1.598)	148 (54.8)	18 (69.2)	0.539 (0.227-1.283)
		T	108 (43.9)	22 (40.7)	0.6712	122 (45.2)	8 (30.8)	0.1572
hsa-mir-4671 rs877722	Chr.: 1 pre-miRNA	AA	91 (74.0)	19 (70.4)	Recessive	97 (71.9)	13 (100)	Dominant
		AT	28 (22.8)	6 (22.2)	2.38 (0.41-13.71)	32 (23.7)	0 (0)	0 (0.0)
		TT	4 (3.3)	2 (7.4)	0.3569	6 (4.4)	0 (0)	**0.02199**
		A	210 (85.4)	44 (81.5)	1.326 (0.612-2.87)	226 (83.7)	26 (100)	0 (0.0)
		T	36 (14.6)	10 (18.5)	0.4731	44 (16.3)	0 (0)	**0.0257**

### *Effects of rs2648841 in miR-1208 secondary structure prediction*

We performed our analysis with the most significant SNP, rs2648841 in miR-1208. In this case, the substitution of the G allele for a T allele induced an energy change ($\Delta\Delta G$) of 3.3 kcal/mol (from -26.1 to -22.8 kcal/mol). This change also showed a modification in the secondary structure (Figure 19).

<p align="center">hsa-mir-1208
rs2648841
$\Delta\Delta G$ = 3.3 Kcal/mol</p>
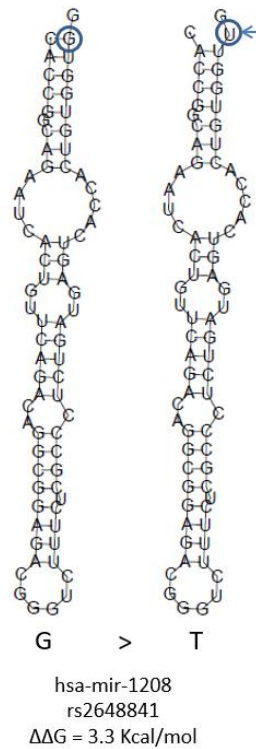
Figure 19. Energy change and minimum free-energy structures of the most significant miRNA SNP due to the presence of different alleles extracted from RNAfold web tool.

miR-1208 target prediction

When we performed the target prediction analysis for miR-1208 we found that this miRNA targeted a total of five genes involved in MTX pathways, three genes of the pharmacodynamic pathway, *DHFR*, *MTHFR* and *MTR*, and two genes involved in pharmacokinetic pathway, *SLCO1A2* and *SLC46A1* (Figure 20).
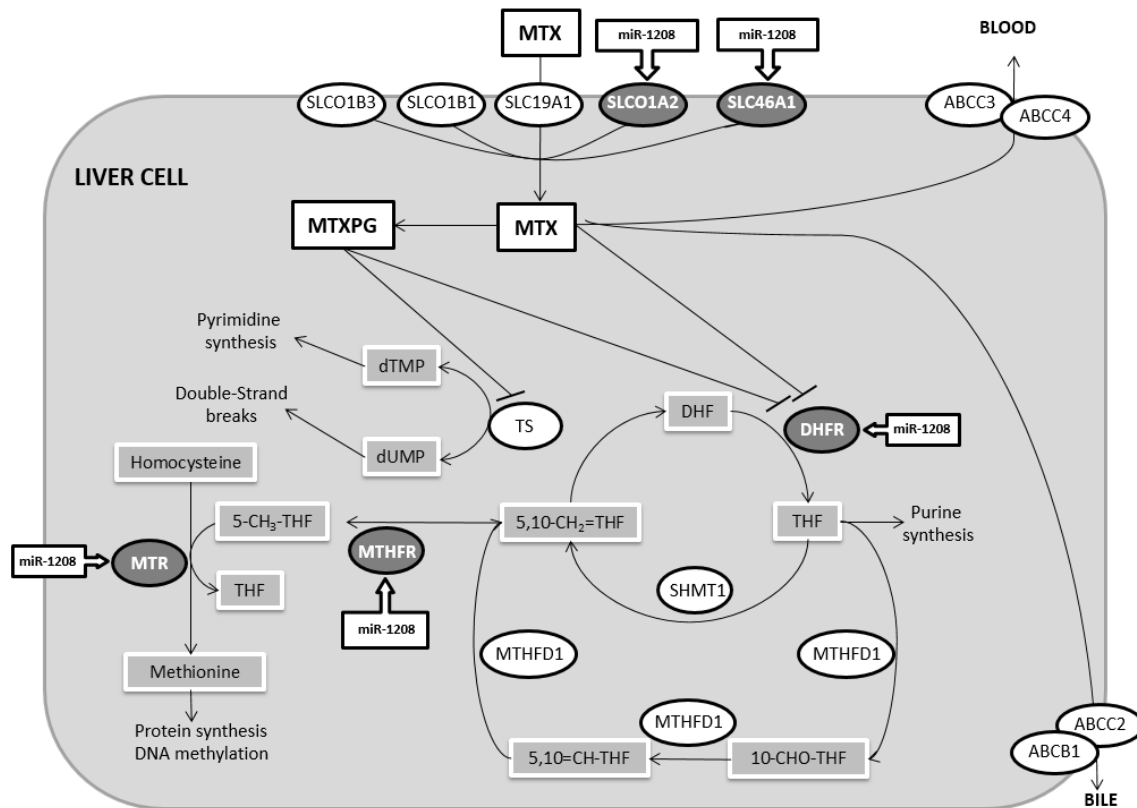
Figure 20. MTX pharmacokinetic and pharmacodynamic pathway genes and miR-1208 pointing out the corresponding target genes.

DISCUSSION

In this study, we evaluated the role of variants in miRNAs described at the time of the study in the hepatotoxicity developed during the treatment of B-ALL. The most significant result was the association of rs2648841 in miR-1208 with transaminases levels during consolidation phase. For this SNP, GT+TT genotype showed the highest association signal with a 0.1-fold decrease risk of toxicity (grade ≥2), which reached the statistical significance when FDR correction was applied. Remarkably, none of the patients with the TT genotype developed toxicity. Interestingly, when we focused our analysis on high transaminases levels (grade ≥3), rs2648841 also showed a significant association and none of the patients with a T allele developed high toxicity.

The SNP rs2648841 is located in the pre-mature sequence of miR-1208. In this miRNA, the T allele induces a positive energy change, which turns the miRNA hairpin from a stable to an unstable status (ΔΔG = 3.3 kcal/mol) (Gruber et al., 2008). It has been proposed that a decrease in the structure stability may reduce the product of the mature miRNA (Gong et al., 2012), and consequently it could lead to an increased expression of its targets. Among the predicted targets for miR-1208, we found three genes of the MTX pharmacodynamic pathway, *DHFR*, *MTR* and *MTHFR,* and two of the pharmacokinetic pathway, *SLCO1A2* and *SLC46A1*. Among them, *DHFR*

is the main target of MTX (Wojtuszkiewicz et al., 2015), therefore higher expression of this gene could mitigate the effect of MTX, contributing to avoid hepatocyte cell death. In fact, high expression of DHFR was associated with MTX resistance (Dulucq et al., 2008), which could explain the protective role of the T allele of rs2648841 in hepatotoxicity. Regarding MTR enzyme, which methylates homocysteine to produce methionine (Krajinovic et al., 2005) and MTHFR, which provides the methyl group for this reaction (Krajinovic et al., 2005) (Figure 20), a high expression of them could lead to decreased levels of homocysteine in the cell. Low levels of homocysteine may protect from apoptosis (Kubota et al., 2014; Yang et al., 2017), that might explain again the protective role of this T allele. Regarding pharmacokinetic pathway, *SLCO1A2* and *SLC46A1* transporters, we consider that these genes are not involved in hepatotoxicity mechanism because they are involved in MTX uptake from the plasma to the liver and MTX plasma levels were not associated with elevation of transaminases in our cohort. In conclusion, the T allele of rs2648841 in miR-1208 could alter the secondary structure, reducing its mature levels. This reduction in miRNA levels could lead to a higher expression of its target genes in pharmacodynamic pathway (*DHFR*, *MTR* and *MTHFR*), protecting the hepatocyte from apoptosis.

On the other hand, another interesting result of this study was the fact that SNPs associated with transaminases levels during induction and consolidation were different. Actually, rs2648841 in miR-1208 was specifically associated with increased transaminases in consolidation, while during induction was not even near of reaching a significant p-value (p=0.21). Moreover, the patients who developed hepatotoxicity during induction were different to the ones who developed it at consolidation, with no association between both events. Therefore, all these data support the idea that the hepatic toxicity in the different phases could be produced by different mechanisms and related to different drugs.

Regarding BI analysis, few patients presented high levels of this toxicity at induction and consolidation and none of the SNPs reached a significant p-value when FDR correction was applied. It would be interesting to study this toxicity in larger cohorts.

This study has some limitations that have to be addressed, such as the relatively high failure rate in genotyping technique. However, this problem was accepted from the beginning of the study, because no other design option to amplify the specific polymorphisms was possible. Moreover, other concomitant drugs, such as 6-mercaptopurine, may also cause hepatotoxicity. In this line, among miR-1208 targets we found *TPMT*, *ABCC5* and *NT5C2*, genes of   pathway.   Reduced miR-1208 levels could lead to higher expression of these genes and then, could contribute to a

higher inactivation of 6-MP (TPMT) (Kotur et al., 2012; Maxwell and Cole, 2017), higher efflux of thiopurines and their metabolites from the hepatocyte (ABCC5) (Krajinovic et al., 2016; Teft et al., 2015) and higher dephosphorylation and inactivation 6-thioinositol monophosphate (NT5C2) (Tzoneva et al., 2013), explaining the protective role of rs2648841. Finally, we have to take into account the inaccuracy of the prediction algorithms of the databases used, but nowadays this limitation has to be assumed.

In summary, we found 5 SNPs in 5 miRNAs that could be involved in the development of hepatotoxicity, measured as a transaminases elevation, during induction and other 11 SNPs in 10 miRNAs that could be associated during consolidation, suggesting different mechanisms involved in hepatotoxicity in each phase. The most significant result was rs2648841 in miR-1208 specifically associated with hepatotoxicity and high hepatotoxicity during consolidation, probably through its involvement in a higher expression of *DHFR*, *MTR* and *MTHFR* genes. It would be interesting to validate the high protection effect of TT genotype in another cohort.

Executive summary

- Due to the success of therapy in childhood ALL, it has gained relevance to reduce toxicity
- One of the most common toxicities in ALL treatment is hepatotoxicity, which could be caused by ASP during the induction and by MTX during consolidation
- Pharmacoepigenetics, which includes the study of miRNAs, is arising as a tool to identify new markers of toxicity
- We analyzed the association of miRNA SNPs in drug-induced hepatotoxicity in two different phases of treatment in a large cohort of Spanish children diagnosed with ALL.
- The development of hepatotoxicity in each phase is not correlated, which suggest that different mechanism could be involved.
- rs2648841 in miR-1208 was associated with hepatotoxicity and high hepatotoxicity, measured as an elevation of transaminases, during consolidation phase after FDR correction.
- Rs2648841 in miR-1208 could affect miRNA levels, and then, affect the expression of its target genes.
- Among miR-1208 targets we found genes of MTX pharmacodynamics pathway that may be involved in hepatocyte death.

ACKNOWLEDGEMENTS

CONFLICTS OF INTEREST

There are no conflicts of interest.

REFERENCES

Amstutz, U., Offer, S.M., Sistonen, J., Joerger, M., Diasio, R.B., and Largiader, C.R. (2015). Polymorphisms in MIR27A Associated with Early-Onset Toxicity in Fluoropyrimidine-Based Chemotherapy. Clin. Cancer Res. 21, 2038–2044.

Bénichou, C. (1990). Criteria of drug-induced liver disorders. Report of an international consensus meeting. J Hepatol. 11, 272–276.

Benjamini, Y., Drai, D., Elmer, G., Kafkafi, N., and Golani, I. (2001). Controlling the false discovery rate in behavior genetics research. Behav. Brain Res. 125, 279–284.

Dulucq, S., St-Onge, G., Gagné, V., Ansari, M., Sinnett, D., Labuda, D., Moghrabi, A., and Krajinovic, M. (2008). DNA variants in the dihydrofolate reductase gene and outcome in childhood ALL. Blood 111, 3692–3700.

Dweep, H., and Gretz, N. (2015). miRWalk2.0: a comprehensive atlas of microRNA-target interactions. Nat. Methods 12, 697.

Erčulj, N., Kotnik, B.F., Debeljak, M., Jazbec, J., and Dolžan, V. (2012). Influence of folate pathway polymorphisms on high-dose methotrexate-related toxicity and survival in childhood acute lymphoblastic leukemia. Leuk. Lymphoma 53, 1096–1104.

Gong, J., Tong, Y., Zhang, H.-M., Wang, K., Hu, T., Shan, G., Sun, J., and Guo, A.-Y. (2012). Genome-wide identification of SNPs in microRNA genes and the SNP effects on microRNA target binding and biogenesis. Hum. Mutat. 33, 254–263.

Gregers, J., Christensen, I.J., Dalhoff, K., Lausen, B., Schroeder, H., Rosthoej, S., Carlsen, N., Schmiegelow, K., and Peterson, C. (2010). The association of reduced folate carrier 80G>A polymorphism to outcome in childhood acute lymphoblastic leukemia interacts with chromosome 21 copy number. Blood 115, 4671–4677.

Gregers, J., Gréen, H., Christensen, I.J., Dalhoff, K., Schroeder, H., Carlsen, N., Rosthoej, S., Lausen, B., Schmiegelow, K., and Peterson, C. (2015a). Polymorphisms in the ABCB1 gene and effect on outcome and toxicity in childhood acute lymphoblastic leukemia. Pharmacogenomics J. 15, 372–379.

Gregers, J., Green, H., Christensen, I.J., Dalhoff, K., Schroeder, H., Carlsen, N., Rosthoej, S., Lausen, B., Schmiegelow, K., and Peterson, C. (2015b). Polymorphisms in the ABCB1 gene and effect on outcome and toxicity in childhood acute lymphoblastic leukemia. Pharmacogenomics J. 15, 372–379.

Gruber, A.R., Lorenz, R., Bernhart, S.H., Neubock, R., and Hofacker, I.L. (2008). The Vienna RNA websuite. Nucleic Acids Res. 36, W70-4.

Gutierrez-Camino, A., Martin-Guerrero, I., and Garcia-Orad, A. (2017a). PNPLA3 rs738409 and Hepatotoxicity in Children With B-cell Acute Lymphoblastic Leukemia: A Validation Study in a Spanish Cohort. Clin. Pharmacol. Ther.

Gutierrez-Camino, A., Oosterom, N., den Hoed, M.A.H., Lopez-Lopez, E., Martin-Guerrero, I., Pluijm, S.M.F., Pieters, R., de Jonge, R., Tissing, W.J.E., Heil, S.G., et al. (2017b). The miR-1206 microRNA variant is associated with

methotrexate-induced oral mucositis in pediatric acute lymphoblastic leukemia. Pharmacogenet. Genomics 27, 303–306.

den Hoed, M.A.H., Lopez-Lopez, E., te Winkel, M.L., Tissing, W., de Rooij, J.D.E., Gutierrez-Camino, A., Garcia-Orad, A., den Boer, E., Pieters, R., Pluijm, S.M.F., et al. (2015). Genetic and metabolic determinants of methotrexate-induced mucositis in pediatric acute lymphoblastic leukemia. Pharmacogenomics J. 15, 248–254.

Iorga, A., Dara, L., and Kaplowitz, N. (2017). Drug-Induced Liver Injury: Cascade of Events Leading to Cell Death, Apoptosis or Necrosis. Int. J. Mol. Sci. 18, 1018.

Iparraguirre, L., Gutierrez-Camino, A., Umerez, M., Martin-Guerrero, I., Astigarraga, I., Navajas, A., Sastre, A., Garcia de Andoin, N., and Garcia-Orad, A. (2016). MiR-pharmacogenetics of methotrexate in childhood B-cell acute lymphoblastic leukemia. Pharmacogenet. Genomics 26, 517–525.

Johnston, W.T., Lightfoot, T.J., Simpson, J., and Roman, E. (2010). Childhood cancer survival: a report from the United Kingdom Childhood Cancer Study. Cancer Epidemiol. 34, 659–666.

Kotur, N., Stankovic, B., Kassela, K., Georgitsi, M., Vicha, A., Leontari, I., Dokmanovic, L., Janic, D., Krstovski, N., Klaassen, K., et al. (2012). 6-mercaptopurine influences TPMT gene transcription in a TPMT gene promoter variable number of tandem repeats-dependent manner. Pharmacogenomics 13, 283–295.

Krajinovic, M., Robaey, P., Chiasson, S., Lemieux-Blanchard, E., Rouillard, M., Primeau, M., Bournissen, F.G., and Moghrabi, A. (2005). Polymorphisms of genes controlling homocysteine levels and IQ score following the treatment for childhood ALL. Pharmacogenomics 6, 293–302.

Krajinovic, M., Elbared, J., Drouin, S., Bertout, L., Rezgui, A., Ansari, M., Raboisson, M.-J., Lipshultz, S.E., Silverman, L.B., Sallan, S.E., et al. (2016). Polymorphisms of ABCC5 and NOS3 genes influence doxorubicin cardiotoxicity in survivors of childhood acute lymphoblastic leukemia. Pharmacogenomics J. 16, 530–535.

Kubota, M., Nakata, R., Adachi, S., Watanabe, K.-I., Heike, T., Takeshita, Y., and Shima, M. (2014). Plasma homocysteine, methionine and S-adenosylhomocysteine levels following high-dose methotrexate treatment in pediatric patients with acute lymphoblastic leukemia or Burkitt lymphoma: association with hepatotoxicity. Leuk. Lymphoma 55, 1591–1595.

Ladas, E.J., Kroll, D.J., Oberlies, N.H., Cheng, B., Ndao, D.H., Rheingold, S.R., and Kelly, K.M. (2010). A randomized, controlled, double-blind, pilot study of milk thistle for the treatment of hepatotoxicity in childhood acute lymphoblastic leukemia (ALL). Cancer 116, 506–513.

Lauschke, V.M., Mkrtchian, S., and Ingelman-Sundberg, M. (2017). The role of microRNAs in liver injury at the crossroad between hepatic cell death and regeneration. Biochem. Biophys. Res. Commun. 482, 399–407.

Liu, Y., Fernandez, C.A., Smith, C., Yang, W., Cheng, C., Panetta, J.C., Kornegay, N., Liu, C., Ramsey, L.B., Karol, S.E., et al. (2017). Genome-Wide Study Links PNPLA3 Variant With Elevated Hepatic Transaminase After Acute Lymphoblastic Leukemia Therapy. Clin. Pharmacol. Ther. 102, 131–140.

Maxwell, R.R., and Cole, P.D. (2017). Pharmacogenetic Predictors of Treatment-Related Toxicity Among Children With Acute Lymphoblastic Leukemia. Curr. Hematol. Malig. Rep. 12, 176–186.

Pui, C.-H., Yang, J.J., Hunger, S.P., Pieters, R., Schrappe, M., Biondi, A., Vora, A., Baruchel, A.A., Silverman, L.B., Schmiegelow, K., et al. (2015). Childhood Acute Lymphoblastic Leukemia: Progress Through Collaboration. J. Clin. Oncol. 33, JCO.2014.59.1636.

Robles-Diaz, M., Lucena, M.I., Kaplowitz, N., Stephens, C., Medina-Cáliz, I., González-Jimenez, A., Ulzurrun, E., Gonzalez, A.F., Fernandez, M.C., Romero-Gómez, M., et al. (2014). Use of Hy's law and a new composite algorithm to predict acute liver failure in patients with drug-induced liver injury. Gastroenterology 147, 109–118.e5.

Rukov, J.L., Wilentzik, R., Jaffe, I., Vinther, J., and Shomron, N. (2014). Pharmaco-miR: linking microRNAs and drug effects. Brief. Bioinform. 15, 648–659.

Salazar, J., Altes, A., del Rio, E., Estella, J., Rives, S., Tasso, M., Navajas, A., Molina, J., Villa, M., Vivanco, J.L., et al. (2012). Methotrexate consolidation treatment according to pharmacogenetics of MTHFR ameliorates event-free survival in childhood acute lymphoblastic leukaemia. Pharmacogenomics J. 12, 379–385.

Sambrook, J, R.D. (2001). Molecular cloning: a laboratory manual (New York: NY: Cold Spring Harbor Laboratory Press).

Teft, W.A., Welch, S., Lenehan, J., Parfitt, J., Choi, Y.-H., Winquist, E., and Kim, R.B. (2015). OATP1B1 and tumour OATP1B3 modulate exposure, toxicity, and survival after irinotecan-based chemotherapy. Br. J. Cancer 112, 857–865.

Tzoneva, G., Perez-Garcia, A., Carpenter, Z., Khiabanian, H., Tosello, V., Allegretta, M., Paietta, E., Racevskis, J., Rowe, J.M., Tallman, M.S., et al. (2013). Activating mutations in the NT5C2 nucleotidase gene drive chemotherapy resistance in relapsed ALL. Nat. Med. 19, 368–371.

Umerez, M., Gutierrez-Camino, Á., Muñoz-Maldonado, C., Martin-Guerrero, I., and Garcia-Orad, A. (2017). MTHFR polymorphisms in childhood acute lymphoblastic leukemia: Influence on methotrexate therapy. Pharmgenomics. Pers. Med. 10, 69–78.

Wojtuszkiewicz, A., Peters, G.J., van Woerden, N.L., Dubbelman, B., Escherich, G., Schmiegelow, K., Sonneveld, E., Pieters, R., van de Ven, P.M., Jansen, G., et al. (2015). Methotrexate resistance in relation to treatment outcome in childhood acute lymphoblastic leukemia. J. Hematol. Oncol. 8, 61.

Yang, A., Sun, Y., Mao, C., Yang, S., Huang, M., Deng, M., Ding, N., Yang, X., Zhang, M., Jin, S., et al. (2017). Folate Protects Hepatocytes of Hyperhomocysteinemia Mice From Apoptosis via Cystic Fibrosis Transmembrane Conductance Regulator (CFTR)-Activated Endoplasmic Reticulum Stress. J. Cell. Biochem. 118, 2921–2932.

Zhan, X., Wu, W., Han, B., Gao, G., Qiao, R., Lv, J., Zhang, S., Zhang, W., Fan, W., Chen, H., et al. (2012). Hsa-miR-196a2 functional SNP is associated with severe toxicity after platinum-based chemotherapy of advanced nonsmall cell lung cancer patients in a Chinese population. J. Clin. Lab. Anal. 26, 441–446.

Involvement of miRNA polymorphisms in mucositis development in childhood acute lymphoblastic leukemia treatment

Umerez, Maitane[1*], PhD student; Gutierrez-Camino, Ángela[1*], PhD; Lopez-Lopez, Elixabet[1], PhD; Santos, Borja[1], PhD; Martin-Guerrero, Idoia[1], PhD; García de Andoin, Nagore[2,3], MD; Sastre, Ana[4],MD; Navajas, Aurora[5,6], PhD; Astigarraga, Itziar[3,5,6], PhD; Garcia-Orad, Africa[1,6], PhD.

*These authors share first authorship

[1]Department of Genetics, Physic Anthropology and Animal Physiology, University of the Basque Country, UPV/EHU, Leioa, Spain; [2]Department of Pediatrics, University Hospital Donostia, San Sebastian, Spain; [3]Department of Pediatrics, University of the Basque Country, UPV/EHU, Leioa, Spain, [4]Department of Oncohematology, University Hospital La Paz, Madrid, Spain; [5]Department of Pediatrics, University Hospital Cruces, Barakaldo, Spain; [6]BioCruces Health Research Institute, Barakaldo, Spain.

Abstract

Mucositis, one of the most debilitating and frequent side effect of childhood acute lymphoblastic leukemia (ALL) therapy, is characterized by inflammation of the mucosa that involves any part of the digestive tract, frequently accompanied by ulcers in the mouth and throat, vomits and diarrhea. As a consequence, treatment could be delayed or even discontinued, which may impair survival. Mucositis can be linked to several antileukemic agents such as methotrexate (MTX), daunorubicin (DNR) or cyclophosphamide (CPA). Nowadays, it is known that miRNAs regulate the expression of genes involved in pharmacokinetic (PK) and pharmacodynamic (PD) pathways of these drugs. SNPs in miRNAs could affect their levels of function, and then, affect their target genes in these pathways. Therefore, the aim of the study was to determine the association between miRNA genetic variants targeting mucositis-related genes and the risk to develop this toxicity. To achieve this aim, we analyzed 213 SNPs in 206 miRNAs in a cohort of 179 Spanish children with B-cell precursor ALL (B-ALL) homogeneously treated with LAL/SHOP protocols. We identified three SNPs in miR-4268, miR-4751 and miR-3117 associated with mucositis, diarrhea and vomits, respectively, which could be explained through the effect on genes related to drug PK and PD, as well as other mucosal injury-related genes.

Keywords: mucositis, acute lymphoblastic leukemia, microRNAs, single nucleotide polymorphisms.

INTRODUCTION

Mucositis is one of the most debilitating and frequent acute side effect of antileukemic chemotherapy in childhood acute lymphoblastic leukemia (ALL) (Sangild et al., 2017; Schmiegelow et al., 2017), the most common pediatric cancer (Johnston et al., 2010). This toxicity is characterized by the breakdown of the mucosal barrier resulting in severe ulceration of the oral cavity and gastrointestinal tract (Van Sebille et al., 2015; Sonis, 2004a, 2004b, 2004c). As a consequence, children suffer from abdominal pain, vomits and diarrhea, which result in weight loss, need for nutritional support and an increased risk of infections (Kuiken et al., 2017). This clinical presentation may cause treatment delays, unplanned interruptions or even premature discontinuation of therapy (Cinausero et al., 2017), which in turn may result in impaired in impaired survival.

Mucositis can be linked to a number of antileukemic agents such as methotrexate (MTX), cytarabine, daunorubicin (DNR) or cyclophosphamide (CPA) (Cinausero et al., 2017; Schmiegelow et al., 2017). Although the prevalence and severity vary according to the type of drug, the cellular events which lead to the mucosal damage seem to be similar (Al-Ansari et al., 2015; Cinausero et al., 2017). This mechanism includes a cascade of critical biologic events such as reactive oxygen species (ROS) generation, NF-κB activation, pro-inflammatory cytokines release, MAPK signaling activation which to contribute to apoptosis, loss of renewal, atrophy and ulceration in the epithelium and submucosa (Cinausero et al., 2017; Le et al., 2017; Sonis et al., 2004, 2013). This mucosal damage could be induced by changes in genes of pharmacokinetic and pharmacodynamic pathways of mucotoxic drugs.

In this line, in childhood ALL treatment, several studies have already found polymorphisms in genes involved in MTX pathway, such as *ABCC1*, *ABCC2* or *ABCC4*, significantly associated with mucositis during consolidation, the phase in which this toxicity is usually assessed and linked to high-dose MTX (den Hoed et al., 2015; Liu et al., 2014b; Lopez-Lopez et al., 2013; Radtke et al., 2013). Variants in these genes of MTX transport could affect their regulation or function (Gervasini et al., 2017; Muralidharan et al., 2015). Interestingly, we recently found a significant association between increased risk of MTX-induced mucositis and GG genotype of rs2114358 in miR-1206 (Gutierrez-Camino et al., 2017b; Lopez-Lopez et al., 2014a). Considering that SNPs in miRNA genes can modify their levels or function, we proposed that these variants might affect MTX pathways genes expression (Gutierrez-Camino et al., 2017b).

In spite of these interesting results found in the consolidation phase, mucositis, as well as other clinical manifestations of mucosal injury such as diarrhea and vomits, are also frequently developed at induction phase. In this phase other mucotoxic drugs such as DNR and CPA are administered in addition to MTX. In consequence, we can hypothesize that variants in miRNAs targeting genes involved in DNR, CPA or MTX pathways, as well as other mucositis-related genes, could also be associated with mucositis during the induction phase of childhood ALL treatment. Therefore, in this study we analyzed the association between this toxicity and all the SNPs in miRNAs with a minor allele frequency (MAF) ≥0.01 described at the moment of the study in a large cohort of 179 Spanish children homogeneously treated for B-ALL. Additionally, we also analyzed diarrhea and vomits, both clinical manifestations related to mucosal damage.

MATERIAL AND METHODS

Patients

This is a retrospective study including 179 Spanish children diagnosed with B-ALL at the Pediatric Oncology Units of three Spanish hospitals (University Hospital Cruces, University Hospital Donostia and University Hospital La Paz from 2000 to 2013). Written informed consent was obtained from all patients or their parents before sample collection. This study obtained the approval (CEISH/102R/2011) of the ethical committee of the University of the Basque Country (UPV/EHU).

Treatment and toxicity evaluation

All the patients included in the study were homogeneously treated with the Spanish standard LAL-SHOP 94/99/2005 protocols. The induction phase of these protocols included two consecutive doses of DNR (120 mg/m^2), 4 doses of vincristine (1.5 mg/m^2 given on a weekly basis), and prednisone (60 mg/m^2/day for 28 days, 30 mg/m^2/day for 4 days and 15 mg/m^2/day the last 4 days). Moreover, 0- 2 doses of CPA depending on treatment arm (1000 mg/m^2/dose), 10 doses of asparaginase (5000–15,000 U/m^2 depending on treatment arm) and 2 or 3 doses of intrathecal MTX-cytarabine-hydrocortisone therapy depending on risk group (low-dose of 8-12 mg of MTX) were also administrated at induction. High-risk patients in the LAL/SHOP 99 also received a single dose of 3 g/m^2 of methotrexate on day +15.

Toxicity data were collected blinded to genotypes from the patients' medical files by the same two expert researchers in all cases. Mucositis was graded from 1 to 4 according to the Spanish Society of Pediatric Hematology and Oncology standards, adapted from the WHO criteria (See Table 9). Additionally, we also collected data of diarrhea and vomits, as both are also clinical

manifestations of mucosal injury. Grades 2 to 4 were considered as toxicity. Other data such as sex and age were systematically recorded from the clinical records.

Genes and polymorphism selection

Taking into account that miRNA targets are not completely defined nowadays and that any miRNA could be implicated direct or indirectly in the regulation of genes involved in mucositis development, we selected all the miRNA genes that have SNPs described at the time of the study (May 2014). Of a total of 1910 SNPs in 969 miRNAs, we selected those SNPs with a MAF>0.01 in European/Caucasoid populations. Mirbase (http://www.mirbase.org/), miRNA SNIPER (http://bioinfo.life.hust.edu.cn/miRNASNP2/index.php), and dbSNP (http://www.ncbi.nlm.nih.gov/SNP/) databases, as well as literature review, were used for the SNP selection (See Table 11).

Genotyping

Genomic DNA was extracted from peripheral blood or bone marrow from patients with ALL in remission using the phenol–chloroform method, as previously described (Sambrook, J, 2001). DNA was quantified using PicoGreen (Invitrogen Corp., Carlsbad, California, USA).

For each sample, 400 ng of DNA was genotyped using the GoldenGate Genotyping Assay (Illumina Inc., San Diego, California, USA) with Veracode technology according to the published Illumina protocol. Data were analyzed with GenomeStudio (Illumina Inc.) software for genotype clustering and calling. Duplicate samples and CEPH trios (Coriell Cell Repository, Camden, New Jersey, USA) were genotyped across the plates. SNPs showing Mendelian allele-transmission errors or showing discordant genotypes were excluded from the analysis.

Statistical analysis

The relationship between toxicities (mucositis, diarrhea and vomits) during induction was measured using univariate logistic regression models and correlation coefficients. To account for the possible confounding effect of age, sex, treatment protocol, risk group and treatment arm on toxicity, univariate and multivariate logistic regressions were used. The association between toxicity and genetic polymorphisms was evaluated by the χ2 or Fisher's exact test. The effect association sizes were estimated by the odds ratios. The most significant test among dominant and recessive models was selected. In all cases the significant level was set at 5 %. The results were adjusted for multiple comparisons using the false discovery rate (FDR) correction (Benjamini et al., 2001). Analyses were performed by using the R v3.3.0. software.

Bioinformatics analysis

- *miRNAs secondary structures prediction*

The RNAfold web tool (http://rna.tbi.univie.ac.at/cgi-bin/RNAWebSuite/RNAfold.cgi) (Gruber et al., 2008) was used to calculate the impact of the SNPs in the minimum free energy secondary structures and the energy change (ΔΔG) of the hairpin structure of the miRNAs significantly associated with toxicity.

- *Gene targets selection and pathway analysis*

MiRNA target genes were selected based on miRWalk database (Dweep and Gretz, 2015). Only those genes confirmed by at least six of the 12 prediction programs hosted in miRWalk (http://www.umm.uni-heidelberg.de/apps/zmf/mirwalk/index.html) were included.

Regarding pathway analysis with significant miRNAs, we first considered genes involved in the pharmacokinetic and pharmacodynamic pathways of DNR (anthracyclines pathway), MTX and CPA, selected based on the Pharmacogenomic Knowledge Base (PharmGKB) (https://www.pharmgkb.org/) and literature review. In a second approach to identify other genes that could be involved in mucosal toxicity, we performed a pathway enrichment analysis using the ConsensusPathDB web tool (CPdB) (http://consensuspathdb.org/) (Kamburov et al., 2013) using the over-representation analysis module. The miRWalk target gene lists were analyzed against the default collections of KEGG (Kanehisa et al., 2017), Reactome (Fabregat et al., 2016) and BioCarta (https://cgap.nci.nih.gov/Pathways/BioCarta_Pathways) pathway databases.

RESULTS

Patient's baseline characteristics

In this study we included a total of 179 pediatric patients. Mucositis data, as well as diarrhea and vomits, were available for 170 patients. During the induction phase, 36 out of 170 patients (21.2%) presented mucositis (grade≥2), 22 (12.9%) diarrhea (grade≥2) and 45 (26.5%) vomits (grade≥2) (Table 25). We found association between mucositis and diarrhea (p=4x10^{-6}) and mucositis and vomits (p=0.0001), as well as between diarrhea and vomiting (p=0.0005). We did not find any association between the covariates (age, sex, treatment protocol, risk group and treatment arm) and toxicities (mucositis, diarrhea and vomits). Thus, we did not include these covariates in the subsequent association analyses.

Table 25. Patients´ characteristics.

Characteristics	Induction phase	Consolidation phase
Number of patients	170	168
Sex, n (%)		
Male	100 (58.8)	100 (59.5)
Female	70 (41.2)	68 (40.5)
Age at diagnosis, mean ± SD (years)	5.22 ± 3.27	5.23 ± 3.27
Male	4.91 ± 3.28	4.84 ± 3.36
Female		
Treatment protocol, n (%)		
LAL/SHOP 94/99	63 (37.1)	62 (36.90)
LAL/SHOP 2005	107 (62.9)	106 (63.10)
Mucositis, n (%)	36 (21.18)	16 (9.52)
Diarrhea, n (%)	22 (12.94)	10 (5.95)
Vomits, n (%)	45 (26.47)	40 (23.81)

Abbreviations: SD, standard deviation.

Genotyping results

Successful genotyping was obtained for 158 out of 179 DNA samples (88.3%) and for 160 SNPs (75.12%). Genotyping failures were due to no PCR amplification, insufficient intensity for cluster separation, or poor or no cluster definition.

Association study

To investigate whether genetic variation in miRNAs influences digestive toxicity, we tested the association between the 160 successfully genotyped polymorphisms in 154 miRNAs and mucositis, diarrhea and vomiting.

Regarding mucositis, a total of 4 SNPs were significantly associated with this toxicity (Table 26). Among them, rs4674470 in miR-4268 was the most statistically significant SNP, the AG+GG genotype showing a 0.3-fold decreased risk of mucositis (p=0.0093) under the dominant model. None of the patients with the CC genotype developed mucositis. The SNP rs6977967 in miR-3683 showed a significant p-value (0.0098) under the recessive model, the GG genotype being the risk genotype. Rs174561 in miR-1908 and rs8078913 in miR-4520a also showed significant results. None of them remained statistically significant after FDR correction.

Table 26. SNPs in miRNAs showing the most significant associations with mucositis during induction phase in pediatric B-ALL. Genotypic and allelic frequencies.

miRNA SNP	Position Localization	Genotype /Allele	MucosInduc (n=170)		Model OR (95% CI) P-value
			NO Tox N=134 (%)	TOX 36 (%)	
hsa-mir-4268 rs4674470	Chr.: 2 pre-miRNA	AA	68 (58.1)	27 (81.8)	Dominant
		AG	39 (33.3)	6 (18.2)	0.31 (0.12-0.80)
		GG	10 (8.5)	0 (0)	**0.009339**
		A	175 (74.8)	60 (90.9)	0.297 (0.122-0.722)
		G	59 (25.2)	6 (9.1)	**0.005**
hsa-mir-3683 rs6977967	Chr.: 7 pre-miRNA	AA	82 (70.1)	22 (66.7)	Recesive
		AG	35 (29.9)	8 (24.2)	0 (0.0)
		GG	0 (0)	3 (9.1)	**0.009897**
		A	199 (85)	52 (78.8)	1.531 (0.767-3.055)
		G	35 (15)	14 (21.2)	0.2247
mir-1908 rs174561	Chr.: 11 pre-miRNA	TT	71 (64)	13 (41.9)	Dominant
		CT	34 (30.6)	16 (51.6)	2.46 (1.09-5.53)
		CC	6 (5.4)	2 (6.5)	**0.02852**
		T	176 (79.3)	42 (67.7)	1.822 (0.977-3.399)
		C	46 (20.7)	20 (32.3)	0.0572
hsa-mir-4520a rs8078913	Chr.: 17 in_mature	CC	38 (35.5)	10 (31.2)	Recesive
		CT	53 (49.5)	12 (37.5)	2.59 (1.03-6.47)
		TT	16 (15)	10 (31.2)	**0.04722**
		C	129 (60.3)	32 (50)	1.518 (0.866-2.66)
		T	85 (39.7)	32 (50)	0.1439

Abbreviations: B-ALL, B cell acute lymphoblastic leukemia; miRNA, microRNA; SNP, single nucleotide polymorphism; Tox, toxicity; OR, odds ratio; CI, confidence interval; Chr, chromosome.
Notes: Bold denote significant P-values.

Regarding diarrhea, we found 6 SNPs significantly associated with toxicity, being rs8667 in miR-4751 the most statistically significant SNP under the dominant model (p=0.0005) (Table 27). The AG+AA genotypes showed an increased risk for developing diarrhea. Other 5 SNPs in miR-146a, miR-605, miR-202, miR-1265 and miR-196a also showed statistically significant results. None of them remained statistically significant after FDR correction.

Table 27. SNPs in miRNAs showing the most significant associations with diarrhea during induction phase in pediatric B-ALL. Genotypic and allelic frequencies.

miRNA SNP	Position Localization	Genotype /Allele	DiarrheaInduc (n=170)		Model OR (95% CI) P-value
			NO Tox N=148 (%)	TOX 22 (%)	
hsa-mir-4751 rs8667	Chr.: 19 pre-miRNA	GG	52 (40.3)	1 (5)	Dominant
		AG	62 (48.1)	15 (75)	12.83 (1.67-98.80)
		AA	15 (11.6)	4 (20)	**0.0005**
		G	166 (64.3)	17 (42.5)	2.441 (1.241-4.803)
		A	92 (35.7)	23 (57.5)	**0.008**
hsa-mir-146a rs2910164	Chr.: 5 in_seed	GG	75 (58.1)	5 (23.8)	Dominant
		CG	44 (34.1)	12 (57.1)	4.44 (1.53-12.87)
		CC	10 (7.8)	4 (19)	**0.002**
		G	194 (75.2)	22 (52.4)	2.756 (1.413-5.376)
		C	64 (24.8)	20 (47.)	**0.0023**
hsa-mir-605 rs2043556	Chr.: 10 pre-miRNA	AA	68 (54)	17 (81)	Dominant
		AG	52 (41.3)	3 (14.3)	0.28 (0.09-0.87)
		GG	6 (4.8)	1 (4.8)	**0.015**
		A	188 (74.6)	37 (88.1)	0.397 (0.15-1.053)
		G	64 (25.4)	5 (11.9)	0.056
hsa-mir-202 rs12355840	Chr.: 10 pre-miRNA	TT	64 (54.7)	15 (83.3)	Dominant
		CT	47 (40.2)	3 (16.7)	0.24 (0.07-0.88)
		CC	6 (5.1)	0 (0)	**0.015**
		T	175 (74.8)	33 (91.7)	0.27 (0.08-0.912)
		C	59 (25.2)	3 (8.3)	0.025
hsa-mir-1265 rs11259096	Chr.: 10 pre-miRNA	TT	116 (89.9)	15 (71.4)	Dominant
		CT	12 (9.3)	6 (28.6)	3.57 (1.18-10.80)
		CC	1 (0.8)	0 (0)	**0.032**
		T	244 (94.6)	36 (85.7)	2.905 (1.049-8.042)
		C	14 (5.4)	6 (14.3)	**0.032**
hsa-mir-196a-2 rs11614913	Chr.: 12 in_mature	CC	63 (48.8)	6 (28.6)	Recesive
		CT	53 (41.1)	9 (42.9)	3.57 (1.18-10.80)
		TT	13 (10.1)	6 (28.6)	**0.0326**
		C	179 (69.4)	21 (50)	2.266 (1.171-4.385)
		T	79 (30.6)	21 (50)	**0.0135**

Abbreviations: B-ALL, B cell acute lymphoblastic leukemia; miRNA, microRNA; SNP, single nucleotide polymorphism; Tox, toxicity; OR, odds ratio; CI, confidence interval; Chr, chromosome.
Notes: Bold denote significant P-values.

In addition, we found a total of 6 SNPs significantly associated with vomits (Table 28). The most statistically significant SNP was rs12402181 in miR-3117, in which AG+AA genotype showed a 0.24-decreased risk of developing vomits under the dominant model (p= 0.004). Other 5 SNPs

in miR-3683, miR-548al, miR-4309, miR-3689d2 and miR-5196 also showed significant results.

None of them remained statistically significant after FDR correction.

Table 28. SNPs in miRNAs showing the most significant associations with vomiting during induction phase in pediatric B-ALL. Genotypic and allelic frequencies.

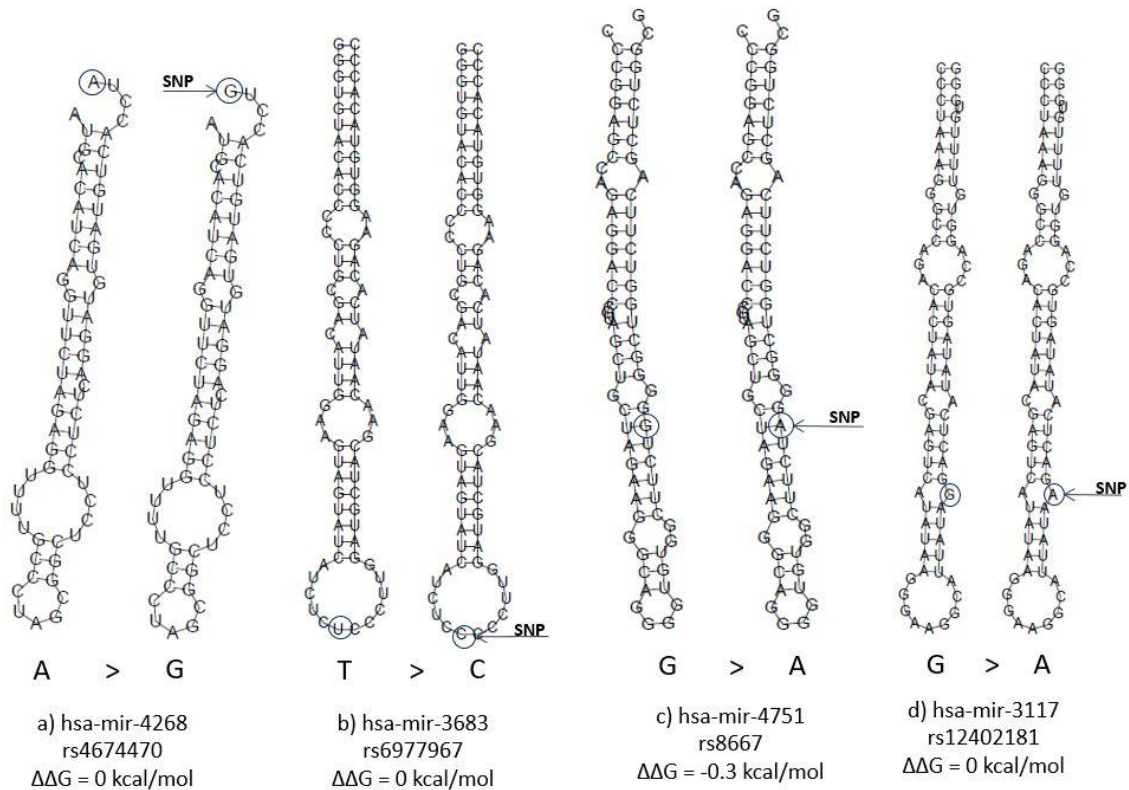| miRNA SNP	Position Localization	Genotype /Allele	VomitingInduc (n=170)		Model OR (95% CI) P-value
			NO Tox N=125 (%)	TOX 45 (%)	
hsa-mir-3117 rs12402181	Chr.: 1 in_seed	GG	75 (25)	34 (89.5)	Dominant
		AG	34 (30.4)	4 (10.5)	0.24 (0.08-0.72)
		AA	3 (2.7)	0 (0)	**0.004**
		G	184 (82.1)	72 (94.7)	0.256 (0.088-0.74)
		A	40 (17.9)	4 (5.3)	**0.007**
hsa-mir-3683 rs6977967	Chr.: 7 pre-miRNA	AA	76 (25.9)	28 (73.7)	Recesive
		AG	36 (32.1)	7 (18.4)	0 (0.0)
		GG	0 (0)	3 (7.9)	**0.015**
		A	188 (83.9)	63 (82.9)	1.078 (0.538-2.16)
		G	36 (16.1)	13 (17.1)	0.833
hsa-mir-548al rs515924	Chr.: 11 in_seed	AA	97 (87.4)	27 (71.1)	Dominant
		AG	14 (12.6)	10 (26.3)	2.82 (1.15-6.93)
		GG	0 (0)	1 (2.6)	**0.026**
		A	208 (93.7)	64 (84.2)	2.786 (1.226-6.327)
		G	14 (6.3)	12 (15.8)	**0.011**
hsa-mir-4309 rs12879262	Chr.: 14 pre-miRNA	GG	75 (25)	32 (84.2)	Dominant
		CG	35 (31.2)	6 (15.8)	0.38 (0.15-0.99)
		CC	2 (1.8)	0 (0)	**0.034**
		G	185 (82.6)	70 (92.1)	0.407 (0.165-1.002)
		C	39 (17.4)	6 (7.9)	0.0447
MIR3689 seq_rs62571442	Chr.: 9 pre-miRNA	AA	32 (28.8)	7 (18.4)	Recesive
		AG	62 (55.9)	19 (50.0)	2.55 (1.08-6.01)
		GG	17 (15.3)	12 (31.6)	**0.035**
		A	126 (56.8)	33 (43.4)	1.71 (1.011-2.893)
		G	96 (43.2)	43 (56.6)	0.044
hsa-mir-5196 rs10406069	Chr.: 19 pre-miRNA	GG	71 (63.4)	17 (44.7)	Dominant
		AG	40 (35.7)	21 (55.3)	2.14 (1.01-4.51)
		AA	1 (0.9)	0 (0.0)	**0.044**
		G	182 (81.3)	55 (72.4)	1.655 (0.904-3.028)
		A	42 (18.8)	21 (27.6)	0.1005

Abbreviations: B-ALL, B cell acute lymphoblastic leukemia; miRNA, microRNA; SNP, single nucleotide polymorphism; Tox, toxicity; OR, odds ratio; CI, confidence interval; Chr, chromosome.
Notes: Bold denote significant P-values.

Bioinformatic analysis

• *Secondary structure prediction*

We performed our analyses with the most statistically significant SNPs, rs4674470 in miR-4268, rs6977967 in miR-3683, rs8667 in miR-4751 and rs12402181 in miR-3117 (Figure 21). Rs4674470 SNP in miR-4268 and rs6977967 in miR-3683 did not modify either the energy change (ΔΔG) or the secondary structure. In the case of rs8667 in miR-4751, the substitution of the G allele for an A allele induced a slight energy change of -0.3 kcal/mol (from -40.2 to -40.5 kcal/mol) with no modification in the secondary structure. Finally, rs12402181 in miR-3117 neither modified the energy change (ΔΔG) nor the secondary structure.

A > G	T > C	G > A	G > A
a) hsa-mir-4268 rs4674470 ΔΔG = 0 kcal/mol	b) hsa-mir-3683 rs6977967 ΔΔG = 0 kcal/mol	c) hsa-mir-4751 rs8667 ΔΔG = -0.3 kcal/mol	d) hsa-mir-3117 rs12402181 ΔΔG = 0 kcal/mol

Figure 21. Energy change and minimum free-energy structures of the most significant miRNA SNPs in mucositis(a and b), diarrhea (c) and vomits (d), due to the presence of different alleles extracted from RNAfold web tool.

- *Pathway analyses*

Following the first approach, we searched for miRNA targets among DNR, CPA and MTX pharmacogenes (Figures 22-24). For mir-4268, we found two genes out of the DNR (anthracyclines) pathway (*NFKBIE*, *CBR1*), three out of the MTX pathway (*MTHFR*, *MTR*, *SLC46A1*), and no genes out of the CPA pathway. For miR-3683 we found one out of MTX (*SHMT1*) and another one of the CPA (*ALDH5A1*). For miR-4751, we found one gene out of the DNR pathway (*NDUFS2*), one out of the MTX (*SLC19A1*) and another one out of the CPA (*ERCC4*) pathway. Finally, for miR-3117 we found one gene out of the DNR pathway (*ABCC1*), four out of the MTX pathway (*PPAT*, *SLC46A1*, *SLCO1A2*, *ABCC1*), and one out of the CPA pathway (*ALDH5A1*).

In a second approach, pathway enrichment analyses were performed for these miRNAs in order to detect other genes related to mucositis, diarrhea and vomits by using the ConsensusPathDB web tool. For miR-4268, we found an over-representation of phospholipase D (PLD) signaling (p-value of 9.1×10^{-8}) among the top ten most significant pathways (Table 29). In this pathway, miR-4268 targeted up to 29 genes (Table 30). This pathway was related with other over-represented pathways such as choline metabolism and glutamatergic and neurotrophin signaling, since 10-12 genes were shared among them.

Table 29. Enriched pathways for miR-4268.

No.	Pathway name	Set size	Candidates	p-value	q-value	Patway source
1	Phospholipase D signaling pathway	144	29 (20.1%)	9.09e-08	0.000116	KEGG
2	Glutamatergic synapse	114	22 (19.3%)	6.67e-06	0.0034	KEGG
3	Signalling by NGF	433	54 (12.5%)	8.8e-06	0.0034	Reactome
4	Transcriptional misregulation in cancer	180	29 (16.1%)	1.07e-05	0.0034	KEGG
5	Transmembrane transport of small molecules	628	70 (11.1%)	2.16e-05	0.00514	Reactome
6	NGF signalling via TRKA from the plasma membrane	340	44 (12.9%)	2.42e-05	0.00514	Reactome
7	Pathways in cancer	397	49 (12.3%)	3.01e-05	0.00549	KEGG
8	Choline metabolism in cancer	101	19 (18.8%)	4.06e-05	0.00647	KEGG
9	Signaling by VEGF	290	38 (13.1%)	6.54e-05	0.00791	Reactome
10	Transmission across Chemical Synapses	218	31 (14.2%)	6.62e-05	0.00791	Reactome

Table 30. Genes of the Phospholipase D signaling pathway targeted by miR-4268

Entrez-gene ID	Entrez-gene name
10411	RAPGEF3 : Rap guanine nucleotide exchange factor 3
2916	GRM6 : glutamate metabotropic receptor 6
5155	PDGFB : platelet derived growth factor subunit B
554	AVPR2 : arginine vasopressin receptor 2
9266	CYTH2 : cytohesin 2
3643	INSR : insulin receptor
1609	DGKQ : diacylglycerol kinase theta
7248	TSC1 : tuberous sclerosis 1
107	ADCY1 : adenylate cyclase 1
108	ADCY2 : adenylate cyclase 2
9846	GAB2 : GRB2 associated binding protein 2
185	AGTR1 : angiotensin II receptor type 1
208	AKT2 : AKT serine/threonine kinase 2
5332	PLCB4 : phospholipase C beta 4
5335	PLCG1 : phospholipase C gamma 1
5337	PLD1 : phospholipase D1
2768	GNA12 : G protein subunit alpha 12
5595	MAPK3 : mitogen-activated protein kinase 3
2912	GRM2 : glutamate metabotropic receptor 2
2914	GRM4 : glutamate metabotropic receptor 4
23396	PIP5K1C : phosphatidylinositol-4-phosphate 5-kinase type 1 gamma
2917	GRM7 : glutamate metabotropic receptor 7
6009	RHEB : Ras homolog enriched in brain
387	RHOA : ras homolog family member A
1956	EGFR : epidermal growth factor receptor
5578	PRKCA : protein kinase C alpha
27128	CYTH4 : cytohesin 4
3577	CXCR1 : C-X-C motif chemokine receptor 1
6654	SOS1 : SOS Ras/Rac guanine nucleotide exchange factor 1

Regarding miR-3683, we found some pathways related to inflammatory processes (Table 31).

Table 31. Enriched pathways for miR-3683.

No.	Pathway name	Set size	Candidates	p-value	q-value	Patway source
1	Activation of BMF and translocation to mitochondria	3	2 (66.7%)	3.34e-05	0.0042	Reactome
2	Effects of PIP2 hydrolysis	27	3 (11.1%)	9.92e-05	0.00625	Reactome
3	Ion homeostasis	56	3 (5.4%)	0.000878	0.0341	Reactome
4	Cardiac conduction	135	4 (3.0%)	0.00108	0.0341	Reactome
5	Aldosterone synthesis and secretion	82	3 (3.7%)	0.00264	0.0613	KEGG
6	Muscle contraction	198	4 (2.0%)	0.00436	0.0613	Reactome
7	Inflammatory mediator regulation of TRP channels	99	3 (3.0%)	0.00449	0.0613	KEGG
8	Platelet calcium homeostasis	31	2 (6.5%)	0.00487	0.0613	Reactome
9	Downstream signaling of activated FGFR1	31	2 (6.5%)	0.00487	0.0613	Reactome
10	Activation of BH3-only proteins	31	2 (6.5%)	0.00487	0.0613	Reactome

For miR-4751, Toll-like receptor (TLR) signaling related pathways were over-represented, including MAPK signaling cascade (Table 32).

Table 32. Enriched pathways for miR-4751.

| No.	Pathway name	Set size	Candidates	p-value	q-value	Patway source
1	Acute myeloid leukemia	57	10 (17.5%)	5.52e-08	3.55e-05	KEGG
2	MAP kinase activation in TLR cascade	62	10 (16.1%)	1.27e-07	4.09e-05	Reactome
3	Nuclear Events (kinase and transcription factor activation)	25	7 (28.0%)	1.91e-07	4.09e-05	Reactome
4	TRAF6 Mediated Induction of proinflammatory cytokines	74	10 (13.5%)	7.05e-07	0.000108	Reactome
5	MAPK targets/ Nuclear events mediated by MAP kinases	31	7 (22.6%)	9.54e-07	0.000108	Reactome
6	TRIF-mediated TLR3/TLR4 signaling	101	11 (10.9%)	1.77e-06	0.000108	Reactome
7	MyD88-independent TLR3/TLR4 cascade	101	11 (10.9%)	1.77e-06	0.000108	Reactome
8	Toll Like Receptor 3 (TLR3) Cascade	101	11 (10.9%)	1.77e-06	0.000108	Reactome
9	MyD88 cascade initiated on plasma membrane	82	10 (12.2%)	1.85e-06	0.000108	Reactome
10	Toll Like Receptor 10 (TLR10) Cascade	82	10 (12.2%)	1.85e-06	0.000108	Reactome

Finally, for miR-3117, MAPK signaling pathways were over-represented (Table 33).

**Table 33.** Enriched pathways for miR-3117-3p.

No.	Pathway name	Set size	Candidates	p-value	q-value	Patway source
1	MAPK signaling pathway - Homo sapiens	257	24 (9.3%)	4.94e-07	0.000322	**KEGG**
2	Ras signaling pathway - Homo sapiens	228	21 (9.2%)	3.24e-06	0.00106	**KEGG**
3	Choline metabolism in cancer - Homo sapiens	101	13 (12.9%)	7.18e-06	0.00149	**KEGG**
4	PDGF signaling pathway	27	7 (25.9%)	9.14e-06	0.00149	**BioCarta**
5	Renal cell carcinoma - Homo sapiens	66	10 (15.2%)	1.95e-05	0.00254	**KEGG**
6	FoxO signaling pathway - Homo sapiens	134	14 (10.4%)	3.61e-05	0.00317	**KEGG**
7	ErbB signaling pathway - Homo sapiens	87	11 (12.6%)	4.32e-05	0.00317	**KEGG**
8	Signaling by EGFR in Cancer	15	5 (33.3%)	4.87e-05	0.00317	**Reactome**
9	Constitutive Signaling by Ligand-Responsive EGFR Cancer Variants	15	5 (33.3%)	4.87e-05	0.00317	**Reactome**
10	Signaling by Ligand-Responsive EGFR Variants in Cancer	15	5 (33.3%)	4.87e-05	0.00317	**Reactome**
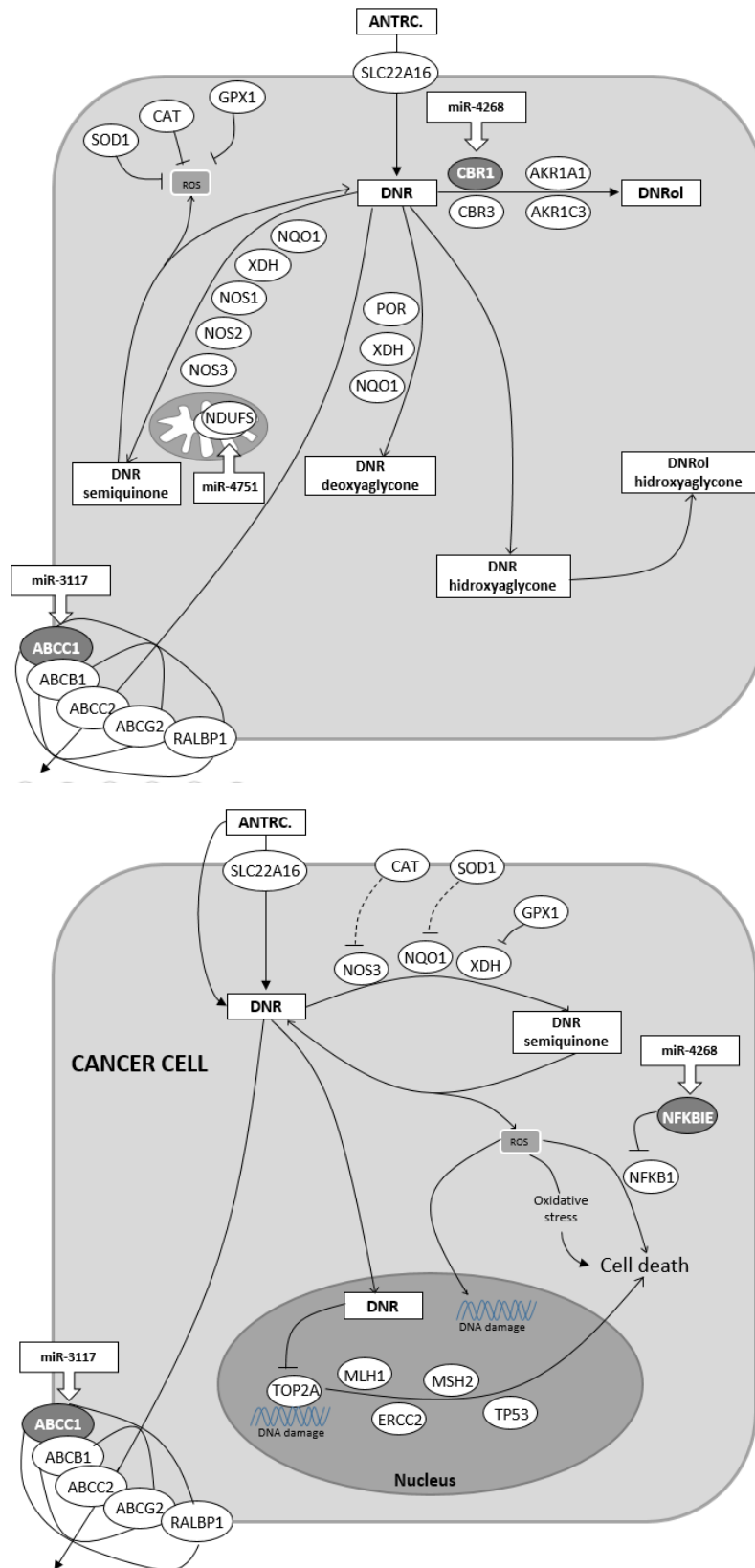
Figure 22. Antrhacyclines PK/PD pathway genes and the most significant miRNAs in this study targeting the corresponding genes.

.
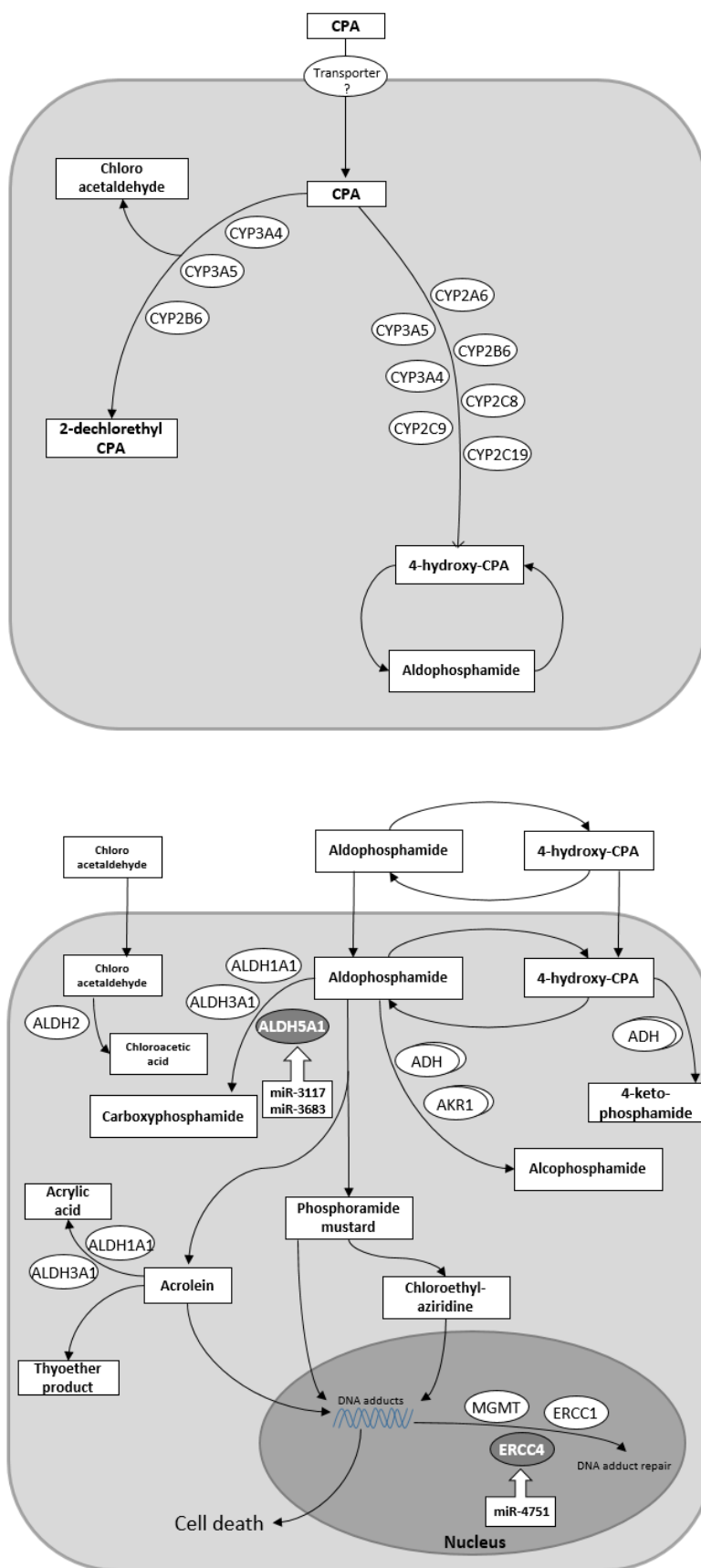
Figure 23. CPA PK/PD pathway genes and the most significant miRNAs in this study targeting the corresponding genes.
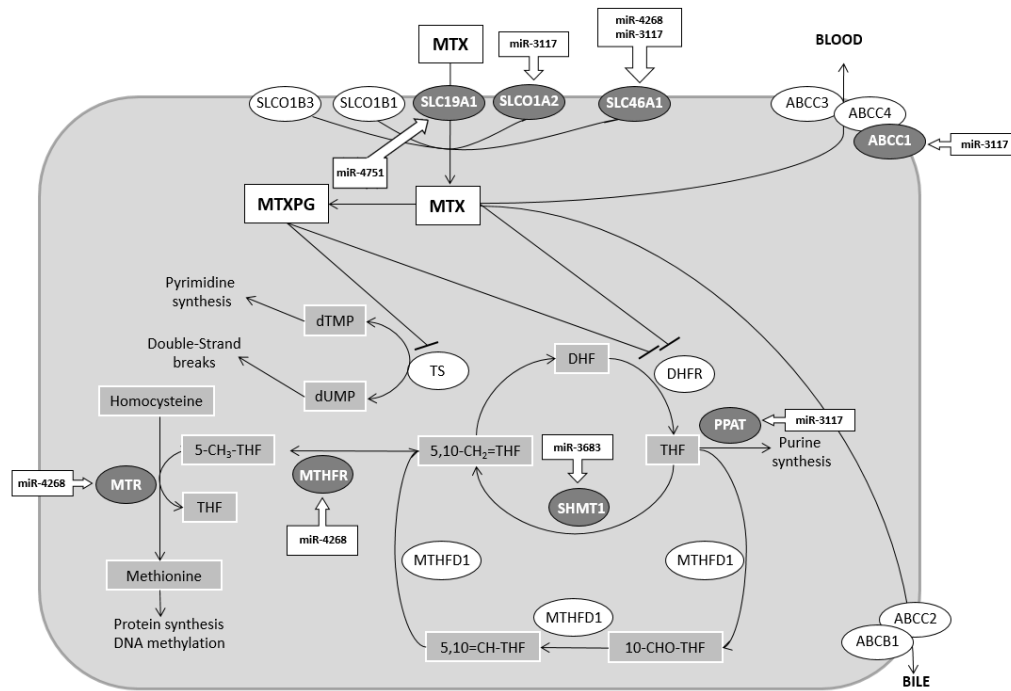
Figure 24. MTX PK/PD pathway genes and the most significant miRNAs in this study targeting the corresponding genes

DISCUSSION

In this study we determined the association between mucositis, diarrhea and vomits and variants in miRNAs that could target genes involved in DNR, MTX or CPA pathways, as well as other mucositis-related genes. We analyzed 213 SNPs in 206 miRNAs in 179 Spanish children diagnosed with B-ALL and homogenously treated with LAL/SHOP protocols.

In mucositis analysis, the most interesting result was the association between AG+GG genotype of rs4674470 in miR-4268 and decreased risk of toxicity (p=0.0093). Interestingly, none of the patients with the GG genotype developed mucositis, indicating a protective role. This SNP is located at the 3´ end position of the miRNA hairpin, but it did not modify either the stability or the secondary structure of the miRNA (Figure 21). However, this position could be crucial for the accurate recognition of a cleavage site between the pri-miRNA and pre-miRNA by the DROSHA. DROSHA generates the termini of pre-miRNAs, determining the mature miRNA sequence, thus, accurate processing by DROSHA is critical for production of functional miRNAs (Fang and Bartel, 2015; Kim et al., 2017). Therefore, the presence of this SNP could lead DROSHA to a misrecognition of the cleavage site and then, to a less production of the miRNA depending on the SNP allele. Of note, this miRNA is represented in the miRbase database, the reference database of miRNAs, with the G allele, which is the minor allele (Kozomara and Griffiths-Jones, 2014). The fact that in the reference database the miRNA sequence is represented with the G

allele could indicate that the miRNA could be more efficiently produced when the G allele is presented because of the recognition of DROSHA of the cleavage site.

Regarding the pathway analysis for this miRNA, we found two genes of DNR pathway (*NFKBIE*, *CBR1*) and three of the MTX pathway (*MTHFR*, *MTR*, *SLC46A1*) following the first approach based on pharmacogenes. However, the deregulation of these genes by miR-4268 could have contradictory effects. For instance, downregulation of *NFKBIE* could protect from cell death (Komissarova et al., 2008), whereas downregulation of *MTHFR* and *MTR* could contribute to apoptosis (Kubota et al., 2014; Yang et al., 2017). In order to identify other mucositis-related genes, we performed a pathway enrichment analysis and we found that miR-4268 targeted the PLD signaling pathway. *PLD* expression has been shown to be up-regulated in inflamed mucosa of inflammatory bowel diseases (Zhou et al., 2016). PLD modulates pro-inflammatory gene expression and has a major role in the secretion of cytokines (Friday and Fox, 2016; Kang et al., 2014), a mechanism involved in mucositis development (Cinausero et al., 2017). Interestingly, silencing of *PLD* effectively blocked the cytokine production (Sethu et al., 2010) and ameliorated intestinal mucosal inflammation (Zhou et al., 2016). This silencing has already been shown that could be mediated by a repertory of miRNAs (Fite et al., 2016). In this context, it is plausible that the rs4674470 GG genotype in miR-4268 could lead to higher miRNA expression due to a more efficient recognition by DROSHA and, in turn, to a lower expression of PLD-related genes, explaining its protective role in mucositis.

Regarding diarrhea, the most statistically significant SNP was rs8667 in miR-4751, the AG+AA genotype showing an increased risk of developing the condition under the dominant model. The SNP is located in the pre-mature sequence of miR-4751 where the A allele slightly modifies the energy, which in turn, could alter the miRNA levels (Gong et al., 2012). We found that miR-4751 targeted several genes out of the DNR (*NDUFS2*), MTX (*SLC19A1*) and CPA (*ERCC4*) pathways. Additionally, pathway enrichment analysis showed that TLR signaling cascades were over-represented. TLRs activation induces pro-inflammatory transcription factors such as NF-kB, which leads to expression of pro-inflammatory genes such as IL-1, IL-6 and TNF (Ramnath et al., 2017), events involved in the pathobiology of mucosal damage. Therefore, rs8667 in miR-4751 could alter the miRNA levels and affect the expression of its target genes in drug pathways and TLR signaling-related genes, contributing to increased toxicity.

Finally, in vomits analysis rs12402181 in miR-3117 was the most statistically significant SNP under the dominant model, in which AG+AA genotypes showed a decreased risk. This SNP is located in the seed sequence of miR-3117-3p, therefore it could affect the accurate recognition

of its target mRNA sequences. Among their target genes, we found genes out of the DNR (*ABCC1*), MTX (*PPAT, SLC46A1*, *SLCO1A2* and *ABCC1*) and CPA (*ALDH5A1*) pathways. By pathway enrichment analysis, we found that MAPK-related pathways were over-represented. MAPK activity is critical for inflammatory response and its activation is a prerequisite for the production of several cytokines, including IL-1, IL-8, IL-6 and TNF (van den Blink et al., 2001; Elsea et al., 2008; Reyes-Gibby et al., 2017). Therefore, failed recognition between miR-3117-3p and its targets mediated by the SNP rs12402181 in the seed region could contribute to mucosal injury by leading to an aberrant activation of the MAPK-related pathways.

This study has some limitations that must be discussed, such as the relatively high failure rate in genotyping technique. However, this high chance of failure was accepted from the beginning of the study because, despite the predicted low score for genotyping, no other design option to amplify the polymorphisms in question was possible. Another possible weakness is that the SNPs did not reach statistical significance when FDR correction was applied. This could be due to the low frequency of SNPs in miRNAs, because they are located in conserved regions (Mishra et al., 2008). Finally, we have to take into account the inaccuracy of the prediction algorithms of the databases used to determine the target gene and pathways, (Akhtar et al., 2016; Lee et al., 2015) but nowadays this limitation has to be assumed.

In conclusion, the most interesting results were three SNPs in miR-4268, miR-4751 and miR-3117 which could be involved in mucositis, diarrhea and vomits, respectively, during the induction phase of childhood ALL therapy. This involvement could be due to their effects on pharmacokinetics and pharmacodynamics of mucotoxic drugs, as well as other mucosal injury-related genes, especially those involved in the inflammatory response. It would be interesting to validate these results in another cohort.

CONFLICT OF INTEREST: Nothing to declare

REFERENCES

Akhtar, M.M., Micolucci, L., Islam, M.S., Olivieri, F., and Procopio, A.D. (2016). Bioinformatic tools for microRNA dissection. Nucleic Acids Res. 44, 24–44.

Al-Ansari, S., Zecha, J.A.E.M., Barasch, A., de Lange, J., Rozema, F.R., and Raber-Durlacher, J.E. (2015). Oral mucositis induced by anticancer therapies. Curr. Oral Heal. Reports 2, 202–211.

Benjamini, Y., Drai, D., Elmer, G., Kafkafi, N., and Golani, I. (2001). Controlling the false discovery rate in behavior genetics research. Behav. Brain Res. 125, 279–284.

van den Blink, B., Juffermans, N.P., ten Hove, T., Schultz, M.J., van Deventer, S.J., van der Poll, T., and Peppelenbosch, M.P. (2001). p38 mitogen-activated protein kinase inhibition increases cytokine release by macrophages in vitro and during infection in vivo. J. Immunol. 166, 582–587.

Cinausero, M., Aprile, G., Ermacora, P., Basile, D., Vitale, M.G., Fanotto, V., Parisi, G., Calvetti, L., and Sonis, S.T. (2017). New frontiers in the pathobiology and treatment of cancer regimen-related mucosal injury. Front. Pharmacol. 8, 354.

Dweep, H., and Gretz, N. (2015). miRWalk2.0: a comprehensive atlas of microRNA-target interactions. Nat. Methods 12, 697.

Elsea, C.R., Roberts, D.A., Druker, B.J., and Wood, L.J. (2008). Inhibition of p38 MAPK suppresses inflammatory cytokine induction by etoposide, 5-fluorouracil, and doxorubicin without affecting tumoricidal activity. PLoS One 3, e2355.

Fabregat, A., Sidiropoulos, K., Garapati, P., Gillespie, M., Hausmann, K., Haw, R., Jassal, B., Jupe, S., Korninger, F., McKay, S., et al. (2016). The Reactome pathway knowledgebase. Nucleic Acids Res. 44, D481-7.

Fang, W., and Bartel, D.P. (2015). The menu of features that define primary microRNAs and enable de novo design of microRNA genes. Mol. Cell 60, 131–145.

Fite, K., Elkhadragy, L., and Gomez-Cambronero, J. (2016). A Repertoire of MicroRNAs Regulates cancer cell starvation by targeting phospholipase D in a feedback loop that operates maximally in cancer cells. Mol. Cell. Biol. 36, 1078–1089.

Friday, S.C., and Fox, D.A. (2016). Phospholipase D enzymes facilitate IL-17- and TNFα-induced expression of proinflammatory genes in rheumatoid arthritis synovial fibroblasts (RASF). Immunol. Lett. 174, 9–18.

Gervasini, G., de Murillo, S.G., Jiménez, M., de la Maya, M.D., and Vagace, J.M. (2017). Effect of polymorphisms in transporter genes on dosing, efficacy and toxicity of maintenance therapy in children with acute lymphoblastic leukemia. Gene 628, 72–77.

Gong, J., Tong, Y., Zhang, H.-M., Wang, K., Hu, T., Shan, G., Sun, J., and Guo, A.-Y. (2012). Genome-wide identification of SNPs in microRNA genes and the SNP effects on microRNA target binding and biogenesis. Hum. Mutat. 33, 254–263.

Gruber, A.R., Lorenz, R., Bernhart, S.H., Neubock, R., and Hofacker, I.L. (2008). The Vienna RNA websuite. Nucleic Acids Res. 36, W70-4.

Gutierrez-Camino, A., Oosterom, N., den Hoed, M.A.H., Lopez-Lopez, E., Martin-Guerrero, I., Pluijm, S.M.F., Pieters, R., de Jonge, R., Tissing, W.J.E., Heil, S.G., et al. (2017). The miR-1206 microRNA variant is associated with methotrexate-induced oral mucositis in pediatric acute lymphoblastic leukemia. Pharmacogenet. Genomics 27, 303–306.

den Hoed, M.A.H., Lopez-Lopez, E., te Winkel, M.L., Tissing, W., de Rooij, J.D.E., Gutierrez-Camino, A., Garcia-Orad, A., den Boer, E., Pieters, R., Pluijm, S.M.F., et al. (2015). Genetic and metabolic determinants of methotrexate-induced mucositis in pediatric acute lymphoblastic leukemia. Pharmacogenomics J. 15, 248–254.

Johnston, W.T., Lightfoot, T.J., Simpson, J., and Roman, E. (2010). Childhood cancer survival: a report from the United Kingdom childhood cancer study. Cancer Epidemiol. 34, 659–666.

Kamburov, A., Stelzl, U., Lehrach, H., and Herwig, R. (2013). The ConsensusPathDB interaction database: 2013 update. Nucleic Acids Res. 41, D793-800.

Kanehisa, M., Furumichi, M., Tanabe, M., Sato, Y., and Morishima, K. (2017). KEGG: new perspectives on genomes, pathways, diseases and drugs. Nucleic Acids Res. 45, D353–D361.

Kang, D.W., Choi, K.-Y., and Min, D.S. (2014). Functional regulation of phospholipase D expression in cancer and inflammation. J. Biol. Chem. 289, 22575–22582.

Kim, B., Jeong, K., and Kim, V.N. (2017). Genome-wide mapping of DROSHA cleavage sites on primary microRNAs and noncanonical substrates. Mol. Cell 66, 258–269.e5.

Komissarova, E. V, Li, P., Uddin, A.N., Chen, X., Nadas, A., and Rossman, T.G. (2008). Gene expression levels in normal human lymphoblasts with variable sensitivities to arsenite: identification of GGT1 and NFKBIE expression levels as possible biomarkers of susceptibility. Toxicol. Appl. Pharmacol. 226, 199–205.

Kozomara, A., and Griffiths-Jones, S. (2014). miRBase: annotating high confidence microRNAs using deep sequencing data. Nucleic Acids Res. 42, D68-73.

Kubota, M., Nakata, R., Adachi, S., Watanabe, K.-I., Heike, T., Takeshita, Y., and Shima, M. (2014). Plasma homocysteine, methionine and S-adenosylhomocysteine levels following high-dose methotrexate treatment in pediatric patients with acute lymphoblastic leukemia or Burkitt lymphoma: association with hepatotoxicity. Leuk. Lymphoma 55, 1591–1595.

Kuiken, N.S.S., Rings, E.H.H.M., Blijlevens, N.M.A., and Tissing, W.J.E. (2017). Biomarkers and non-invasive tests for gastrointestinal mucositis. Support. Care Cancer 25, 2933–2941.

Le, Z., Niu, X., Chen, Y., Ou, X., Zhao, G., Liu, Q., Tu, W., Hu, C., Kong, L., and Liu, Y. (2017). Predictive single nucleotide polymorphism markers for acute oral mucositis in patients with nasopharyngeal carcinoma treated with radiotherapy. Oncotarget 8, 63026–63037.

Lee, Y.J.D., Kim, V., Muth, D.C., and Witwer, K.W. (2015). Validated microRNA target databases: an evaluation. Drug Dev. Res. 76, 389–396.

Liu, Y., Yin, Y., Sheng, Q., Lu, X., Wang, F., Lin, Z., Tian, H., Xu, A., and Zhang, J. (2014). Association of ABCC2 -24C>T polymorphism with high-dose methotrexate plasma concentrations and toxicities in childhood acute lymphoblastic leukemia. PLoS One 9, e82681.

Lopez-Lopez, E., Ballesteros, J., Pinan, M.A., Sanchez de Toledo, J., Garcia de Andoin, N., Garcia-Miguel, P., Navajas, A., and Garcia-Orad, A. (2013). Polymorphisms in the methotrexate transport pathway: a new tool for MTX plasma level prediction in pediatric acute lymphoblastic leukemia. Pharmacogenet. Genomics 23, 53–61.

Lopez-Lopez, E., Gutierrez-Camino, A., Pinan, M.A., Sanchez-Toledo, J., Uriz, J.J., Ballesteros, J., Garcia-Miguel, P., Navajas, A., and Garcia-Orad, A. (2014). Pharmacogenetics of microRNAs and microRNAs biogenesis machinery in pediatric acute lymphoblastic leukemia. PLoS One 9, e91261.

Mishra, P.J., Mishra, P.J., Banerjee, D., and Bertino, J.R. (2008). MiRSNPs or MiR-polymorphisms, new players in microRNA mediated regulation of the cell: Introducing microRNA pharmacogenomics. Cell Cycle 7, 853–858.

Muralidharan, N., Antony, P.T., Jain, V.K., Mariaselvam, C.M., and Negi, V.S. (2015). Multidrug resistance 1 (MDR1) 3435C>T gene polymorphism influences the clinical phenotype and methotrexate-induced adverse events in South Indian Tamil rheumatoid arthritis. Eur. J. Clin. Pharmacol. 71, 959–965.

Radtke, S., Zolk, O., Renner, B., Paulides, M., Zimmermann, M., Moricke, A., Stanulla, M., Schrappe, M., and Langer, T. (2013). Germline genetic variations in methotrexate candidate genes are associated with pharmacokinetics, toxicity, and outcome in childhood acute lymphoblastic leukemia. Blood 121, 5145–5153.

Ramnath, D., Powell, E.E., Scholz, G.M., and Sweet, M.J. (2017). The toll-like receptor 3 pathway in homeostasis, responses to injury and wound repair. Semin. Cell Dev. Biol. 61, 22–30.

Reyes-Gibby, C.C., Melkonian, S.C., Wang, J., Yu, R.K., Shelburne, S.A., Lu, C., Gunn, G.B., Chambers, M.S., Hanna, E.Y., Yeung, S.-C.J., et al. (2017). Identifying novel genes and biological processes relevant to the development of cancer therapy-induced mucositis: An informative gene network analysis. PLoS One 12, e0180396.

Sambrook, J, R.D. (2001). Molecular cloning: a laboratory manual (New York: NY: Cold Spring Harbor Laboratory Press).

Sangild, P.T., Shen, R.L., Pontoppidan, P.E.L., and Rathe, M. (2017). Animal models of chemotherapy-induced mucositis: translational relevance and challenges. Am. J. Physiol. - Gastrointest. Liver Physiol. ajpgi.00204.2017.

Schmiegelow, K., Müller, K., Mogensen, S.S., Mogensen, P.R., Wolthers, B.O., Stoltze, U.K., Tuckuviene, R., and Frandsen, T. (2017). Open peer review non-infectious chemotherapy-associated acute toxicities during childhood acute lymphoblastic leukemia therapy. F 1000 Res. 1–14.

Van Sebille, Y.Z.A., Stansborough, R., Wardill, H.R., Bateman, E., Gibson, R.J., and Keefe, D.M. (2015). Management of mucositis during chemotherapy: from pathophysiology to pragmatic therapeutics. Curr. Oncol. Rep. 17, 50.

Sethu, S., Pushparaj, P.N., and Melendez, A.J. (2010). Phospholipase D1 mediates TNFalpha-induced inflammation in a murine model of TNFalpha-induced peritonitis. PLoS One 5, e10506.

Sonis, S.T. (2004a). The pathobiology of mucositis. Nat. Rev. Cancer 4, 277–284.

Sonis, S.T. (2004b). Oral mucositis in cancer therapy. J. Support. Oncol. 2, 3–8.

Sonis, S.T. (2004c). A biological approach to mucositis. J. Support. Oncol. 2, 21-32-6.

Sonis, S.T., Elting, L.S., Keefe, D., Peterson, D.E., Schubert, M., Hauer-Jensen, M., Bekele, B.N., Raber-Durlacher, J., Donnelly, J.P., Rubenstein, E.B., et al. (2004). Perspectives on cancer therapy-induced mucosal injury: pathogenesis, measurement, epidemiology, and consequences for patients. Cancer 100, 1995–2025.

Sonis, S.T., Antin, J., Tedaldi, M., and Alterovitz, G. (2013). SNP-based Bayesian networks can predict oral mucositis risk in autologous stem cell transplant recipients. Oral Dis. 19, 721–727.

Staley, J.R., Blackshaw, J., Kamat, M.A., Ellis, S., Surendran, P., Sun, B.B., Paul, D.S., Freitag, D., Burgess, S., Danesh, J., et al. (2016). PhenoScanner: a database of human genotype-phenotype associations. Bioinformatics 32, 3207–3209.

Yang, A., Sun, Y., Mao, C., Yang, S., Huang, M., Deng, M., Ding, N., Yang, X., Zhang, M., Jin, S., et al. (2017). Folate protects hepatocytes of hyperhomocysteinemia mice from apoptosis via cystic fibrosis transmembrane conductance regulator (CFTR)-activated endoplasmic reticulum stress. J. Cell. Biochem. 118, 2921–2932.

Zhou, G., Yu, L., Yang, W., Wu, W., Fang, L., and Liu, Z. (2016). Blockade of PLD2 ameliorates intestinal mucosal inflammation of inflammatory bowel disease. Mediators Inflamm. 2016, 2543070.

MiR-pharmacogenetics of methotrexate in childhood B-cell acute lymphoblastic leukemia

Leire Iparraguirre[1]; Angela Gutierrez-Camino[1]; Maitane Umerez[1]; Idoia Martin-Guerrero[1]; Itziar Astigarraga[2,3]; Aurora Navajas[,2,3]; Ana Sastre[4]; Nagore Garcia de Andoin[5] and Africa Garcia-Orad[1,3].

[1]Department of Genetics, Physical Anthropology and Animal Physiology, Faculty of Medicine and Odontology, University of the Basque Country (UPV/EHU), Leioa, Spain; [2]Department of Pediatric Hematology/Oncology, University Hospital Cruces, Bilbao, Spain; [3]Department of Pediatrics, BioCruces Health Research Institute, Barakaldo, Spain; [4]Department of Pediatric Oncohematology, University Hospital La Paz, Madrid, Spain; [5]Department of Pediatric Oncohematology, University Hospital Donostia, San Sebastian, Spain.

Abstract

Objectives: Methotrexate (MTX), the key drug in childhood B-cell acute lymphoblastic leukemia (B-ALL) therapy, often causes toxicity. An association between genetic variants in MTX transport genes and toxicity has been found. It is known that these transporters are regulated by microRNAs (miRNAs), and miRNA single nucleotide polymorphisms (SNPs) interfere with miRNA levels or function. With regard to B-cell ALL, we have previously found rs56103835 in miR-323b that targets *ABCC4* associated with MTX plasma levels. Despite these evidences and that nowadays a large amount of new miRNAs have been annotated, studies of miRNA polymorphisms and MTX toxicity are almost absent. Therefore, the aim of this study was to determine whether there are other variants in miRNAs associated with MTX levels. **Patients and methods:** Blood samples of 167 Spanish patients with pediatric B-cell ALL treated with the LALSHOP protocol were analyzed. We selected all the SNPs described in pre-miRNAs with a minor allele frequency more than 1% (213 SNPs in 206 miRNAs) that could regulate MTX transporters because the miRNAs that target MTX transporter genes are not completely defined. Genotyping was performed with VeraCode GoldenGate platform. **Results:** Among the most significant results, we found rs56292801 in miR-5189, rs4909237 in miR-595, and rs78790512 in miR-6083 to be associated with MTX plasma levels. These miRNAs were predicted, in silico, to regulate genes involved in MTX uptake: *SLC46A1*, *SLC19A1*, and *SLCO1A2*. **Conclusion:** In this study, we detected three SNPs in miR-5189, miR-595, and miR-6083 that might affect SLC46A1, SLC19A1, and SLCO1A2 MTX transport gene regulation and could affect MTX levels in patients with pediatric B-cell ALL.

Keywords: B-cell acute lymphoblastic leukemia, methotrexate, microRNAs, single nucleotide polymorphisms.

INTRODUCTION

Acute lymphoblastic leukemia (ALL) is the most common childhood cancer (Johnston et al., 2010). During the past 20 years, survival rates for ALL have improved markedly because of advances in chemotherapy (Pui, 2010). An important component of ALL therapy is methotrexate (MTX). Despite its clinical efficacy, high doses of MTX often cause toxicity, requiring a dose reduction or cessation of treatment, which may have an impact on survival (Evans et al., 1998; Salazar et al., 2012; Treon and Chabner, 1996). Therefore, one of the challenges for modern medicine is to predict which patients will develop toxicity in advance, in order to adjust the treatment from the beginning.

In the past few years, a large number of studies have analyzed the relationship between genetic variants and MTX toxicity (Lopez-Lopez et al., 2014b; Moriyama et al., 2015; Pui et al., 2015; Trevino et al., 2009). Some of the most interesting results have been found in MTX transporters. Treviño et al. (Trevino et al., 2009) found for the first time that single nucleotide polymorphisms (SNPs) rs4149081 and rs11045879 in SLCO1B1 were strongly associated with MTX clearance in patients with ALL. After that first report, these variants and others in SLCO1B1 have been confirmed in subsequent studies (Lopez-Lopez et al., 2011, 2013; Radtke et al., 2013; Ramsey et al., 2012, 2013). As a result of these studies, other works have focused their interest on the analysis of variants in MTX transporters, finding several SNPs in genes such as SLC19A1, ABCC4, or ABCC2 also associated with MTX levels (Laverdiere et al., 2002; Lopez-Lopez et al., 2013).

At present, it is known that MTX transporter genes, as well as the 50% of our genes, are regulated at the post transcriptional level by microRNAs (miRNAs) (Rukov and Shomron, 2011). Therefore, changes in miRNA levels or function might affect its target gene expression. Considering that SNPs in miRNA genes can modify their levels or function, we could expect that these variants might affect MTX transport gene regulation. These variants have already been related with other drug toxicities (Amstutz et al., 2015; Meulendijks et al., 2016; Zhan et al., 2012). With regard to childhood B-cell acute lymphoblastic leukemia (B-ALL), there is a previous study performed by our group in which we analyzed 46 SNPs in 42 pre-miRNAs and found one SNP, rs56103835, in miR-453 (also known as miR-323b) to be significantly associated with MTX plasma clearance during the consolidation phase. Interestingly, this miRNA has as putative target gene ABCC4, which is involved in MTX transport (Lopez-Lopez et al., 2014a).

Taking into account that after our previous study the number of annotated miRNAs has increased substantially (Kozomara and Griffiths-Jones, 2014) and that nowadays miRNA targets

are not completely defined and any miRNA could be involved in regulation of MTX transporter genes, the aim of this study was to determine whether any of the currently described variants in miRNAs are associated with MTX plasma levels in childhood ALL patients. To achieve this aim, we have analyzed all miRNA variants with a minor allele frequency more than 0.01 in a large B-ALL Spanish population.

PATIENTS AND METHODS

Patients

The patients included in this retrospective study were 167 Spanish childhood B-ALL patients diagnosed at the Pediatric Oncology Units of three Spanish hospitals (University Hospital Cruces, University Hospital Donostia and University Hospital La Paz from 2000 to 2013). Written informed consent was obtained from all patients or their parents before sample collection. This study obtained the board approval (CEISH/102R/2011) of the University of the Basque Country (UPV/EHU).

Treatment and toxicity evaluation

All patients included in the study were homogeneously treated with the LAL-SHOP 94/99 and 2005 protocols. These protocols included in the consolidation phase three MTX doses (each dose consisted of 3 or 5 g/m^2), 6-mercaptopurine (30 mg/m^2/day for 6 weeks), four doses of cytarabine (1 g/m^2), and four doses of triple intrathecal therapy. Each of the three MTX doses was given in a 24 h infusion with homogeneous folinic acid rescue. After each dose, MTX plasma concentration was monitored by a fluorescence polarization immunoassay on a TDx system (Abbott Laboratories, Abbott Park, Illinois, USA). Measurements were recorded daily until the concentration was below 0.2 µmol/l.

MTX plasma-level data were collected in consolidation phase at 48, 72, and 96 h right after the start of the infusion. Data were collected objectively, blinded to genotypes, from the patients' medical files. MTX levels were considered high if the concentration was over 1 µmol/l at 48 h or over 0.2 µmol/l at 72 or 96 h after at least one of the three doses, as previously described (Lopez-Lopez et al., 2013; Suthandiram et al., 2014). In addition, global high MTX plasma levels were considered if the MTX levels were higher than the established threshold in any of the cycles during the consolidation phase. Sex and age data were systematically recorded from the clinical records.

Genes and polymorphism selection

Taking into account that, on one hand, miRNAs that target MTX transporters are not completely defined nowadays and that, on the other hand, any miRNA could be implicated direct or indirectly in the regulation of MTX transporters, we selected all the miRNA genes that have SNPs described at the time of the study (May 2014). Of a total of 1910 SNPs in 969 miRNAs, we selected those SNPs with a minor allele frequency more than 0.01 in European/Caucasoid populations. For the SNP selection, we used mirbase (http://www.mirbase.org/), miRNA SNIPER (http://bioinfo.life.hust.edu.cn/miRNASNP2/index.php), and dbSNP (http://www.ncbi.nlm.nih.gov/SNP/) databases, as well as literature review.

A total of 213 SNPs in 206 miRNAs were selected for the study (See Table 11).

Genotyping

Genomic DNA was extracted from patients' remission peripheral blood or bone marrow using the phenol–chloroform method, as previously described (Sambrook, J, 2001). DNA was quantified using PicoGreen (Invitrogen Corp., Carlsbad, California, USA).

For each sample, 400 ng of DNA was genotyped using the GoldenGate Genotyping Assay (Illumina Inc., San Diego, California, USA) with Veracode technology according to the published Illumina protocol. Data were analyzed with GenomeStudio (Illumina Inc.) software for genotype clustering and calling. Duplicate samples and CEPH trios (Coriell Cell Repository, Camden, New Jersey, USA) were genotyped across the plates. SNPs showing Mendelian allele-transmission errors or showing discordant genotypes were excluded from the analysis.

Statistical analysis

The $\chi 2$ or Fisher's exact test was used to determine the effect of MTX levels. The effect sizes of the associations were estimated by the odds ratios. To account for the possible confounding effect of MTX dose, multivariate logistic regressions were used. In addition, we analyzed independently the population treated with a 5 g/m^2 dose by univariate logistic regression. We performed this analysis considering that the 5 g/m^2 dose could have a major contribution in significant results. The most significant test among dominant and recessive genetic models was selected. In all cases the significance level was set at 5%. The results were adjusted for multiple comparisons using the false discovery rate (FDR) correction (Benjamini et al., 2001). Analyses were performed by using the R v3.3.0. software.

Bioinformatics analysis

MiRNA target genes were selected based on miRWalk database. Only those genes confirmed by at least six of the 12 prediction programs hosted in miRWalk (http://www.umm.uni-heidelberg.de/apps/zmf/mirwalk/index.html) (Dweep et al., 2011) were included. To identify genes involved in the MTX pathway among the total of the target genes, the Pharmacogenomic Knowledge Base (PharmGKB) (https://www.pharmgkb.org/) was used. The RNAfold web tool (http://rna.tbi.univie.ac.at/cgi-bin/RNAfold.cgi) (Gruber et al., 2008) was used to calculate the impact of the SNPs in the minimum free energy secondary structures and the energy change ($\Delta\Delta G$) of the hairpin structure of the miRNAs showing significant results.

RESULTS

Patients´ baseline characteristics

In this study, we included a total of 167 childhood B-ALL patients from whom MTX level data were available at least at one point during the consolidation phase. A slight male preponderance was observed, as 59.88% (n= 100) were male and 40.12% (n =67) were female. Mean age did not differ between both groups (Table 34).

MTX plasma-level data were available for 159 patients at 48 h, for 163 patients at 72 h, and for 152 patients at 96 h (Table 35). Among the patients who had high MTX plasma levels at any time during the consolidation phase (n= 62, 37.13%), the frequency of high MTX plasma levels was higher for the patients who had received a 5 g/m^2 dose than for the ones receiving the 3 g/m^2 dose (3.4 : 1). This difference was also maintained at 48 h (3.3 : 1) and 72 h (2.5 : 1) and increased at 96 h (4.5 : 1) (Table 35).

Genotyping results

Successful genotyping was carried out for 147 out of 167 DNA samples (88.02%). During the genotyping process, 53 out of 213 SNPs (24.88%) (See Table 12) failed in more than 20% of the samples and were eliminated from the study. These failures were due to no PCR amplification, insufficient intensity for cluster separation, or poor or no cluster definition. Successful genotyping was obtained for 160 SNPs (75.12%).

Table 34. Characteristics of the childhood B-ALL patients.

Number of patients, n	167
Sex, n (%)	
Female	67(40.12)
Male	100 (59.88)
Mean age at diagnosis ± SD, years	5.2 ± 3.26
Female	5.0 ± 3.13
Male	5.3 ± 3.23
Treatment protocol, n (%)	
LAL-SHOP 94/99	65 (38.92)
LAL-SHOP 2005	102 (61.08)
MTX dose in consolidation, n (%)	
$3g/m^2$	72 (43.11)
$5g/m^2$	95 (56.89)
Global MTX levels in plasma, n (%)	
High MTX plasma levels	62 (37.13)
Normal MTX plasma levels	105 (62.87)

Table 35. MTX plasma levels data.

	Global	48h	72h	96h
$5 g/m^2$ (n=95)				
Normal levels, n (%)	47 (49.48)	57 (60.0)	49 (51.58)	59 (62.10)
High levels, n (%)	48 (50.52)	33 (34.74)	43 (45.26)	27 (28.42)
NA, n (%)	0 (0.0)	5 (5.26)	3 (3.16)	9 (9.48)
$3 g/m^2$ (n=72)				
Normal levels, n (%)	58 (80.56)	59 (81.94)	58 (80.55)	60 (83.33)
High levels, n (%)	14 (19.44)	10 (13.88)	17 (23.61)	6 (8.33)
NA, n (%)	0 (0.0)	3 (4.18)	1 (4.16)	6 (8.34)
$5 g/m^2$ and $3 g/m^2$ (n=167)				
Normal levels, n (%)	105 (62.87)	116 (69.46)	107 (64.07)	119 (71.25)
High levels, n (%)	62 (37.13)	43 (25.75)	56 (33.53)	33 (19.76)
NA, n (%)	0 (0.0)	8 (4.79)	4 (2.4)	15 (8.99)

Abbreviations: NA, data not available at that time point

Association study

To investigate whether genetic variation in miRNAs influences MTX levels, we tested the association between the 160 successfully genotyped polymorphisms in 154 miRNAs and MTX plasma concentration. The analysis was performed at any time during MTX infusion, at 48, 72, and 96 h in a cohort of 147 Spanish childhood B-ALL patients who were homogeneously treated. A total of 15 polymorphisms in 15 miRNA genes showed a significant association ($P < 0.05$) with MTX plasma levels (Tables 36 and 37). The most significant associations, which in addition were consistent along time, were found for miR-5189, miR-595, and miR-6083 (Table 36). These SNPs did not reach the significant value when FDR correction was applied.

In miR-5189, rs56292801 AA+AG genotypes showed a 0.4-fold decreased risk of high MTX plasma levels in all the analyses (Table 36). When we performed the analysis in the group of patients who received the 5 g/m^2 dose, the association showed a more significant P-value, and moreover another SNP in the same miRNA, rs35613341, showed a significant result (Table 38).

For miR-595, rs4909237 TT genotype was associated with a 5.7-fold increased risk of high global MTX plasma levels (P = 0.028), and it showed significant results at 48 h (P = 0.031) and at 72 h (P =0.015). At 96 h, although it did not reach a significant P-value, it was nearly significant (P = 0.065).

In the case of miR-6083, rs78790512 AA genotype was never found in patients with high MTX plasma levels. A significant value was found for global MTX plasma levels (P = 0.007), as well as at 48 h (P =0.026) and 72 h (P = 0.011). In addition, at 96 h it was almost significant (P = 0.051), showing the same trend as the previous time points. When we performed the analysis in the group of patients who received the 5 g/m^2 dose, it was also associated with high MTX plasma levels (Table 38).

Other 12 SNPs in 12 miRNAs were significantly associated with MTX plasma levels in at least one of the analyses. However, these associations were not consistent at the different time points analyzed (Table 37).

Table 36. SNPs in miRNAs showing the most significant associations with MTX plasma levels in childhood B-ALL patients.

miRNA SNP	Position Location	Genotype	Global (n=147) Normal levels N=90	High levels N=57	Model OR. CI (95%) P-value	48h (n=139) Normal levels N=98	High levels N=41	Model OR. CI (95%) P-value	72h (n=143) Normal levels N=92	High levels N=51	Model OR. CI (95%) P-value	96h (n=133) Normal levels N=102	High levels N=31	Model OR. CI (95%) P-value
hsa-mir-5189 rs56292801	Chr:16 Pre-mature	GG	41 (45.6)	36 (64.3)	Dominant	44 (44.4)	26 (65.0)	Dominant	42 (45.7)	32 (64.0)	Dominant	48 (46.6)	21 (67.7)	Dominant
		AG	40 (44.4)	18 (32.1)	0.42 (0.20-0.89)	44 (44.4)	13 (32.5)	0.4 (0.18-0.89)	41 (44.6)	16 (32.0)	0.42 (0.19-0.90)	44 (42.7)	9 (29.0)	0.41 (0.17-0.99)
		AA	9 (10.0)	2 (3.6)	**0.021**	11 (11.1)	1 (2.5)	**0.021**	9 (9.8)	2 (4.0)	**0.022**	11 (10.7)	1 (3.2)	**0.041**
hsa-mir-595 rs4909237	Chr:2 Pre-mature	CC	59 (65.6)	35 (62.5)	Recessive	64 (64.6)	23 (57.5)	Recessive	60 (65.2)	31 (62.0)	Recessive	67 (65.0)	18 (58.1)	Recessive
		CT	29 (32.2)	14 (25.0)	5.70 (1.02-31.70)	32 (32.3)	11 (27.5)	4.94 (1.08-22.6)	30 (32.6)	12 (24.0)	6.69 (1.21-37.04)	33 (32.0)	9 (29.0)	4.72 (0.89-24.94)
		TT	2 (2.2)	7 (12.5)	**0.028**	3 (3.0)	6 (15.0)	**0.031**	2 (2.2)	7 (14.0)	**0.015**	3 (2.9)	4 (12.9)	0.065
hsa-mir-6083 rs78790512	Chr:3 Pre-mature	GG	60 (66.7)	41 (71.9)	Recessive	66 (66.7)	30 (73.2)	Recessive	62 (67.4)	36 (70.6)	Recessive	69 (67.0)	24 (77.4)	Recessive
		AG	24 (26.7)	16 (28.1)	0.0 (0.0)	27 (27.3)	11 (26.8)	0.0 (0.0)	24 (26.1)	15 (29.4)	0.0 (0.0)	28 (27.2)	7 (22.6)	0.0 (0.0)
		AA	6 (6.7)	0 (0.0)	**0.007**	6 (6.1)	0 (0.0)	**0.026**	6 (6.5)	0 (0.0)	**0.011**	6 (5.8)	0 (0.0)	0.051

Abbreviations: OR, Odds-ratio; CI., confidence interval
Notes: Bold denote significant P-values; MTX plasma levels data for some patients were not available at 48h (NA=8), 72h (NA=4) and 96h (NA=14).

Table 37. SNPs in miRNAs not consistently associated with MTX plasma levels in childhood B-cell ALL patients.

miRNA SNP	Position Location	Genotype	Global (n=147)		Model OR. CI (95%) P-value	48h (n=139)		Model OR. CI (95%) P-value	72h (n=143)		Model OR. CI (95%) P-value	96h (n=133)		Model OR. CI (95%) P-value
			Normal levels N=90	High levels N=57		Normal levels N=98	High levels N=41		Normal levels N=92	High levels N=51		Normal levels N=102	High levels N=31	
hsa-mir-1206 rs2114358	Chr:8 Pre-mature	TT	27 (30.0)	25 (45.0)	Dominant. 0.37 (0.17-0.82)	31 (31.3)	16 (41.0)	Dominant 0.50 (0.21-1.15)	27 (29.3)	23 (70.6)	Dominant 0.32 (0.14-0.73)	33 (32.0)	14 (45.2)	Dominant 0.45 (0.19-1.10)
		CT	45 (50.0)	24 (43.6)		49 (49.5)	19 (48.7)		47 (51.1)	21 (42.9)		52 (50.5)	13 (41.9)	
		CC	18 (20.0)	6 (10.9)	**0.012**	19 (19.2)	4 (10.3)	0.103	18 (19.6)	5 (10.2)	**0.005**	18 (17.5)	4 (12.9)	0.079
hsa-mir-4792 rs11714172	Chr:3 Pre-mature	TT	37 (41.6)	18 (31.6)	Dominant 1.78 (0.84-3.78)	41 (41.8)	11 (26.8)	Dominant 2.25 (0.97-5.21)	38 (41.8)	14 (27.5)	Dominant 2.23 (1.01-4.92)	42 (41.2)	7 (22.6)	Dominant 2.67 (1.04-5.99)
		GT	37 (41.6)	32 (56.1)		40 (40.8)	27 (65.9)		38 (41.8)	31 (60.8)		43 (42.2)	20 (64.5)	
		GG	15 (16.9)	7 (12.3)	0.128	17 (17.3)	3 (7.3)	0.050	15 (16.5)	6 (1.8)	**0.043**	17 (16.7)	4 (12.9)	**0.037**
hsa-mir-5007 rs1572687	Chr:13 Pre-mature	CC	32 (35.6)	15 (26.3)	Recessive 1.84 (0.75-4.52)	33 (33.3)	13 (31.7)	Recessive 2.31 (0.92-2.18)	33 (35.9)	14 (27.5)	Recessive 1.88 (0.76-4.66)	33 (32.0)	11 (35.5)	Recessive 3.86 (1.46-10.19)
		CT	44 (48.9)	28 (49.1)		51 (51.5)	16 (39.0)		45 (48.9)	24 (47.1)		55 (53.4)	8 (25.8)	
		TT	14 (15.6)	14 (24.6)	0.180	15 (15.2)	12 (29.3)	0.920	14 (15.2)	13 (25.5)	0.171	15 (14.6)	12 (38.7)	**0.006**
hsa-mir-4700 rs1055070	Chr:12 Mature	TT	76 (84.4)	56 (98.2)	Dominant 0.11 (0.01-0.90)	85 (85.9)	40 (97.6)	Dominant 0.18 (0.02-1.46)	78 (84.8)	50 (98.0)	Dominant 0.13 (0.02-1.04)	89 (86.4)	30 (96.8)	Dominant 0.26 (0.03-2.14)
		GT	13 (14.4)	1 (1.8)		13 (13.1)	1 (2.4)		13 (14.1)	1 (2.0)		13 (12.6)	1 (3.2)	
		GG	1 (1.1)	0 (0.0)	**0.007**	1 (1.0)	0 (0.0)	0.048	1 (1.1)	0 (0.0)	0.014	1 (1.0)	0 (0.0)	0.142
hsa-mir-323b rs56103835	Chr:14 Pre-mature	TT	66 (73.3)	35 (61.4)	Dominant 1.88 (0.87-4.05)	70 (70.7)	28 (68.3)	Dominant 1.15 (0.50-2.63)	67 (72.8)	33 (64.7)	Recessive 0.0 (0.0)	73 (70.9)	21 (67.7)	Recessive 0.0 (0.0)
		CT	19 (21.1)	21 (36.8)		24 (24.2)	12 (29.3)		19 (20.7)	18 (35.3)		24 (23.3)	10 (32.3)	
		CC	5 (5.6)	1 (1.8)	0.107	5 (5.1)	1 (2.4)	0.740	6 (6.5)	0 (0.0)	**0.021**	6 (5.8)	0 (0.0)	0.078
hsa-mir-4432 rs243080	Chr:2 Pre-mature	CC	25 (28.1)	16 (29.6)	Recessive 2.15 (0.96-4.85)	26 (26.5)	14 (36.8)	Recessive 1.75 (0.74-4.12)	27 (29.7)	13 (27.1)	Recessive 2.56 (1.12-5.83)	28 (27.7)	12 (40.0)	Recessive 1.80 (0.73-4.46)
		CT	47 (52.8)	17 (31.5)		51 (52.0)	10 (26.3)		47 (51.6)	15 (31.2)		50 (49.5)	6 (20.0)	
		TT	17 (19.1)	21 (38.9)	0.063	21 (21.4)	14 (36.8)	0.204	17 (18.7)	20 (41.7)	**0.025**	23 (22.8)	12 (40.0)	0.206
hsa-mir-4268 rs4674470	Chr:2 Pre-mature	TT	61 (67.8)	31 (54.4)	Dominant 2.33 (1.08-5.00)	66 (66.7)	23 (56.1)	Dominant 1.95 (0.88-4.35)	61 (66.3)	29 (56.9)	Dominant 1.82 (0.85-3.92)	68 (66.0)	17 (54.8)	Dominant 2.00 (0.83-4.79)
		CT	24 (26.7)	21 (36.8)		27 (27.3)	16 (39.0)		26 (28.3)	18 (35.3)		28 (27.2)	13 (41.9)	
		CC	5 (5.6)	5 (8.8)	**0.027**	6 (6.1)	2 (4.9)	0.101	5 (5.4)	4 (7.8)	0.121	7 (6.8)	1 (3.2)	0.121
hsa-mir-4520a rs8078913	Chr:17 Mature	CC	26 (31.0)	21 (40.4)	Recessive 2.22 (0.81-6.12)	29 (31.9)	14 (36.8)	Recessive 3.23 (1.11-9.36)	27 (31.4)	18 (39.1)	Recessive 2.18 (0.79-6.06)	32 (33.0)	11 (37.9)	Recessive 2.67 (0.86-8.29)
		CT	44 (52.4)	20 (38.5)		48 (52.7)	14 (36.8)		45 (52.3)	18 (39.1)		50 (51.5)	11 (37.9)	
		TT	14 (16.7)	11 (21.2)	0.118	14 (15.4)	10 (26.3)	**0.029**	14 (16.3)	10 (21.7)	0.132	15 (15.5)	7 (24.1)	0.09
hsa-mir-4467 rs60871950	Chr:7 Mature	AA	28 (31.1)	14 (25.9)	Recessive 0.61 (0.26-1.41)	29 (29.3)	10 (26.3)	Recessive 0.35 (0.13-0.97)	28 (30.4)	11 (22.9)	Recessive 0.68 (0.29-1.60)	28 (27.2)	9 (30.0)	Recessive 0.38 (0.13-1.13)
		AG	34 (37.8)	28 (51.9)		37 (37.4)	22 (57.9)		36 (39.1)	26 (54.2)		41 (39.8)	16 (53.3)	
		GG	28 (31.1)	12 (22.2)	0.244	33 (33.3)	6 (15.8)	**0.033**	28 (30.4)	11 (22.9)	0.370	34 (33.0)	5 (16.7)	0.065
hsa-mir-604 rs2368392	Chr: 10 Pre-mature	CC	55 (61.1)	31 (54.4)	Dominant 1.76 (0.84-3.71)	61 (61.6)	21 (51.2)	Dominant 1.88 (0.86-4.13)	56 (60.9)	27 (52.9)	Dominant 1.75 (0.82-3.72)	63 (61.2)	14 (45.2)	Dominant 2.50 (1.04-5.99)
		CT	32 (35.6)	24 (42.1)		35 (35.4)	18 (43.9)		33 (35.9)	22 (43.1)		37 (35.9)	15 (48.4)	
		TT	3 (3.3)	2 (3.5)	0.133	3 (3.0)	2 (4.9)	0.112	3 (3.3)	2 (3.9)	0.142	3 (2.9)	2 (6.5)	**0.037**
hsa-mir.4745 rs10422347	Chr: 19 Mature	CC	73 (83.9)	44 (78.6)	Recessive 0.0 (0.0)	81 (84.4)	32 (80.0)	Recessive 0.0 (0.0)	73 (82)	42 (84)	Recessive 0.0 (0.0)	83 (83.0)	25 (80.6)	Recessive 0.0 (0.0)
		CT	14 (16.1)	10 (17.9)		15 (15.6)	6 (15.0)		16 (18)	6 (12)		17 (17.0)	4 (12.9)	
		TT	0 (0.0)	2 (3.6)	0.114	0 (0.0)	2 (5.0)	0.056	0 (0)	2 (4)	0.092	0 (0.0)	2 (6.5)	**0.037**
hsa-mir-1265 rs11259096	Chr:10 Pre-mature	TT	82 (91.1)	47 (82.5)	Dominant 2.35 (0.80-6.94)	91 (91.9)	33 (80.5)	Dominant 3.23 (1.03-10.12)	83 (90.2)	43 (84.3)	Dominant 1.83 (0.61-5.47)	92 (89.3)	27 (87.1)	Dominant 1.37 (0.37-4.98)
		CT	7 (7.8)	10 (17.5)		7 (7.1)	8 (19.5)		8 (8.7)	8 (15.7)		10 (9.7)	4 (12.9)	
		CC	1 (1.1)	0 (0.0)	0.118	1 (1.0)	0 (0.0)	**0.044**	1 (1.1)	0 (0.0)	0.284	1 (1.0)	0 (0.0)	0.641

Abbreviations: OR, Odds-ratio; CI., confidence interval. **Notes:** Bold denote significant P-values; MTX plasma levels data for some patients were not available at 48h (NA=8), 72h (NA=4) and 96h (NA=14).

Table 38. SNPs in miRNAs associated with MTX plasma levels in childhood B-ALL patients treated with 5g/m^2 MTX dose.

miRNA SNP	Position Location	Genotype	Global (n=86)		Model OR. CI (95%) p-value	48h (n=81)		Model OR. IC (95%) p-value	72h (n=83)		Model OR. IC (95%) p-value	96h (n=77)		Model OR. IC (95%) p-value
			Normal levels N=40	High levels N=46		Normal levels N=48	High levels N=33		Normal levels N=42	High levels N=41		Normal levels N=51	High levels N=26	
hsa-mir-5189 rs56292801	Chr:16 Pre-mature	GG	15 (37.5)	31 (67.4)	Dominant	18 (37.5)	23 (69.7)	Dominant	16 (38.1)	27 (65.9)	Dominant	21 (41.2)	20 (76.9)	Dominant
		AG	22 (55.0)	13 (28.3)	0.29 (0.12-0.71)	26 (54.2)	9 (27.3)	0.26 (0.10-0.67)	23 (54.8)	12 (29.3)	0.32 (0.13-0.78)	26 (51.0)	5 (19.2)	0.21 (0.07-0.61)
		AA	3 (7.5)	2 (4.3)	**0.005**	4 (8.3)	1 (3.0)	**0.004**	3 (7.1)	2 (4.9)	**0.010**	4 (7.8)	1 (3.8)	**0.002**
rs35613341		CC	15 (37.5)	28 (60.9)	Dominant	18 (37.5)	21 (63.6)	Dominant	16 (38.1)	25 (61.0)	Dominant	21 (41.2)	18 (69.2)	Dominant
		CG	20 (50.0)	15 (32.6)	0.39 (0.16-0.92)	23 (47.9)	11 (33.3)	0.34 (0.14-0.86)	21 (50.0)	13 (31.7)	0.39 (0.16-0.95)	23 (45.1)	7 (26.9)	0.31 (0.11-0.85)
		GG	5 (12.5)	3 (6.5)	**0.029**	7 (14.6)	1 (3.0)	**0.020**	5 (11.9)	3 (7.3)	**0.036**	7 (13.7)	1 (3.8)	**0.018**
hsa-mir-6083 rs78790512	Chr:3 Pre-mature	GG	23 (57.5)	36 (78.3)	Dominant	28 (58.3)	27 (81.8)	Dominant	25 (59.5)	32 (78.0)	Dominant	30 (58.8)	23 (88.5)	Dominant
		AG	3 (32.5)	10 (21.7)	0.38 (0.15-0.96)	16 (33.3)	6 (18.2)	0.31 (0.11-0.89)	13 (31.0)	9 (22.0)	0.41 (0.16-1.08)	17 (33.3)	3 (11.5)	0.19 (0.05-0.70)
		AA	4 (10.0)	0 (0.0)	**0.038**	4 (8.3)	0 (0.0)	**0.022**	4 (9.5)	0 (0.0)	0.067	4 (7.8)	0 (0.0)	**0.005**
hsa-mir-5007 rs1572687	Chr:3 Pre-mature	CC	12 (30.0)	12 (26.1)	Recessive	13 (27.1)	11 (33.3)	Recessive	13 (31.0)	11 (26.8)	Recessive	13 (25.5)	9 (34.6)	Recessive
		CT	23 (57.5)	22 (47.8)	2.47 (0.79-7.76)	29 (60.4)	11 (33.3)	3.50 (1.14-10.73)	24 (57.1)	18 (43.9)	3.06 (0.97-9.68)	32 (62.7)	6 (23.1)	5.50 (1.74-17.43)
		TT	5 (12.5)	12 (26.1)	0.109	6 (12.5)	11 (33.3)	**0.024**	5 (11.9)	12 (29.3)	0.047	6 (11.8)	11 (42.3)	**0.002**
hsa-mir-604 rs2368392	Chr: 12 Pre-mature	CC	29 (72.5)	26 (56.5)	Dominant	35 (72.9)	16 (48.5)	Dominant	30 (71.4)	22 (53.7)	Dominant	36 (70.6)	12 (46.2)	Dominant
		CT	10 (25.0)	18 (39.1)	2.03 (0.82-5.02)	12 (25.0)	15 (45.5)	2.86 (1.12-7.28)	11 (26.2)	17 (41.5)	2.16 (0.87-5.35)	14 (27.5)	12 (46.2)	2.80 (1.05-7.45)
		TT	1 (2.5)	2 (4.3)	0.121	1 (2.1)	2 (6.1)	**0.025**	1 (2.4)	2 (4.9)	0.093	1 (2.0)	2 (7.7)	**0.037**
hsa-mir-4792 rs11714172	Chr:3 Pre-mature	TT	19 (47.5)	15 (32.6)	Dominant	23 (47.9)	9 (27.3)	Dominant	20 (47.6)	12 (29.3)	Dominant	24 (47.1)	5 (19.2)	Dominant
		GT	11 (27.5)	24 (52.2)	1.87 (0.78-4.48)	13 (27.1)	21 (63.6)	2.45 (0.95-6.36)	12 (28.6)	23 (56.1)	2.20 (0.89-5.43)	15 (29.4)	17 (65.4)	3.73 (1.22-11.44)
		GG	10 (25.0)	7 (15.2)	0.158	12 (25.0)	3 (9.1)	0.059	10 (23.8)	6 (14.6)	0.084	12 (23.5)	4 (15.4)	**0.014**
hsa-mir-4432 rs243080	Chr:2 Pre-mature	TT	9 (23.1)	19 (43.2)	Dominant	13 (27.7)	12 (38.7)	Dominant	9 (22.0)	18 (46.2)	Dominant	14 (28.6)	11 (44.0)	Dominant
		CT	19 (48.7)	13 (29.5)	0.39 (0.15-1.03)	22 (46.8)	9 (29.0)	0.61 (0.23-1.59)	19 (46.3)	12 (30.8)	0.33 (0.12-0.87)	21 (42.9)	6 (24.0)	0.51 (0.19-1.39)
		CC	11 (28.2)	12 (27.3)	0.051	12 (25.5)	10 (32.3)	0.308	13 (31.7)	9 (23.1)	**0.021**	14 (28.6)	8 (32.0)	0.188
hsa-mir-4520a rs8078913	Chr.17 Mature	CC	12 (32.4)	18 (42.9)	Recessive	14 (32.6)	12 (38.7)	Recessive	13 (33.3)	15 (40.5)	Recessive	17 (35.4)	9 (37.5)	Recessive
		CT	22 (59.5)	17 (40.5)	2.27 (0.54-9.50)	26 (60.5)	12 (38.7)	3.89 (0.92-16.48)	23 (59.0)	15 (40.5)	2.80 (0.67-11.78)	28 (58.3)	9 (37.5)	5.00 (1.13-22.18)
		TT	3 (8.1)	7 (16.7)	0.246	3 (7.0)	7 (22.6)	0.053	3 (7.7)	7 (18.9)	0.143	3 (6.2)	6 (25.0)	**0.028**
hsa-mir-4268 rs4674470	Chr: 2 Pre-mature	TT	31 (77.5)	26 (56.5)	Dominant	35 (72.9)	20 (60.6)	Dominant	31 (73.8)	24 (58.5)	Dominant	36 (70.6)	16 (61.5)	Dominant
		CT	9 (22.5)	15 (32.6)	2.65 (1.03-6.81)	12 (25.0)	11 (33.3)	1.75 (0.68-4.50)	11 (26.2)	13 (31.7)	2.00 (0.79-5.04)	13 (25.5)	9 (34.6)	1.50 (0.56-4.05)
		CC	0 (0.0)	5 (10.9)	**0.038**	1 (2.1)	2 (6.1)	0.245	0 (0.0)	4 (9.8)	0.140	2 (3.9)	1 (3.8)	0.425
hsa-miR-3689 rs62571442	Chr:9 Pre-mature	AA	13 (33.3)	8 (17.4)	Dominant	15 (31.9)	4 (12.1)	Dominant	13 (31.7)	6 (14.6)	Dominant	16 (32.0)	3 (11.5)	Dominant
		AG	19 (48.7)	30 (65.2)	2.37 (0.86-6.54)	23 (48.9)	24 (72.7)	3.40 (1.01-11.42)	21 (51.2)	27 (65.9)	2.71 (0.91-8.04)	26 (52.0)	18 (69.2)	3.61 (0.94-13.80)
		GG	7 (17.9)	8 (17.4)	0.089	9 (19.1)	5 (15.2)	**0.034**	7 (17.1)	8 (19.5)	0.064	8 (16.0)	5 (19.2)	0.040
hsa-mir-4494 rs215383	Chr:12 Pre-mature	GG	29 (72.5)	28 (63.6)	Recessive	33 (70.2)	21 (65.6)	Recessive	31 (73.8)	23 (59.0)	Recessive	36 (72.0)	15 (57.7)	Recessive
		AG	11 (27.5)	12 (27.3)	0.00 (0.0)	13 (27.7)	8 (25.0)	4.76 (0.47-47.96)	11 (26.2)	12 (30.8)	0.00 (0.0)	13 (26.0)	8 (30.8)	6.39 (0.63-64.83)
		AA	0 (0.0)	4 (9.1)	0.117	1 (2.1)	3 (9.4)	0.150	0 (0.0)	4 (10.3)	**0.049**	1 (2.0)	3 (11.5)	0.086

Abbreviations: OR., Odds-ratio; CI., confidence interval. **Notes**: Bold denote significant P-values; MTX plasma levels data for some patients were not available at 48h (NA=5), 72h (NA=3) and 96h (NA=9).

Bioinformatics analysis

- *Effects of genetic variants on the pre-miRNA secondary structure*

The three most significant SNPs found in this study were located in the pre-miRNA sequence. In-silico analysis predicted that their allelic change has an impact in the secondary structure of the miRNAs because it causes a change in the energy of the hairpin structure. The modification was especially pronounced for rs56292801 in miR-5189, in which the substitution of the G allele for an A allele induced an energy change ($\Delta\Delta G$) of 5.3 kcal/mol (from -55.9 to -50.6 kcal/mol). This allelic change also induced a drastic change on the secondary structure (Figure 25). For rs4909237 in miR-595, the substitution of the C allele for a T allele induced a modest energy change of -0.5 kcal/mol (from -29.20 to -29.70 kcal/mol) and a pronounced change on the secondary structure. Finally, in the case of rs78790512 in miR-6083, the substitution of the G allele for an A allele caused a minor energy change ($\Delta\Delta G=0.2$ kcal/mol; from -30.9 to -30.70 kcal/mol) and a small structure change (Figure 25).
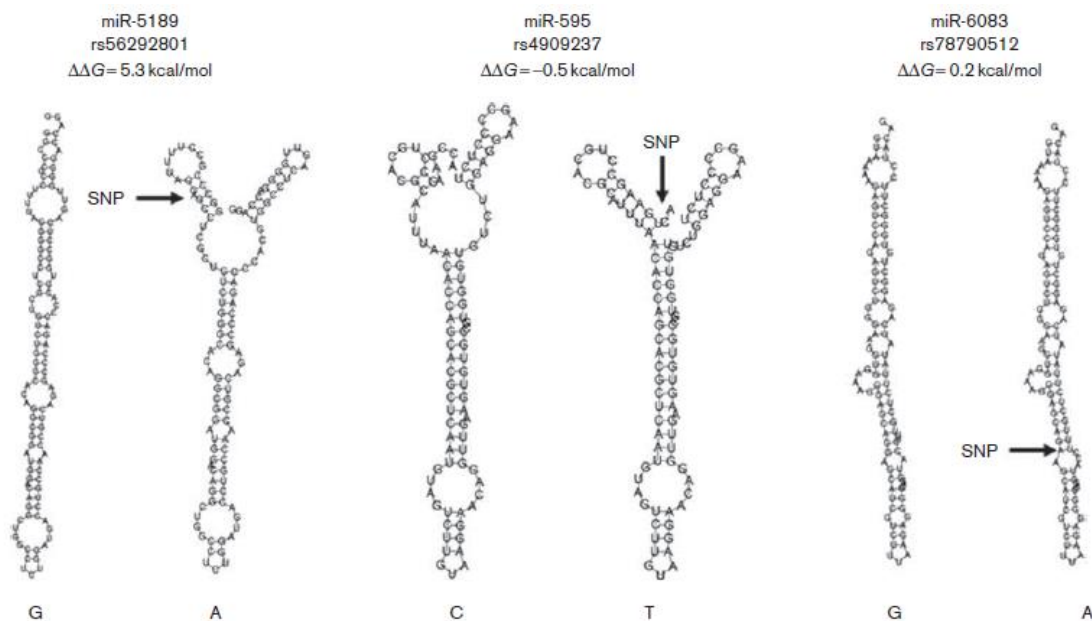
Figure 25. Energy change and minimum free-energy structures of the three most significant miRNA SNPs due to the presence of different alleles extracted from RNAfold web tool.

- *Target prediction*

In-silico analysis predicted that miR-5189 and miR-595 target three of the 14 MTX transporter genes: SLC19A1, SLCO1A2, and SLC46A1. The most remarkable result was found for miR-595, which regulates the three of them. For miR-6083, at the moment, there are no predicted targets among the MTX transporter genes (Figure 26).
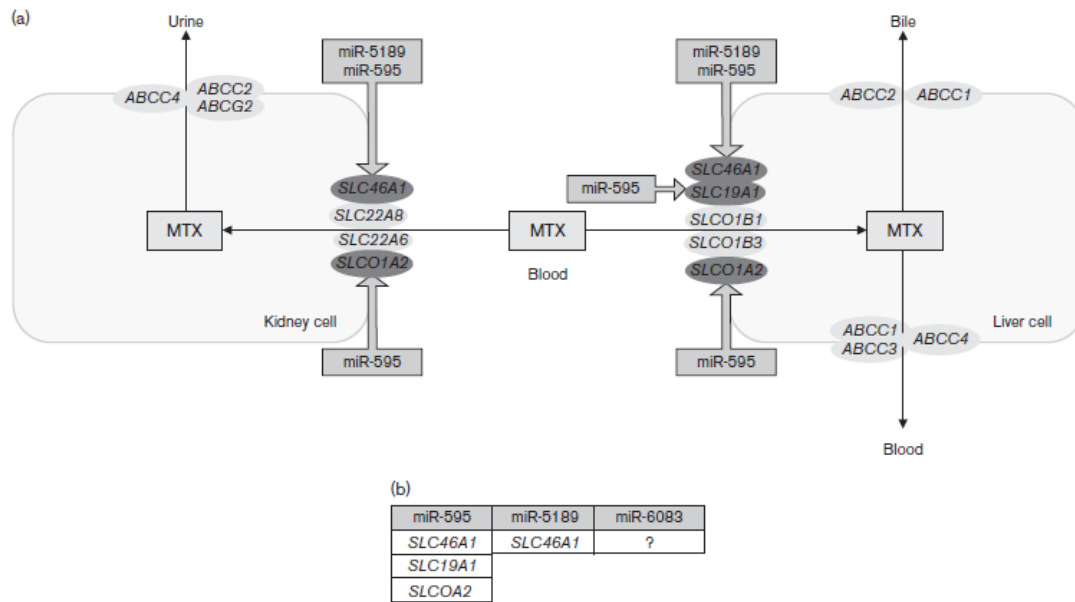
Figure 26. Genes of the MTX transport pathway regulated by at least one of the most significant miRNAs in the study. (a) Genes in the MTX transport pathway targeted by miR-595 and miR-5189. (b) Summary table of the microRNA targets.

DISCUSSION

In this study, we have evaluated the role of all variants in miRNAs described at the time of the selection in the alteration of MTX plasma levels considering its possible effect on MTX transport genes. Hence, we evaluated the correlation between 160 SNPs in 154 miRNAs and MTX plasma levels in 147 children diagnosed with B-ALL and homogenously treated with LAL-SHOP 94/99 and 2005 protocols. The three most significant SNPs consistently associated with MTX plasma levels along the different time points analyzed were located in miR-5189, miR-595, and miR-6083.

We found that the rs56292801 AA genotype in pre-miR-5189 showed a protective role for MTX accumulation along time. Interestingly, this genotype showed an increased association in patients treated with the 5 g/m^2 dose. In addition, in these patients another SNP in the same miRNA, rs35613341, was significantly associated with MTX plasma levels, suggesting an important role of miR-5189 at high doses of MTX. In this miRNA, the rs56292801 A allele induces a positive energy change, which has been suggested to turn the miRNA hairpin from a stable to an unstable status ($\Delta\Delta G$= 5.3 kcal/mol). It has been proposed that the decrease in the structure stability may reduce the product of the mature miRNA (Gong et al., 2012), and therefore it could lead to an increased expression of its targets. Among the targets predicted for miR-5189, we found SLC46A1, which encodes for the proton coupled folate transporter, involved in MTX

transport (Deng et al., 2009; Qiu et al., 2007; Zhao et al., 2008) (Figure 26). Some of the major sites of SLC46A1 expression include the kidney and the liver (Desmoulin et al., 2012; Hou and Matherly, 2014; Qiu et al., 2006). It has been reported that proton coupled folate transporter may contribute to folate analog internalization, such as MTX, when their levels are sufficiently elevated (Desmoulin et al., 2012). Therefore, the protective role of the A allele can be explained by its impact on the stability of the miR-5189, which may reduce the mature product – increasing SLC46A1 expression – and may in turn facilitate MTX clearance. This is the first time that this miRNA is associated with MTX plasma levels, presumably because it has been recently described. Further studies are needed to confirm this result.

The second most significant result was observed for rs4909237 TT genotype in miR-595, which has shown to increase the risk of having MTX high plasma levels along time. In-silico data indicate that the T allele slightly modifies the energy ($\Delta\Delta G = -0.5$ kcal/mol) but has a major impact on the secondary structure. Interestingly, miR-595 targets, apart from SLC46A1 previously mentioned, other two transporter genes SLC19A1 and SLCO1A2, which are also involved in MTX uptake (Figure 26). SLC19A1 encodes for the reduced folate carrier (RFC1), the major folate transporter, which is mainly expressed in the liver and mediates the uptake of MTX into the cells (Desmoulin et al., 2012). Polymorphisms in this gene have been associated with MTX toxicities and plasma concentrations in pediatric ALL (Faganel Kotnik et al., 2011; Imanishi et al., 2007; Laverdiere et al., 2002; Lopez-Lopez et al., 2013; Shimasaki et al., 2006; Suthandiram et al., 2014). Supporting our results, Wang et al. found an SNP that creates a miRNA-binding site for miR-595 in the 3´UTR region of SLC19A1 associated with high MTX plasma levels (Wang et al., 2014). Both the association found by our group and the one found by Wang and colleagues suggest that miR-595 could have an important role in SLC19A1 regulation and therefore affect MTX transport. The third gene regulated by this miRNA is SLCO1A2, expressed in liver and kidney. This transporter contributes to MTX uptake (Badagnani et al., 2006; Callens et al., 2015; Desmoulin et al., 2012). In addition, variants in SLCO1A2 have shown to alter MTX transport and may have a role in MTX disposition and toxicity (Badagnani et al., 2006; Zhou et al., 2013). To sum up, an increase in the mature miR-595 levels due to the effect of the SNP may decrease the expression of these three transporters and reduce both MTX biliary and urinary elimination, leading to drug accumulation in plasma.

The third most significant association was found between rs78790512 GG+AG genotype in miR-6083 and high MTX concentration along time. In-silico data indicate that the substitution of the G allele for an A allele caused minor energy ($\Delta\Delta G = 0.2$ kcal/mol) and structure changes. In this

case, the A allele seems to have a role in protection from high MTX levels, as none of the patients with the rs78790512 AA genotype presented high MTX levels in plasma. We cannot explain this association based on the energy or secondary structure change (Figure 25). We neither can explain this association based on its targets, because nowadays there are no predicted targets for miR-6083 among MTX transporter genes, although it could have an indirect effect regulating other noncoding RNAs.

In the present study, with the increase in the patients' sample, three of the SNPs in miRNAs analyzed in our previous study that did not reach a significant value in association with MTX plasma levels obtained significant results (rs2114358 in miR-1206, rs2368392 in miR-604, and rs11259096 in miR-1265). Remarkably, the rs56103835 in miR-323b, which was previously associated with MTX clearance, was also associated with high MTX plasma levels at 72 h (P =0.021) in this study (Table 37). Interestingly, this miRNA targets the ABCC4 gene, which encodes for multidrug resistance protein 4 (MRP4), involved mainly in the efflux of MTX in the kidney (van Aubel et al., 2002; El-Sheikh et al., 2007). In line with our results, it has already been suggested that variants in ABCC4 can affect MTX levels and toxicity (Ansari et al., 2009; den Hoed et al., 2015; Krishnamurthy et al., 2008; Lopez-Lopez et al., 2013; Low et al., 2009; Nicoletti et al., 2012). In addition, other 8 new miRNAs with significant SNPs were associated with high MTX plasma levels at some of the time points analyzed. All these results were not consistent at the different time points analyzed, and thus they have to be considered with caution.

This study has some limitations that might be addressed, such as the relatively high failure rate in genotyping technique. However, this high chance of failure was accepted from the beginning of the study, because despite the predicted low score for genotyping, no other design option to amplify the polymorphisms in question was possible. Another possible weakness is that the SNPs did not reach a significant P-value when FDR was applied. However, it is interesting to point that for some of the SNPs, such as rs78790512 in miR-6083, none of the patients with high MTX levels present the AA genotype. Therefore, the lack of significant values after FDR could be due to low statistical power because of the low frequency of patients with high MTX levels. Finally, we have to take into account the inaccuracy of the prediction algorithms of the databases used (Akhtar et al., 2016; Lee et al., 2015), but nowadays this limitation has to be assumed.

CONCLUSION

In this study we detected three SNPs in three miRNAs that could modify the expression of miR-5189, miR-595, and miR-6083, which, up to now, could target three MTX transport genes (SLC19A1, SLCO1A, and SLC46A1). This finding points out the possible involvement of miRNA variants in MTX transport gene regulation.

CONFLICTS OF INTEREST

There are no conflicts of interest.

REFERENCES

Akhtar, M.M., Micolucci, L., Islam, M.S., Olivieri, F., and Procopio, A.D. (2016). Bioinformatic tools for microRNA dissection. Nucleic Acids Res. 44, 24–44.

Amstutz, U., Offer, S.M., Sistonen, J., Joerger, M., Diasio, R.B., and Largiader, C.R. (2015). Polymorphisms in MIR27A Associated with Early-Onset Toxicity in Fluoropyrimidine-Based Chemotherapy. Clin. Cancer Res. 21, 2038–2044.

Ansari, M., Sauty, G., Labuda, M., Gagne, V., Laverdiere, C., Moghrabi, A., Sinnett, D., and Krajinovic, M. (2009). Polymorphisms in multidrug resistance-associated protein gene 4 is associated with outcome in childhood acute lymphoblastic leukemia. Blood 114, 1383–1386.

van Aubel, R.A.M.H., Smeets, P.H.E., Peters, J.G.P., Bindels, R.J.M., and Russel, F.G.M. (2002). The MRP4/ABCC4 gene encodes a novel apical organic anion transporter in human kidney proximal tubules: putative efflux pump for urinary cAMP and cGMP. J. Am. Soc. Nephrol. 13, 595–603.

Badagnani, I., Castro, R.A., Taylor, T.R., Brett, C.M., Huang, C.C., Stryke, D., Kawamoto, M., Johns, S.J., Ferrin, T.E., Carlson, E.J., et al. (2006). Interaction of methotrexate with organic-anion transporting polypeptide 1A2 and its genetic variants. J. Pharmacol. Exp. Ther. 318, 521–529.

Benjamini, Y., Drai, D., Elmer, G., Kafkafi, N., and Golani, I. (2001). Controlling the false discovery rate in behavior genetics research. Behav. Brain Res. 125, 279–284.

Callens, C., Debled, M., Delord, M., Turbiez-Stalain, I., Veyret, C., Bieche, I., and Brain, E. (2015). High-throughput pharmacogenetics identifies SLCO1A2 polymorphisms as candidates to elucidate the risk of febrile neutropenia in the breast cancer RAPP-01 trial. Breast Cancer Res. Treat. 153, 383–389.

Deng, Y., Zhou, X., Kugel Desmoulin, S., Wu, J., Cherian, C., Hou, Z., Matherly, L.H., and Gangjee, A. (2009). Synthesis and biological activity of a novel series of 6-substituted thieno[2,3-d]pyrimidine antifolate inhibitors of purine biosynthesis with selectivity for high affinity folate receptors over the reduced folate carrier and proton-coupled folate transpo. J. Med. Chem. 52, 2940–2951.

Desmoulin, S.K., Hou, Z., Gangjee, A., and Matherly, L.H. (2012). The human proton-coupled folate transporter: Biology and therapeutic applications to cancer. Cancer Biol. Ther. 13, 1355–1373.

Dweep, H., Sticht, C., Pandey, P., and Gretz, N. (2011). miRWalk--database: prediction of possible miRNA binding sites by "walking" the genes of three genomes. J. Biomed. Inform. 44, 839–847.

El-Sheikh, A.A.K., van den Heuvel, J.J.M.W., Koenderink, J.B., and Russel, F.G.M. (2007). Interaction of nonsteroidal anti-inflammatory drugs with multidrug resistance protein (MRP) 2/ABCC2- and MRP4/ABCC4-mediated methotrexate transport. J. Pharmacol. Exp. Ther. 320, 229–235.

Evans, W.E., Relling, M. V, Rodman, J.H., Crom, W.R., Boyett, J.M., and Pui, C.H. (1998). Conventional compared with individualized chemotherapy for childhood acute lymphoblastic leukemia. N. Engl. J. Med. 338, 499–505.

Faganel Kotnik, B., Grabnar, I., Bohanec Grabar, P., Dolzan, V., and Jazbec, J. (2011). Association of genetic polymorphism in the folate metabolic pathway with methotrexate pharmacokinetics and toxicity in childhood acute lymphoblastic leukaemia and malignant lymphoma. Eur. J. Clin. Pharmacol. 67, 993–1006.

Gong, J., Tong, Y., Zhang, H.-M., Wang, K., Hu, T., Shan, G., Sun, J., and Guo, A.-Y. (2012). Genome-wide identification of SNPs in microRNA genes and the SNP effects on microRNA target binding and biogenesis. Hum. Mutat. 33, 254–263.

Gruber, A.R., Lorenz, R., Bernhart, S.H., Neubock, R., and Hofacker, I.L. (2008). The Vienna RNA websuite. Nucleic Acids Res. 36, W70-4.

den Hoed, M.A.H., Lopez-Lopez, E., te Winkel, M.L., Tissing, W., de Rooij, J.D.E., Gutierrez-Camino, A., Garcia-Orad, A., den Boer, E., Pieters, R., Pluijm, S.M.F., et al. (2015). Genetic and metabolic determinants of methotrexate-induced mucositis in pediatric acute lymphoblastic leukemia. Pharmacogenomics J. 15, 248–254.

Hou, Z., and Matherly, L.H. (2014). Biology of the major facilitative folate transporters SLC19A1 and SLC46A1. Curr. Top. Membr. 73, 175–204.

Imanishi, H., Okamura, N., Yagi, M., Noro, Y., Moriya, Y., Nakamura, T., Hayakawa, A., Takeshima, Y., Sakaeda, T., Matsuo, M., et al. (2007). Genetic polymorphisms associated with adverse events and elimination of methotrexate in childhood acute lymphoblastic leukemia and malignant lymphoma. J. Hum. Genet. 52, 166–171.

Johnston, W.T., Lightfoot, T.J., Simpson, J., and Roman, E. (2010). Childhood cancer survival: a report from the United Kingdom Childhood Cancer Study. Cancer Epidemiol. 34, 659–666.

Kozomara, A., and Griffiths-Jones, S. (2014). miRBase: annotating high confidence microRNAs using deep sequencing data. Nucleic Acids Res. 42, D68-73.

Krishnamurthy, P., Schwab, M., Takenaka, K., Nachagari, D., Morgan, J., Leslie, M., Du, W., Boyd, K., Cheok, M., Nakauchi, H., et al. (2008). Transporter-mediated protection against thiopurine-induced hematopoietic toxicity. Cancer Res. 68, 4983–4989.

Laverdiere, C., Chiasson, S., Costea, I., Moghrabi, A., and Krajinovic, M. (2002). Polymorphism G80A in the reduced folate carrier gene and its relationship to methotrexate plasma levels and outcome of childhood acute lymphoblastic leukemia. Blood 100, 3832–3834.

Lee, Y.J.D., Kim, V., Muth, D.C., and Witwer, K.W. (2015). Validated MicroRNA Target Databases: An Evaluation. Drug Dev. Res. 76, 389–396.

Lopez-Lopez, E., Martin-Guerrero, I., Ballesteros, J., Pinan, M.A., Garcia-Miguel, P., Navajas, A., and Garcia-Orad, A. (2011). Polymorphisms of the SLCO1B1 gene predict methotrexate-related toxicity in childhood acute lymphoblastic leukemia. Pediatr. Blood Cancer 57, 612–619.

Lopez-Lopez, E., Ballesteros, J., Pinan, M.A., Sanchez de Toledo, J., Garcia de Andoin, N., Garcia-Miguel, P., Navajas, A., and Garcia-Orad, A. (2013). Polymorphisms in the methotrexate transport pathway: a new tool for MTX plasma level prediction in pediatric acute lymphoblastic leukemia. Pharmacogenet. Genomics 23, 53–61.

Lopez-Lopez, E., Gutierrez-Camino, A., Bilbao-Aldaiturriaga, N., Pombar-Gomez, M., Martin-Guerrero, I., and Garcia-Orad, A. (2014a). Pharmacogenetics of childhood acute lymphoblastic leukemia. Pharmacogenomics 15, 1383–1398.

Lopez-Lopez, E., Gutierrez-Camino, A., Pinan, M.A., Sanchez-Toledo, J., Uriz, J.J., Ballesteros, J., Garcia-Miguel, P., Navajas, A., and Garcia-Orad, A. (2014b). Pharmacogenetics of microRNAs and microRNAs biogenesis machinery in pediatric acute lymphoblastic leukemia. PLoS One 9, e91261.

Low, S.-K., Kiyotani, K., Mushiroda, T., Daigo, Y., Nakamura, Y., and Zembutsu, H. (2009). Association study of genetic polymorphism in ABCC4 with cyclophosphamide-induced adverse drug reactions in breast cancer patients. J. Hum. Genet. 54, 564–571.

Meulendijks, D., Henricks, L.M., Amstutz, U., Froehlich, T.K., Largiader, C.R., Beijnen, J.H., de Boer, A., Deenen, M.J., Cats, A., and Schellens, J.H.M. (2016). Rs895819 in MIR27A improves the predictive value of DPYD variants to identify patients at risk of severe fluoropyrimidine-associated toxicity. Int. J. Cancer 138, 2752–2761.

Moriyama, T., Relling, M. V, and Yang, J.J. (2015). Inherited genetic variation in childhood acute lymphoblastic leukemia. Blood 125, 3988–3995.

Nicoletti, P., Cartsos, V.M., Palaska, P.K., Shen, Y., Floratos, A., and Zavras, A.I. (2012). Genomewide pharmacogenetics of bisphosphonate-induced osteonecrosis of the jaw: the role of RBMS3. Oncologist 17, 279–287.

Pui, C.-H. (2010). Recent research advances in childhood acute lymphoblastic leukemia. J. Formos. Med. Assoc. 109, 777–787.

Pui, C.-H., Yang, J.J., Hunger, S.P., Pieters, R., Schrappe, M., Biondi, A., Vora, A., Baruchel, A.A., Silverman, L.B., Schmiegelow, K., et al. (2015). Childhood Acute Lymphoblastic Leukemia: Progress Through Collaboration. J. Clin. Oncol. 33, JCO.2014.59.1636.

Qiu, A., Jansen, M., Sakaris, A., Min, S.H., Chattopadhyay, S., Tsai, E., Sandoval, C., Zhao, R., Akabas, M.H., and Goldman, I.D. (2006). Identification of an intestinal folate transporter and the molecular basis for hereditary folate malabsorption. Cell 127, 917–928.

Qiu, A., Min, S.H., Jansen, M., Malhotra, U., Tsai, E., Cabelof, D.C., Matherly, L.H., Zhao, R., Akabas, M.H., and Goldman, I.D. (2007). Rodent intestinal folate transporters (SLC46A1): secondary structure, functional properties, and response to dietary folate restriction. Am. J. Physiol. Cell Physiol. 293, C1669-78.

Radtke, S., Zolk, O., Renner, B., Paulides, M., Zimmermann, M., Moricke, A., Stanulla, M., Schrappe, M., and Langer, T. (2013). Germline genetic variations in methotrexate candidate genes are associated with pharmacokinetics, toxicity, and outcome in childhood acute lymphoblastic leukemia. Blood 121, 5145–5153.

Ramsey, L.B., Bruun, G.H., Yang, W., Trevino, L.R., Vattathil, S., Scheet, P., Cheng, C., Rosner, G.L., Giacomini, K.M., Fan, Y., et al. (2012). Rare versus common variants in pharmacogenetics: SLCO1B1 variation and methotrexate disposition. Genome Res. 22, 1–8.

Ramsey, L.B., Panetta, J.C., Smith, C., Yang, W., Fan, Y., Winick, N.J., Martin, P.L., Cheng, C., Devidas, M., Pui, C.-H.C.-H., et al. (2013). Genome-wide study of methotrexate clearance replicates SLCO1B1. Blood 121, 898–904.

Rukov, J.L., and Shomron, N. (2011). MicroRNA pharmacogenomics: post-transcriptional regulation of drug response. Trends Mol. Med. 17, 412–423.

Salazar, J., Altes, A., del Rio, E., Estella, J., Rives, S., Tasso, M., Navajas, A., Molina, J., Villa, M., Vivanco, J.L., et al. (2012). Methotrexate consolidation treatment according to pharmacogenetics of MTHFR ameliorates event-free survival in childhood acute lymphoblastic leukaemia. Pharmacogenomics J. 12, 379–385.

Sambrook, J, R.D. (2001). Molecular cloning: a laboratory manual (New York: NY: Cold Spring Harbor Laboratory Press).

Shimasaki, N., Mori, T., Samejima, H., Sato, R., Shimada, H., Yahagi, N., Torii, C., Yoshihara, H., Tanigawara, Y., Takahashi, T., et al. (2006). Effects of methylenetetrahydrofolate reductase and reduced folate carrier 1 polymorphisms on high-dose methotrexate-induced toxicities in children with acute lymphoblastic leukemia or lymphoma. J. Pediatr. Hematol. Oncol. 28, 64–68.

Suthandiram, S., Gan, G.-G., Zain, S.M., Bee, P.-C., Lian, L.-H., Chang, K.-M., Ong, T.-C., and Mohamed, Z. (2014). Effect of polymorphisms within methotrexate pathway genes on methotrexate toxicity and plasma levels in adults with hematological malignancies. Pharmacogenomics 15, 1479–1494.

Treon, S.P., and Chabner, B.A. (1996). Concepts in use of high-dose methotrexate therapy. Clin. Chem. 42, 1322–1329.

Trevino, L.R., Shimasaki, N., Yang, W., Panetta, J.C., Cheng, C., Pei, D., Chan, D., Sparreboom, A., Giacomini, K.M., Pui, C.-H., et al. (2009). Germline genetic variation in an organic anion transporter polypeptide associated with methotrexate pharmacokinetics and clinical effects. J. Clin. Oncol. 27, 5972–5978.

Wang, S., Sun, L., Zeng, W., Wu, W., and Zhang, G. (2014). Effects of a microRNA binding site polymorphism in SLC19A1 on methotrexate concentrations in Chinese children with acute lymphoblastic leukemia. Med. Oncol. 31, 62.

Zhan, X., Wu, W., Han, B., Gao, G., Qiao, R., Lv, J., Zhang, S., Zhang, W., Fan, W., Chen, H., et al. (2012). Hsa-miR-196a2 functional SNP is associated with severe toxicity after platinum-based chemotherapy of advanced nonsmall cell lung cancer patients in a Chinese population. J. Clin. Lab. Anal. 26, 441–446.

Zhao, R., Qiu, A., Tsai, E., Jansen, M., Akabas, M.H., and Goldman, I.D. (2008). The proton-coupled folate transporter: impact on pemetrexed transport and on antifolates activities compared with the reduced folate carrier. Mol. Pharmacol. 74, 854–862.

Zhou, F., Zheng, J., Zhu, L., Jodal, A., Cui, P.H., Wong, M., Gurney, H., Church, W.B., and Murray, M. (2013). Functional analysis of novel polymorphisms in the human SLCO1A2 gene that encodes the transporter OATP1A2. AAPS J. 15, 1099–1108.

DISCUSSION

During the last decades, childhood ALL survival rates have reached up to 90 % (Pui et al., 2015; Tasian and Hunger, 2017) at least in part, due to advances in treatment protocols. However, the chemotherapeutic agents are also a source of concern due to their toxicities, because the patients suffering severe toxicity often require a dose reduction or even treatment discontinuation, with the consequent negative impact on survival (Evans et al., 1998; Salazar et al., 2012; Treon and Chabner, 1996). In this scenario, where the toxicities are not presented homogeneously and with the same severity between the affected children, research on predictive markers is of great interest to further guide clinicians on the dose individualization. Pharmacogenomic studies have already proposed several polymorphisms in coding regions of drug PK/PD pathways. Nowadays it is known that miRNAs regulate these genes involved in PK and PD pathways. Polymorphisms in miRNAs can modify miRNA levels or function, consequently affecting the expression of their target genes.

In this context, the main goal of the present study was to identify new genetic markers in miRNAs targeting drug-related genes or other genes involved in toxicity development, that could explain the most common toxicities developed during childhood B-ALL therapy. These markers could make possible the adjustment of the treatment from the beginning, minimizing toxicity. We focused our efforts in peripheral neurotoxicity, hepatic toxicity and gastrointestinal toxicity, three main toxicities of childhood B-ALL therapy, as well as in MTX plasmatic levels, which are strictly monitored during high dose MTX treatment. In order to discover new markers in miRNAs that could predict these toxicities, in the present study, we evaluated the association of polymorphisms in all the miRNAs described at the moment of the selection with a MAF higher than 1 % (213 SNPs in 206 miRNAs) in a group of 179 children diagnosed with B-ALL and homogeneously treated according to the standardized LAL/SHOP protocol.

Regarding peripheral neurotoxicity, we identified two SNPs in miRNAs that could potentially explain the development of this adverse event during induction phase. The most significant association was found for the rs12402181 in mir-3117, in which AG+AA genotypes showed a decreased risk of peripheral neurotoxicity. This SNP is located in the seed region of miR-3117-3p, in which the change of the G allele for the A variant allele could affect the accurate recognition of its target mRNA sequences. Among their target genes we found *ABCC1* and *RALBP1*, both genes have been described in the literature as transporters implicated in the removal of VCR from the cells (Awasthi et al., 2005; Franca et al., 2017; Kunicka and Soucek, 2014). Indeed, polymorphisms in *ABCC1* have already been associated with VCR-related neuropathy (Franca et al., 2017; Lopez-Lopez et al., 2016) and RALBP1 inhibition has been

associated with drug accumulation and enhanced cytotoxicity (Drake et al., 2007). Therefore, the rs12402181 A variant allele could affect the binding of miR-3117-3p with the mRNAs of *ABCC1* and *RALBP1*, resulting in their increased expression. This higher expression of *ABCC1* and *RALBP1* genes could promote a greater VCR efflux from the cell, explaining the decreased risk of VCR-induced peripheral neurotoxicity.

The second most significant result for neurotoxicity induced by VCR was observed for rs7896283 in miR-4481, in which CT+CC genotype showed a risk role. This SNP is located in the pre-miRNA sequence, where the substitution of the T allele for a C allele shows a negative energy change. This negative energy change indicates a turn of the miRNA hairpin from an unstable to a stable status, and it has been proposed that the increase in the structure stability may enhance the product of the mature miRNA (Gong et al., 2012) with the consequent decreased expression of its targets. Although we did not found any VCR PK/PD pathway genes potentially targeted by miR-4481, the pathway enrichment analysis predicted axon guidance as the most significant pathway targeted by miR-4481. Axon guidance is involved in spontaneous regeneration of peripheral nerves when they are damaged (Chiono and Tonda-Turo, 2015) therefore, the rs7896283 C risk allele may increase miR-4481 stability and in consequence its mature levels, leading to a decrease in the expression of its target genes. Then, less expression of genes involved in peripheral nerves regeneration could be the explanation of the increased peripheral neuropathy.

The second toxicity analyzed was hepatotoxicity measured as transaminases elevation. We analyzed its association during induction and consolidation phases, observing that the SNPs associated with hypertransaminasemia during these two phases were different, what supports the idea that the hepatic toxicity in these two phases could be produced by different mechanisms and related to different drugs. The most interesting result found in our study was the association of rs2648841 in miR-1208 with transaminases levels during consolidation phase. Our results showed that GT+TT genotype conferred a decreased risk of liver toxicity (grade ≥2), and high hepatotoxicity (grade ≥3). Remarkably, none of the patients with the TT genotype developed low grade toxicity, neither high grade toxicity. The T variant allele of rs2648841, located in the pre-mature sequence of miR-1208, would turn the miRNA hairpin to a more unstable status, reducing the product of the mature miRNA and then, increasing the expression of its targets. Interestingly miR-1208 targets three genes of the MTX pharmacodynamic pathway, *DHFR*, *MTR* and *MTHFR*. The T allele protective role against blood transaminases elevation could be explained first, due to the higher expression of *DHFR*. MTX exerts its cytotoxic

function through DHFR inhibition, which results in the interruption of purine and pyrimidine bases synthesis and consequent cell death. Thus, a higher expression of DHFR would mitigate the effect of MTX contributing to avoid hepatocyte death. In fact, high expression of DHFR has been reported to be associated with MTX resistance (Dulucq et al., 2008). On the other hand, the higher expression of *MTR* (gene coding for the enzyme responsible for homocysteine methylation to give methionine) and *MTHFR* (gene that codifies the enzyme that catalyzes the reaction to provide the methyl-group) (Krajinovic et al., 2005), would promote the homocysteine to methionine reaction decreasing intracellular homocysteine levels. These homocysteine lower levels may protect from apoptosis (Kubota et al., 2014; Yang et al., 2017), explaining again the protective role of this T allele.

Regarding gastrointestinal toxicity, the third toxicity analyzed, we focus our study in mucositis and its clinical manifestations diarrhea and vomits. In mucositis analysis, the most interesting result was the association between AG+GG genotype of rs4674470 in miR-4268 and decreased risk of toxicity. Interestingly, none of the patients with the GG genotype developed mucositis, indicating a protective role. This SNP is located at the 3´ end position of the miRNA hairpin. Although it did not modify either the stability or the secondary structure of the miRNA, this position could be crucial for the accurate recognition of a cleavage site between the pri-miRNA and pre-miRNA by DROSHA. DROSHA generates the termini of pre-miRNAs, determining the mature miRNA sequence, thus, accurate processing by DROSHA is critical for production of functional miRNAs (Fang and Bartel, 2015; Kim et al., 2017). Therefore, the presence of this SNP could lead DROSHA to a misrecognition of the cleavage site and then, to a less production of the miRNA depending on the SNP allele. Of note, this miRNA is represented in the miRbase database, the reference database of miRNAs, with the G allele, which is the minor allele (Kozomara and Griffiths-Jones, 2014). The fact that in the reference database the miRNA sequence is represented with the G allele could indicate that the miRNA could be more efficiently produced when the G allele is presented because of the recognition of DROSHA of the cleavage site.

Regarding the pathway analysis for this miRNA, we found two genes of DNR pathway (*NFKBIE*, *CBR1*) and three of the MTX pathway (*MTHFR*, *MTR*, *SLC46A1*) following the first approach based on pharmacogenes. However, the deregulation of these genes could have contradictory effects. For instance, downregulation of *NFKBIE* could protect from cell death (Komissarova et al., 2008), whereas downregulation of *MTHFR* and *MTR* could contribute to apoptosis (Kubota et al., 2014; Yang et al., 2017). In order to identify other mucositis-related genes, we performed a pathway enrichment analysis and we found that miR-4268 targeted PLD signaling pathway. *PLD*

Discussion

expression has been shown to be up-regulated in inflamed mucosa of inflammatory bowel diseases (Zhou et al., 2016). PLD modulates pro-inflammatory gene expression and has a major role in the secretion of cytokines (Friday and Fox, 2016; Kang et al., 2014), a mechanism involved in mucositis development (Cinausero et al., 2017). Interestingly, silencing of *PLD* effectively blocked cytokine production (Sethu et al., 2010) and ameliorated intestinal mucosal inflammation (Zhou et al., 2016). This silencing has already been shown that could be mediated by a repertory of miRNAs (Fite et al., 2016). In this context, it is plausible that the rs4674470 GG genotype in miR-4268 could lead to higher miRNA expression due to a more efficient recognition by DROSHA and, in turn, to a lower expression of PLD-related genes, explaining its protective role in mucositis.

In diarrhea and vomits analyses, the most statistically significant SNPs were rs8667 in miR-4751 and rs12402181 in miR-3117, respectively. The SNP rs8667 in miR-4751 is located in the pre-mature sequence where the A allele slightly modifies the energy, which in turn, could alter the miRNA levels (Gong et al., 2012). The SNP rs12402181 in miR-3117 is located in the seed sequence and could affect the accurate recognition of its target mRNA sequences. Among their target genes, we found several genes of DNR, MTX and CPA pathways, and more interestingly, both miRNAs targeted pathways related with inflammatory response. Activation of this response is a prerequisite for the production of several cytokines, including IL-1, IL-8, IL-6 and TNF (van den Blink et al., 2001; Elsea et al., 2008; Reyes-Gibby et al., 2017), events involved in the pathobiology of mucosal damage. Therefore, rs8667 in miR-4751 and rs12402181 in miR-3117 could alter the miRNA levels and function and affect the expression of their target genes in drug pathways and inflamatory response-related genes, contributing to toxicity.

Finally with regard to MTX plasma levels during high-dose consolidation phase, we pointed out as the most interesting results to rs56292801 in miR-5189 and rs4909237 in miR-595, which were the two SNPs consistently associated with MTX plasma levels along the different time points analyzed. The most interesting result was for rs56292801 in miR-5189 pre-mature sequence, in which the AG+AA genotype showed a protective role against MTX accumulation along time. The importance of miR-5189 in plasmatic high MTX levels is supported by the fact that the association with the plasmatic high levels became even stronger when only patients treated with the 5 g/m^2 dose where analyzed. In this miRNA, a positive energy change was caused by the A variant allele, what suggests that this decrease in the structure stability may reduce the mature miR-5189 expression and therefore lead to an increased expression of its targets. Among the targets predicted for miR-5189, we found *SLC46A1*, which encodes for the

proton coupled folate transporter, which may contribute to folate analog internalization, such as MTX (Deng et al., 2009; Qiu et al., 2007; Zhao et al., 2008), when their levels are sufficiently elevated (Desmoulin et al., 2012). Some of the major sites of SLC46A1 expression include the kidney (Desmoulin et al., 2012; Hou and Matherly, 2014; Qiu et al., 2006), key route of excretion for MTX. Therefore, the protective role of the A allele can be explained by its impact on the stability of the miR-5189, which may reduce the mature product, increasing *SLC46A1* expression and facilitating in turn MTX clearance.

The second most significant result for MTX plasma levels was observed for rs4909237 TT genotype in miR-595, which has shown to increase the risk of having MTX high plasma levels along time. Although the T variant allele *in silico* showed a slight minimum free energy change, it had a major impact on the secondary structure, what could affect miR-595 processing. Interestingly, miR-595 targets, apart from *SLC46A1* previously mentioned, other two MTX transporter genes *SLC19A1* and *SLCO1A2*, which are also involved in MTX uptake. *SLC19A1* encodes for the reduced folate carrier (RFC1), the major folate transporter, which is mainly expressed in the liver and mediates the uptake of MTX into the cells (Desmoulin et al., 2012). Supporting our results, Wang et al. found an SNP that creates a miRNA-binding site for miR-595 in the 3´UTR region of *SLC19A1* associated with high MTX plasma levels (Wang et al., 2014)(Gong et al., 2012)(Gong et al., 2012)(Gong et al., 2012)(Gong et al., 2012)(Gong et al., 2012)(Gong et al., 2012)(Gong et al., 2012)(Gong et al., 2012)(Gong et al., 2012)(Gong et al., 2012)(Gong et al., 2012). Both the association found by our group and the one found by Wang and colleagues suggest that miR-595 could have an important role in *SLC19A1* regulation and therefore affect MTX transport. The third gene regulated by this miRNA is *SLCO1A2*, expressed in liver and kidney. This transporter also contributes to MTX uptake (Badagnani et al., 2006; Callens et al., 2015; Desmoulin et al., 2012). To sum up, an increase in the mature miR-595 levels due to the effect of the SNP may decrease the expression of these three transporters and reduce both MTX biliary and urinary elimination, leading to drug accumulation in plasma.

In summary, our study has identified 8 new candidate markers for toxicity prediction in childhood patients with ALL: rs12402181 in miR-3117 and rs7896283 in miR-4481 for VCR induced peripheral neurotoxicity during induction; rs2648841 in miR-1208 for transaminases elevation caused by MTX during consolidation; rs4674470 in miR-4268 for mucositis, rs8667 in miR-4751 for diarrhea and rs12402181 in miR-3117 for vomits during induction and finally rs56292801 in miR-5189 and rs4909237 in miR-595 for elevated plasmatic MTX levels. It would

be interesting to confirm these results in other populations and to validate them through functional studies.

CONCLUSIONS

1. First, in neurotoxicity induced by VCR we found AG+AA genotype of rs12402181 of miR-3117 associated with toxicity. This could be due to an overexpression of its VCR transport targets *ABCC1* and *RALBP1*. We also found association between CT+CC genotype of rs7896283 in miR-4481 and neurotoxicity that could be explain through axon guidance genes downregulation.

2. Regarding hepatic toxicity, we found GT+TT genotypes of rs2648841 in miR-1208 were associated with transaminases levels elevation during consolidation phase. This association could be explained by the upregulation of MTX PD pathway genes *DHFR*, *MTR* and *MTHFR*.

3. Concerning gastrointestinal toxicity, AA+AG genotypes of rs4674470 in miR-4268, AA+AG genotypes of rs8667 in miR-4751 and AA+AG genotypes of rs12402181 in miR-3117 could be involved in mucositis, diarrhea and vomits, respectively, during the induction phase. This involvement could be due to their effects on pharmacokinetic and pharmacodynamic genes of mucotoxic drugs such as DNR, MTX and CPA, as well as other mucosal injury-related genes, especially those of inflammatory response.

4. For high MTX plasma levels during consolidation phase we found the SNPs AG+AA genotypes of rs56292801 in miR-5189 and TT genotype of rs4909237 in miR-595 which could modify miRNA expression and then affect the expression of their target genes *SLC46A1*, *SLC19A1* and *SLCO1A2*.

In summary, our study has identified variants in miRNAs as new toxicity markers for childhood ALL therapy. We propose that these variants could serve to adjust treatment before toxicities appear. We open a new investigation field for ALL treatment based on the study of miRNA.

REFERENCES - ERREFERENTZIAK

REFERENCES - ERREFERENTZIAK

1000 Genomes Project Consortium, R.M., Abecasis, G.R., Altshuler, D., Auton, A., Brooks, L.D., Durbin, R.M., Gibbs, R.A., Hurles, M.E., McVean, G.A., Donnelly, P., et al. (2010). A map of human genome variation from population-scale sequencing. Nature *467*, 1061–1073.

Abe, T., Unno, M., Onogawa, T., Tokui, T., Kondo, T.N., Nakagomi, R., Adachi, H., Fujiwara, K., Okabe, M., Suzuki, T., et al. (2001). LST-2, a human liver-specific organic anion transporter, determines methotrexate sensitivity in gastrointestinal cancers. Gastroenterology *120*, 1689–1699.

Accord Healthcare S.L.U. (2017a). Methotrexate [medicinal product official information].

Accord Healthcare S.L.U. (2017b). Citarabine [medicinal product official information].

Akhtar, M.M., Micolucci, L., Islam, M.S., Olivieri, F., and Procopio, A.D. (2016). Bioinformatic tools for microRNA dissection. Nucleic Acids Res. *44*, 24–44.

Al-Ansari, S., Zecha, J.A.E.M., Barasch, A., de Lange, J., Rozema, F.R., and Raber-Durlacher, J.E. (2015). Oral mucositis induced by anticancer therapies. Curr. Oral Heal. Reports *2*, 202–211.

Amstutz, U., Offer, S.M., Sistonen, J., Joerger, M., Diasio, R.B., and Largiader, C.R. (2015). Polymorphisms in MIR27A Associated with Early-Onset Toxicity in Fluoropyrimidine-Based Chemotherapy. Clin. Cancer Res. *21*, 2038–2044.

Ansari, M., and Krajinovic, M. (2007). Pharmacogenomics in cancer treatment defining genetic bases for inter-individual differences in responses to chemotherapy. Curr. Opin. Pediatr. *19*, 15–22.

Ansari, M., Sauty, G., Labuda, M., Gagne, V., Laverdiere, C., Moghrabi, A., Sinnett, D., and Krajinovic, M. (2009). Polymorphisms in multidrug resistance-associated protein gene 4 is associated with outcome in childhood acute lymphoblastic leukemia. Blood *114*, 1383–1386.

Argyriou, A.A., Bruna, J., Marmiroli, P., and Cavaletti, G. (2012). Chemotherapy-induced peripheral neurotoxicity (CIPN): An update. Crit. Rev. Oncol. Hematol. *82*, 51–77.

van Aubel, R.A.M.H., Smeets, P.H.E., Peters, J.G.P., Bindels, R.J.M., and Russel, F.G.M. (2002). The MRP4/ABCC4 gene encodes a novel apical organic anion transporter in human kidney proximal tubules: putative efflux pump for urinary cAMP and cGMP. J. Am. Soc. Nephrol. *13*, 595–603.

Awasthi, S., Hallene, K.L., Fazio, V., Singhal, S.S., Cucullo, L., Awasthi, Y.C., Dini, G., and Janigro, D. (2005). RLIP76, a non-ABC transporter, and drug resistance in epilepsy. BMC Neurosci. *6*, 61.

Badagnani, I., Castro, R.A., Taylor, T.R., Brett, C.M., Huang, C.C., Stryke, D., Kawamoto, M., Johns, S.J., Ferrin, T.E., Carlson, E.J., et al. (2006). Interaction of methotrexate with organic-anion transporting polypeptide 1A2 and its genetic variants. J. Pharmacol. Exp. Ther. *318*, 521–529.

Baxter Oncology GmbH (2017). Cyclophosphamide [medicinal product official information].

Bektaş-Kayhan, K., Küçükhüseyin, Ö., Karagöz, G., Ünür, M., Öztürk, O., Ünüvar, A., Devecioğlu, Ö., and Yilmaz-Aydoğan, H. (2012). Is the MDR1 C3435T polymorphism responsible for oral mucositis in children with acute lymphoblastic leukemia? Asian Pac. J. Cancer Prev. *13*, 5251–5255.

Bénichou, C. (1990). Criteria of drug-induced liver disorders. Report of an international consensus meeting. J Hepatol. *11*, 272–276.

Benjamini, Y., Drai, D., Elmer, G., Kafkafi, N., and Golani, I. (2001). Controlling the false discovery rate in behavior genetics research. Behav. Brain Res. *125*, 279–284.

References-Erreferentziak

van den Bent, M.J. (2005). Prevention of Chemotherapy-Induced Neuropathy: Leukemia Inhibitory Factor. Clin. Cancer Res. *11*, 1691–1693.

Bhojwani, D., Yang, J.J., and Pui, C.-H. (2015). Biology of Childhood Acute Lymphoblastic Leukemia. Pediatr. Clin. North Am. *62*, 47–60.

van den Blink, B., Juffermans, N.P., ten Hove, T., Schultz, M.J., van Deventer, S.J., van der Poll, T., and Peppelenbosch, M.P. (2001). p38 mitogen-activated protein kinase inhibition increases cytokine release by macrophages in vitro and during infection in vivo. J. Immunol. *166*, 582–587.

Bohnsack, M.T., Czaplinski, K., and Gorlich, D. (2004). Exportin 5 is a RanGTP-dependent dsRNA-binding protein that mediates nuclear export of pre-miRNAs. RNA *10*, 185–191.

Callens, C., Debled, M., Delord, M., Turbiez-Stalain, I., Veyret, C., Bieche, I., and Brain, E. (2015). High-throughput pharmacogenetics identifies SLCO1A2 polymorphisms as candidates to elucidate the risk of febrile neutropenia in the breast cancer RAPP-01 trial. Breast Cancer Res. Treat. *153*, 383–389.

Carozzi, V.A., Canta, A., and Chiorazzi, A. (2015). Chemotherapy-induced peripheral neuropathy: What do we know about mechanisms? Neurosci. Lett. *596*, 90–107.

Celtikci, B., Lawrance, A.K., Wu, Q., and Rozen, R. (2009). Methotrexate-induced apoptosis is enhanced by altered expression of methylenetetrahydrofolate reductase. Anticancer. Drugs *20*, 787–793.

Ceppi, F., Langlois-Pelletier, C., Gagne, V., Rousseau, J., Ciolino, C., De Lorenzo, S., Kevin, K.M., Cijov, D., Sallan, S.E., Silverman, L.B., et al. (2014). Polymorphisms of the vincristine pathway and response to treatment in children with childhood acute lymphoblastic leukemia. Pharmacogenomics *15*, 1105–1116.

Cinausero, M., Aprile, G., Ermacora, P., Basile, D., Vitale, M.G., Fanotto, V., Parisi, G., Calvetti, L., and Sonis, S.T. (2017). New frontiers in the pathobiology and treatment of cancer regimen-related mucosal injury. Front. Pharmacol. *8*, 354.

Chiono, V., and Tonda-Turo, C. (2015). Trends in the design of nerve guidance channels in peripheral nerve tissue engineering. Prog. Neurobiol. *131*, 87–104.

Dávila-Fajardo, C.L., Swen, J.J., Cabeza Barrera, J., and Guchelaar, H.-J. (2013). Genetic risk factors for drug-induced liver injury in rheumatoid arthritis patients using low-dose methotrexate. Pharmacogenomics *14*, 63–73.

Deng, Y., Zhou, X., Kugel Desmoulin, S., Wu, J., Cherian, C., Hou, Z., Matherly, L.H., and Gangjee, A. (2009). Synthesis and biological activity of a novel series of 6-substituted thieno[2,3-d]pyrimidine antifolate inhibitors of purine biosynthesis with selectivity for high affinity folate receptors over the reduced folate carrier and proton-coupled folate transpo. J. Med. Chem. *52*, 2940–2951.

Dennison, J.B., Kulanthaivel, P., Barbuch, R.J., Renbarger, J.L., Ehlhardt, W.J., and Hall, S.D. (2006). Selective metabolism of vincristine in vitro by CYP3A5. Drug Metab. Dispos. *34*, 1317–1327.

Desmoulin, S.K., Hou, Z., Gangjee, A., and Matherly, L.H. (2012). The human proton-coupled folate transporter: Biology and therapeutic applications to cancer. Cancer Biol. Ther. *13*, 1355–1373.

Diouf, B., Crews, K.R., Lew, G., Pei, D., Cheng, C., Bao, J., Zheng, J.J., Yang, W., Fan, Y., Wheeler, H.E., et al. (2015). Association of an inherited genetic variant with vincristine-related peripheral neuropathy in children with acute lymphoblastic leukemia. JAMA *313*, 815–823.

Dougherty, P.M., Cata, J.P., Burton, A.W., Vu, K., and Weng, H.-R. (2007). Dysfunction in multiple primary afferent fiber subtypes revealed by quantitative sensory testing in patients with chronic vincristine-induced pain. J. Pain Symptom Manage. *33*, 166–179.

Drake, K.J., Singhal, J., Yadav, S., Nadkar, A., Pungaliya, C., Singhal, S.S., and Awasthi, S. (2007). RALBP1/RLIP76 mediates multidrug resistance. Int. J. Oncol. *30*, 139–144.

Dulucq, S., St-Onge, G., Gagné, V., Ansari, M., Sinnett, D., Labuda, D., Moghrabi, A., and Krajinovic, M. (2008). DNA variants in the dihydrofolate reductase gene and outcome in childhood ALL. Blood *111*, 3692–3700.

Dweep, H., and Gretz, N. (2015). miRWalk2.0: a comprehensive atlas of microRNA-target interactions. Nat. Methods *12*, 697.

Dweep, H., Sticht, C., Pandey, P., and Gretz, N. (2011). miRWalk--database: prediction of possible miRNA binding sites by "walking" the genes of three genomes. J. Biomed. Inform. *44*, 839–847.

Egbelakin, A., Ferguson, M.J., MacGill, E.A., Lehmann, A.S., Topletz, A.R., Quinney, S.K., Li, L., McCammack, K.C., Hall, S.D., and Renbarger, J.L. (2011). Increased risk of vincristine neurotoxicity associated with low CYP3A5 expression genotype in children with acute lymphoblastic leukemia. Pediatr. Blood Cancer *56*, 361–367.

El-Sheikh, A.A.K., van den Heuvel, J.J.M.W., Koenderink, J.B., and Russel, F.G.M. (2007). Interaction of nonsteroidal anti-inflammatory drugs with multidrug resistance protein (MRP) 2/ABCC2- and MRP4/ABCC4-mediated methotrexate transport. J. Pharmacol. Exp. Ther. *320*, 229–235.

Elsea, C.R., Roberts, D.A., Druker, B.J., and Wood, L.J. (2008). Inhibition of p38 MAPK suppresses inflammatory cytokine induction by etoposide, 5-fluorouracil, and doxorubicin without affecting tumoricidal activity. PLoS One *3*, e2355.

Erčulj, N., Kotnik, B.F., Debeljak, M., Jazbec, J., and Dolžan, V. (2012). Influence of folate pathway polymorphisms on high-dose methotrexate-related toxicity and survival in childhood acute lymphoblastic leukemia. Leuk. Lymphoma *53*, 1096–1104.

Evans, W.E., Relling, M. V, Rodman, J.H., Crom, W.R., Boyett, J.M., and Pui, C.H. (1998). Conventional compared with individualized chemotherapy for childhood acute lymphoblastic leukemia. N. Engl. J. Med. *338*, 499–505.

Fabregat, A., Sidiropoulos, K., Garapati, P., Gillespie, M., Hausmann, K., Haw, R., Jassal, B., Jupe, S., Korninger, F., McKay, S., et al. (2016). The Reactome pathway knowledgebase. Nucleic Acids Res. *44*, D481-7.

Faganel Kotnik, B., Grabnar, I., Bohanec Grabar, P., Dolzan, V., and Jazbec, J. (2011). Association of genetic polymorphism in the folate metabolic pathway with methotrexate pharmacokinetics and toxicity in childhood acute lymphoblastic leukaemia and malignant lymphoma. Eur. J. Clin. Pharmacol. *67*, 993–1006.

Fang, W., and Bartel, D.P. (2015). The menu of features that define primary microRNAs and enable de novo design of microRNA genes. Mol. Cell *60*, 131–145.

Fite, K., Elkhadragy, L., and Gomez-Cambronero, J. (2016). A Repertoire of MicroRNAs Regulates cancer cell starvation by targeting phospholipase D in a feedback loop that operates maximally in cancer cells. Mol. Cell. Biol. *36*, 1078–1089.

Franca, R., Rebora, P., Bertorello, N., Fagioli, F., Conter, V., Biondi, A., Colombini, A., Micalizzi, C., Zecca, M., Parasole, R., et al. (2017). Pharmacogenetics and induction/consolidation therapy toxicities in acute lymphoblastic leukemia patients treated with AIEOP-BFM ALL 2000 protocol. Pharmacogenomics J. *17*, 4–10.

Friday, S.C., and Fox, D.A. (2016). Phospholipase D enzymes facilitate IL-17- and TNFα-induced expression of proinflammatory genes in rheumatoid arthritis synovial fibroblasts (RASF). Immunol. Lett. *174*, 9–18.

References-Erreferentziak

Friedman, R.C., Farh, K.K.-H., Burge, C.B., and Bartel, D.P. (2008). Most mammalian mRNAs are conserved targets of microRNAs. Genome Res. *19*, 92–105.

Fukuda, Y., Li, Y., and Segal, R.A. (2017). A Mechanistic Understanding of Axon Degeneration in Chemotherapy-Induced Peripheral Neuropathy. Front. Neurosci. *11*, 481.

Geng, L., and Wang, X. (2015). Epstein-Barr Virus-associated lymphoproliferative disorders: experimental and clinical developments. Int. J. Clin. Exp. Med. *8*, 14656–14671.

Gervasini, G., de Murillo, S.G., Jiménez, M., de la Maya, M.D., and Vagace, J.M. (2017). Effect of polymorphisms in transporter genes on dosing, efficacy and toxicity of maintenance therapy in children with acute lymphoblastic leukemia. Gene *628*, 72–77.

Gong, J., Tong, Y., Zhang, H.-M., Wang, K., Hu, T., Shan, G., Sun, J., and Guo, A.-Y. (2012). Genome-wide identification of SNPs in microRNA genes and the SNP effects on microRNA target binding and biogenesis. Hum. Mutat. *33*, 254–263.

Gregers, J., Christensen, I.J., Dalhoff, K., Lausen, B., Schroeder, H., Rosthoej, S., Carlsen, N., Schmiegelow, K., and Peterson, C. (2010). The association of reduced folate carrier 80G>A polymorphism to outcome in childhood acute lymphoblastic leukemia interacts with chromosome 21 copy number. Blood *115*, 4671–4677.

Gregers, J., Green, H., Christensen, I.J., Dalhoff, K., Schroeder, H., Carlsen, N., Rosthoej, S., Lausen, B., Schmiegelow, K., and Peterson, C. (2015a). Polymorphisms in the ABCB1 gene and effect on outcome and toxicity in childhood acute lymphoblastic leukemia. Pharmacogenomics J. *15*, 372–379.

Gregers, J., Gréen, H., Christensen, I.J., Dalhoff, K., Schroeder, H., Carlsen, N., Rosthoej, S., Lausen, B., Schmiegelow, K., and Peterson, C. (2015b). Polymorphisms in the ABCB1 gene and effect on outcome and toxicity in childhood acute lymphoblastic leukemia. Pharmacogenomics J. *15*, 372–379.

Gregory, R.I., Chendrimada, T.P., and Shiekhattar, R. (2006). MicroRNA biogenesis: isolation and characterization of the microprocessor complex. Methods Mol. Biol. *342*, 33–47.

Groninger, E., Meeuwsen-de Boer, T., Koopmans, P., Uges, D., Sluiter, W., Veerman, A., Kamps, W., and de Graaf, S. (2005). Vincristine pharmacokinetics and response to vincristine monotherapy in an up-front window study of the Dutch Childhood Leukaemia Study Group (DCLSG). Eur. J. Cancer *41*, 98–103.

Gruber, A.R., Lorenz, R., Bernhart, S.H., Neubock, R., and Hofacker, I.L. (2008). The Vienna RNA websuite. Nucleic Acids Res. *36*, W70-4.

Gutierrez-Camino, A., Martin-Guerrero, I., Lopez-Lopez, E., Echebarria-Barona, A., Zabalza, I., Ruiz, I., Guerra-Merino, I., and Garcia-Orad, A. (2016). Lack of association of the CEP72 rs924607 TT genotype with vincristine-related peripheral neuropathy during the early phase of pediatric acute lymphoblastic leukemia treatment in a Spanish population. Pharmacogenet. Genomics *26*, 100–102.

Gutierrez-Camino, A., Martin-Guerrero, I., and Garcia-Orad, A. (2017a). PNPLA3 rs738409 and Hepatotoxicity in Children With B-cell Acute Lymphoblastic Leukemia: A Validation Study in a Spanish Cohort. Clin. Pharmacol. Ther. *102*, 906.

Gutierrez-Camino, A., Oosterom, N., den Hoed, M.A.H., Lopez-Lopez, E., Martin-Guerrero, I., Pluijm, S.M.F., Pieters, R., de Jonge, R., Tissing, W.J.E., Heil, S.G., et al. (2017b). The miR-1206 microRNA variant is associated with methotrexate-induced oral mucositis in pediatric acute lymphoblastic leukemia. Pharmacogenet. Genomics *27*, 303–306.

Hartman, A., van Schaik, R.H.N., van der Heiden, I.P., Broekhuis, M.J.C., Meier, M., den Boer, M.L., and Pieters, R. (2010). Polymorphisms in genes involved in vincristine pharmacokinetics or pharmacodynamics are not related to impaired motor performance in children with leukemia. Leuk. Res. *34*, 154–159.

Hashimoto, M., Yamashita, Y., and Mori, N. (2002). Immunohistochemical detection of CD79a expression in precursor T cell lymphoblastic lymphoma/leukaemias. J. Pathol. *197*, 341–347.

Ho, D.H., Whitecar, J.P., Luce, J.K., and Frei, E. (1970). L-asparagine requirement and the effect of L-asparaginase on the normal and leukemic human bone marrow. Cancer Res. *30*, 466–472.

den Hoed, M.A.H., Lopez-Lopez, E., te Winkel, M.L., Tissing, W., de Rooij, J.D.E., Gutierrez-Camino, A., Garcia-Orad, A., den Boer, E., Pieters, R., Pluijm, S.M.F., et al. (2015). Genetic and metabolic determinants of methotrexate-induced mucositis in pediatric acute lymphoblastic leukemia. Pharmacogenomics J. *15*, 248–254.

Hou, Z., and Matherly, L.H. (2014). Biology of the major facilitative folate transporters SLC19A1 and SLC46A1. Curr. Top. Membr. *73*, 175–204.

Hunger, S.P., Winick, N.J., Sather, H.N., and Carroll, W.L. (2005). Therapy of low-risk subsets of childhood acute lymphoblastic leukemia: when do we say enough? Pediatr. Blood Cancer *45*, 876–880.

Hutvágner, G., McLachlan, J., Pasquinelli, A.E., Bálint, E., Tuschl, T., and Zamore, P.D. (2001). A cellular function for the RNA-interference enzyme Dicer in the maturation of the let-7 small temporal RNA. Science *293*, 834–838.

Imanishi, H., Okamura, N., Yagi, M., Noro, Y., Moriya, Y., Nakamura, T., Hayakawa, A., Takeshima, Y., Sakaeda, T., Matsuo, M., et al. (2007). Genetic polymorphisms associated with adverse events and elimination of methotrexate in childhood acute lymphoblastic leukemia and malignant lymphoma. J. Hum. Genet. *52*, 166–171.

Inada, T., and Makino, S. (2014). Novel roles of the multi-functional CCR4-NOT complex in post-transcriptional regulation. Front. Genet. *5*, 135.

Iorga, A., Dara, L., and Kaplowitz, N. (2017). Drug-Induced Liver Injury: Cascade of Events Leading to Cell Death, Apoptosis or Necrosis. Int. J. Mol. Sci. *18*, 1018.

Iparraguirre, L., Gutierrez-Camino, A., Umerez, M., Martin-Guerrero, I., Astigarraga, I., Navajas, A., Sastre, A., Garcia de Andoin, N., and Garcia-Orad, A. (2016). MiR-pharmacogenetics of methotrexate in childhood B-cell acute lymphoblastic leukemia. Pharmacogenet. Genomics *26*, 517–525.

Islam, M.N., and Iskander, M.N. (2004). Microtubulin binding sites as target for developing anticancer agents. Mini Rev. Med. Chem. *4*, 1077–1104.

Johnston, W.T., Lightfoot, T.J., Simpson, J., and Roman, E. (2010). Childhood cancer survival: a report from the United Kingdom childhood cancer study. Cancer Epidemiol. *34*, 659–666.

Jordan, M.A., and Wilson, L. (2004). Microtubules as a target for anticancer drugs. Nat. Rev. Cancer *4*, 253–265.

Kamburov, A., Stelzl, U., Lehrach, H., and Herwig, R. (2013). The ConsensusPathDB interaction database: 2013 update. Nucleic Acids Res. *41*, D793-800.

Kanehisa, M., Furumichi, M., Tanabe, M., Sato, Y., and Morishima, K. (2017). KEGG: new perspectives on genomes, pathways, diseases and drugs. Nucleic Acids Res. *45*, D353–D361.

Kang, D.W., Choi, K.-Y., and Min, D.S. (2014). Functional regulation of phospholipase D expression in cancer and inflammation. J. Biol. Chem. *289*, 22575–22582.

Kim, V.N. (2004). MicroRNA precursors in motion: exportin-5 mediates their nuclear export. Trends Cell Biol. *14*, 156–159.

References-Erreferentziak

Kim, B., Jeong, K., and Kim, V.N. (2017). Genome-wide mapping of DROSHA cleavage sites on primary microRNAs and noncanonical substrates. Mol. Cell *66*, 258–269.e5.

Komissarova, E. V, Li, P., Uddin, A.N., Chen, X., Nadas, A., and Rossman, T.G. (2008). Gene expression levels in normal human lymphoblasts with variable sensitivities to arsenite: identification of GGT1 and NFKBIE expression levels as possible biomarkers of susceptibility. Toxicol. Appl. Pharmacol. *226*, 199–205.

Kotur, N., Stankovic, B., Kassela, K., Georgitsi, M., Vicha, A., Leontari, I., Dokmanovic, L., Janic, D., Krstovski, N., Klaassen, K., et al. (2012). 6-mercaptopurine influences TPMT gene transcription in a TPMT gene promoter variable number of tandem repeats-dependent manner. Pharmacogenomics *13*, 283–295.

Kozomara, A., and Griffiths-Jones, S. (2014). miRBase: annotating high confidence microRNAs using deep sequencing data. Nucleic Acids Res. *42*, D68-73.

Krajinovic, M., and Moghrabi, A. (2004). Pharmacogenetics of methotrexate. Pharmacogenomics *5*, 819–834.

Krajinovic, M., Robaey, P., Chiasson, S., Lemieux-Blanchard, E., Rouillard, M., Primeau, M., Bournissen, F.G., and Moghrabi, A. (2005). Polymorphisms of genes controlling homocysteine levels and IQ score following the treatment for childhood ALL. Pharmacogenomics *6*, 293–302.

Krajinovic, M., Elbared, J., Drouin, S., Bertout, L., Rezgui, A., Ansari, M., Raboisson, M.-J., Lipshultz, S.E., Silverman, L.B., Sallan, S.E., et al. (2016). Polymorphisms of ABCC5 and NOS3 genes influence doxorubicin cardiotoxicity in survivors of childhood acute lymphoblastic leukemia. Pharmacogenomics J. *16*, 530–535.

Krishnamurthy, P., Schwab, M., Takenaka, K., Nachagari, D., Morgan, J., Leslie, M., Du, W., Boyd, K., Cheok, M., Nakauchi, H., et al. (2008). Transporter-mediated protection against thiopurine-induced hematopoietic toxicity. Cancer Res. *68*, 4983–4989.

Kubota, M., Nakata, R., Adachi, S., Watanabe, K.-I., Heike, T., Takeshita, Y., and Shima, M. (2014). Plasma homocysteine, methionine and S-adenosylhomocysteine levels following high-dose methotrexate treatment in pediatric patients with acute lymphoblastic leukemia or Burkitt lymphoma: association with hepatotoxicity. Leuk. Lymphoma *55*, 1591–1595.

Kuiken, N.S.S., Rings, E.H.H.M., Blijlevens, N.M.A., and Tissing, W.J.E. (2017). Biomarkers and non-invasive tests for gastrointestinal mucositis. Support. Care Cancer *25*, 2933–2941.

Kunicka, T., and Soucek, P. (2014). Importance of ABCC1 for cancer therapy and prognosis. Drug Metab. Rev. *46*, 325–342.

Ladas, E.J., Kroll, D.J., Oberlies, N.H., Cheng, B., Ndao, D.H., Rheingold, S.R., and Kelly, K.M. (2010). A randomized, controlled, double-blind, pilot study of milk thistle for the treatment of hepatotoxicity in childhood acute lymphoblastic leukemia (ALL). Cancer *116*, 506–513.

Lauschke, V.M., Mkrtchian, S., and Ingelman-Sundberg, M. (2017). The role of microRNAs in liver injury at the crossroad between hepatic cell death and regeneration. Biochem. Biophys. Res. Commun. *482*, 399–407.

Laverdiere, C., Chiasson, S., Costea, I., Moghrabi, A., and Krajinovic, M. (2002). Polymorphism G80A in the reduced folate carrier gene and its relationship to methotrexate plasma levels and outcome of childhood acute lymphoblastic leukemia. Blood *100*, 3832–3834.

Le, Z., Niu, X., Chen, Y., Ou, X., Zhao, G., Liu, Q., Tu, W., Hu, C., Kong, L., and Liu, Y. (2017). Predictive single nucleotide polymorphism markers for acute oral mucositis in patients with nasopharyngeal carcinoma treated with radiotherapy. Oncotarget *8*, 63026–63037.

Lee, W.M. (2003). Drug-Induced Hepatotoxicity. N. Engl. J. Med. *349*, 474–485.

Lee, Y.J.D., Kim, V., Muth, D.C., and Witwer, K.W. (2015). Validated microRNA target databases: an evaluation. Drug Dev. Res. *76*, 389–396.

Legha, S.S. (1986). Vincristine neurotoxicity. Pathophysiology and management. Med. Toxicol. *1*, 421–427.

Leveque, D., and Jehl, F. (2007). Molecular pharmacokinetics of catharanthus (vinca) alkaloids. J. Clin. Pharmacol. *47*, 579–588.

Lewis, B.P., Burge, C.B., and Bartel, D.P. (2005). Conserved seed pairing, often flanked by adenosines, indicates that thousands of human genes are microRNA targets. Cell *120*, 15–20.

Li, M.-P., Hu, Y.-D., Hu, X.-L., Zhang, Y.-J., Yang, Y.-L., Jiang, C., Tang, J., and Chen, X.-P. (2016). MiRNAs and miRNA Polymorphisms Modify Drug Response. Int. J. Environ. Res. Public Health *13*.

Li, S., Wang, L., Fu, B., Berman, M.A., Diallo, A., and Dorf, M.E. (2014). TRIM65 regulates microRNA activity by ubiquitination of TNRC6. Proc. Natl. Acad. Sci. *111*, 6970–6975.

Li, Y., Zhu, X., Gu, J., Dong, D., Yao, J., Lin, C., Huang, K., and Fei, J. (2010). Anti-miR-21 oligonucleotide sensitizes leukemic K562 cells to arsenic trioxide by inducing apoptosis. Cancer Sci. *101*, 948–954.

Liang, D.-C., Yang, C.-P., Lin, D.-T., Hung, I.-J., Lin, K.-H., Chen, J.-S., Hsiao, C.-C., Chang, T.-T., Peng, C.-T., Lin, M.-T., et al. (2010). Long-term results of Taiwan Pediatric Oncology Group studies 1997 and 2002 for childhood acute lymphoblastic leukemia. Leukemia *24*, 397–405.

Lim, J.Y.-S., Bhatia, S., Robison, L.L., and Yang, J.J. (2014). Genomics of racial and ethnic disparities in childhood acute lymphoblastic leukemia. Cancer *120*, 955–962.

Liu, W., Baker, R.D., Bhatia, T., Zhu, L., and Baker, S.S. (2016). Pathogenesis of nonalcoholic steatohepatitis. Cell. Mol. Life Sci. *73*, 1969–1987.

Liu, Y., Yin, Y., Sheng, Q., Lu, X., Wang, F., Lin, Z., Tian, H., Xu, A., and Zhang, J. (2014a). Association of ABCC2 −24C>T Polymorphism with High-Dose Methotrexate Plasma Concentrations and Toxicities in Childhood Acute Lymphoblastic Leukemia. PLoS One *9*, e82681.

Liu, Y., Yin, Y., Sheng, Q., Lu, X., Wang, F., Lin, Z., Tian, H., Xu, A., and Zhang, J. (2014b). Association of ABCC2 -24C>T polymorphism with high-dose methotrexate plasma concentrations and toxicities in childhood acute lymphoblastic leukemia. PLoS One *9*, e82681.

Liu, Y., Fernandez, C.A., Smith, C., Yang, W., Cheng, C., Panetta, J.C., Kornegay, N., Liu, C., Ramsey, L.B., Karol, S.E., et al. (2017). Genome-Wide Study Links PNPLA3 Variant With Elevated Hepatic Transaminase After Acute Lymphoblastic Leukemia Therapy. Clin. Pharmacol. Ther. *102*, 131–140.

Lopez-Lopez, E., Martin-Guerrero, I., Ballesteros, J., Pinan, M.A., Garcia-Miguel, P., Navajas, A., and Garcia-Orad, A. (2011). Polymorphisms of the SLCO1B1 gene predict methotrexate-related toxicity in childhood acute lymphoblastic leukemia. Pediatr. Blood Cancer *57*, 612–619.

Lopez-Lopez, E., Ballesteros, J., Pinan, M.A., Sanchez de Toledo, J., Garcia de Andoin, N., Garcia-Miguel, P., Navajas, A., and Garcia-Orad, A. (2013). Polymorphisms in the methotrexate transport pathway: a new tool for MTX plasma level prediction in pediatric acute lymphoblastic leukemia. Pharmacogenet. Genomics *23*, 53–61.

Lopez-Lopez, E., Gutierrez-Camino, A., Pinan, M.A., Sanchez-Toledo, J., Uriz, J.J., Ballesteros, J., Garcia-Miguel, P., Navajas, A., and Garcia-Orad, A. (2014a). Pharmacogenetics of microRNAs and microRNAs biogenesis machinery in pediatric acute lymphoblastic leukemia. PLoS One *9*, e91261.

Lopez-Lopez, E., Gutierrez-Camino, A., Bilbao-Aldaiturriaga, N., Pombar-Gomez, M., Martin-Guerrero, I., and Garcia-Orad, A. (2014b). Pharmacogenetics of childhood acute lymphoblastic leukemia.

References-Erreferentziak

Pharmacogenomics *15*, 1383–1398.

Lopez-Lopez, E., Gutierrez-Camino, A., Astigarraga, I., Navajas, A., Echebarria-Barona, A., Garcia-Miguel, P., Garcia de Andoin, N., Lobo, C., Guerra-Merino, I., Martin-Guerrero, I., et al. (2016). Vincristine pharmacokinetics pathway and neurotoxicity during early phases of treatment in pediatric acute lymphoblastic leukemia. Pharmacogenomics *17*, 731–741.

Lopomo, A., and Coppedè, F. (2017). Pharmacoepigenetics and pharmacoepigenomics of gastrointestinal cancers. Expert Rev. Gastroenterol. Hepatol. *12*, 1–14.

Low, S.-K., Kiyotani, K., Mushiroda, T., Daigo, Y., Nakamura, Y., and Zembutsu, H. (2009). Association study of genetic polymorphism in ABCC4 with cyclophosphamide-induced adverse drug reactions in breast cancer patients. J. Hum. Genet. *54*, 564–571.

Malouf, C., and Ottersbach, K. (2017). Molecular processes involved in B cell acute lymphoblastic leukaemia. Cell. Mol. Life Sci.

Maxwell, R.R., and Cole, P.D. (2017). Pharmacogenetic Predictors of Treatment-Related Toxicity Among Children With Acute Lymphoblastic Leukemia. Curr. Hematol. Malig. Rep. *12*, 176–186.

Merritt, W.M., Bar-Eli, M., and Sood, A.K. (2010). The dicey role of Dicer: implications for RNAi therapy. Cancer Res. *70*, 2571–2574.

Meulendijks, D., Henricks, L.M., Amstutz, U., Froehlich, T.K., Largiader, C.R., Beijnen, J.H., de Boer, A., Deenen, M.J., Cats, A., and Schellens, J.H.M. (2016). Rs895819 in MIR27A improves the predictive value of DPYD variants to identify patients at risk of severe fluoropyrimidine-associated toxicity. Int. J. Cancer *138*, 2752–2761.

Mikkelsen, T.S., Thorn, C.F., Yang, J.J., Ulrich, C.M., French, D., Zaza, G., Dunnenberger, H.M., Marsh, S., McLeod, H.L., Giacomini, K., et al. (2011). PharmGKB summary: methotrexate pathway. Pharmacogenet. Genomics *21*, 679–686.

Mishra, P.J., Mishra, P.J., Banerjee, D., and Bertino, J.R. (2008). MiRSNPs or MiR-polymorphisms, new players in microRNA mediated regulation of the cell: Introducing microRNA pharmacogenomics. Cell Cycle *7*, 853–858.

Mitchell, C., Richards, S., Harrison, C.J., and Eden, T. (2010). Long-term follow-up of the United Kingdom medical research council protocols for childhood acute lymphoblastic leukaemia, 1980–2001. Leukemia *24*, 406–418.

Moore, A.S., Norris, R., Price, G., Nguyen, T., Ni, M., George, R., van Breda, K., Duley, J., Charles, B., and Pinkerton, R. (2011). Vincristine pharmacodynamics and pharmacogenetics in children with cancer: a limited-sampling, population modelling approach. J. Paediatr. Child Health *47*, 875–882.

Möricke, A., Zimmermann, M., Reiter, A., Henze, G., Schrauder, A., Gadner, H., Ludwig, W.D., Ritter, J., Harbott, J., Mann, G., et al. (2010). Long-term results of five consecutive trials in childhood acute lymphoblastic leukemia performed by the ALL-BFM study group from 1981 to 2000. Leukemia *24*, 265–284.

Moriyama, T., Relling, M. V, and Yang, J.J. (2015). Inherited genetic variation in childhood acute lymphoblastic leukemia. Blood *125*, 3988–3995.

Muralidharan, N., Antony, P.T., Jain, V.K., Mariaselvam, C.M., and Negi, V.S. (2015). Multidrug resistance 1 (MDR1) 3435C>T gene polymorphism influences the clinical phenotype and methotrexate-induced adverse events in South Indian Tamil rheumatoid arthritis. Eur. J. Clin. Pharmacol. *71*, 959–965.

Nakajima, M., and Yokoi, T. (2011). MicroRNAs from biology to future pharmacotherapy: regulation of

cytochrome P450s and nuclear receptors. Pharmacol. Ther. *131*, 330–337.

Navarro, V.J., and Senior, J.R. (2006). Drug-Related Hepatotoxicity. N. Engl. J. Med. *354*, 731–739.

Nicoletti, P., Cartsos, V.M., Palaska, P.K., Shen, Y., Floratos, A., and Zavras, A.I. (2012). Genomewide pharmacogenetics of bisphosphonate-induced osteonecrosis of the jaw: the role of RBMS3. Oncologist *17*, 279–287.

Onuma, T., Waligunda, J., and Holland, J.F. (1971). Amino acid requirements in vitro of human leukemic cells. Cancer Res. *31*, 1640–1644.

Pfizer, S.. (2017a). Vincristine [medicinal product official information].

Pfizer, S.L. (2017b). Daunorubicin [medicinal product official information].

Plasschaert, S.L.A., Groninger, E., Boezen, M., Kema, I., de Vries, E.G.E., Uges, D., Veerman, A.J.P., Kamps, W.A., Vellenga, E., de Graaf, S.S., et al. (2004). Influence of functional polymorphisms of the MDR1 gene on vincristine pharmacokinetics in childhood acute lymphoblastic leukemia. Clin. Pharmacol. Ther. *76*, 220–229.

Postma, T.J., Benard, B.A., Huijgens, P.C., Ossenkoppele, G.J., and Heimans, J.J. (1993). Long-term effects of vincristine on the peripheral nervous system. J. Neurooncol. *15*, 23–27.

Preskorn, S.H., and Hatt, C.R. (2013). How pharmacogenomics (PG) are changing practice: implications for prescribers, their patients, and the healthcare system (PG series part I). J. Psychiatr. Pract. *19*, 142–149.

Pui, C.-H. (2010). Recent research advances in childhood acute lymphoblastic leukemia. J. Formos. Med. Assoc. *109*, 777–787.

Pui, C.-H., and Evans, W.E. (2013). A 50-year journey to cure childhood acute lymphoblastic leukemia. Semin. Hematol. *50*, 185–196.

Pui, C.-H., Yang, J.J., Hunger, S.P., Pieters, R., Schrappe, M., Biondi, A., Vora, A., Baruchel, A.A., Silverman, L.B., Schmiegelow, K., et al. (2015). Childhood Acute Lymphoblastic Leukemia: Progress Through Collaboration. J. Clin. Oncol. *33*, JCO.2014.59.1636.

Qiu, A., Jansen, M., Sakaris, A., Min, S.H., Chattopadhyay, S., Tsai, E., Sandoval, C., Zhao, R., Akabas, M.H., and Goldman, I.D. (2006). Identification of an intestinal folate transporter and the molecular basis for hereditary folate malabsorption. Cell *127*, 917–928.

Qiu, A., Min, S.H., Jansen, M., Malhotra, U., Tsai, E., Cabelof, D.C., Matherly, L.H., Zhao, R., Akabas, M.H., and Goldman, I.D. (2007). Rodent intestinal folate transporters (SLC46A1): secondary structure, functional properties, and response to dietary folate restriction. Am. J. Physiol. Cell Physiol. *293*, C1669-78.

Radtke, S., Zolk, O., Renner, B., Paulides, M., Zimmermann, M., Moricke, A., Stanulla, M., Schrappe, M., and Langer, T. (2013). Germline genetic variations in methotrexate candidate genes are associated with pharmacokinetics, toxicity, and outcome in childhood acute lymphoblastic leukemia. Blood *121*, 5145–5153.

Ramnath, D., Powell, E.E., Scholz, G.M., and Sweet, M.J. (2017). The toll-like receptor 3 pathway in homeostasis, responses to injury and wound repair. Semin. Cell Dev. Biol. *61*, 22–30.

Ramsey, L.B., Bruun, G.H., Yang, W., Trevino, L.R., Vattathil, S., Scheet, P., Cheng, C., Rosner, G.L., Giacomini, K.M., Fan, Y., et al. (2012). Rare versus common variants in pharmacogenetics: SLCO1B1 variation and methotrexate disposition. Genome Res. *22*, 1–8.

Ramsey, L.B., Panetta, J.C., Smith, C., Yang, W., Fan, Y., Winick, N.J., Martin, P.L., Cheng, C., Devidas, M.,

References-Erreferentziak

Pui, C.-H.C.-H., et al. (2013). Genome-wide study of methotrexate clearance replicates SLCO1B1. Blood *121*, 898–904.

Reyes-Gibby, C.C., Melkonian, S.C., Wang, J., Yu, R.K., Shelburne, S.A., Lu, C., Gunn, G.B., Chambers, M.S., Hanna, E.Y., Yeung, S.-C.J., et al. (2017). Identifying novel genes and biological processes relevant to the development of cancer therapy-induced mucositis: An informative gene network analysis. PLoS One *12*, e0180396.

Rice, T., Schork, N., and Rao, D. (2008). Genetic Dissection of Complex Traits.

Robles-Diaz, M., Lucena, M.I., Kaplowitz, N., Stephens, C., Medina-Cáliz, I., González-Jimenez, A., Ulzurrun, E., Gonzalez, A.F., Fernandez, M.C., Romero-Gómez, M., et al. (2014). Use of Hy's law and a new composite algorithm to predict acute liver failure in patients with drug-induced liver injury. Gastroenterology *147*, 109–118.e5.

Rosenthal, S., and Kaufman, S. (1974). Vincristine neurotoxicity. Ann. Intern. Med. *80*, 733–737.

Rukov, J.L., and Shomron, N. (2011). MicroRNA pharmacogenomics: post-transcriptional regulation of drug response. Trends Mol. Med. *17*, 412–423.

Rukov, J.L., Wilentzik, R., Jaffe, I., Vinther, J., and Shomron, N. (2014). Pharmaco-miR: linking microRNAs and drug effects. Brief. Bioinform. *15*, 648–659.

Ryan, B.M., Robles, A.I., and Harris, C.C. (2010). Genetic variation in microRNA networks: the implications for cancer research. Nat. Rev. Cancer *10*, 389–402.

Salazar, J., Altes, A., del Rio, E., Estella, J., Rives, S., Tasso, M., Navajas, A., Molina, J., Villa, M., Vivanco, J.L., et al. (2012). Methotrexate consolidation treatment according to pharmacogenetics of MTHFR ameliorates event-free survival in childhood acute lymphoblastic leukaemia. Pharmacogenomics J. *12*, 379–385.

Sambrook, J, R.D. (2001). Molecular cloning: a laboratory manual (New York: NY: Cold Spring Harbor Laboratory Press).

Sangild, P.T., Shen, R.L., Pontoppidan, P.E.L., and Rathe, M. (2017). Animal models of chemotherapy-induced mucositis: translational relevance and challenges. Am. J. Physiol. - Gastrointest. Liver Physiol. ajpgi.00204.2017.

Schmiegelow, K., Müller, K., Mogensen, S.S., Mogensen, P.R., Wolthers, B.O., Stoltze, U.K., Tuckuviene, R., and Frandsen, T. (2017). Open peer review non-infectious chemotherapy-associated acute toxicities during childhood acute lymphoblastic leukemia therapy. F 1000 Res. 1–14.

Van Sebille, Y.Z.A., Stansborough, R., Wardill, H.R., Bateman, E., Gibson, R.J., and Keefe, D.M. (2015). Management of mucositis during chemotherapy: from pathophysiology to pragmatic therapeutics. Curr. Oncol. Rep. *17*, 50.

Sethu, S., Pushparaj, P.N., and Melendez, A.J. (2010). Phospholipase D1 mediates TNFalpha-induced inflammation in a murine model of TNFalpha-induced peritonitis. PLoS One *5*, e10506.

Shimasaki, N., Mori, T., Samejima, H., Sato, R., Shimada, H., Yahagi, N., Torii, C., Yoshihara, H., Tanigawara, Y., Takahashi, T., et al. (2006). Effects of methylenetetrahydrofolate reductase and reduced folate carrier 1 polymorphisms on high-dose methotrexate-induced toxicities in children with acute lymphoblastic leukemia or lymphoma. J. Pediatr. Hematol. Oncol. *28*, 64–68.

Silver pharma S.L. (2017). Mercaptopurine [medicinal product official information].

Silverman, L.B., Declerck, L., Gelber, R.D., Dalton, V.K., Asselin, B.L., Barr, R.D., Clavell, L.A., Hurwitz, C.A.,

Moghrabi, A., Samson, Y., et al. (2000). Results of Dana-Farber Cancer Institute Consortium protocols for children with newly diagnosed acute lymphoblastic leukemia (1981-1995). Leukemia *14*, 2247–2256.

Slaby, O., Bienertova-Vasku, J., Svoboda, M., and Vyzula, R. (2012). Genetic polymorphisms and microRNAs: new direction in molecular epidemiology of solid cancer. J. Cell. Mol. Med. *16*, 8–21.

Song, J.-J., Liu, J., Tolia, N.H., Schneiderman, J., Smith, S.K., Martienssen, R.A., Hannon, G.J., and Joshua-Tor, L. (2003). The crystal structure of the Argonaute2 PAZ domain reveals an RNA binding motif in RNAi effector complexes. Nat. Struct. Biol. *10*, 1026–1032.

Sonis, S.T. (2004a). The pathobiology of mucositis. Nat. Rev. Cancer *4*, 277–284.

Sonis, S.T. (2004b). Oral mucositis in cancer therapy. J. Support. Oncol. *2*, 3–8.

Sonis, S.T. (2004c). A biological approach to mucositis. J. Support. Oncol. *2*, 21-32-6.

Sonis, S.T. (2007). The pathobiology of oral mucositis. Community Support. Oncol. *5*, 3–11.

Sonis, S.T., Elting, L.S., Keefe, D., Peterson, D.E., Schubert, M., Hauer-Jensen, M., Bekele, B.N., Raber-Durlacher, J., Donnelly, J.P., Rubenstein, E.B., et al. (2004). Perspectives on cancer therapy-induced mucosal injury: pathogenesis, measurement, epidemiology, and consequences for patients. Cancer *100*, 1995–2025.

Sonis, S.T., Antin, J., Tedaldi, M., and Alterovitz, G. (2013). SNP-based Bayesian networks can predict oral mucositis risk in autologous stem cell transplant recipients. Oral Dis. *19*, 721–727.

Spezialpräparate, M.G. für klinische (2017). Asparaginase [medicinal product official information].

Sullivan, K.M., Dean, A., and Soe, M.M. (2009). OpenEpi: a web-based epidemiologic and statistical calculator for public health. Public Health Rep. *124*, 471–474.

Suthandiram, S., Gan, G.-G., Zain, S.M., Bee, P.-C., Lian, L.-H., Chang, K.-M., Ong, T.-C., and Mohamed, Z. (2014). Effect of polymorphisms within methotrexate pathway genes on methotrexate toxicity and plasma levels in adults with hematological malignancies. Pharmacogenomics *15*, 1479–1494.

Swerdlow, S., Campo, E., Harris, N., Jaffe, E., Pileri, S., Stein, H., Thiele, J., and Vardiman, J. (2008). WHO Classification of Tumours of Haematopoietic and Lymphoid Tissues (Lyon:IARC;2008).

Swerts, K., De Moerloose, B., Dhooge, C., Laureys, G., Benoit, Y., and Philippé, J. (2006). Prognostic significance of multidrug resistance-related proteins in childhood acute lymphoblastic leukaemia. Eur. J. Cancer *42*, 295–309.

Tasian, S.K., and Hunger, S.P. (2017). Genomic characterization of paediatric acute lymphoblastic leukaemia: an opportunity for precision medicine therapeutics. Br. J. Haematol. *176*, 867–882.

Teft, W.A., Welch, S., Lenehan, J., Parfitt, J., Choi, Y.-H., Winquist, E., and Kim, R.B. (2015). OATP1B1 and tumour OATP1B3 modulate exposure, toxicity, and survival after irinotecan-based chemotherapy. Br. J. Cancer *112*, 857–865.

Treon, S.P., and Chabner, B.A. (1996). Concepts in use of high-dose methotrexate therapy. Clin. Chem. *42*, 1322–1329.

Trevino, L.R., Shimasaki, N., Yang, W., Panetta, J.C., Cheng, C., Pei, D., Chan, D., Sparreboom, A., Giacomini, K.M., Pui, C.-H., et al. (2009). Germline genetic variation in an organic anion transporter polypeptide associated with methotrexate pharmacokinetics and clinical effects. J. Clin. Oncol. *27*, 5972–5978.

Turner, R.M., Park, B.K., and Pirmohamed, M. (2015). Parsing interindividual drug variability: an emerging

References-Erreferentziak

role for systems pharmacology. Wiley Interdiscip. Rev. Syst. Biol. Med. *7*, 221–241.

Tzoneva, G., Perez-Garcia, A., Carpenter, Z., Khiabanian, H., Tosello, V., Allegretta, M., Paietta, E., Racevskis, J., Rowe, J.M., Tallman, M.S., et al. (2013). Activating mutations in the NT5C2 nucleotidase gene drive chemotherapy resistance in relapsed ALL. Nat. Med. *19*, 368–371.

Umerez, M., Gutierrez-Camino, Á., Muñoz-Maldonado, C., Martin-Guerrero, I., and Garcia-Orad, A. (2017). MTHFR polymorphisms in childhood acute lymphoblastic leukemia: Influence on methotrexate therapy. Pharmgenomics. Pers. Med. *10*, 69–78.

Wang, S., Sun, L., Zeng, W., Wu, W., and Zhang, G. (2014). Effects of a microRNA binding site polymorphism in SLC19A1 on methotrexate concentrations in Chinese children with acute lymphoblastic leukemia. Med. Oncol. *31*, 62.

Wojtuszkiewicz, A., Peters, G.J., van Woerden, N.L., Dubbelman, B., Escherich, G., Schmiegelow, K., Sonneveld, E., Pieters, R., van de Ven, P.M., Jansen, G., et al. (2015). Methotrexate resistance in relation to treatment outcome in childhood acute lymphoblastic leukemia. J. Hematol. Oncol. *8*, 61.

Xia, L., Zhang, D., Du, R., Pan, Y., Zhao, L., Sun, S., Hong, L., Liu, J., and Fan, D. (2008). miR-15b and miR-16 modulate multidrug resistance by targeting BCL2 in human gastric cancer cells. Int. J. Cancer *123*, 372–379.

Yang, A., Sun, Y., Mao, C., Yang, S., Huang, M., Deng, M., Ding, N., Yang, X., Zhang, M., Jin, S., et al. (2017). Folate protects hepatocytes of hyperhomocysteinemia mice from apoptosis via cystic fibrosis transmembrane conductance regulator (CFTR)-activated endoplasmic reticulum stress. J. Cell. Biochem. *118*, 2921–2932.

Zhan, X., Wu, W., Han, B., Gao, G., Qiao, R., Lv, J., Zhang, S., Zhang, W., Fan, W., Chen, H., et al. (2012). Hsa-miR-196a2 functional SNP is associated with severe toxicity after platinum-based chemotherapy of advanced nonsmall cell lung cancer patients in a Chinese population. J. Clin. Lab. Anal. *26*, 441–446.

Zhao, R., Qiu, A., Tsai, E., Jansen, M., Akabas, M.H., and Goldman, I.D. (2008). The proton-coupled folate transporter: impact on pemetrexed transport and on antifolates activities compared with the reduced folate carrier. Mol. Pharmacol. *74*, 854–862.

Zhou, F., Zheng, J., Zhu, L., Jodal, A., Cui, P.H., Wong, M., Gurney, H., Church, W.B., and Murray, M. (2013). Functional analysis of novel polymorphisms in the human SLCO1A2 gene that encodes the transporter OATP1A2. AAPS J. *15*, 1099–1108.

Zhou, G., Yu, L., Yang, W., Wu, W., Fang, L., and Liu, Z. (2016). Blockade of PLD2 ameliorates intestinal mucosal inflammation of inflammatory bowel disease. Mediators Inflamm. *2016*, 2543070.